



Vaango Theory Guide

Version Version 23 .4 .6

April 6, 2023

Biswajit Banerjee

and

The Uintah team

Copyright © 2015-2023 Biswajit Banerjee

The contents of this manual can and will change significantly over time. Please make sure that all the information is up to date.



Contents

1	The Material Point Method	9
1.1	Introduction	9
1.2	Weak form of the momentum equation	10
1.3	Information transfer from particles to grid and back	11
1.3.1	Traditional MPM	13
1.3.2	GIMP	14
1.3.3	CPDI	14
1.3.4	Transfer to and from grid	14
1.4	MPM discretization of the weak form	15
1.4.1	Damping	18
1.5	Algorithm Description	18
1.5.1	Deformation gradient computation	20
1.6	Shape functions for MPM, GIMP, and CPDI	21
1.6.1	MPM	22
1.6.2	GIMP	23
1.6.3	UGIMP and cpGIMP	23
1.6.4	CPDI	25
1.7	Contact algorithms	26
1.7.1	Definitions	26
1.7.2	Computing surface normals and tractions	27
1.7.3	Basic contact algorithm	27
1.7.4	Contact with a specified master	27
1.7.5	Frictional contact algorithms	28
1.8	Implicit time integration	32
1.8.1	Newton's method	32
1.8.2	Tangent stiffness matrix	33
1.8.3	External force stiffness matrix	37
1.8.4	Body force stiffness matrix	37

1.9	Pseudocode of explicit MPM algorithm in Vaango	37
1.9.1	Initialization	38
1.9.2	Time advance	38
2	MPM Material Models	47
2.1	Notation and definitions	47
2.1.1	Volumetric-deviatoric decomposition	47
2.1.2	Stress invariants	48
2.1.3	Effective stress and strain	48
2.1.4	Equivalent strain rate and plastic strain	49
2.1.5	Velocity gradient, rate-of-deformation, deformation gradient	49
2.1.6	Eigenvectors and coordinate transformations	49
2.2	Material models available in Vaango	50
3	Special material models	55
3.1	Rigid material	55
3.2	Ideal gas material	55
3.3	Water material	56
3.4	Murnaghan material	56
3.5	JWL++ material	56
4	Elastic material models	59
4.1	Hypoelastic material	59
4.2	Hyperelastic Material Models	59
4.2.1	Compressible neo-Hookean material	60
4.2.2	Compressible Mooney-Rivlin material	60
4.2.3	Transversely isotropic hyperelastic material	61
4.3	Elastic modulus models	61
4.3.1	Support vector regression model	62
5	Plasticity	65
6	Equation of state models	67
6.1	Hypoelastic equation of state	67
6.2	Default hyperelastic equation of state	68
6.3	Mie-Gruneisen equation of state	68
6.4	Equations of state used in the ARENA model	69
6.4.1	Solid matrix material	69
6.4.2	Pore water	69
6.4.3	Pore air	70
7	Deviatoric stress models	71
7.1	Shear modulus models	71
7.1.1	Constant shear modulus	71
7.1.2	Mechanical Threshold Stress shear modulus	72

7.1.3	SCG shear modulus	72
7.1.4	Nadal-LePoac (NP) shear modulus	72
7.1.5	Preston-Tonks-Wallace (PTW) shear modulus	73
7.1.6	Borja's shear modulus model	73
8	Yield condition	75
8.1	von Mises yield	75
8.2	The Gurson-Tvergaard-Needleman (GTN) yield condition	76
8.3	The Rousselier yield condition	77
9	Flow rule	79
9.1	Associated plasticity	79
9.2	Non-associated plasticity	79
10	Isotropic hardening models	81
10.1	Linear hardening model	81
10.2	Johnson-Cook model	81
10.3	Steinberg-Guinan model	82
10.4	Zerilli-Armstrong model	83
10.5	Polymer Zerilli-Armstrong model	83
10.6	Mechanical threshold stress model	84
10.7	Preston-Tonks-Wallace model	85
10.8	SUVIC-I model	86
11	Kinematic hardening models	89
11.1	Ziegler-Prager model	89
11.2	Armstrong-Frederick model	89
12	Internal variable evolution	91
12.1	Equivalent plastic strain	91
12.2	Porosity	91
12.3	Backstress	92
12.4	Damage	92
12.5	Temperature	92
13	Melting temperature models	95
13.1	Constant melting temperature	95
13.2	Steinberg-Cochran-Guinan melting temperature	95
13.3	Burakovsky-Preston-Silbar melting temperature	96

14	Adiabatic heating and specific heat	97
14.1	Constant specific heat model	97
14.2	Specific heat model for copper	97
14.3	Specific heat model for steel	98
15	Damage models	99
15.1	Hancock-MacKenzie model	99
15.2	Johnson-Cook model	99
16	Material failure	101
16.1	Introduction	101
16.2	Erosion algorithm	101
16.3	Material stability conditions	102
16.3.1	Drucker's condition	102
16.3.2	Acoustic tensor criterion	102
16.3.3	Becker's simplification	105
17	Isotropic metal plasticity	107
17.1	The model	107
17.1.1	Purely elastic loading/unloading	108
17.1.2	Yield condition	108
17.1.3	Flow rule	109
17.1.4	Isotropic and kinematic hardening/softening rules	109
17.1.5	Elastic-plastic loading/unloading	110
17.1.6	Consistency condition	111
17.2	Stress update	111
17.2.1	Iterative solution	112
17.2.2	Stress update in reduced stress space	116
17.2.3	Algorithm 1	118
17.2.4	Algorithm 2	120
17.3	Example 1: von Mises plasticity	122
17.4	Example 2: Gurson-type model	123
17.5	Example 3: Nonlinear elasticity and isotropic hardening	124
18	Metal plasticity : traditional approach	127
18.1	Preamble	127
18.2	Elastic relation	128
18.3	Flow rule	128
18.4	Hardening, porosity evolution, and plastic dissipation	129
18.5	Yield condition	129
18.6	Continuum elastic-plastic tangent modulus	130
18.6.1	J ₂ plasticity	131
18.6.2	J ₂ -I ₁ plasticity	132

18.7	Stress update	132
18.7.1	Integrating the rate equations	133
18.7.2	Newton iterations	135
18.7.3	Algorithm	138
18.8	Examples	139
18.8.1	Example 1	139
18.8.2	Example 2	141



1 — The Material Point Method

1.1 Introduction

The **MPM** component solves the momentum equations

$$\nabla \cdot \sigma + \rho \mathbf{b} = \rho \dot{\mathbf{v}} \quad (1.1)$$

using an updated Lagrangian formulation. The momentum solve for solid materials is complicated by the fact that the equations need material constitutive models for closure. These material constitutive models vary significantly between materials and contribute a large fraction of the computational cost of a simulation.

The material point method (MPM) was described by Sulsky et al. [1, 2] as an extension to the FLIP (Fluid-Implicit Particle) method of Brackbill [3], which itself is an extension of the particle-in-cell (PIC) method of Harlow [4].

Interestingly, the name “material point method” first appeared in the literature two years later in a description of an axisymmetric form of the method [5].

In both FLIP and **MPM**, the basic idea is the same: objects are discretized into particles, or material points, each of which contains all state data for the small region of material that it represents. Particles do not interact with each other directly, rather the particle information is accumulated to a background grid, where the equations of motion (1.1) are integrated forward in time. This time advanced solution is then used to update the particle state. Particle state data includes the position, mass, volume, velocity, stress, state of deformation of that material, and a number of time-dependent internal material variables.

MPM differs from other “mesh-free” particle methods in that, while each object is primarily represented by a collection of particles, a computational mesh is also an important part of the calculation. This mesh reduces the computational cost of searching for neighboring particles.

MPM usually uses a regular structured grid as a computational mesh. While this grid, in principle, deforms as the material that it is representing deforms, at the end of each timestep, it is reset to its original undeformed position, in effect providing a new computational grid for each timestep. The use of a regular structured grid for each time step has a number of computational advantages. Computation of spatial gradients is simplified. Mesh entanglement, which can plague fully Lagrangian techniques, such as the Finite Element Method (FEM), is avoided.

MPM has also been successful in solving problems involving contact between colliding objects, having an

advantage over FEM in that the use of the regular grid eliminates the need for doing costly searches for contact surfaces[6].

In addition to the advantages that **MPM** brings, as with any numerical technique, it has its own set of shortcomings. It is computationally more expensive than a comparable FEM code. Accuracy for **MPM** is typically lower than FEM, and errors associated with particles moving around the computational grid can introduce non-physical oscillations into the solution. Finally, numerical difficulties can still arise in simulations involving large deformation that will prematurely terminate the simulation. The severity of all of these issues (except for the expense) has been significantly reduced with the introduction of the Generalized Interpolation Material Point Method, or **GIMP** [7]. Newer developments such as the **CPDI MPM** method [8] have also been incorporated into the explicit time integrated **MPM** in VAANGO. Implementation of other approaches along the line of **CPDI** such as **CPDI2** [9] and **CPTI** [10] is also being considered for future versions.

In addition, **MPM** can be incorporated with a multi-material CFD algorithm as the structural component in a fluid-structure interaction formulation. This capability was first demonstrated in the CFDLIB codes from Los Alamos by Bryan Kashiwa and co-workers[11]. There, as in the MPMICE component, **MPM** serves as the Lagrangian description of the solid material in a multimaterial CFD code. Certain elements of the solution procedure are based in the Eulerian CFD algorithm, including intermaterial heat and momentum transfer as well as satisfaction of a multimaterial equation of state. The use of a Lagrangian method such as **MPM** to advance the solution of the solid material eliminates the diffusion typically associated with Eulerian methods.

1.2 Weak form of the momentum equation

To derive the weak form of the momentum equation (1.1), we multiply the momentum equation with a vector-valued weighting function (\mathbf{w}) and integrate over the domain (Ω). The weighting function (\mathbf{w}) satisfies velocity boundary conditions on the parts of the boundary where velocities are prescribed. Then,

$$\int_{\Omega} \mathbf{w} \cdot [\nabla \cdot \boldsymbol{\sigma} + \rho \mathbf{b}] d\Omega = \int_{\Omega} \rho \mathbf{w} \cdot \dot{\mathbf{v}} d\Omega. \quad (1.2)$$

Using the identity $\mathbf{v} \cdot (\nabla \cdot \mathbf{S}) = \nabla \cdot (\mathbf{S}^T \cdot \mathbf{v}) - \mathbf{S} : \nabla \mathbf{v}$, where \mathbf{S} is a second-order tensor valued field and \mathbf{v} is a vector valued field, we have

$$\int_{\Omega} \{ \nabla \cdot (\boldsymbol{\sigma}^T \cdot \mathbf{w}) - \boldsymbol{\sigma} : \nabla \mathbf{w} + \rho \mathbf{w} \cdot \mathbf{b} \} d\Omega = \int_{\Omega} \rho \mathbf{w} \cdot \dot{\mathbf{v}} d\Omega.$$

Application the divergence theorem to the divergence of the weighted stress leads to

$$\int_{\Gamma} \mathbf{n} \cdot (\boldsymbol{\sigma}^T \cdot \mathbf{w}) d\Gamma + \int_{\Omega} \{ -\boldsymbol{\sigma} : \nabla \mathbf{w} + \rho \mathbf{w} \cdot \mathbf{b} \} d\Omega = \int_{\Omega} \rho \mathbf{w} \cdot \dot{\mathbf{v}} d\Omega$$

where \mathbf{n} is the outward normal to the surface Γ . Rearranging,

$$\int_{\Gamma} (\boldsymbol{\sigma} \cdot \mathbf{n}) \cdot \mathbf{w} d\Gamma - \int_{\Omega} \boldsymbol{\sigma} : \nabla \mathbf{w} d\Omega + \int_{\Omega} \rho \mathbf{w} \cdot \mathbf{b} d\Omega = \int_{\Omega} \rho \mathbf{w} \cdot \dot{\mathbf{v}} d\Omega. \quad (1.3)$$

If the applied surface traction is $\bar{\mathbf{t}} := \boldsymbol{\sigma} \cdot \mathbf{n}$, since \mathbf{w} is zero on the part of the boundary where velocities/displacements are specified, we get the **weak form**

$$\int_{\Gamma_t} \bar{\mathbf{t}} \cdot \mathbf{w} d\Gamma - \int_{\Omega} \boldsymbol{\sigma} : \nabla \mathbf{w} d\Omega + \int_{\Omega} \rho \mathbf{w} \cdot \mathbf{b} d\Omega = \int_{\Omega} \rho \mathbf{w} \cdot \dot{\mathbf{v}} d\Omega. \quad (1.4)$$

1.3 Information transfer from particles to grid and back

The goal of **MPM** is to find a unique function $f(\mathbf{x}, t)$ that satisfies the governing equations (1.1) for a given initial set of objects and a set of initial and boundary conditions.

An important underlying assumption in **MPM** is that continuum field quantities have two equivalent representations – a grid representation and a particle representation. For instance, the representation of a vector field \mathbf{f} can be both

$$\boxed{\mathbf{f}(\mathbf{x}) = \sum_g \mathbf{f}(\mathbf{x}_g) S_g(\mathbf{x}) = \sum_g \mathbf{f}_g S_g(\mathbf{x})} \quad \text{and} \quad \boxed{\mathbf{f}(\mathbf{x}) = \sum_p \mathbf{f}(\mathbf{x}_p) \chi_p(\mathbf{x}) = \sum_p \mathbf{f}_p \chi_p(\mathbf{x})} \quad (1.5)$$

where the subscript g indicates a grid nodal quantity and the subscript p indicates a particle quantity. A particle centroid is at the location \mathbf{x}_p while a grid node is at \mathbf{x}_g . The functions S_g are interpolation functions (also called shape functions) that take values from the grid nodes to points in the computational domain. On the other hand, the functions χ_p are particle characteristic functions. We assume that both these representations are partitions of unity. In the above we have ignored time-dependence for simplicity.

The **MPM** algorithm is particle-centered. We start with information on particles and then project that information to the grid nodes for the solution of (1.1). After the equations have been solved, the information on the grid can be interpolated back to the particles in preparation for the next timestep. The projection operation from particles to the grid is not as obvious as the interpolation from the grid back to particles and requires some explanation.

Ideally we would like the two representations in (1.5) to produce identical results. However, due to approximation errors, they usually do not. Let $\mathbf{e}(\mathbf{x})$ be the error. Then we can pose a least-squares error minimization problem as

$$\text{Find } \mathbf{f}_g \text{ that minimizes } E = \int_{\Omega} w(\mathbf{x}) \|\mathbf{e}(\mathbf{x})\|^2 d\Omega \text{ where } \int_{\Omega} w(\mathbf{x}) d\Omega = 1. \quad (1.6)$$

The domain of integration is the volume Ω and $w(\mathbf{x})$ is a weighting function. Then the minimum of the functional E can be found using

$$\frac{\partial E}{\partial \mathbf{f}_g} = \mathbf{0} \implies \int_{\Omega} w(\mathbf{x}) \left[\frac{\partial \mathbf{e}}{\partial \mathbf{f}_g} \cdot \mathbf{e}(\mathbf{x}) + \mathbf{e}(\mathbf{x}) \cdot \frac{\partial \mathbf{e}}{\partial \mathbf{f}_g} \right] d\Omega = \mathbf{0} \quad (1.7)$$

From (1.5),

$$\frac{\partial \mathbf{e}}{\partial \mathbf{f}_g} = \frac{\partial}{\partial \mathbf{f}_g} \left[\sum_{g'} \mathbf{f}_{g'} S_{g'}(\mathbf{x}) - \sum_p \mathbf{f}_p \chi_p(\mathbf{x}) \right] = \sum_{g'} \frac{\partial \mathbf{f}_{g'}}{\partial \mathbf{f}_g} S_{g'}(\mathbf{x}) = S_g(\mathbf{x}) \mathbf{I}. \quad (1.8)$$

Therefore,

$$\int_{\Omega} w(\mathbf{x}) S_g(\mathbf{x}) \mathbf{e}(\mathbf{x}) d\Omega = \mathbf{0} \implies \int_{\Omega} w(\mathbf{x}) S_g(\mathbf{x}) \left[\sum_{g'} \mathbf{f}_{g'} S_{g'}(\mathbf{x}) - \sum_p \mathbf{f}_p \chi_p(\mathbf{x}) \right] d\Omega = \mathbf{0}. \quad (1.9)$$

If we note that the particle characteristic function (χ_p) is required to be zero outside the domain of particle p and 1 inside, rearrangement of the above equation leads to

$$\sum_g \mathbf{f}_g \int_{\Omega} w(\mathbf{x}) S_{g'}(\mathbf{x}) S_g(\mathbf{x}) d\Omega = \sum_p \mathbf{f}_p \int_{\Omega_p} w(\mathbf{x}) S_{g'}(\mathbf{x}) d\Omega. \quad (1.10)$$

Define

$$\boxed{A_{g'g} := \int_{\Omega} w(\mathbf{x}) S_{g'}(\mathbf{x}) S_g(\mathbf{x}) d\Omega \quad \text{and} \quad B_{g'p} := \int_{\Omega_p} w(\mathbf{x}) S_{g'}(\mathbf{x}) d\Omega.} \quad (1.11)$$

Equation (1.10) can now be expressed as

$$\sum_g A_{g'g} \mathbf{f}_g = \sum_p B_{g'p} \mathbf{f}_p. \quad (1.12)$$

Inverting the relation, we have

$$\mathbf{f}_g = [\mathbb{A}^{-1}]_{gg'} \sum_p B_{g'p} \mathbf{f}_p = \sum_p [\mathbb{A}^{-1}]_{gg'} B_{g'p} \mathbf{f}_p \quad (1.13)$$

where \mathbb{A} is the matrix representation of $A_{g'g}$ in (1.12). We can rewrite the above equation as

$$\boxed{\mathbf{f}_g = \sum_p \psi_{gp} \mathbf{f}_p} \quad (1.14)$$

where

$$\boxed{\psi_{gp} := [\mathbb{A}^{-1}]_{gg'} B_{g'p}.} \quad (1.15)$$

The map in equation (1.14) can be used to project particle quantities to grid nodes. However, some simplification is needed to avoid the need to invert a large matrix.

We can remove the need to invert \mathbb{S} if we diagonalize $S_{g'g}$ using a lumped approximation. In that case

$$A_{g'} = \sum_g A_{g'g} = \int_{\Omega} w(\mathbf{x}) S_{g'}(\mathbf{x}) \sum_g S_g(\mathbf{x}) d\Omega = \int_{\Omega} w(\mathbf{x}) S_{g'}(\mathbf{x}) d\Omega \quad (1.16)$$

where we have used the partition of unity property of the grid nodal interpolation function. Now note that the integral over the domain Ω can be split into a sum of integrals over particles.

The particle-to-grid projection operations in equations (1.14) and (1.15) can then be expressed as

$$\mathbf{f}_g = \sum_p \psi_{gp} \mathbf{f}_p \quad \text{where} \quad \psi_{gp} = \frac{B_{gp}}{A_g}, \quad A_g = \sum_p B_{gp}, \quad B_{gp} = \int_{\Omega_p} w(\mathbf{x}) S_g(\mathbf{x}) d\Omega. \quad (1.17)$$

Going back to (1.5), recall that we had assumed that \mathbf{f}_p was the value of the function $\mathbf{f}(\mathbf{x})$ at the particle centroid, \mathbf{x}_p . However, this requirement is not necessary for the development of the projection from particles to the grid. We may, alternatively, define \mathbf{f}_p as

$$\mathbf{f}_p = \frac{1}{W_p} \int_{\Omega_p} \mathbf{f}(\mathbf{x}) \omega_p(\mathbf{x}) d\Omega, \quad W_p := \int_{\Omega_p} \omega_p(\mathbf{x}) d\Omega \quad (1.18)$$

where Ω_p is the particle domain and $\omega_p(\mathbf{x})$ is a weighting function. Also recall that the grid interpolation function has the form

$$\mathbf{f}(\mathbf{x}) = \sum_g \mathbf{f}_g S_g(\mathbf{x}). \quad (1.19)$$

Therefore, we can compute the value of a quantity at a particle using the grid interpolation functions by substituting (1.19) into (1.18) to get

$$\mathbf{f}_p = \frac{1}{W_p} \int_{\Omega_p} \left[\sum_g \mathbf{f}_g S_g(\mathbf{x}) \right] \omega_p(\mathbf{x}) d\Omega = \sum_g \mathbf{f}_g \left[\frac{1}{W_p} \int_{\Omega_p} S_g(\mathbf{x}) \omega_p(\mathbf{x}) d\Omega \right]. \quad (1.20)$$

Since the particle domain Ω_p is never known exactly and we would like to avoid determining that domain, we approximate the above equation as

$$\mathbf{f}_p \approx \sum_g \mathbf{f}_g \left[\frac{1}{W_p^*} \int_{\Omega_p^*} S_g(\mathbf{x}) \omega_p^*(\mathbf{x}) d\Omega \right], \quad W_p^* := \int_{\Omega_p^*} \omega_p^*(\mathbf{x}) d\Omega \quad (1.21)$$

where the alternative weight function $\omega_p^*(\mathbf{x})$ is defined as

$$\omega_p^*(\mathbf{x}) := \omega_p(\mathbf{x}) \chi_p^*(\mathbf{x}) d\Omega. \quad (1.22)$$

The function $\chi_p^*(\mathbf{x})$ is called the **particle averaging function** since it is **not** identical to the **particle characteristic function** $\chi_p(\mathbf{x})$. All that is needed is that the function have compact support in a neighborhood Ω_p^* containing particle p .

The grid-to-particle interpolation function can then be expressed as

$$\mathbf{f}_p \approx \sum_g \mathbf{f}_g \langle S_{gp} \rangle \quad \text{where} \quad \langle S_{gp} \rangle := \frac{\int_{\Omega_p^*} S_g(\mathbf{x}) \omega_p^*(\mathbf{x}) d\Omega}{\int_{\Omega_p^*} \omega_p^*(\mathbf{x}) d\Omega}, \quad \omega_p^*(\mathbf{x}) := \omega_p(\mathbf{x}) \chi_p^*(\mathbf{x}) d\Omega. \quad (1.23)$$

A more compact matrix notation is used in [12]:

$$\mathbf{f}_p = \mathbb{S} \mathbf{f}_g \quad (1.24)$$

where \mathbf{f}_p is a particle-based quantity matrix that has size $N_p \times 1$ for scalars, $N_p \times 3$ for vectors, and $N_p \times 6$ for symmetric second-order tensors. The matrix \mathbf{f}_g are the corresponding grid quantities that have sizes $N_g \times 1$ for scalars, $N_g \times 3$ for vectors and $N_g \times 6$ for symmetric 2-tensors. The \mathbb{S} matrix has size $N_p \times N_g$ with components $\langle S_{gp} \rangle$.

We can now make some special assumptions about the weight functions in (1.17) to reduce the projection operation to that use in tradition **MPM** approaches. Let us assume that

$$B_{gp} = V_p \langle S_{gp} \rangle \implies \int_{\Omega_p} S_g(\mathbf{x}) \omega_p(\mathbf{x}) d\Omega = V_p \frac{\int_{\Omega_p} S_g(\mathbf{x}) \omega_p(\mathbf{x}) d\Omega}{\int_{\Omega_p} \omega_p(\mathbf{x}) d\Omega} \quad (1.25)$$

With that assumption, the particle-to-grid projection operations in equations (1.17) become

$$\mathbf{f}_g = \sum_p \psi_{gp} \mathbf{f}_p \quad \text{where} \quad \psi_{gp} = \frac{V_p \langle S_{gp} \rangle}{\sum_p V_p \langle S_{gp} \rangle}, \quad \sum_p \psi_{gp} = 1. \quad (1.26)$$

The matrix notation used for the above relation in [12] is

$$\mathbf{f}_g = \mathbb{S}^+ \mathbf{f}_p \quad (1.27)$$

where \mathbb{S}^+ is a $N_g \times N_p$ matrix.

1.3.1 Traditional MPM

If we wish to recover the traditional **MPM** formulation [2], take $\omega_p(\mathbf{x}) = 1$ and $\chi_p^*(\mathbf{x}) = V_p \delta(\mathbf{x} - \mathbf{x}_p)$ where V_p is the volume of $\Omega_p^* = \Omega_p$ and $\delta(\mathbf{x})$ is the Dirac delta function, we have

$$\bar{S}_{gp} := \langle S_{gp} \rangle = \frac{\int_{\Omega_p} S_g(\mathbf{x}) V_p \delta(\mathbf{x} - \mathbf{x}_p) d\Omega}{\int_{\Omega_p} V_p \delta(\mathbf{x} - \mathbf{x}_p) d\Omega} = S_g(\mathbf{x}_p). \quad (1.28)$$

The gradient of the interpolation function evaluated at the particle is

$$\bar{\mathbf{G}}_{gp} = \langle \nabla S_{gp} \rangle = \frac{\int_{\Omega_p} \nabla S_g(\mathbf{x}) V_p \delta(\mathbf{x} - \mathbf{x}_p) d\Omega}{\int_{\Omega_p} V_p \delta(\mathbf{x} - \mathbf{x}_p) d\Omega} = \nabla S_g(\mathbf{x}_p). \quad (1.29)$$

1.3.2 GIMP

To recover the **GIMP** formulation [7], we take $\omega_p(\mathbf{x}) = 1$ and the square pulse function $\chi_p^*(\mathbf{x}) = 1$ for $\mathbf{x} \in \Omega_p^*$ and $\chi_p^*(\mathbf{x}) = 0$ otherwise. The particle domain Ω_p^* is assumed to be a rectangular parallelepiped. Then

$$\bar{S}_{gp} := \langle S_{gp} \rangle = \begin{cases} \frac{1}{V_p^*} \int_{\Omega_p^*} S_g(\mathbf{x}) d\Omega & \text{for } \mathbf{x} \in \Omega_p^* \\ 0 & \text{otherwise.} \end{cases} \quad (1.30)$$

The gradient of the interpolation function is

$$\bar{\mathbf{G}}_{gp} = \langle \nabla S_{gp} \rangle = \begin{cases} \frac{1}{V_p^*} \int_{\Omega_p^*} \nabla S_g(\mathbf{x}) d\Omega & \text{for } \mathbf{x} \in \Omega_p^* \\ 0 & \text{otherwise.} \end{cases} \quad (1.31)$$

1.3.3 CPDI

For the **CPDI** formulation [8], we take $\omega_p^*(\mathbf{x}) = 1$ and the particle domain Ω_p^* is assumed to be a general parallelepiped that deforms based on the particle deformation gradient. The expression for ϕ_{gp} is similar to that for **GIMP** except that a modified shape function is used for interpolation:

$$\bar{S}_{gp} := \langle S_{gp} \rangle = \begin{cases} \frac{1}{V_p^*} \int_{\Omega_p^*} S_g^*(\mathbf{x}) d\Omega & \text{for } \mathbf{x} \in \Omega_p^* \\ 0 & \text{otherwise.} \end{cases} \quad (1.32)$$

The gradient of the interpolation function is

$$\bar{\mathbf{G}}_{gp} = \langle \nabla S_{gp} \rangle = \begin{cases} \frac{1}{V_p^*} \int_{\Omega_p^*} \nabla S_g^*(\mathbf{x}) d\Omega & \text{for } \mathbf{x} \in \Omega_p^* \\ 0 & \text{otherwise.} \end{cases} \quad (1.33)$$

1.3.4 Transfer to and from grid

For the interpolation from grid nodes to particles, the above relations indicate a general relation (see (1.23))

$$\mathbf{f}_p = \sum_g \mathbf{f}_g \bar{S}_{gp}. \quad (1.34)$$

In matrix form (see (1.24))

$$\mathbf{f}_p = \mathbb{S} \mathbf{f}_g. \quad (1.35)$$

For the particle-to-grid projection (see (1.17)), consider the case where $w(\mathbf{x}) = \rho(\mathbf{x})$ where ρ is the mass density. Then,

$$A_g = \int_{\Omega} \rho(\mathbf{x}) S_g(\mathbf{x}) d\Omega = m_g, \quad B_{gp} = \int_{\Omega} \rho(\mathbf{x}) S_g(\mathbf{x}) \chi_p(\mathbf{x}) d\Omega \quad (1.36)$$

and

$$\boxed{m_g \mathbf{f}_g = \sum_p \mathbf{f}_p \int_{\Omega} \rho(x) S_g(x) \chi_p(\mathbf{x}) d\Omega = \sum_p \mathbf{f}_p m_p \bar{S}_{gp}.} \quad (1.37)$$

where m_g is the grid node mass and m_p is the particle mass. In matrix form equation 1.37 can be written as (see (1.27))

$$\mathbf{f}_g = \mathbb{S}^+ \mathbf{f}_p \quad \text{where} \quad \mathbb{S}^+ := \mathbf{m}_g^{-1} \mathbb{S}^T \mathbf{m}_p \quad (1.38)$$

where \mathbf{m}_g is a $N_g \times N_g$ diagonal matrix that is invertible as long as $m_g \neq 0$, \mathbf{m}_p is a $N_p \times N_p$ diagonal matrix, and \mathbb{S} is a $N_p \times N_g$ matrix.

On the other hand, if $w(\mathbf{x}) = 1$, we have

$$A_g = \int_{\Omega} S_g(\mathbf{x}) d\Omega = V_g, \quad B_{gp} = \int_{\Omega} S_g(\mathbf{x}) \chi_p(\mathbf{x}) d\Omega \quad (1.39)$$

and

$$V_g \mathbf{f}_g = \sum_p \mathbf{f}_p \int_{\Omega} S_g(x) \chi_p(\mathbf{x}) d\Omega = \sum_p \mathbf{f}_p V_p \bar{S}_{gp}. \quad (1.40)$$

where V_g is the grid node volume and V_p is the particle volume. In matrix form equation (1.40) can be written as

$$\mathbf{f}_g = \mathbb{S}_V^+ \mathbf{f}_p \quad \text{where} \quad \mathbb{S}_V^+ := \mathbf{V}_g^{-1} \mathbb{S}^T \mathbf{V}_p \quad (1.41)$$

where \mathbf{V}_g is a $N_g \times N_g$ diagonal matrix that is invertible as long as $V_g \neq 0$, and \mathbf{V}_p is a $N_p \times N_p$ diagonal matrix.

In traditional **MPM**, the velocity (\mathbf{v}) is projected using mass weighting as per (1.37), i.e.,

$$m_g \mathbf{v}_g = \sum_p m_p \mathbf{v}_p \bar{S}_{gp} \quad \text{or} \quad \mathbf{v}_g = \mathbb{S}^+ \mathbf{v}_p. \quad (1.42)$$

This implies that the mass density (ρ) and the momentum *per unit volume* ($\mathbf{P} = \rho \mathbf{v}$) are projected to grid nodes using the volume-weighted approach in (1.40):

$$\begin{aligned} V_g \rho_g &= \sum_p V_p \rho_p \bar{S}_{gp} \quad \text{or} \quad \mathbf{m}_g = \mathbb{S}^T \mathbf{m}_p \\ V_g \mathbf{P}_g &= \sum_p V_p \mathbf{P}_p \bar{S}_{gp} \quad \text{or} \quad \mathbf{p}_g = \mathbb{S}^T \mathbf{p}_p \end{aligned} \quad (1.43)$$

where \mathbf{p} is a matrix of *total* momentum. Further details of the actual projection operators used in VAANGO are discussed next.

1.4 MPM discretization of the weak form

The weak form of the momentum equation is

$$\int_{\Gamma_t} \bar{\mathbf{t}} \cdot \mathbf{w} d\Gamma - \int_{\Omega} \boldsymbol{\sigma} : \nabla \mathbf{w} d\Omega + \int_{\Omega} \rho \mathbf{w} \cdot \mathbf{b} d\Omega = \int_{\Omega} \rho \mathbf{w} \cdot \dot{\mathbf{v}} d\Omega. \quad (1.44)$$

To discretize the weak form we can use either of the assumed description of field variables shown in (1.5). The grid node-based discretization is used in finite elements while **MPM** uses the particle-based discretization but also a grid-based approximation.

Recall from (1.5) and (1.26) that

$$\mathbf{f}(\mathbf{x}) = \sum_g \mathbf{f}_g S_g(\mathbf{x}) \quad \text{and} \quad \mathbf{f}_g = \sum_p \psi_{gp} \mathbf{f}_p, \quad \psi_{gp} = \frac{V_p \langle S_{gp} \rangle}{\sum_p V_p \langle S_{gp} \rangle}, \quad \sum_p \psi_{gp} = 1. \quad (1.45)$$

Therefore, we can write

$$\mathbf{f}(\mathbf{x}) = \sum_g \sum_p \psi_{gp} \mathbf{f}_p S_g(\mathbf{x}) = \sum_p \mathbf{f}_p \sum_g \psi_{gp} S_g(\mathbf{x}) = \sum_p \mathbf{f}_p Y_p(\mathbf{x}) \quad (1.46)$$

where the **particle basis functions**, Y_p , are defined as

$$Y_p(\mathbf{x}) := \sum_g \psi_{gp} S_g(\mathbf{x}) = \frac{V_p \sum_g \langle S_{gp} \rangle S_g(\mathbf{x})}{\sum_p V_p \langle S_{gp} \rangle} \quad (1.47)$$

If we compare (1.46) with the particle representation in (1.5):

$$\mathbf{f}(\mathbf{x}) = \sum_p \mathbf{f}_p \chi_p(\mathbf{x}) \quad (1.48)$$

we see that for the grid-based and particle-based representations to be both accurate representations of the field we need the χ_p and Y_p values to be related by

$$\int_{\Omega} w(\mathbf{x}) \chi_p(\mathbf{x}) = \int_{\Omega} w(\mathbf{x}) Y_p(\mathbf{x}) \quad (1.49)$$

because they cannot be point-wise identical unless the particle characteristic functions satisfy the Kronecker property exactly. We will use the Y_p **particle basis functions** to discretize the momentum equation.

The first step in the MPM discretization is to convert the integrals over Ω in (1.44) into a sum of integrals over particles using the particle basic functions, Y_p :

$$\begin{aligned} \int_{\Gamma_t} \bar{\mathbf{t}}(\mathbf{x}) \cdot \mathbf{w}(\mathbf{x}) d\Gamma - \sum_p \int_{\Omega_p} Y_p(\mathbf{x}) \boldsymbol{\sigma}_p : \nabla \mathbf{w} d\Omega + \sum_p \int_{\Omega_p} Y_p(\mathbf{x}) \rho_p \mathbf{w}(\mathbf{x}) \cdot \mathbf{b}_p d\Omega \\ = \sum_p \int_{\Omega_p} Y_p(\mathbf{x}) \rho_p \mathbf{w}(\mathbf{x}) \cdot \dot{\mathbf{v}}(\mathbf{x}) d\Omega. \end{aligned} \quad (1.50)$$

The weighting function, the velocity, and the material time derivative of \mathbf{v} are approximated as (see [2]):

$$\mathbf{w}(\mathbf{x}) = \sum_g \mathbf{w}_g S_g(\mathbf{x}), \quad \mathbf{v}(\mathbf{x}) = \sum_h \mathbf{v}_h S_h(\mathbf{x}), \quad \dot{\mathbf{v}}(\mathbf{x}) \approx \sum_h \dot{\mathbf{v}}_h S_h(\mathbf{x}). \quad (1.51)$$

Plugging these into the left hand side of (1.50) we get

$$\begin{aligned} \text{LHS} = \int_{\Gamma_t} \bar{\mathbf{t}}(\mathbf{x}) \cdot \left[\sum_g \mathbf{w}_g S_g(\mathbf{x}) \right] d\Gamma - \sum_p \int_{\Omega_p} Y_p(\mathbf{x}) \boldsymbol{\sigma}_p : \left[\sum_g \mathbf{w}_g \otimes \nabla S_g \right] d\Omega \\ + \sum_p \int_{\Omega_p} Y_p(\mathbf{x}) \rho_p \left[\sum_g \mathbf{w}_g S_g(\mathbf{x}) \right] \cdot \mathbf{b}_p d\Omega \end{aligned} \quad (1.52)$$

Rearranging,

$$\begin{aligned} \text{LHS} = \sum_g \mathbf{w}_g \cdot \left[\int_{\Gamma_t} \bar{\mathbf{t}}(\mathbf{x}) S_g(\mathbf{x}) d\Gamma - \sum_p \int_{\Omega_p} Y_p(\mathbf{x}) \boldsymbol{\sigma}_p \cdot \nabla S_g d\Omega \right. \\ \left. + \sum_p \int_{\Omega_p} \rho_p Y_p(\mathbf{x}) S_g(\mathbf{x}) \mathbf{b}_p d\Omega \right] \end{aligned} \quad (1.53)$$

Similarly, the right hand side of (1.50) can be written as

$$\text{RHS} = \sum_p \int_{\Omega_p} Y_p(\mathbf{x}) \rho_p \left[\sum_g \mathbf{w}_g S_g(\mathbf{x}) \right] \cdot \left[\sum_h \dot{\mathbf{v}}_h S_h(\mathbf{x}) \right] d\Omega. \quad (1.54)$$

Rearrangement leads to

$$\text{RHS} = \sum_g \mathbf{w}_g \cdot \sum_h \left[\sum_p \int_{\Omega_p} \rho_p Y_p(\mathbf{x}) S_g(\mathbf{x}) S_h(\mathbf{x}) \dot{\mathbf{v}}_h d\Omega \right]. \quad (1.55)$$

Combining the left and right hand sides and invoking the arbitrariness of \mathbf{w}_g , for N_g grid points we get equations for $g = 1, 2, \dots, N_g$:

$$\begin{aligned} \int_{\Gamma_t} \bar{\mathbf{t}}(\mathbf{x}) S_g(\mathbf{x}) d\Gamma - \sum_p \int_{\Omega_p} Y_p(\mathbf{x}) \boldsymbol{\sigma}_p \cdot \nabla S_g d\Omega + \sum_p \int_{\Omega_p} \rho_p Y_p(\mathbf{x}) S_g(\mathbf{x}) \mathbf{b}_p d\Omega \\ = \sum_h \left[\sum_p \int_{\Omega_p} \rho_p Y_p(\mathbf{x}) S_g(\mathbf{x}) S_h(\mathbf{x}) \dot{\mathbf{v}}_h d\Omega \right]. \end{aligned} \quad (1.56)$$

We can simplify the above equations further by taking the particle variables outside the integral by assuming they are constant over a particle domain:

$$\begin{aligned} \int_{\Gamma_t} \bar{\mathbf{t}}(\mathbf{x}) S_g(\mathbf{x}) d\Gamma - \sum_p \boldsymbol{\sigma}_p \cdot \left[\int_{\Omega_p} Y_p(\mathbf{x}) \nabla S_g d\Omega \right] + \sum_p \rho_p \mathbf{b}_p \left[\int_{\Omega_p} Y_p(\mathbf{x}) S_g(\mathbf{x}) d\Omega \right] \\ = \sum_h \sum_p \rho_p \left[\int_{\Omega_p} Y_p(\mathbf{x}) S_g(\mathbf{x}) S_h(\mathbf{x}) d\Omega \right] \dot{\mathbf{v}}_h. \end{aligned} \quad (1.57)$$

Recalling that Y_p has the same effect as χ_p when integrated over a particle volume, we can write

$$\langle S_{gp} \rangle := \frac{1}{V_p} \int_{\Omega_p} Y_p(\mathbf{x}) S_g(\mathbf{x}) d\Omega. \quad (1.58)$$

Then (1.57) can be expressed as

$$\begin{aligned} \int_{\Gamma_t} \bar{\mathbf{t}}(\mathbf{x}) S_g(\mathbf{x}) d\Gamma - \sum_p V_p \boldsymbol{\sigma}_p \cdot \langle \nabla S_{gp} \rangle + \sum_p V_p \rho_p \mathbf{b}_p \langle S_{gp} \rangle \\ = \sum_h \sum_p \rho_p \left[\int_{\Omega_p} Y_p(\mathbf{x}) S_g(\mathbf{x}) S_h(\mathbf{x}) d\Omega \right] \dot{\mathbf{v}}_h. \end{aligned} \quad (1.59)$$

Define the mass matrix (\mathbf{M}), the internal force vector ($\mathbf{f}_g^{\text{int}}$), the body force vector ($\mathbf{f}_g^{\text{body}}$), and the external force vector ($\mathbf{f}_g^{\text{ext}}$) at grid node g as

$$\begin{aligned} M_{gh} &:= \sum_p \rho_p \int_{\Omega_p} Y_p(\mathbf{x}) S_g(\mathbf{x}) S_h(\mathbf{x}) d\Omega \\ \mathbf{f}_g^{\text{int}} &:= \sum_p V_p \boldsymbol{\sigma}_p \cdot \langle \nabla S_{gp} \rangle \\ \mathbf{f}_g^{\text{body}} &:= \sum_p m_p \mathbf{b}_p \langle S_{gp} \rangle \\ \mathbf{f}_g^{\text{ext}} &:= \int_{\Gamma_t} \bar{\mathbf{t}}(\mathbf{x}) S_g(\mathbf{x}) d\Gamma. \end{aligned} \quad (1.60)$$

Then, from (1.59) we get the semi-discrete system of equations

$$\sum_h M_{gh} \dot{\mathbf{v}}_h = \mathbf{f}_g^{\text{ext}} - \mathbf{f}_g^{\text{int}} + \mathbf{f}_g^{\text{body}}; \quad g = 1 \dots N_g \quad (1.61)$$

The mass matrix is typically lumped such that

$$\begin{aligned} m_g = \sum_h M_{gh} = \sum_p \rho_p \int_{\Omega_p} Y_p(\mathbf{x}) S_g(\mathbf{x}) \left[\sum_h S_h(\mathbf{x}) \right] d\Omega = \sum_p \rho_p \int_{\Omega_p} Y_p(\mathbf{x}) S_g(\mathbf{x}) d\Omega \\ = \sum_p \rho_p V_p \langle S_{gp} \rangle = \sum_p m_p \langle S_{gp} \rangle. \end{aligned} \quad (1.62)$$

In that case the semi-discrete system of equations simplifies to

$$m_g \dot{\mathbf{v}}_g = \mathbf{f}_g^{\text{ext}} - \mathbf{f}_g^{\text{int}} + \mathbf{f}_g^{\text{body}} ; \quad g = 1 \dots N_g \quad (1.63)$$

The external force at grid nodes is more difficult to estimate and is typically computed from particle values using

$$\mathbf{f}_g^{\text{ext}} = \sum_p \mathbf{f}_p^{\text{ext}} \langle S_{gp} \rangle . \quad (1.64)$$

1.4.1 Damping

Two types of artificial damping are implemented in VAANGO . The first approach modifies the acceleration in (1.63) such that

$$m_g \dot{\mathbf{v}}_g = \mathbf{f}_g^{\text{ext}} - \mathbf{f}_g^{\text{int}} + \mathbf{f}_g^{\text{body}} - \alpha_d \mathbf{v}_g ; \quad g = 1 \dots N_g \quad (1.65)$$

where α_d is a damping coefficient.

The second approach uses Richtmyer-von Neumann artificial viscosity to damp out large oscillations in high strain-rate simulations. VAANGO uses a three-dimensional form of the Richtmyer-von Neumann artificial viscosity ([13, 14], p.29). The viscosity factor takes the form

$$q = C_0 \rho l \sqrt{\frac{K}{\rho}} |\text{tr} \mathbf{d}| + C_1 \rho l^2 (\text{tr} \mathbf{d})^2 \quad (1.66)$$

where C_0 and C_1 are constants, ρ is the mass density, K is the bulk modulus, \mathbf{d} is the rate of deformation tensor, and l is a characteristic length (usually the grid cell size). Typical values of the coefficients are $C_0 = 0.2$ and $C_1 = 2.0$.

The factor q is used to decrease the particle stress:

$$\boldsymbol{\sigma}_p = \boldsymbol{\sigma}_p - q \mathbf{I} \quad (1.67)$$

before it is projected to grid nodes for internal force calculations.

1.5 Algorithm Description

The interested reader should consult [1, 2] for the development of the discrete equations in MPM discussed in this section, and [7] for the development of the equations for the GIMP method. These end up being very similar, the differences in how the two developments affect implementation will be described in Section 1.6.

In solving a structural mechanics problem with MPM , one begins by discretizing the object of interest into a suitable number of particles, or “material points”.

What constitutes a suitable number is something of an open question, but it is typically advisable to use at least two particles in each computational cell in each direction, i.e. 4 particles per cell (PPC) in 2-D, 8 PPC in 3-D.

In choosing the resolution of the computational grid, similar considerations apply as for any computational method (trade-off between time to solution and accuracy, use of resolution studies to ensure convergence in results, etc.). Each of these particles will carry, minimally, the following variables:

- position - \mathbf{x}_p
- mass - m_p
- volume - V_p

- velocity - \mathbf{v}_p
- stress - $\boldsymbol{\sigma}_p$
- deformation gradient - \mathbf{F}_p

The description that follows is a recipe for advancing each of these variables from the current (discrete) time t_n to the subsequent time t_{n+1} . Note that particle mass, m_p , typically remains constant throughout a simulation unless solid phase reaction models are utilized, a feature that is not present in VAANGO MPM . (Such models are available in MPMICE , see Section ??.) It is also important to point out that the algorithm for advancing the timestep is based on the so-called Update Stress Last (USL) algorithm.

The superiority of this approach over the Update Stress First (USF) approach was clearly demonstrated by Wallstedt and Guilkey [15]. USF was the formulation used in Uintah until mid-2008.

The discrete momentum equation that results from the weak form is given as:

$$\mathbf{M}\mathbf{a} = \mathbf{f}^{\text{ext}} - \mathbf{f}^{\text{int}} + \mathbf{f}^{\text{body}} \quad (1.68)$$

where \mathbf{M} is the mass matrix, \mathbf{a} is the acceleration vector, \mathbf{f}^{ext} is the external force vector (sum of the body forces and tractions), and \mathbf{f}^{int} is the internal force vector resulting from the divergence of the material stresses. The construction of each of these quantities, which are based at the nodes of the computational grid, will be described below.

The solution begins by projecting the particle state to the nodes of the computational grid, to form the mass matrix \mathbf{M} and to find the nodal external forces \mathbf{f}^{ext} , and velocities, \mathbf{v} . In practice, a lumped mass matrix is used to avoid the need to invert a system of equations to solve Eq. (1.68) for acceleration. These quantities are calculated at individual nodes by the following equations, where the \sum_p represents a summation over all particles:

$$m_g = \sum_p m_p \bar{S}_{gp}, \quad \mathbf{v}_g = \frac{\sum_p m_p \mathbf{v}_p \bar{S}_{gp}}{m_g}, \quad \mathbf{f}_g^{\text{ext}} = \sum_p \mathbf{f}_p^{\text{ext}} \bar{S}_{gp} \quad (1.69)$$

and g refers to individual nodes of the grid, m_p is the particle mass, \mathbf{v}_p is the particle velocity, and $\mathbf{f}_p^{\text{ext}}$ is the external force on the particle. The external forces that start on the particles typically the result of tractions, the application of which is discussed in the VAANGO User manual. $\bar{S}_{gp} = \langle S_{gp} \rangle$ is the shape function of the g -th node evaluated at the particle p as discussed in the section 1.3 equation (1.23). The functional form of the shape functions differs between MPM , GIMP , and CPDI . Further details of the difference are given in Section 1.6.

Following the operations in Eq. 1.69, \mathbf{f}^{int} is still required in order to solve for acceleration at the nodes. This is computed at the nodes as a volume integral of the divergence of the stress on the particles, specifically:

$$\mathbf{f}_g^{\text{int}} = \sum_p V_p \boldsymbol{\sigma}_p \bar{\mathbf{G}}_{gp} \quad (1.70)$$

where $\bar{\mathbf{G}}_{gp}$ is the gradient of the shape function of the g -th node evaluated at the particle p , and $\boldsymbol{\sigma}_p$ and V_p are the time t_n values of particle stress and volume respectively.

Equation (1.68) can then be solved for \mathbf{a} .

$$\mathbf{a}_g = \frac{\mathbf{f}_g^{\text{ext}} - \mathbf{f}_g^{\text{int}} + \mathbf{f}_g^{\text{body}}}{m_g} \quad (1.71)$$

In the explicit version of MPM implemented in VAANGO , a forward Euler method is used for the time integration:

$$\mathbf{v}_g^L = \mathbf{v}_g + \mathbf{a}_g \Delta t \quad \text{where} \quad \Delta t = t_{n+1} - t_n. \quad (1.72)$$

The time advanced grid velocity, \mathbf{v}_g^L is used to compute a velocity gradient at each particle according to:

$$\nabla \mathbf{v}_p = \sum_g \mathbf{v}_g^L \bar{\mathbf{G}}_{gp}. \quad (1.73)$$

This velocity gradient is used to update the particle's deformation gradient, volume and stress. First, an incremental deformation gradient is computed using the velocity gradient:

$$\Delta \mathbf{F}_p^{n+1} = (\mathbf{I} + \nabla \mathbf{v}_p \Delta t) \quad (1.74)$$

Particle volume and deformation gradient are updated by:

$$V_p^{n+1} = \det(\Delta \mathbf{F}_p^{n+1}) V_p^n, \quad \mathbf{F}_p^{n+1} = \Delta \mathbf{F}_p^{n+1} \cdot \mathbf{F}_p^n. \quad (1.75)$$

Finally, the velocity gradient, and/or the deformation gradient are provided to a constitutive model, which outputs a time advanced stress at the particles.

At this point in the timestep, the particle position and velocity are explicitly updated by:

$$\begin{aligned} \mathbf{v}_p(t + \Delta t) &= \mathbf{v}_p(t) + \sum_g \bar{S}_{gp} \mathbf{a}_g \Delta t \\ \mathbf{x}_p(t + \Delta t) &= \mathbf{x}_p(t) + \sum_g \bar{S}_{gp} \mathbf{v}_g^L \Delta t \end{aligned} \quad (1.76)$$

This completes one timestep, in that the update of all six of the variables enumerated above (with the exception of mass, which is assumed to remain constant) has been accomplished. Conceptually, one can imagine that, since an acceleration and velocity were computed at the grid, and an interval of time has passed, the grid nodes also experienced a displacement. This displacement also moved the particles in an isoparametric fashion. In practice, particle motion is accomplished by Equation 1.76, and the grid never deforms. So, while the **MPM** literature will often refer to resetting the grid to its original configuration, in fact, this isn't necessary as the grid nodes never leave that configuration. Regardless, at this point, one is ready to advance to the next timestep.

The algorithm described above is the core of the VAANGO **MPM** implementation. However, it neglects a number of important considerations. The first is kinematic boundary conditions on the grid for velocity and acceleration. Next, is the use of advanced contact algorithms. By default, **MPM** enforces no-slip, no-interpenetration contact. This feature is extremely useful, but it also means that two bodies initially in "contact" (meaning that they both contain particles whose data are accumulated to common nodes) behave as if they are a single body. To enable multi-field simulations with frictional contact, or to impose displacement based boundary conditions, e.g. a rigid piston, additional steps must be taken. These steps implement contact formulations such as that described by Bardenhagen, et al.[16]. The use of the contact algorithms is described briefly in this manual, but the reader will be referred to the relevant literature for their development. Lastly, heat conduction is also available in the explicit **MPM** code, although it may be neglected via a run time option in the input file. Explicit **MPM** is typically used for high-rate simulations in which heat conduction is negligible.

1.5.1 Deformation gradient computation

The deformation gradient computation involves the solution of a first-order differential equation:

$$\dot{\mathbf{F}} = \mathbf{I} \cdot \mathbf{F} = \nabla \mathbf{v} \cdot \mathbf{F} \quad (1.77)$$

which, for constant \mathbf{I} and initial condition $\mathbf{F} = \mathbf{F}_0$, has the exact solution

$$\mathbf{F}(t) = \exp(t \mathbf{I}) \cdot \mathbf{F}_0 = \exp(t \nabla \mathbf{v}) \cdot \mathbf{F}_0. \quad (1.78)$$

Expanded in series form, and considering only the time step Δt with initial condition $\mathbf{F} = \mathbf{F}_p^n$, we have

$$\mathbf{F}_p(t) = \left[\mathbf{I} + \Delta t \nabla \mathbf{v}_p + \frac{1}{2!} (\Delta t \nabla \mathbf{v}_p)^2 + \frac{1}{3!} (\Delta t \nabla \mathbf{v}_p)^3 + \dots \right] \cdot \mathbf{F}_p^n. \quad (1.79)$$

The approach in (1.74) is a first-order approximation of the Taylor series expansion for the deformation gradient:

$$\mathbf{F}_p^{n+1} = (\mathbf{I} + \nabla \mathbf{v}_p \Delta t) \mathbf{F}_p^n. \quad (1.80)$$

This is the most commonly used method of computing the deformation gradient. VAANGO also allows for an alternative estimate of the deformation gradient by subcycling after dividing Δt into k smaller increments:

$$\mathbf{F}_p^{n+1} = \left[\prod_k (\mathbf{I} + \nabla \mathbf{v}_p \Delta t_k) \right] \mathbf{F}_p^n. \quad (1.81)$$

Alternatively, multiple terms of the expansion in (1.79) can be evaluated by choosing an appropriate flag in the input file.

Finally, VAANGO also provides an option to compute the matrix exponential using the [Cayley-Hamilton theorem](#). However, all these approaches assume that the velocity gradient remains constant over a time step.

Pressure stabilization

A pressure stabilization step may be required during the computation of deformation gradients of materials that are nearly incompressible. The algorithm involves computing the particle volumes inside each grid cell (ignoring volume that may extend outside cell boundaries):

$$V_{co} = \sum_{p \in c} \frac{m_p}{\rho_o}, \quad V_c = \sum_{p \in c} V_p \quad (1.82)$$

where V_{co} is an estimate of the initial volume in a cell and V_c is the current volume in the cell. The initial density is ρ_o . An estimate of the volume change is computed using

$$J_c = \frac{V_c}{V_{co}}. \quad (1.83)$$

A correction is applied to the particle deformation gradient using

$$\mathbf{F}_p \leftarrow \left(\frac{J_c}{\det(\mathbf{F}_p)} \right)^{1/3} \mathbf{F}_p. \quad (1.84)$$

1.6 Shape functions for MPM, GIMP, and CPDI

In both [MPM](#) and [GIMP](#), the basic idea is the same: objects are discretized into particles, or material points, each of which contains all state data for the small region of material that it represents. In [MPM](#), these particles are spatially Dirac delta functions, meaning that the material that each represents is assumed to exist at a single point in space, namely the position of the particle. Interactions between the particles and the grid take place using weighting functions, also known as shape functions or interpolation functions. These are typically, but not necessarily, linear, bilinear or trilinear in one, two and three dimensions, respectively.

Bardenhagen and Kober [7] generalized the development that gives rise to [MPM](#), and suggested that [MPM](#) may be thought of as a subset of their “Generalized Interpolation Material Point” ([GIMP](#)) method.

As discussed in Section 1.3, in the family of **GIMP** methods one chooses a characteristic function χ_p to represent the particles and a shape function S_g as a basis of support on the computational nodes. An effective shape function \bar{S}_{gp} is found by the convolution of χ_p and S_g which is written as:

$$\bar{S}_{gp}(\mathbf{x}_p) = \frac{1}{V_p} \int_{\Omega_p \cap \Omega} \chi_p(\mathbf{x} - \mathbf{x}_p) S_g(\mathbf{x}) d\mathbf{x}. \quad (1.85)$$

While the user has significant latitude in choosing these two functions, in practice, the choice of S_g is usually given (in one-dimension) as,

$$S_g(x) = \begin{cases} 1 + (x - x_g)/h & -h < x - x_g \leq 0 \\ 1 - (x - x_g)/h & 0 < x - x_g \leq h \\ 0 & \text{otherwise,} \end{cases} \quad (1.86)$$

where x_g is the vertex location, and h is the cell width, assumed to be constant in this formulation, although this is not a general restriction on the method. Multi-dimensional versions are constructed by forming tensor products of the one-dimensional version in the orthogonal directions. In three dimensions,

$$S_g^\alpha(r, s, t) = \frac{1}{8} (1 + r r_\alpha) (1 + s s_\alpha) (1 + t t_\alpha) \quad (1.87)$$

and $r, s, t \in [-1, 1]$ are the natural coordinates of the support domain. A plot of the basis function in two-dimensions is shown in Figure 1.1.

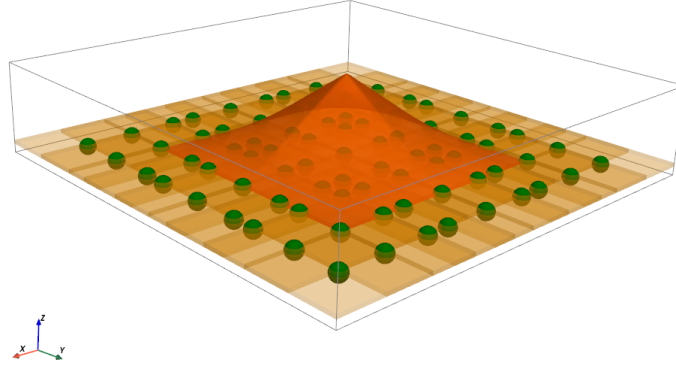


Figure 1.1: Linear grid node shape functions for 2D traditional **MPM**.

1.6.1 MPM

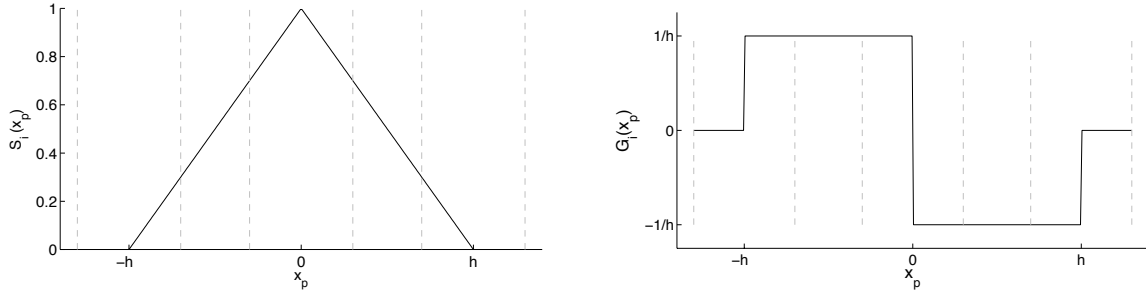
When the choice of characteristic function is the Dirac delta,

$$\chi_p(\mathbf{x}) = \delta(\mathbf{x} - \mathbf{x}_p) V_p, \quad (1.88)$$

where \mathbf{x}_p is the particle position, and V_p is the particle volume, then traditional **MPM** is recovered. In that case, the effective shape function is still that given by Equation (1.86). Its gradient is given by:

$$G_g(x) = \begin{cases} 1/h & -h < x - x_g \leq 0 \\ -1/h & 0 < x - x_g \leq h \\ 0 & \text{otherwise,} \end{cases} \quad (1.89)$$

Plots of Equations 1.86 and 1.89 are shown below. The discontinuity in the gradient gives rise to poor accuracy and stability properties.



(a) Effective shape function when using traditional MPM . (b) Gradient of the effective shape function when using traditional MPM .

1.6.2 GIMP

Typically, when an analyst indicates that they are “using GIMP ” this implies use of the linear grid basis function given in Eq. 1.86 and a “top-hat” characteristic function, given by (in one-dimension),

$$\chi_p(x) = H(x - (x_p - l_p)) - H(x - (x_p + l_p)), \quad (1.90)$$

where $H(x)$ is the Heaviside function ($H(x) = 0$ if $x < 0$ and $H(x) = 1$ if $x \geq 0$) and l_p is the half-length of the particle. When the convolution indicated in Eq. 1.85 is carried out using the expressions in Eqns. 1.86 and 1.90, a closed form for the effective shape function can be written as:

$$\bar{S}_{gp}(x_p) = \begin{cases} \frac{(h+l_p+(x_p-x_g))^2}{4hl_p} & -h-l_p < x_p-x_g \leq -h+l_p \\ 1 + \frac{(x_p-x_g)}{h} & -h+l_p < x_p-x_g \leq -l_p \\ 1 - \frac{(x_p-x_g)^2+l_p^2}{2hl_p} & -l_p < x_p-x_g \leq l_p \\ 1 - \frac{(x_p-x_g)}{h} & l_p < x_p-x_g \leq h-l_p \\ \frac{(h+l_p-(x_p-x_g))^2}{4hl_p} & h-l_p < x_p-x_g \leq h+l_p \\ 0 & \text{otherwise,} \end{cases} \quad (1.91)$$

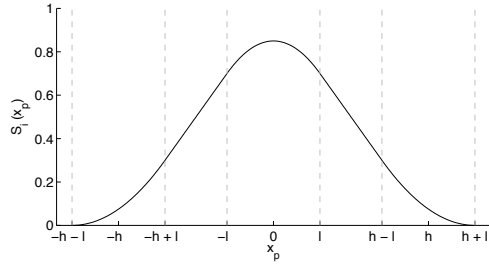
The gradient of which is:

$$\bar{G}_{gp}(x_p) = \begin{cases} \frac{h+l_p+(x_p-x_g)}{2hl_p} & -h-l_p < x_p-x_g \leq -h+l_p \\ \frac{1}{h} & -h+l_p < x_p-x_g \leq -l_p \\ -\frac{(x_p-x_g)}{hl_p} & -l_p < x_p-x_g \leq l_p \\ -\frac{1}{h} & l_p < x_p-x_g \leq h-l_p \\ -\frac{h+l_p-(x_p-x_g)}{2hl_p} & h-l_p < x_p-x_g \leq h+l_p \\ 0 & \text{otherwise,} \end{cases} \quad (1.92)$$

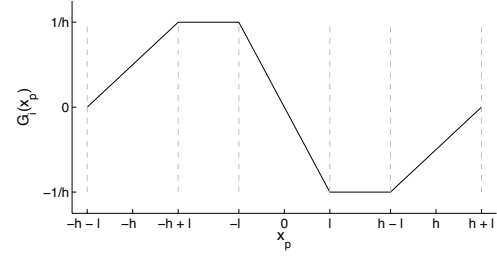
Plots of Equations 1.91 and 1.92 are shown in Figure 1.3. The continuous nature of the gradients are largely responsible for the improved robustness and accuracy of GIMP over MPM .

1.6.3 UGIMP and cpGIMP

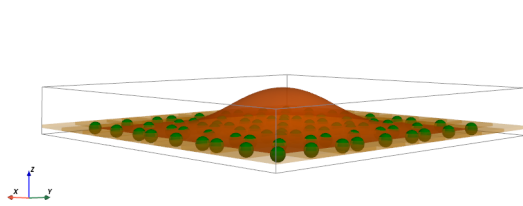
The GIMP effective shape functions in (1.91) are valid only for particle sizes that are smaller than the grid spacing. In Figure 1.4 we see that discontinuities appear in the effective shape function for particles for which $l_p > 0.5h$.



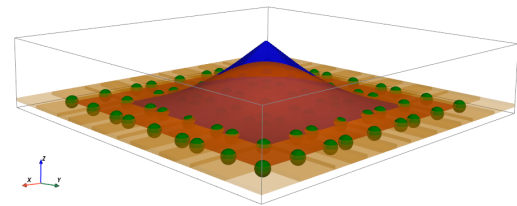
(a) One-dimensional shape function.



(b) Gradient of the one-dimensional shape function.

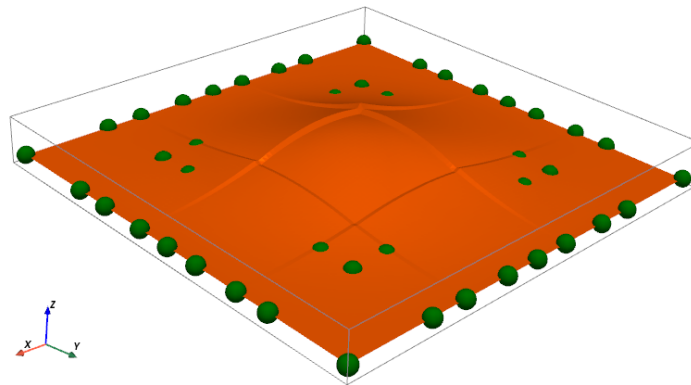


(c) Two-dimensional shape function.



(d) Two-dimensional GIMP compared to MPM (blue).

Figure 1.3: GIMP effective shape functions and their gradients.

Figure 1.4: Two-dimensional GIMP effective shape functions (\bar{S}_{gp}) for $l_p = 0.7h$.

There is one further consideration in defining the effective shape function, and that is whether or not the size (length in 1-D) of the particle is kept fixed (denoted as **UGIMP** here) or is allowed to evolve due to material deformations (“Finite GIMP” or “Contiguous GIMP” and **cpGIMP** here). In one-dimensional simulations, evolution of the particle (half-)length is straightforward,

$$l_p^n = \mathbf{F}_p^n l_p^0, \quad (1.93)$$

where \mathbf{F}_p^n is the deformation gradient at time n . A similar approach is used in **CPDI**.

In multi-dimensional simulations, a similar approach can be used, assuming an initially rectangular or cuboid particle, to find the current particle shape. The difficulty arises in evaluating Eq. (1.85) for these general shapes. One approach, apparently effective, has been to create a cuboid that circumscribes the deformed particle shape [17]. Alternatively, one can assume that the particle size remains constant (insofar as it applies to the effective shape function evaluations only).

1.6.4 CPDI

The **CPDI** formulation [8] is a more recent method for calculating the quantities

$$\langle S_{gp} \rangle = \frac{1}{V_p} \int_{\Omega_p} Y_p(\mathbf{x}) \tilde{S}_g(\mathbf{x}) d\Omega \quad \text{and} \quad \langle \nabla S_{gp} \rangle = \frac{1}{V_p} \int_{\Omega_p} Y_p(\mathbf{x}) \nabla \tilde{S}_g(\mathbf{x}) d\Omega \quad (1.94)$$

where Y_p are the particle basis functions and \tilde{S}_g are approximate grid basis functions. Figure 1.5 shows examples of two-dimensional grid and particle basis functions that are used in **CPDI**.

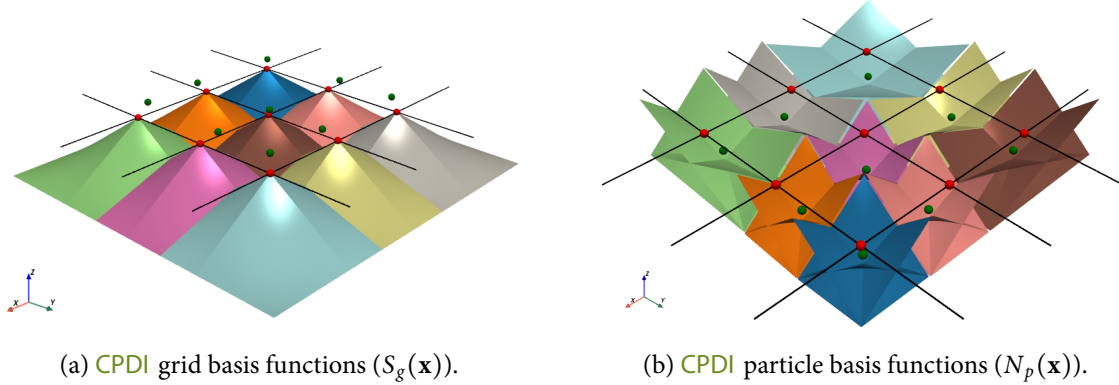


Figure 1.5: Two-dimensional **CPDI** grid and particle basis functions.

In the reference state, the domain Ω_{p0} for particle p is assumed to be a parallelepiped spanned by the three vectors \mathbf{r}_p^{io} , $i = 1, 2, 3$ with origin at the centroid. In the deformed state, these vectors become $\mathbf{r}_p^i = \mathbf{F}_p \cdot \mathbf{r}_p^{io}$ where \mathbf{F}_p is the deformation gradient. The corners of the deformed parallelepiped are used in CPDI to create the grid basis functions:

$$\tilde{S}_g(\mathbf{x}) = \sum_{\alpha=1}^8 N_p^\alpha(\mathbf{x}) S_g(\mathbf{x}_p^\alpha) \quad \text{on } \Omega_p \quad (1.95)$$

where α are the indices of the vertices of the particle parallelepiped,

$$N_p^\alpha(r, s, t) = \frac{1}{8} (1 + r r_\alpha) (1 + s s_\alpha) (1 + t t_\alpha) \quad (1.96)$$

and r, s, t the natural coordinates of the parallelepiped that range from -1 to 1. The functions $S_g(\mathbf{x})$ are typically chosen to be the hat functions of classical MPM. Figure 1.6 shows the particle domains and the effective grid shape functions produced by the **CPDI** relation in (1.95).

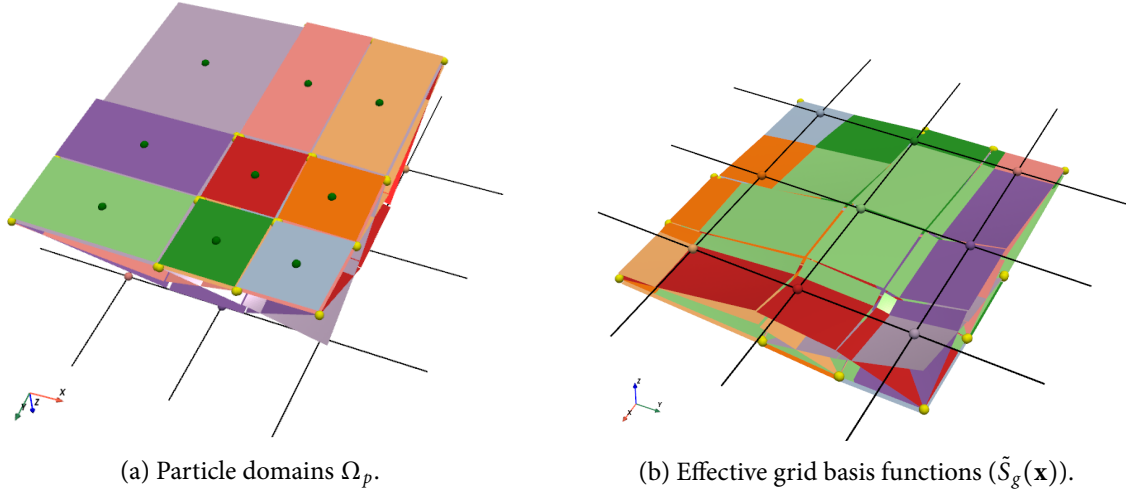


Figure 1.6: Two-dimensional CPDI particle domains and effective grid basis functions.

We can compute the quantities in (1.94) as follows.

Let

$$\mathbf{s}_p^o = [\mathbf{r}_p^{1o} \quad \mathbf{r}_p^{2o} \quad \mathbf{r}_p^{3o}] \quad \text{and} \quad \mathbf{s}_p = [\mathbf{r}_p^1 \quad \mathbf{r}_p^2 \quad \mathbf{r}_p^3] \quad \text{and} \quad \mathbf{F}_p = \begin{bmatrix} F_{11} & F_{12} & F_{13} \\ F_{21} & F_{22} & F_{23} \\ F_{31} & F_{32} & F_{33} \end{bmatrix}. \quad (1.97)$$

Then $\mathbf{s}_p = \mathbf{F}_p \mathbf{s}_p^o$. Let

$$\mathbf{S}_{gp} = [S_g(\mathbf{x}_p^1) \quad S_g(\mathbf{x}_p^2) \quad S_g(\mathbf{x}_p^3) \quad S_g(\mathbf{x}_p^4) \quad S_g(\mathbf{x}_p^5) \quad S_g(\mathbf{x}_p^6) \quad S_g(\mathbf{x}_p^7) \quad S_g(\mathbf{x}_p^8)]. \quad (1.98)$$

Also, let

$$\mathbf{R} = \begin{bmatrix} -1 & 1 & 1 & -1 & -1 & 1 & 1 & -1 \\ -1 & -1 & 1 & 1 & -1 & -1 & 1 & 1 \\ -1 & -1 & -1 & -1 & 1 & 1 & 1 & 1 \end{bmatrix} \quad (1.99)$$

Then,

$$\bar{S}_{gp} = \langle S_{gp} \rangle = \text{mean}(\mathbf{S}_{gp}) \quad \text{and} \quad \bar{\mathbf{G}}_{gp} = \langle \nabla S_{gp} \rangle = \frac{1}{8} \mathbf{s}_p^{-T} \mathbf{R}^T \mathbf{S}_{gp}^T. \quad (1.100)$$

1.7 Contact algorithms

The default behavior of MPM is to handle interactions between objects using velocities on the background grid. However, beyond some simple situations, contact requires the application of contact laws. In the VAANGO implementation of friction contact, Coulomb friction is assumed. Alternative types of contact, such as adhesive contact, could also be implemented by changing the contact law.

The purpose of the various contact algorithms in VAANGO is to correct the grid velocities such that a particular set of contact assumptions are satisfied. Many of these algorithms require the computation of surface normals.

1.7.1 Definitions

Let $m_p, \mathbf{v}_p, \mathbf{p}_p$ be the mass, velocity, and momentum of particle p . Also, let $m_g, \mathbf{v}_g, \mathbf{p}_g$ be the mass, velocity, and momentum at a grid point g due to nearby particles in the region of influence. Consider N_α objects

that can potentially be in contact and index then by the superscript α . Then, from (1.43), we have

$$\mathbf{m}_g^\alpha = V_g^\alpha \rho_g^\alpha = \sum_p V_p^\alpha \rho_p^\alpha \bar{S}_{gp} = \sum_p m_p^\alpha \bar{S}_{gp} \quad \text{and} \quad \mathbf{p}_g^\alpha = \sum_p \mathbf{p}_p^\alpha \bar{S}_{gp}. \quad (1.101)$$

In matrix notation,

$$\mathbf{m}_g^\alpha = \mathbb{S}^T \mathbf{m}_p^\alpha \quad \text{and} \quad \mathbf{p}_g^\alpha = \mathbb{S}^T \mathbf{p}_p^\alpha. \quad (1.102)$$

Similarly, from (1.42), we have

$$m_g^\alpha \mathbf{v}_g^\alpha = \sum_p m_p^\alpha \mathbf{v}_p^\alpha \bar{S}_{gp} \implies \mathbf{v}_g^\alpha = \frac{1}{m_g^\alpha} \sum_p m_p^\alpha \mathbf{v}_p^\alpha \bar{S}_{gp}. \quad (1.103)$$

In matrix form,

$$\mathbf{v}_g^\alpha = \mathbb{S}_\alpha^+ \mathbf{v}_p^\alpha \quad \text{where} \quad \mathbb{S}_\alpha^+ = (\mathbf{m}_g^\alpha)^{-1} \mathbb{S}^T \mathbf{m}_p^\alpha. \quad (1.104)$$

Based on a local conservation of momentum, we define a **center-of-mass velocity**, \mathbf{v}_g^{cm} , at grid node g for all the contacting objects:

$$\mathbf{v}_g^{\text{cm}} = \frac{\sum_\alpha m_g^\alpha \mathbf{v}_g^\alpha}{\sum_\alpha m_g^\alpha}. \quad (1.105)$$

We also define an **effective grid mass**, m_g^{eff} , as

$$\frac{1}{m_g^{\text{eff}}} = \sum_\alpha \frac{1}{m_g^\alpha}. \quad (1.106)$$

1.7.2 Computing surface normals and tractions

Surface normals are typically estimated from the gradient of mass at grid nodes. If m_p is the mass of particle p , then the normal at grid node g due to the particles in its region of influence is

$$\mathbf{n}_g = \sum_p m_p \nabla \bar{S}_{gp}. \quad (1.107)$$

Normals are converted to unit vectors before they are used in VAANGO computations.

Surface tractions at the nodes are computed by projecting particle stresses ($\boldsymbol{\sigma}_p$) to grid nodes:

$$\bar{\mathbf{t}}_g = \mathbf{n}_g \cdot \left(\sum_p \boldsymbol{\sigma}_p \bar{S}_{gp} \right). \quad (1.108)$$

1.7.3 Basic contact algorithm

The most basic contact algorithm in VAANGO is called “single-velocity contact”. The center-of-mass velocity is computed using (1.105). Upon contact detection, grid nodes that participate are assigned this velocity:

$$\mathbf{v}_g = \mathbf{v}_g^{\text{cm}}. \quad (1.109)$$

1.7.4 Contact with a specified master

A slightly more complex algorithm is the “master”-based contact which is called “specified-velocity contact” in VAANGO. In this model, a selected master material is assigned velocities, $\mathbf{v}_g^m = \mathbf{v}^m(t)$, where m is the index of the master material. The grid node velocities of the materials are then adjusted according to

$$\mathbf{v}_g \leftarrow \mathbf{v}_g - [\mathbf{n}_g^m \cdot (\mathbf{v}_g - \mathbf{v}_g^m)] \mathbf{n}_g^m \quad (1.110)$$

where \mathbf{n}_g^m is the normal for the master material computed using (1.107). This type of contact is useful for imposing boundary conditions on objects.

1.7.5 Frictional contact algorithms

The two main frictional contact algorithms are `friction_bard`, which is based on [16], and `friction_LR`, which is described in [12].

Bardenhagen et al. algorithm

In the algorithm developed in [16], a contact interface is defined as the set of nodes for which individual grid velocities associated with each object differ from the center of mass velocity:

$$\mathbf{v}_g^\alpha - \mathbf{v}_g^{\text{cm}} \neq \mathbf{0}. \quad (1.111)$$

Once this condition is identified, the surface normal \mathbf{n}_g^α is computed from the mass distribution around node g , and the surface normal traction \mathbf{t}_g^α is computed from the stresses in surrounding material points.

The contact condition is

$$(\mathbf{v}_g^\alpha - \mathbf{v}_g^{\text{cm}}) \cdot \mathbf{n}_g^\alpha > 0 \quad \text{and} \quad \mathbf{t}_g^\alpha \cdot \mathbf{n}_g^\alpha < 0. \quad (1.112)$$

This condition indicates compressive stress at node g . If this condition is not satisfied, the objects are assumed to have separated.

To enforce (1.112), the grid node velocities are adjusted such that momentum is conserved, i.e.,

$$\Delta(v_n)_g^\alpha = \Delta \mathbf{v}_g^\alpha \cdot \mathbf{n}_g^\alpha \quad \text{and} \quad \Delta(v_t)_g^\alpha = \Delta \mathbf{v}_g^\alpha \cdot \left[\mathbf{n}_g^\alpha \times \frac{\Delta \mathbf{v}_g^\alpha \times \mathbf{n}_g^\alpha}{\|\Delta \mathbf{v}_g^\alpha \times \mathbf{n}_g^\alpha\|} \right] \quad (1.113)$$

where

$$\Delta \mathbf{v}_g^\alpha := \mathbf{v}_g^\alpha - \mathbf{v}_g^{\text{cm}}. \quad (1.114)$$

Normal contact is enforced by adjusting material velocities by $\Delta(v_n)_g^\alpha$. The tangential contact is enforced using Coulomb friction with the tangential velocity determined using $\mu \Delta(v_n)_g^\alpha$ where μ is the friction coefficient. If $\Delta(v_t)_g^\alpha < \mu \Delta(v_n)_g^\alpha$, the no-slip condition is enforced. Otherwise, the tangential components of the nodal velocities are updated with a reduced friction coefficient

$$\mu_{\text{red}} = \min \left(\mu, \frac{|\Delta(v_t)_g^\alpha|}{|\Delta(v_n)_g^\alpha|} \right). \quad (1.115)$$

Returning to the problem of computing object outward normals at a grid point, the traditional approach is to compute volume gradients using the set of particles influencing a node:

$$\mathbf{g}_g^\alpha = \sum_{p^\alpha} \bar{\mathbf{G}}_{gp} V_p \quad (1.116)$$

where the gradients $\bar{\mathbf{G}}_{gp}$ are as defined in (1.29), (1.31), and (1.33). The normal to an object is calculated using

$$\mathbf{n}^\alpha = \frac{\mathbf{g}_g^\alpha}{\|\mathbf{g}_g^\alpha\|}. \quad (1.117)$$

For multiple objects, an average gradient can be computed for better accuracy.

Nairn et al. algorithm

The more recent algorithm by [12] uses a logistic regression step to determine contact. The underlying approach is similar to that used in [16]. Since the approach is at its simplest when only two objects are involved at a grid point, we will describe only that case below. Most situations with contact between multiple objects see [12].

Let the two objects be indexed by α and β . Let $\mathbf{p}_g^{\alpha o}$ and $\mathbf{p}_g^{\beta o}$ be the particle momenta projected to the grid. We would like to compute the momentum correction $\Delta \mathbf{p}$ so that momentum is conserved after contact. Let the corrected momenta be

$$\mathbf{p}_g^\alpha = \mathbf{p}_g^{\alpha o} + \Delta \mathbf{p} \quad \text{and} \quad \mathbf{p}_g^\beta = \mathbf{p}_g^{\beta o} - \Delta \mathbf{p}. \quad (1.118)$$

If we restrict relative motion between objects at a grid point to the tangent plane, and let $\hat{\mathbf{t}}$ be the direction of relative motion, then

$$\mathbf{v}_g^\beta - \mathbf{v}_g^\alpha = k \hat{\mathbf{t}} \implies \frac{\mathbf{p}_g^\beta}{m_g^\beta} - \frac{\mathbf{p}_g^\alpha}{m_g^\alpha} = k \hat{\mathbf{t}} \implies m_g^\alpha \mathbf{p}_g^\beta - m_g^\beta \mathbf{p}_g^\alpha = m_g^\alpha m_g^\beta k \hat{\mathbf{t}}. \quad (1.119)$$

From the definition of the center-of-mass velocity in (1.105) and the effective grid mass (1.106), we have

$$\mathbf{v}_g^{\text{cm}} = \frac{m_g^\alpha \mathbf{v}_g^\alpha + m_g^\beta \mathbf{v}_g^\beta}{m_g^\alpha + m_g^\beta} = \frac{\mathbf{p}_g^\alpha + \mathbf{p}_g^\beta}{m_g^\alpha + m_g^\beta} \quad \text{and} \quad m_g^{\text{eff}} = \frac{m_g^\alpha m_g^\beta}{m_g^\alpha + m_g^\beta}. \quad (1.120)$$

Therefore,

$$\mathbf{p}_g^\alpha + \mathbf{p}_g^\beta = \frac{\mathbf{v}_g^{\text{cm}} m_g^\alpha m_g^\beta}{m_g^{\text{eff}}}. \quad (1.121)$$

Solving for $\mathbf{p}_g^\alpha, \mathbf{p}_g^\beta$ from equations (1.119) and (1.121), we have

$$\mathbf{p}_g^\alpha = m_g^\alpha \mathbf{v}_g^{\text{cm}} - m_g^{\text{eff}} k \hat{\mathbf{t}} \quad \text{and} \quad \mathbf{p}_g^\beta = m_g^\beta \mathbf{v}_g^{\text{cm}} + m_g^{\text{eff}} k \hat{\mathbf{t}}. \quad (1.122)$$

Therefore, from (1.118),

$$\Delta \mathbf{p} = \mathbf{p}_g^\alpha - \mathbf{p}_g^{\alpha o} = m_g^\alpha \mathbf{v}_g^{\text{cm}} - m_g^{\text{eff}} k \hat{\mathbf{t}} - m_g^\alpha \mathbf{v}_g^{\alpha o} = m_g^\alpha (\mathbf{v}_g^{\text{cm}} - \mathbf{v}_g^{\alpha o}) - m_g^{\text{eff}} k \hat{\mathbf{t}}. \quad (1.123)$$

The quantity

$$\Delta \mathbf{p}^o := m_g^\alpha (\mathbf{v}_g^{\text{cm}} - \mathbf{v}_g^{\alpha o}) \quad (1.124)$$

is the initial change of momentum before tangential correction. Since the contact force (\mathbf{f}^c) is given by the rate of change of momentum due to contact, we have

$$\mathbf{f}^{\text{co}} = \frac{\Delta \mathbf{p}^o}{\Delta t} \quad \text{and} \quad \mathbf{f}^c = \frac{\Delta \mathbf{p}}{\Delta t} = \mathbf{f}^{\text{co}} - \frac{m_g^{\text{eff}} k \hat{\mathbf{t}}}{\Delta t}. \quad (1.125)$$

where Δt is the timestep size. The contact compressive traction is found from the normal component of the contact force needed to prevent interpenetration:

$$T_n^c = -\frac{1}{A^c} \mathbf{f}^{\text{co}} \cdot \mathbf{n} \quad (1.126)$$

where A^c is the contact area. The tangential contact traction can be found using a contact law:

$$T_t^c = \frac{1}{A^c} \mathbf{f}^c \cdot \hat{\mathbf{t}} = \frac{1}{A^c} \left[\mathbf{f}^{\text{co}} \cdot \hat{\mathbf{t}} - \frac{m_g^{\text{eff}} k}{\Delta t} \right]. \quad (1.127)$$

Therefore, if $T_t^c = T_t^c(T_n^c)$ is a contact law,

$$k = \frac{\Delta t}{m_g^{\text{eff}}} [\mathbf{f}^{\text{co}} \cdot \hat{\mathbf{t}} - A^c T_t^c(T_n^c)] . \quad (1.128)$$

We can compute k using the contact law $T_t^c(T_n^c)$ and then adjust \mathbf{v}_g^α and \mathbf{v}_g^β using (1.118). Note that this process is identical to that used in the Bardenhagen et al. algorithm. The main difficulty is in finding where contact has occurred and the quantities \mathbf{n} , $\hat{\mathbf{t}}$, and A^c .

The basic contact identification condition used in this approach, and in the Bardenhagen et al. approach, is

$$(\mathbf{v}_g^\beta - \mathbf{v}_g^\alpha) \cdot \frac{\mathbf{g}_g^\alpha - \mathbf{g}_g^\beta}{\|\mathbf{g}_g^\alpha - \mathbf{g}_g^\beta\|} < 0 \quad \text{and} \quad T_n^c > 0 \quad (1.129)$$

where \mathbf{g}_g is the volume gradient defined in (1.116). This condition is a variation of (1.112) and is a necessary, but not sufficient, condition to detect whether the two objects are approaching each other and in contact. However, $T_n^c > 0$ even when the objects are not touching and a separation condition is needed to correctly identify contact.

The logistic regression approach developed in [12] attempts to identify contact without having to rely purely on grid information. This approach requires a set of particles (point-cloud) in the neighborhood of a grid point that satisfies (1.129). The aim of this technique is to identify a plane within the point-cloud that best separates the two objects. The normal to this plane is the contact normal \mathbf{n}_g . The logistic function penalizes points as a function of their distance from a preferred separation plane.

The logistic regression method for separation detection is described next. Let \mathbf{x}_p be the homogeneous coordinate representation of a particle position, i.e., $\mathbf{X}_p = (\mathbf{x}_p, 1) =: (X_1, X_2, X_3, X_4)$, where $\mathbf{x}_p = (x_p^1, x_p^2, x_p^3)$ is the particle position. Let \mathbf{N} be the corresponding normal vector of the separation plane, i.e., $\mathbf{N} = (\mathbf{n}, N_4)$ where $\mathbf{n} = (n_1, n_2, n_3) =: (N_1, N_2, N_3)$ is the normal to the separation plane and n_4 is an offset. The equation of the desired separation plane is

$$\mathbf{X} \cdot \mathbf{N} = 0 \quad (1.130)$$

where \mathbf{X} is the vector of particle positions. Let there be P particles in the point-cloud consisting of points from objects α and β . Define a particle label c_p as:

$$c_p = \begin{cases} -1 & \text{for particles in object } \alpha \\ 1 & \text{for particles in object } \beta. \end{cases} \quad (1.131)$$

The objective function that has to be minimized is the error

$$E = \sum_{p=1}^P w_p [\mathcal{L}(\mathbf{X}_p, \mathbf{N}) - c_p]^2 + \sum_{j=1}^4 \lambda_j^2 N_j^2 \quad (1.132)$$

where w_p are weights, λ_j^2 are penalty factors that help regularize the error function and \mathcal{L} is the logistic function given by

$$\mathcal{L}(\mathbf{X}, \mathbf{N}) = \frac{2}{1 + \exp(-\mathbf{X} \cdot \mathbf{N})} - 1. \quad (1.133)$$

The minimum of E is achieved when $\frac{\partial E}{\partial \mathbf{N}} = 0$ and $\frac{\partial E}{\partial \lambda} = 0$. From the first requirement

$$\frac{\partial E}{\partial N_i} = 2 \sum_{p=1}^P w_p [\mathcal{L}(\mathbf{X}_p, \mathbf{N}) - c_p] \frac{\partial \mathcal{L}}{\partial N_i} + 2 \sum_{j=1}^4 \lambda_j^2 N_j \frac{\partial N_j}{\partial N_i} = 0 \quad (1.134)$$

where

$$\begin{aligned}\frac{\partial \mathcal{L}}{\partial N_i} &= 2 \frac{\partial}{\partial N_i} [1 + \exp(-X_m N_m)]^{-1} = -2 [1 + \exp(-X_m N_m)]^{-2} \frac{\partial}{\partial N_i} \exp(-X_m N_m) \\ &= 2 [1 + \exp(-X_m N_m)]^{-2} \exp(-X_m N_m) X_m \frac{\partial N_m}{\partial N_i} \\ &= 2 [1 + \exp(-X_m N_m)]^{-2} \exp(-X_m N_m) X_i.\end{aligned}\quad (1.135)$$

Define

$$\theta_p := -\mathbf{X}_p \cdot \mathbf{N} \quad \text{and} \quad \phi_p := 1 + \exp(\theta_p). \quad (1.136)$$

Then, in vector form,

$$\frac{\partial \mathcal{L}}{\partial \mathbf{N}} = \frac{2 \exp(\theta_p)}{\phi_p^2} \mathbf{X} \quad \text{and} \quad \mathcal{L}(\mathbf{X}_p, \mathbf{N}) = \frac{2}{\phi_p} - 1. \quad (1.137)$$

Returning to (1.134), we can write

$$\frac{\partial E}{\partial N_i} = 2 \sum_{p=1}^P w_p [\mathcal{L}(\mathbf{X}_p, \mathbf{N}) - c_p] \frac{\partial \mathcal{L}}{\partial N_i} + 2 \lambda_i^2 N_i = 0. \quad (1.138)$$

Similarly,

$$\frac{\partial E}{\partial \lambda_i} = 2 \sum_{j=1}^4 \lambda_j \frac{\partial \lambda_j}{\partial \lambda_i} N_j^2 = \lambda_i N_i^2 = 0 \quad (1.139)$$

Then, in vector form, the system of equations needed to solve for \mathbf{N} and $\boldsymbol{\lambda}$ is

$$\boxed{\begin{aligned} \sum_{p=1}^P w_p [\mathcal{L}(\mathbf{X}_p, \mathbf{N}) - c_p] \frac{\partial \mathcal{L}}{\partial \mathbf{N}} + (\boldsymbol{\lambda} \odot \boldsymbol{\lambda}) \odot \mathbf{N} &= \mathbf{0} \quad \text{and} \\ \boldsymbol{\lambda} \odot (\mathbf{N} \odot \mathbf{N}) &= \mathbf{0} \end{aligned}} \quad (1.140)$$

where

$$\mathbf{N} = (N_1, N_2, N_3, N_4), \quad \boldsymbol{\lambda} = (\lambda_1, \lambda_2, \lambda_3, \lambda_4), \quad \mathbf{a} \odot \mathbf{b} = (a_1 b_1, a_2 b_2, a_3 b_3, a_4 b_4). \quad (1.141)$$

The second set of equations in (1.140) suggest that the solution will improve as $\boldsymbol{\lambda} \rightarrow \mathbf{0}$. Given a vector $\boldsymbol{\lambda}$, the first equation in (1.140) can be solved for \mathbf{N} using Newton's method. Define

$$\mathbf{Y}(\mathbf{N}) := \sum_{p=1}^P w_p [\mathcal{L}(\mathbf{X}_p, \mathbf{N}) - c_p] \frac{\partial \mathcal{L}}{\partial \mathbf{N}} + (\boldsymbol{\lambda} \odot \boldsymbol{\lambda}) \odot \mathbf{N}. \quad (1.142)$$

Then, with \mathbf{I} denoting the 4×4 identity matrix,

$$\frac{\partial \mathbf{Y}}{\partial \mathbf{N}} = \sum_{p=1}^P w_p \left[\frac{\partial \mathcal{L}}{\partial \mathbf{N}} \otimes \frac{\partial \mathcal{L}}{\partial \mathbf{N}} + [\mathcal{L}(\mathbf{X}_p, \mathbf{N}) - c_p] \frac{\partial^2 \mathcal{L}}{\partial \mathbf{N}^2} \right] + (\boldsymbol{\lambda} \odot \boldsymbol{\lambda}) \mathbf{I}. \quad (1.143)$$

Then Newton's method gives the iterative rule

$$\mathbf{N}^{k+1} = \mathbf{N}^k - \left[\frac{\partial \mathbf{Y}}{\partial \mathbf{N}} \right]_{\mathbf{N}^k}^{-1} \cdot \mathbf{Y}(\mathbf{N}^k) \quad (1.144)$$

Given appropriate starting values, this method will converge to the solution except in situations where $\mathbf{X} \cdot \mathbf{N} < 0$. It is preferable to normalize \mathbf{N} in those situations where the exponential becomes too large.

Once the \mathbf{N} vector has been found, the unit normal to the separation plane is determined by normalizing $\mathbf{n} = (N_1, N_2, N_3)$. Contact occurs at particle p if

$$\min_{p \in \beta} (\mathbf{x}_p \cdot \frac{\mathbf{n}}{\|\mathbf{n}\|} - R_p) - \max_{p \in \alpha} (\mathbf{x}_p \cdot \frac{\mathbf{n}}{\|\mathbf{n}\|} + R_p) < 0 \quad (1.145)$$

where R_p is the distance from the centroid of particle p to its deformed edge along \mathbf{n} .

1.8 Implicit time integration

Recall from equation (1.61) that the MPM discretized momentum equations can be written as a semi-algebraic system

$$\sum_h M_{gh} \dot{\mathbf{v}}_h = \mathbf{f}_g^{\text{ext}} - \mathbf{f}_g^{\text{int}} + \mathbf{f}_g^{\text{body}} ; \quad g = 1 \dots N_g \quad (1.146)$$

where the mass matrix (\mathbf{M}), the internal force vector ($\mathbf{f}_g^{\text{int}}$), the body force vector ($\mathbf{f}_g^{\text{body}}$), and the external force vector ($\mathbf{f}_g^{\text{ext}}$) at grid node g as

$$\begin{aligned} M_{gh} &:= \sum_p \rho_p \int_{\Omega_p} Y_p(\mathbf{x}) S_g(\mathbf{x}) S_h(\mathbf{x}) d\Omega \\ \mathbf{f}_g^{\text{int}} &:= \sum_p V_p \boldsymbol{\sigma}_p \cdot \langle \nabla S_{gp} \rangle \\ \mathbf{f}_g^{\text{body}} &:= \sum_p m_p \mathbf{b}_p \langle S_{gp} \rangle \\ \mathbf{f}_g^{\text{ext}} &:= \int_{\Gamma_t} \bar{\mathbf{t}}(\mathbf{x}) S_g(\mathbf{x}) d\Gamma. \end{aligned} \quad (1.147)$$

While the MPM background grid is reset after each time increment, MPM does not require it to be reset during each iteration of an implicit integration process. Therefore, during a time step, we can carry a grid displacement variable \mathbf{u} that can be used to compute grid accelerations $\mathbf{a}_g = \dot{\mathbf{v}}_g$ and discarded at the end of a time step.

Let us express (1.146) in matrix form as

$$\mathbf{M}_g \mathbf{a}_g = \mathbf{f}_g^{\text{ext}} - \mathbf{f}_g^{\text{int}} + \mathbf{f}_g^{\text{body}} \quad (1.148)$$

Define the residual as

$$\mathbf{r}(\mathbf{u}_g^{n+1}, t_{n+1}) = \mathbf{M}_g \mathbf{a}_g^{n+1} - \mathbf{f}_g^{\text{ext}}(\mathbf{u}_g^{n+1}, t_{n+1}) + \mathbf{f}_g^{\text{int}}(\mathbf{u}_g^{n+1}, t_{n+1}) - \mathbf{f}_g^{\text{body}}(\mathbf{u}_g^{n+1}, t_{n+1}) = \mathbf{0}. \quad (1.149)$$

where the superscript $n + 1$ indicates quantities at time t_{n+1} and \mathbf{u}_g is the $N_g \times 3$ matrix of grid node displacements. We use a Newmark- β method to integrate the acceleration:

$$\begin{aligned} \mathbf{u}_g^{n+1} &= \mathbf{u}^* + \beta \mathbf{a}_g^{n+1} (\Delta t)^2 \\ \mathbf{v}_g^{n+1} &= \mathbf{v}^* + \gamma \mathbf{a}_g^{n+1} \Delta t \end{aligned} \quad (1.150)$$

where

$$\begin{aligned} \mathbf{u}^* &= \mathbf{u}_g^n + \mathbf{v}_g^n \Delta t + \frac{1}{2} (1 - 2\beta) \mathbf{a}_g^n (\Delta t)^2 \\ \mathbf{v}^* &= \mathbf{v}_g^n + (1 - \gamma) \mathbf{a}_g^n \Delta t. \end{aligned} \quad (1.151)$$

1.8.1 Newton's method

In the VAANGO implementation, the residual is expressed in terms of the displacement. We are required to do this because tangents needed in Newton's method are easier to compute when forces can be expressed in the form

$$\mathbf{f} = \mathbf{K} \cdot \mathbf{u} \quad (1.152)$$

where \mathbf{K} is the stiffness matrix. If we were to use the velocity as the primary variable, as in explicit MPM, we would need rates of the forces instead:

$$\dot{\mathbf{f}} = \mathbf{K} \cdot \mathbf{v} + \dot{\mathbf{K}} \cdot \mathbf{u}. \quad (1.153)$$

The extra term involving the rate of change of the stiffness matrix complicates the process and we avoid it in VAANGO.

Then, using (1.149) and (1.150), we have

$$\mathbf{r}(\mathbf{u}_g^{n+1}, t_{n+1}) = \frac{1}{\beta \Delta t^2} \mathbf{M}_g(\mathbf{u}_g^{n+1} - \mathbf{u}^*) - \mathbf{f}^{\text{ext}}(\mathbf{u}_g^{n+1}, t_{n+1}) + \mathbf{f}^{\text{int}}(\mathbf{u}_g^{n+1}, t_{n+1}) - \mathbf{f}^{\text{body}}(\mathbf{u}_g^{n+1}, t_{n+1}) = \mathbf{0}. \quad (1.154)$$

The problem then reduces to finding the solution \mathbf{u}_g^{n+1} of the nonlinear system of equations (1.154). Newton's method is used in VAANGO with the starting value of $\mathbf{u}_g^{n+1} = \mathbf{u}_g^*$. Dropping the subscript g temporarily for convenience, and denoting the current Newton iteration by the subscript k , we can linearize the residual at \mathbf{u}_k^{n+1} using a Taylor expansion:

$$\mathbf{0} = \mathbf{r}(\mathbf{u}_{k+1}^{n+1}, t_{n+1}) = \mathbf{r}(\mathbf{u}_k^{n+1}, t_{n+1}) + \frac{\partial \mathbf{r}(\mathbf{u}_k^{n+1}, t_{n+1})}{\partial \mathbf{u}} (\mathbf{u}_{k+1}^{n+1} - \mathbf{u}_k^{n+1}). \quad (1.155)$$

Rearranging the above equation,

$$\Delta \mathbf{u} = \mathbf{u}_{k+1}^{n+1} - \mathbf{u}_k^{n+1} = - \left[\frac{\partial \mathbf{r}(\mathbf{u}_k^{n+1}, t_{n+1})}{\partial \mathbf{u}} \right]^{-1} \mathbf{r}(\mathbf{u}_k^{n+1}, t_{n+1}) = -\mathbf{K}^{-1} \mathbf{r}(\mathbf{u}_k^{n+1}, t_{n+1}). \quad (1.156)$$

This iterative process is continued until $\Delta \mathbf{u}$ is smaller than a given tolerance. The tangent matrix \mathbf{K} , of size $N_g \times N_g$, is

$$\mathbf{K} = \frac{\partial \mathbf{r}(\mathbf{u}_k^{n+1}, t_{n+1})}{\partial \mathbf{u}}. \quad (1.157)$$

This matrix is decomposed and evaluated separately for the internal and external forces, i.e.,

$$\mathbf{K} = \frac{\partial \mathbf{r}(\mathbf{u}_k^{n+1}, t_{n+1})}{\partial \mathbf{u}} = \frac{1}{\beta \Delta t^2} \mathbf{M}_g - \frac{\partial}{\partial \mathbf{u}} [\mathbf{f}^{\text{ext}}(\mathbf{u}_g^{n+1}, t_{n+1})] + \frac{\partial}{\partial \mathbf{u}} [\mathbf{f}^{\text{int}}(\mathbf{u}_g^{n+1}, t_{n+1})] - \frac{\partial}{\partial \mathbf{u}} [\mathbf{f}^{\text{body}}(\mathbf{u}_g^{n+1}, t_{n+1})]. \quad (1.158)$$

Alternatively,

$$\mathbf{K} = \frac{1}{\beta \Delta t^2} \mathbf{M}_g - \mathbf{K}^{\text{ext}}(\mathbf{u}_g^{n+1}, t_{n+1}) + \mathbf{K}^{\text{int}}(\mathbf{u}_g^{n+1}, t_{n+1}) - \mathbf{K}^{\text{body}}(\mathbf{u}_g^{n+1}, t_{n+1}). \quad (1.159)$$

1.8.2 Tangent stiffness matrix

The contribution to the tangent matrix (\mathbf{K}) from the internal forces is called the **tangent stiffness matrix** (\mathbf{K}^{int}). Since an updated Lagrangian formulation is used in MPM, we can compute the tangent stiffness using the configuration at time t_n as the reference configuration.

Recall from (1.147) that for explicit MPM we used

$$\mathbf{f}_g^{\text{int}} = \sum_p V_p \boldsymbol{\sigma}_p \cdot \langle \nabla S_{gp} \rangle \quad \text{where} \quad \langle S_{gp} \rangle := \frac{1}{V_p} \int_{\Omega_p} Y_p(\mathbf{x}) S_g(\mathbf{x}) d\Omega. \quad (1.160)$$

For the computation of the tangent matrix, it is preferable to start from the weak form of the momentum equation (1.4):

$$I = \int_{\Omega} \boldsymbol{\sigma} : \nabla \mathbf{w} d\Omega \quad (1.161)$$

which leads to integral form of equation (1.160) (see (1.56)):

$$\mathbf{f}_g^{\text{int}} = \sum_p \int_{\Omega_p} Y_p(\mathbf{x}) \boldsymbol{\sigma}_p \cdot \nabla S_g d\Omega. \quad (1.162)$$

Also, since we are typically working with rates of stress in the constitutive models, it is preferable to express all quantities in terms of stress rates that are objective. It is easier to work with the Lagrangian PK-1 stress (\mathbf{P}) at the beginning of the timestep rather than the spatial Cauchy stress ($\boldsymbol{\sigma}$).

To convert from the spatial description (1.161) to a Lagrangian material description, observe that

$$\nabla_{n+1} \mathbf{w} = \frac{\partial \mathbf{w}}{\partial \mathbf{x}^{n+1}} = \frac{\partial \mathbf{w}}{\partial \mathbf{x}^n} \cdot \frac{\partial \mathbf{x}^n}{\partial \mathbf{x}^{n+1}} = \frac{\partial \mathbf{w}}{\partial \mathbf{x}^n} \cdot (\Delta \mathbf{F}_n^{n+1})^{-1} = \frac{\partial \mathbf{w}}{\partial \mathbf{x}^n} \cdot \frac{\Delta \mathbf{F}_c^T}{J_n^{n+1}} = \nabla_n \mathbf{w} \cdot \frac{\Delta \mathbf{F}_c^T}{J_n^{n+1}} \quad (1.163)$$

where, with \mathbf{F} as the deformation gradient,

$$\mathbf{F}^{n+1} = \Delta \mathbf{F}_n^{n+1} \mathbf{F}^n, \quad J_n^{n+1} = \det(\Delta \mathbf{F}_n^{n+1}), \quad \Delta \mathbf{F}_c = \text{cofactor}(\Delta \mathbf{F}_n^{n+1}). \quad (1.164)$$

Therefore,

$$\begin{aligned} I &= \int_{\Omega^{n+1}} \boldsymbol{\sigma}^{n+1} : \nabla_{n+1} \mathbf{w} \, d\Omega^{n+1} = \int_{\Omega^n} \boldsymbol{\sigma}^{n+1} : \nabla_n \mathbf{w} J_n^{n+1} \, d\Omega^n \\ &= \int_{\Omega^n} \boldsymbol{\sigma}^{n+1} : \left(\nabla_n \mathbf{w} \cdot \Delta \mathbf{F}_c^T \right) \, d\Omega^n = \int_{\Omega^n} (\boldsymbol{\sigma}^{n+1} \cdot \Delta \mathbf{F}_c) : \nabla_n \mathbf{w} \, d\Omega^n \\ &= \int_{\Omega^n} \mathbf{P}^n : \nabla_n \mathbf{w} \, d\Omega^n \end{aligned} \quad (1.165)$$

where \mathbf{P}^n is the first Piola-Kirchhoff stress. Following the same process as used to derive (1.56), we get

$$\mathbf{f}_g^{\text{int}} = \sum_p \int_{\Omega_p^n} Y_p(\mathbf{x}^n) \mathbf{P}_p^n \cdot \nabla_n S_g \, d\Omega^n. \quad (1.166)$$

Taking the material time derivative of (1.166), we have

$$\dot{\mathbf{f}}_g^{\text{int}} = \sum_p \int_{\Omega_p^n} Y_p(\mathbf{x}^n) \dot{\mathbf{P}}_p^n \cdot \nabla_n S_g \, d\Omega^n. \quad (1.167)$$

Since the rate of the first Piola-Kirchhoff stress is not objective, it is easier to work with the rate of the second Piola-Kirchhoff stress (\mathbf{S}):

$$\mathbf{P} = \mathbf{F} \cdot \mathbf{S} \quad \implies \quad \dot{\mathbf{P}} = \dot{\mathbf{F}} \cdot \mathbf{S} + \mathbf{F} \cdot \dot{\mathbf{S}}. \quad (1.168)$$

Substitution of (1.168) into (1.167) gives

$$\dot{\mathbf{f}}_g^{\text{int}} = \sum_p \int_{\Omega_p^n} Y_p(\mathbf{x}^n) \left[\dot{\mathbf{F}}_p^{n+1} \cdot \mathbf{S}_p^n + \mathbf{F}_p^{n+1} \cdot \dot{\mathbf{S}}_p^n \right] \cdot \nabla_n S_g \, d\Omega^n. \quad (1.169)$$

Separating out the two components, we have

$$\dot{\mathbf{f}}_g^{\text{int}} = \sum_p \int_{\Omega_p^n} Y_p(\mathbf{x}^n) \dot{\mathbf{F}}_p^{n+1} \cdot \mathbf{S}_p^n \cdot \nabla_n S_g \, d\Omega^n + \sum_p \int_{\Omega_p^n} Y_p(\mathbf{x}^n) \mathbf{F}_p^{n+1} \cdot \dot{\mathbf{S}}_p^n \cdot \nabla_n S_g \, d\Omega^n. \quad (1.170)$$

The rate of the internal force can then be expressed as

$$\dot{\mathbf{f}}_g^{\text{int}} = \dot{\mathbf{f}}_g^{\text{geo}} + \dot{\mathbf{f}}_g^{\text{mat}} \quad (1.171)$$

where the geometric and material rates of the internal forces are defined as

$$\begin{aligned} \dot{\mathbf{f}}_g^{\text{geo}} &:= \sum_p \int_{\Omega_p^n} Y_p(\mathbf{x}^n) \dot{\mathbf{F}}_p^{n+1} \cdot \mathbf{S}_p^n \cdot \nabla_n S_g \, d\Omega^n \\ \dot{\mathbf{f}}_g^{\text{mat}} &:= \sum_p \int_{\Omega_p^n} Y_p(\mathbf{x}^n) \mathbf{F}_p^{n+1} \cdot \dot{\mathbf{S}}_p^n \cdot \nabla_n S_g \, d\Omega^n. \end{aligned} \quad (1.172)$$

We can now use the constitutive relation between the second Piola-Kirchhoff stress and the Green strain (\mathbf{E}), the expression for the Green strain in terms of the deformation gradient, the relationship between the velocity gradient (\mathbf{I}) and the rate of change of the deformation gradient, and the definition of the rate-of-deformation (\mathbf{d})

$$\dot{\mathbf{S}} = \mathcal{C} : \dot{\mathbf{E}}, \quad \mathbf{E} = \frac{1}{2} (\mathbf{F}^T \cdot \mathbf{F} - \mathbf{I}), \quad \dot{\mathbf{F}} = \mathbf{I} \cdot \mathbf{F}, \quad \text{and} \quad \mathbf{d} = \frac{1}{2} (\mathbf{I} + \mathbf{I}^T) \quad (1.173)$$

to write the material and geometric rates of the internal force in (1.172) as

$$\begin{aligned} \dot{\mathbf{f}}_g^{\text{mat}} &= \sum_p \int_{\Omega_p^n} Y_p(\mathbf{x}^n) \mathbf{F}_p^{n+1} \cdot [\mathcal{C}_p^n : \dot{\mathbf{E}}_p^n] \cdot \nabla S_g \, d\Omega^n \\ &= \frac{1}{2} \sum_p \int_{\Omega_p^n} Y_p(\mathbf{x}^n) \mathbf{F}_p^{n+1} \cdot \left[\mathcal{C}_p^n : \left((\dot{\mathbf{F}}_p^{n+1})^T \cdot \mathbf{F}_p^{n+1} + (\mathbf{F}_p^{n+1})^T \cdot \dot{\mathbf{F}}_p^{n+1} \right) \right] \cdot \nabla S_g \, d\Omega^n \\ &= \frac{1}{2} \sum_p \int_{\Omega_p^n} Y_p(\mathbf{x}^n) \mathbf{F}_p^{n+1} \cdot \left[\mathcal{C}_p^n : \left((\mathbf{F}_p^{n+1})^T \cdot (\mathbf{I}_p^{n+1})^T \cdot \mathbf{F}_p^{n+1} + (\mathbf{F}_p^{n+1})^T \cdot \mathbf{I}_p^{n+1} \cdot \mathbf{F}_p^{n+1} \right) \right] \cdot \nabla S_g \, d\Omega^n \quad (1.174) \\ &= \sum_p \int_{\Omega_p^n} Y_p(\mathbf{x}^n) \mathbf{F}_p^{n+1} \cdot \left[\mathcal{C}_p^n : \left((\mathbf{F}_p^{n+1})^T \cdot \mathbf{d}_p^{n+1} \cdot \mathbf{F}_p^{n+1} \right) \right] \cdot \nabla S_g \, d\Omega^n \\ \dot{\mathbf{f}}_g^{\text{geo}} &:= \sum_p \int_{\Omega_p^n} Y_p(\mathbf{x}^n) \left[(\mathbf{F}_p^{n+1})^T \cdot (\mathbf{I}_p^{n+1})^T \right] \cdot \mathbf{S}_p^n \cdot \nabla S_g \, d\Omega^n. \end{aligned}$$

Recall the interpolation of the velocity from the grid nodes (h) to particles (p) can be computed using

$$\mathbf{v}_p(\mathbf{x}^{n+1}) = \sum_h \mathbf{v}_h^{n+1} S_h(\mathbf{x}^{n+1}) \quad (1.175)$$

Therefore,

$$\begin{aligned} \mathbf{I}_p^{n+1} &= \nabla_{n+1} \mathbf{v}_p^{n+1}(\mathbf{x}^{n+1}) = \sum_h \mathbf{v}_h^{n+1} \otimes \nabla_{n+1} S_h \\ \mathbf{d}_p^{n+1} &= \frac{1}{2} \sum_h \left[\mathbf{v}_h^{n+1} \otimes \nabla_{n+1} S_h + \nabla_{n+1} S_h \otimes \mathbf{v}_h^{n+1} \right]. \end{aligned} \quad (1.176)$$

Using (1.176) in (1.174), we have

$$\begin{aligned} \dot{\mathbf{f}}_g^{\text{mat}} &= \frac{1}{2} \sum_h \sum_p \int_{\Omega_p^n} Y_p(\mathbf{x}^n) \mathbf{F}_p^{n+1} \cdot \left[\mathcal{C}_p^n : \left((\mathbf{F}_p^{n+1})^T \cdot \left[\nabla_{n+1} S_h \otimes \mathbf{v}_h^{n+1} + \mathbf{v}_h^{n+1} \otimes \nabla_{n+1} S_h \right] \cdot \mathbf{F}_p^{n+1} \right) \right] \cdot \nabla S_g \, d\Omega^n \\ \dot{\mathbf{f}}_g^{\text{geo}} &= \sum_h \sum_p \int_{\Omega_p^n} Y_p(\mathbf{x}^n) \left[(\mathbf{F}_p^{n+1})^T \cdot \left(\nabla_{n+1} S_h \otimes \mathbf{v}_h^{n+1} \right) \right] \cdot \mathbf{S}_p^n \cdot \nabla S_g \, d\Omega^n. \end{aligned} \quad (1.177)$$

Since both the second Piola-Kirchhoff stress and the Green strain are symmetric, the tensor \mathcal{C} has the symmetries $C_{ijkl} = C_{jikl} = C_{jilk}$. For hyperelastic materials we have the additional symmetry $C_{ijkl} = C_{klij}$. We can take advantage of these symmetries to simplify the above expressions. The first term in the expression for the rate of the material internal force contains an expression of the form

$$\mathbf{A} := \mathbf{F} \cdot \left[\mathcal{C} : \left(\mathbf{F}^T \cdot \left[\tilde{\mathbf{G}} \otimes \mathbf{v} \right] \cdot \mathbf{F} \right) \right] \cdot \mathbf{G} =: \boldsymbol{\alpha} \cdot \mathbf{v} \quad (1.178)$$

while the second term contains

$$\mathbf{B} := \mathbf{F} \cdot \left[\mathcal{C} : \left(\mathbf{F}^T \cdot \left[\mathbf{v} \otimes \tilde{\mathbf{G}} \right] \cdot \mathbf{F} \right) \right] \cdot \mathbf{G} =: \boldsymbol{\beta} \cdot \mathbf{v} \quad (1.179)$$

where

$$\mathbf{G} = \mathbf{G}_g := \nabla_n S_g \quad \text{and} \quad \tilde{\mathbf{G}} = \mathbf{G}_h := \nabla_{n+1} S_h. \quad (1.180)$$

In index notation,

$$\begin{aligned}
 A_r &= F_{ri} C_{ijk\ell} F_{km}^T \tilde{G}_m v_n F_{n\ell} G_j = F_{ri} C_{ijk\ell} F_{mk} \tilde{G}_m F_{n\ell} G_j v_n = G_j (F \cdot C \cdot F^T)_{rjkn} (\tilde{G} \cdot F)_k v_n \\
 &= G_j (\tilde{G} \cdot F)_k (F \cdot C \cdot F^T)_{rjkn} v_n =: \alpha_{rn} v_n \\
 B_r &= F_{ri} C_{ijk\ell} F_{kn}^T v_n \tilde{G}_m F_{m\ell} G_j = F_{ri} C_{ijk\ell} F_{nk} \tilde{G}_m F_{m\ell} G_j v_n = G_j (F \cdot C \cdot F^T)_{rj\ell n} (\tilde{G} \cdot F)_\ell v_n \\
 &= G_j (\tilde{G} \cdot F)_\ell (F \cdot C \cdot F^T)_{rj\ell n} v_n =: \beta_{rn} v_n = \alpha_{rn} v_n = A_r
 \end{aligned} \tag{1.181}$$

Similarly for the geometrically nonlinear component, we have

$$\mathbf{C} := [\mathbf{F}^T \cdot (\tilde{\mathbf{G}} \otimes \mathbf{v})] \cdot \mathbf{S} \cdot \mathbf{G} =: \boldsymbol{\gamma} \cdot \mathbf{v}. \tag{1.182}$$

In index notation

$$C_r = F_{ri} \tilde{G}_i v_n S_{nk} G_k = (\tilde{\mathbf{G}} \cdot \mathbf{F}^T)_r (\mathbf{G} \cdot \mathbf{S})_n v_n =: \gamma_{rn} v_n. \tag{1.183}$$

We can now express (1.177) as

$$\begin{aligned}
 \dot{\mathbf{f}}_g^{\text{mat}} &= \sum_h \left[\sum_p \int_{\Omega_p^n} Y_p(\mathbf{x}^n) \boldsymbol{\alpha} d\Omega^n \right] \cdot \mathbf{v}_h^{n+1} \\
 \dot{\mathbf{f}}_g^{\text{geo}} &= \sum_h \left[\sum_p \int_{\Omega_p^n} Y_p(\mathbf{x}^n) \boldsymbol{\gamma} d\Omega^n \right] \cdot \mathbf{v}_h^{n+1}
 \end{aligned} \tag{1.184}$$

where

$$\begin{aligned}
 [\boldsymbol{\alpha}]_{i\ell} &= G_j [\tilde{\mathbf{G}} \cdot \mathbf{F}_p^{n+1}]_k [\mathbf{F}_p^{n+1} \cdot \mathcal{C}_p^n \cdot (\mathbf{F}_p^{n+1})^T]_{ijk\ell} \\
 [\boldsymbol{\gamma}]_{i\ell} &= [\tilde{\mathbf{G}} \cdot (\mathbf{F}_p^{n+1})^T]_i [\mathbf{G} \cdot \mathbf{S}_p^n]_\ell
 \end{aligned} \tag{1.185}$$

Using

$$\dot{\mathbf{f}} = \frac{\partial \mathbf{f}}{\partial \mathbf{u}} \cdot \mathbf{v} \tag{1.186}$$

where \mathbf{u} is the displacement, we notice from (1.184) that

$$\begin{aligned}
 (\mathbf{K}^{\text{mat}})_{gh} &= \frac{\partial \dot{\mathbf{f}}_g^{\text{mat}}}{\partial \mathbf{u}_h^{n+1}} = \sum_p \int_{\Omega_p^n} Y_p(\mathbf{x}^n) \boldsymbol{\alpha} d\Omega^n \\
 (\mathbf{K}^{\text{geo}})_{gh} &= \frac{\partial \dot{\mathbf{f}}_g^{\text{geo}}}{\partial \mathbf{u}_h^{n+1}} = \sum_p \int_{\Omega_p^n} Y_p(\mathbf{x}^n) \boldsymbol{\gamma} d\Omega^n.
 \end{aligned} \tag{1.187}$$

If we now set the current configuration as the reference configuration (see [18], section 6.1.3), we have

$$\mathbf{F}_p^{n+1} = \mathbf{I}, \quad \mathbf{S}_p^n = \boldsymbol{\sigma}_p^{n+1}, \quad \mathbf{x}^n = \mathbf{x}^{n+1}, \quad d\Omega_n = d\Omega_{n+1}, \quad \mathbf{G} = \tilde{\mathbf{G}}, \quad \mathcal{C}_p^n = (\mathcal{C}^\sigma)_p^{n+1}. \tag{1.188}$$

Therefore,

$$(\mathbf{K}^{\text{int}})_{gh}(\mathbf{u}_g^{n+1}, t_{n+1}) = (\mathbf{K}^{\text{mat}})_{gh} + (\mathbf{K}^{\text{geo}})_{gh} \tag{1.189}$$

where

$$\begin{aligned}
 (\mathbf{K}^{\text{mat}})_{gh} &= \sum_p \int_{\Omega_p^{n+1}} Y_p(\mathbf{x}^{n+1}) \tilde{\mathbf{G}}_g \cdot (\mathcal{C}^\sigma)_p^{n+1} \cdot \tilde{\mathbf{G}}_h d\Omega^{n+1} \\
 (\mathbf{K}^{\text{geo}})_{gh} &= \sum_p \int_{\Omega_p^{n+1}} Y_p(\mathbf{x}^{n+1}) (\tilde{\mathbf{G}}_h \otimes \tilde{\mathbf{G}}_g) \cdot \boldsymbol{\sigma}_p^{n+1} d\Omega^{n+1}.
 \end{aligned} \tag{1.190}$$

An efficient way of converting these relations to Voigt form is possible only in the case where the grid basis functions are trilinear. For **GIMP** and **CPDI** basis functions, the problem becomes more complex and have not been implemented in **VAANGO**.

1.8.3 External force stiffness matrix

Recall from (1.60) that the external force is given by

$$\mathbf{f}_g^{\text{ext}} := \int_{\Gamma_t} \tilde{\mathbf{t}}(\mathbf{x}) S_g(\mathbf{x}) d\Gamma. \quad (1.191)$$

To find the contribution to the stiffness matrix from the external force, note that

$$\dot{\mathbf{f}}_g^{\text{ext}} := \int_{\Gamma_t} \left[\dot{\tilde{\mathbf{t}}}(\mathbf{x}) S_g(\mathbf{x}) + \tilde{\mathbf{t}}(\mathbf{x}) (\nabla S_g \cdot \mathbf{v}_g) \right] d\Gamma = \int_{\Gamma_t} \left[\dot{\tilde{\mathbf{t}}}(\mathbf{x}) S_g(\mathbf{x}) + (\tilde{\mathbf{t}}(\mathbf{x}) \otimes \tilde{\mathbf{G}}_g) \cdot \mathbf{v}_g \right] d\Gamma \quad (1.192)$$

We make the simplifying assumption that

$$\dot{\tilde{\mathbf{t}}}(\mathbf{x}) = \tilde{t}(\mathbf{x}) \mathbf{v}_g \quad (1.193)$$

to get

$$\dot{\mathbf{f}}_g^{\text{ext}} := \int_{\Gamma_t} \left[\tilde{t}(\mathbf{x}) S_g(\mathbf{x}) \mathbf{I} + \tilde{\mathbf{t}}(\mathbf{x}) \otimes \tilde{\mathbf{G}}_g \right] \cdot \mathbf{v}_g d\Gamma \quad (1.194)$$

Therefore,

$$(\mathbf{K}^{\text{ext}})_{gh} = \int_{\Gamma_t} \left[\tilde{t}(\mathbf{x}) S_g(\mathbf{x}) \mathbf{I} + \tilde{\mathbf{t}}(\mathbf{x}) \otimes \tilde{\mathbf{G}}_g \right] \delta_{gh} d\Gamma \quad (1.195)$$

1.8.4 Body force stiffness matrix

The body force is given by

$$\mathbf{f}_g^{\text{ext}} := \sum_p \int_{\Omega_p} \rho_p Y_p(\mathbf{x}) S_g(\mathbf{x}) \mathbf{b}_p d\Omega \quad (1.196)$$

In VAANGO we assume that the body force does not vary with deformation. Therefore,

$$(\mathbf{K}^{\text{body}})_{gh} = 0. \quad (1.197)$$

1.9 Pseudocode of explicit MPM algorithm in Vaango

The momentum equation is solved using the **MPM** algorithm while forward Euler time-stepping is used to integrate time derivatives. The pseudocode of the overall algorithm is given below. The main quantities of interest are:

- t_{max} : The maximum time until which the simulation is to run.
- $t, \Delta t$: The current time ($t = t_n$) and the time step.
- \mathbf{h}_g : The grid spacing vector.
- m_p : The particle mass.
- V_p^n, V_p^{n+1} : The particle volume at $t = t_n$ and $t = t_{n+1}$.
- $\mathbf{x}_p^n, \mathbf{x}_p^{n+1}$: The particle position at $t = t_n$ and $t = t_{n+1}$.
- $\mathbf{u}_p^n, \mathbf{u}_p^{n+1}$: The particle displacement at $t = t_n$ and $t = t_{n+1}$.
- $\mathbf{v}_p^n, \mathbf{v}_p^{n+1}$: The particle velocity at $t = t_n$ and $t = t_{n+1}$.
- $\boldsymbol{\sigma}_p^n, \boldsymbol{\sigma}_p^{n+1}$: The particle Cauchy stress at time $t = t_n$ and $t = t_{n+1}$.
- $\mathbf{F}_p^n, \mathbf{F}_p^{n+1}$: The particle deformation gradient at time $t = t_n$ and $t = t_{n+1}$.

1.9.1 Initialization

An outline of the initialization process is described below. Specific details have been discussed in earlier reports. The new quantities introduced in this section are

- n_p : The number of particles used to discretize a body.
- $\mathbf{b}_p^n, \mathbf{b}_p^{n+1}$: The particle body force acceleration at $t = t_n$ and $t = t_{n+1}$.
- D_p^n, D_p^{n+1} : The particle damage parameter at $t = t_n$ and $t = t_{n+1}$.
- $\mathbf{f}_p^{\text{ext},n}, \mathbf{f}_p^{\text{ext},n+1}$: The particle external force at $t = t_n$ and $t = t_{n+1}$.

Algorithm 1 Initialization

Require: `xmlProblemSpec`, `defGradComputer`, `constitutiveModel`, `damageModel`, `particleBC`,

\hookrightarrow `mpmFlags` `materialList`,

```

1: procedure INITIALIZE
2:   for matl in materialList do
3:      $n_p[\text{matl}], \mathbf{x}_p^o[\text{matl}], \mathbf{u}_p^o[\text{matl}], m_p[\text{matl}], V_p^o[\text{matl}], \mathbf{v}_p^o[\text{matl}], \mathbf{b}_p^o[\text{matl}],$ 
        $\hookrightarrow \mathbf{f}_p^{\text{ext},o}[\text{matl}] \leftarrow \text{matl.CREATEPARTICLES}()$ 
4:      $\mathbf{F}_p^o[\text{matl}] \leftarrow \text{defGradComputer.INITIALIZE}(\text{matl})$ 
5:      $\boldsymbol{\sigma}_p^o[\text{matl}] \leftarrow \text{constitutiveModel.INITIALIZE}(\text{matl})$ 
6:      $D_p^o[\text{matl}] \leftarrow \text{damageModel.INITIALIZE}(\text{matl})$ 
7:   end for
8:   if mpmFlags.initializeStressWithBodyForce = TRUE then
9:      $\mathbf{b}_p^o \leftarrow \text{INITIALIZEBODYFORCE}()$ 
10:     $\boldsymbol{\sigma}_p^o, \mathbf{F}_p^o \leftarrow \text{INITIALIZESTRESSANDDEFGRADFROMBODYFORCE}()$ 
11:   end if
12:   if mpmFlags.applyParticleBCs = TRUE then
13:      $\mathbf{f}_p^{\text{ext},o} \leftarrow \text{particleBC.INITIALIZEPRESSUREBCs}()$ 
14:   end if
15:   return  $n_p, \mathbf{x}_p^o, \mathbf{u}_p^o, m_p, V_p^o, \mathbf{v}_p^o, \mathbf{b}_p^o, \mathbf{f}_p^{\text{ext},o}, \mathbf{F}_p^o, \boldsymbol{\sigma}_p^o, D_p^o$ 
16: end procedure

```

1.9.2 Time advance

The operations performed during a timestep are shown in the pseudocode below.

Algorithm 2 The MPM time advance algorithm

```

1: procedure TIMEADVANCE( $\mathbf{h}_g, \mathbf{x}_p^n, \mathbf{u}_p^n, m_p, V_p^n, \mathbf{v}_p^n, \mathbf{f}_p^{\text{ext},n}, \mathbf{d}_p^n$ )
2:    $\mathbf{b}_p^n \leftarrow \text{COMPUTEPARTICLEBODYFORCE}()$   $\triangleright$  Compute the body force term
3:    $\mathbf{f}_p^{\text{ext},n+1} \leftarrow \text{APPLYEXTERNALLOADS}()$   $\triangleright$  Apply external loads to the particles
4:    $m_g, V_g, \mathbf{v}_g, \mathbf{b}_g, \mathbf{f}_g^{\text{ext}} \leftarrow \text{INTERPOLATEPARTICLESTOGRID}()$   $\triangleright$  Interpolate particle data to the grid
5:    $\text{EXCHANGEMOMENTUMINTERPOLATED}()$   $\triangleright$  Exchange momentum between bodies on grid.
        $\hookrightarrow$  Not discussed in this report.
6:    $\mathbf{f}_g^{\text{int}}, \boldsymbol{\sigma}_g, \mathbf{v}_g \leftarrow \text{COMPUTEINTERNALFORCE}()$   $\triangleright$  Compute the internal force at the grid nodes
7:    $\mathbf{v}_g^*, \mathbf{a}_g \leftarrow \text{COMPUTEANDINTEGRATEACCELERATION}()$   $\triangleright$  Compute the grid velocity
        $\hookrightarrow$  and grid acceleration
8:    $\text{EXCHANGEMOMENTUMINTEGRATED}()$   $\triangleright$  Exchange momentum between bodies on grid
        $\hookrightarrow$  using integrated values. Not discussed in this report.
9:    $\mathbf{v}_g^*, \mathbf{a}_g \leftarrow \text{SETGRIDBOUNDARYCONDITIONS}()$   $\triangleright$  Update the grid velocity and grid
        $\hookrightarrow$  acceleration using the BCs
10:   $\mathbf{l}_p^n, \mathbf{F}_p^{n+1}, V_p^{n+1} \leftarrow \text{COMPUTEDFORMATIONGRADIENT}()$   $\triangleright$  Compute the velocity gradient
        $\hookrightarrow$  and the deformation gradient

```

```

11:   $\sigma_p^{n+1}, \eta_p^{n+1} \leftarrow \text{COMPUTESTRESSTENSOR}()$  ▷ Compute the updated stress and
    ↪ internal variables (if any)
12:   $\sigma_p^{n+1}, \eta_p^{n+1}, \chi_p^{n+1}, D_p^{n+1} \leftarrow \text{COMPUTE BASICDAMAGE}()$  ▷ Compute the damage parameter
    ↪ and update the stress and internal variables
13:   $\chi_p^{n+1}, D_p^{n+1} \leftarrow \text{UPDATEEROSIONPARAMETER}()$  ▷ Update the indicator variable that is used
    ↪ to delete particles at the end of a time step
14:   $V_p^{n+1}, \mathbf{u}_p^{n+1}, \mathbf{v}_p^{n+1}, \mathbf{x}_p^{n+1}, m_p, \mathbf{h}_p^{n+1} \leftarrow \text{INTERPOLATE TOPARTICLESANDUPDATE}()$  ▷ Update the
    ↪ particle variables after interpolating grid quantities to particles
15:  end procedure

```

The algorithms used for the above operations are discussed next.

Computing the body force

The body force consists of a gravitational term and, optionally, centrifugal and coriolis terms that are needed for simulations inside a rotating frame such as a centrifuge.

Algorithm 3 Computing the body force on particles

Require: $\mathbf{x}_p^n, \mathbf{v}_p^n$, materialList, particleList, mpmFlags

```

1:  procedure COMPUTEPARTICLEBODYFORCE
2:    for matl in materialList do
3:      if mpmFlags.rotatingCoordSystem = TRUE then
4:         $\mathbf{g} \leftarrow \text{mpmFlags.gravityAcceleration}$ 
5:         $\mathbf{b}_p^n[\text{matl}] \leftarrow \mathbf{g}$ 
6:      else
7:        for part in particleList do
8:           $\mathbf{g} \leftarrow \text{mpmFlags.gravityAcceleration}$ 
9:           $\mathbf{x}_{rc} \leftarrow \text{mpmFlags.coordRotationCenter}$ 
10:          $\mathbf{z}_r \leftarrow \text{mpmFlags.coordRotationAxis}$ 
11:          $\omega \leftarrow \text{mpmFlags.coordRotationSpeed}$ 
12:          $\boldsymbol{\omega} \leftarrow \omega \mathbf{z}_r$  ▷ Compute angular velocity vector
13:          $\mathbf{a}_{\text{corolis}} \leftarrow 2\boldsymbol{\omega} \times \mathbf{v}_p^n[\text{matl}, \text{part}]$  ▷ Compute Coriolis acceleration
14:          $\mathbf{r} \leftarrow \mathbf{x}_p^n[\text{matl}, \text{part}] - \mathbf{x}_{rc}$ 
15:          $\mathbf{a}_{\text{centrifugal}} \leftarrow \boldsymbol{\omega} \times \boldsymbol{\omega} \times \mathbf{r}$  ▷ Compute the centrifugal body force acceleration
16:          $\mathbf{b}_p^n[\text{matl}, \text{part}] \leftarrow \mathbf{g} - \mathbf{a}_{\text{centrifugal}} - \mathbf{a}_{\text{corolis}}$  ▷ Compute the body force acceleration
17:       end for
18:     end if
19:   end for
20:   return  $\mathbf{b}_p^n$ 
21: end procedure

```

Applying external loads

Note that the updated deformation gradient has not been computed yet at this stage and the particle force is applied based on the deformation gradient at the beginning of the timestep. The new quantities introduced in this section are:

- \mathbf{h}_p^n : The particle size matrix at time $t = t_n$.

Algorithm 4 Applying external loads to particles

Require: $t_{n+1}, \mathbf{x}_p^n, \mathbf{h}_p^n, \mathbf{u}_p^n, \mathbf{f}_p^{\text{ext}, n}, \mathbf{F}_p^n$, materialList, particleList, mpmFlags, particleBC

```

1:  procedure APPLYEXTERNALLOADS

```

```

2:    $f_p \leftarrow 0$ 
3:   if mpmFlags.useLoadCurves = TRUE then
4:      $f_p \leftarrow \text{particleBC.COMPUTEFORCEPERPARTICLE}(t^{n+1})$  ▷Compute the force per particle
        $\hookrightarrow$  due to the applied pressure
5:   end if
6:   for matl in materialList do
7:     if mpmFlags.useLoadCurves = TRUE then
8:       for part in particleList do
9:          $\mathbf{f}_p^{\text{ext},n+1}[\text{matl},\text{part}] \leftarrow \text{particleBC.GETFORCEVECTOR}(t_{n+1}, \mathbf{x}_p^n, \mathbf{h}_p^n, \mathbf{u}_p^n,$ 
            $\hookrightarrow f_p, \mathbf{F}_p^n)$  ▷Compute the applied force vector at each particle
10:        end for
11:      else
12:         $\mathbf{f}_p^{\text{ext},n+1}[\text{matl}] \leftarrow \mathbf{f}_p^{\text{ext},n}[\text{matl}]$ 
13:      end if
14:    end for
15:    return  $\mathbf{f}_p^{\text{ext},n+1}$ 
16:  end procedure

```

Interpolating particles to grid

The grid quantities computed during this procedure and not stored for the next timestep except for the purpose of visualization. The new quantities introduced in this section are

- m_g : The mass at a grid node.
- V_g : The volume at a grid node.
- \mathbf{v}_g : The velocity at a grid node.
- $\mathbf{f}_g^{\text{ext}}$: The external force at a grid node.
- \mathbf{b}_g : The body force at a grid node.

Algorithm 5 Interpolating particle data to background grid

Require: $m_p, V_p^n, \mathbf{x}_p^n, \mathbf{h}_p^n, \mathbf{b}_p^n, \mathbf{f}_p^{\text{ext},n+1}, \mathbf{F}_p^n, \text{materialList}, \text{particleList}, \text{gridNodeList}$ mpmFlags, particleBC

```

1: procedure INTERPOLATEPARTICLESTOGRID
2:   interpolator  $\leftarrow \text{CREATEINTERPOLATOR}(\text{mpmFlags})$  ▷Create the interpolator
        $\hookrightarrow$  and find number of grid nodes that can affect a particle
3:   for matl in materialList do
4:     for part in particleList do
5:        $n_{gp}, S_{gp} \leftarrow \text{interpolator.FINDCELLSANDWEIGHTS}(\mathbf{x}_p^n, \mathbf{h}_p^n, \mathbf{F}_p^n)$  ▷Find the node
            $\hookrightarrow$  indices of the cells affecting the particle and the interpolation weights
6:        $\mathbf{p}_p \leftarrow m_p[\text{matl}][\text{part}] \mathbf{v}_p^n[\text{matl}][\text{part}]$  ▷Compute particle momentum
7:       for node in  $n_{gp}$  do
8:          $m_g[\text{matl}][\text{node}] \leftarrow m_g[\text{matl}][\text{node}] + m_p[\text{matl}][\text{part}] S_{gp}[\text{node}]$ 
9:          $V_g[\text{matl}][\text{node}] \leftarrow V_g[\text{matl}][\text{node}] + V_p^n[\text{matl}][\text{part}] S_{gp}[\text{node}]$ 
10:         $\mathbf{v}_g[\text{matl}][\text{node}] \leftarrow \mathbf{v}_g[\text{matl}][\text{node}] + \mathbf{p}_p S_{gp}[\text{node}]$ 
11:         $\mathbf{f}_g^{\text{ext}}[\text{matl}][\text{node}] \leftarrow \mathbf{f}_g^{\text{ext}}[\text{matl}][\text{node}] + \mathbf{f}_p^{\text{ext},n+1}[\text{matl}][\text{part}] S_{gp}[\text{node}]$ 
12:         $\mathbf{b}_g[\text{node}] \leftarrow \mathbf{b}_g[\text{node}] + m_p[\text{matl}][\text{part}] \mathbf{b}_p^n[\text{matl}][\text{part}] S_{gp}[\text{node}]$ 
13:      end for
14:    end for
15:    for node in gridNodeList do
16:       $\mathbf{v}_g[\text{matl}][\text{node}] \leftarrow \mathbf{v}_g[\text{matl}][\text{node}] / m_g[\text{matl}][\text{node}]$ 
17:    end for
18:     $\mathbf{v}_g[\text{matl}] \leftarrow \text{APPLYSYMMETRYVELOCITYBC}(\mathbf{v}_g[\text{matl}])$  ▷Apply any symmetry
        $\hookrightarrow$  velocity BCs that may be applicable

```

```

19:   end for
20:   return  $m_g, V_g, \mathbf{v}_g, \mathbf{b}_g, \mathbf{f}_g^{\text{ext}}$ 
21: end procedure

```

Exchanging momentum using interpolated grid values

The exchange of momentum is carried out using a contact model. Details can be found in the Uintah Developers Manual.

Computing the internal force

This procedure computes the internal force at the grid nodes. The new quantities introduced in this section are

- n_{gp} : The number of grid nodes that are used to interpolate from particle to grid.
- S_{gp} : The nodal interpolation function evaluated at a particle
- \mathbf{G}_{gp} : The gradient of the nodal interpolation function evaluated at a particle
- σ_v : A volume weighted grid node stress.
- $\mathbf{f}_g^{\text{int}}$: The internal force at a grid node.

Algorithm 6 Computing the internal force

Require: $h_g, V_g, V_p^n, \mathbf{x}_p^n, \mathbf{h}_p^n, \sigma_p^n, \mathbf{F}_p^n, \text{materialList}, \text{particleList}, \text{gridNodeList}, \text{mpmFlags}$

```

1: procedure COMPUTEINTERNALFORCE
2:   interpolator ← CREATEINTERPOLATOR(mpmFlags) ▷ Create the interpolator and
   ↪ find number of grid nodes that can affect a particle
3:   for matl in materialList do
4:     for part in particleList do
5:        $n_{gp}, S_{gp}, \mathbf{G}_{gp} \leftarrow$ 
   ↪ interpolator.FINDCELLSANDWEIGHTSANDSHAPEDERIVATIVES( $\mathbf{x}_p^n, \mathbf{h}_p^n, \mathbf{F}_p^n$ )
   ↪ Find the node indices of the cells affecting the particle and
   ↪ the interpolation weights and gradients
6:        $\sigma_v \leftarrow V_p[\text{matl}][\text{part}] \sigma_p^n[\text{matl}][\text{part}]$ 
7:       for node in  $n_{gp}$  do
8:          $\mathbf{f}_g^{\text{int}}[\text{matl}][\text{node}] \leftarrow \mathbf{f}_g^{\text{int}}[\text{matl}][\text{node}] - (\mathbf{G}_{gp}[\text{node}]/h_g) \cdot \sigma_p^n[\text{matl}][\text{part}] V_p^n[\text{part}]$ 
9:          $\sigma_g[\text{matl}][\text{node}] \leftarrow \sigma_g[\text{matl}][\text{node}] + \sigma_v S_{gp}[\text{node}]$ 
10:      end for
11:    end for
12:    for node in gridNodeList do
13:       $\sigma_g[\text{matl}][\text{node}] \leftarrow \sigma_g[\text{matl}][\text{node}]/V_g[\text{matl}][\text{node}]$ 
14:    end for
15:     $\mathbf{v}_g[\text{matl}] \leftarrow \text{APPLYSYMMETRYTRACTIONBC}()$  ▷ Apply any symmetry tractions BCs
   ↪ that may be applicable
16:  end for
17:  return  $\mathbf{f}_g^{\text{int}}, \sigma_g, \mathbf{v}_g$ 
18: end procedure

```

Computing and integrating the acceleration

This procedure computes the accelerations at the grid nodes and integrates the grid accelerations using forward Euler to compute grid velocities. The new quantities introduced in this section are

- \mathbf{a}_g : The grid accelerations.
- \mathbf{v}_g^* : The integrated grid velocities.

Algorithm 7 Computing and integrating the acceleration**Require:** $\Delta t, m_g, \mathbf{f}_g^{\text{int}}, \mathbf{f}_g^{\text{ext}}, \mathbf{b}_g, \mathbf{v}_g, \text{materialList}, \text{gridNodeList}, \text{mpmFlags}$

```

1: procedure COMPUTEANDINTEGRATEACCELERATION
2:   for  $\text{matl}$  in  $\text{materialList}$  do
3:     for  $\text{node}$  in  $\text{gridNodeList}$  do
4:        $\mathbf{a}_g[\text{matl}][\text{node}] \leftarrow (\mathbf{f}_g^{\text{int}}[\text{matl}][\text{node}] + \mathbf{f}_g^{\text{ext}}[\text{matl}][\text{node}] + \mathbf{b}_g[\text{matl}][\text{node}]) / m_g[\text{matl}][\text{node}]$ 
5:        $\mathbf{v}_g^* \leftarrow \mathbf{v}_g[\text{matl}][\text{node}] + \mathbf{a}_g[\text{matl}][\text{node}] * \Delta t$ 
6:     end for
7:   end for
8:   return  $\mathbf{v}_g^*, \mathbf{a}_g$ 
9: end procedure

```

Exchanging momentum using integrated grid values

The exchange of momentum is carried out using a contact model. Details can be found in the Uintah Developers Manual.

Setting grid boundary conditions**Algorithm 8** Setting grid boundary conditions**Require:** $\Delta t, \mathbf{a}_g, \mathbf{v}_g^*, \mathbf{v}_g, \text{materialList}, \text{gridNodeList}, \text{mpmFlags}$

```

1: procedure SETGRIDBOUNDARYCONDITIONS
2:   for  $\text{matl}$  in  $\text{materialList}$  do
3:      $\mathbf{v}_g^*[\text{matl}] \leftarrow \text{APPLYSYMMETRYVELOCITYBC}(\mathbf{v}_g^*[\text{matl}])$ 
4:     for  $\text{node}$  in  $\text{gridNodeList}$  do
5:        $\mathbf{a}_g[\text{matl}][\text{node}] \leftarrow (\mathbf{v}_g^*[\text{matl}][\text{node}] - \mathbf{v}_g[\text{matl}][\text{node}]) / \Delta t$ 
6:     end for
7:   end for
8:   return  $\mathbf{v}_g^*, \mathbf{a}_g$ 
9: end procedure

```

Computing the deformation gradient

The velocity gradient is computed using the integrated grid velocities and then used to compute the deformation gradient. The new quantities introduced in this section are

- $\Delta \mathbf{F}_p^n$: The increment of the particle deformation gradient.
- \mathbf{l}_p^{n+1} : The particle velocity gradient.
- ρ_o : The initial mass density of the material.

Algorithm 9 Computing the velocity gradient and deformation gradient**Require:** $\Delta t, \mathbf{x}_p^n, m_p, V_p^n, \mathbf{h}_p^n, \mathbf{v}_p^n, \mathbf{l}_p^n, \mathbf{F}_p^n, \mathbf{h}_g, \mathbf{v}_g, \mathbf{v}_g^*, \rho_o, \text{materialList}, \text{gridNodeList}, \text{mpmFlags}, \text{velGradComputer}$

```

1: procedure COMPUTEDEFORMATIONGRADIENT
2:    $\text{interpolator} \leftarrow \text{CREATEINTERPOLATOR}(\text{mpmFlags})$ 
3:   for  $\text{matl}$  in  $\text{materialList}$  do
4:     for  $\text{part}$  in  $\text{particleList}$  do
5:        $\mathbf{l}_p^{n+1}[\text{matl}, \text{part}] \leftarrow \text{velGradComputer.COMPUTEVELGRAD}(\text{interpolator}, \mathbf{h}_g, \mathbf{x}_p^n[\text{matl}, \text{part}],$ 
         $\hookrightarrow \mathbf{h}_p^n[\text{matl}, \text{part}], \mathbf{F}_p^n[\text{matl}, \text{part}], \mathbf{v}_g^*[\text{matl}])$   $\triangleright \text{Compute the velocity gradient}$ 
6:        $\mathbf{F}_p^{n+1}[\text{matl}, \text{part}], \Delta \mathbf{F}_p^{n+1} \leftarrow \text{COMPUTEDEFORMATIONGRADIENTFROMVELOCITY}(\mathbf{l}_p^n[\text{matl}, \text{part}],$ 
         $\hookrightarrow \mathbf{l}_p^{n+1}[\text{matl}, \text{part}], \mathbf{F}_p^n[\text{matl}, \text{part}])$   $\triangleright \text{Compute the deformation gradient}$ 
7:        $V_p^{n+1}[\text{matl}, \text{part}] \leftarrow m_p[\text{matl}, \text{part}] / \rho_o * \det(\mathbf{F}_p^{n+1}[\text{matl}, \text{part}])$ 

```

```

8:         end for
9:     end for
10:    return  $l_p^{n+1}, F_p^{n+1}, V_p^{n+1}$ 
11: end procedure

```

Algorithm 10 Computing the deformation gradient using the velocity gradient

Require: $\Delta t, l_p^{n+1}, F_p^n, \text{mpmFlags}$

```

1: procedure COMPUTEDEFORMATIONGRADIENTFROMVELOCITY
2:   if  $\text{mpmFlags.defGradAlgorithm} = \text{"first\_order"}$  then
3:      $F_p^{n+1}, \Delta F_p^{n+1} \leftarrow \text{SERIESUPDATECONSTANTVELGRAD}(\text{numTerms} = 1, \Delta t, l_p^{n+1}, F_p^n)$ 
4:   else if  $\text{mpmFlags.defGradAlgorithm} = \text{"subcycle"}$  then
5:      $F_p^{n+1}, \Delta F_p^{n+1} \leftarrow \text{SUBCYCLEUPDATECONSTANTVELGRAD}(\Delta t, l_p^{n+1}, F_p^n)$ 
6:   else if  $\text{mpmFlags.defGradAlgorithm} = \text{"taylor\_series"}$  then
7:      $F_p^{n+1}, \Delta F_p^{n+1} \leftarrow \text{SERIESUPDATECONSTANTVELGRAD}(\text{numTerms} = \text{mpmFlags.numTaylorSeriesTerms},$ 
       $\Delta t, l_p^{n+1}, F_p^n)$ 
8:   else
9:      $F_p^{n+1}, \Delta F_p^{n+1} \leftarrow \text{CAYLEYUPDATECONSTANTVELGRAD}(\Delta t, l_p^{n+1}, F_p^n)$ 
10:  end if
11:  return  $F_p^{n+1}, \Delta F_p^{n+1}$ 
12: end procedure

```

Computing the stress tensor

The stress tensor is compute by individual constitutive models. Details of the Arena partially saturated model are given later. The new quantities introduced in this section are

- η_p^n, η_p^{n+1} : The internal variables needed by the constitutive model.

Algorithm 11 Computing the stress tensor

Require: $\Delta t, \mathbf{x}_p^n, m_p, V_p^{n+1}, h_p^n, l_p^{n+1}, F_p^{n+1}, \sigma_p^n, \eta_p^n, \rho_o, \text{materialList}, \text{mpmFlags}, \text{constitutiveModel}$

```

1: procedure COMPUTESTRESS TENSOR
2:   for  $\text{matl}$  in  $\text{materialList}$  do
3:      $\sigma_p^{n+1}, \eta_p^{n+1} \leftarrow \text{constitutiveModel}[\text{matl}].\text{COMPUTESTRESS TENSOR}(\Delta t, \mathbf{x}_p^n, m_p, V_p^{n+1}, h_p^n,$ 
       $\hookrightarrow l_p^{n+1}, F_p^{n+1}, \sigma_p^n, \eta_p^n, \rho_o, \text{mpmFlags})$  ▷ Update the stress and any
      ↪ internal variables needed by the constitutive model
4:   end for
5:   return  $\sigma_p^{n+1}, \eta_p^{n+1}$ 
6: end procedure

```

Computing the basic damage parameter

The damage parameter is updated and the particle stress is modified in this procedure. The new quantities introduced in this section are

- $\epsilon_p^{f,n}, \epsilon_p^{f,n+1}$: The particle strain to failure at $t = T_n$ and $t = T_{n+1}$.
- χ_p^n, χ_p^{n+1} : An indicator function that identifies whether a particle has failed completely.
- $t_p^{\chi,n}, t_p^{\chi,n+1}$: The time to failure of a particle.
- D_p^n, D_p^{n+1} : A particle damage parameter that can be used to modify the stress.

Algorithm 12 Computing the damage parameter

Require: $t^{n+1}, V_p^{n+1}, F_p^{n+1}, \sigma_p^{n+1}, D_p^n, \epsilon_p^{f,n}, \chi_p^n, t_p^{\chi,n}, \text{materialList}, \text{mpmFlags}$

```

1: procedure COMPUTEDAMAGE
2:   for matl in materialList do
3:     for part in particleList do
4:       if brittleDamage = TRUE then
5:          $\sigma_p^{n+1}, \varepsilon_p^{f,n+1}, \chi_p^{n+1}, t_p^{\chi,n+1}, D_p^{n+1} \leftarrow \text{UPDATE DAMAGE AND MODIFY STRESS}(V_p^{n+1}, \mathbf{F}_p^{n+1},$ 
            $\hookrightarrow \sigma_p^{n+1}, D_p^n, \varepsilon_p^{f,n}, \chi_p^n, t_p^{\chi,n})$  ▷ Update the damage parameters and stress
6:       else
7:          $\sigma_p^{n+1}, \varepsilon_p^{f,n+1}, \chi_p^{n+1}, t_p^{\chi,n+1} \leftarrow \text{UPDATE FAILED PARTICLES AND MODIFY STRESS}(V_p^{n+1}, \mathbf{F}_p^{n+1},$ 
            $\hookrightarrow \sigma_p^{n+1}, \varepsilon_p^{f,n}, \chi_p^n, t_p^{\chi,n}, t^{n+1})$  ▷ Update the failed particles and stress
8:       end if
9:     end for
10:  end for
11:  return  $\sigma_p^{n+1}, \varepsilon_p^{f,n+1}, \chi_p^{n+1}, t_p^{\chi,n+1}, D_p^{n+1}$ 
12: end procedure

```

Updating the particle erosion parameter

The particle failure indicator function is updated in this procedure and used later for particle deletion if needed.

Algorithm 13 Updating the particle erosion parameter

Require: D_p^n, χ_p^n materialList, mpmFlags, constitutiveModel

```

1: procedure UPDATEEROSIONPARAMETER
2:   for matl in materialList do
3:     for part in particleList do
4:       if matl.doBasicDamage = TRUE then
5:          $\chi_p^{n+1} \leftarrow \text{damageModel.GETLOCALIZATIONPARAMETER}()$  ▷ Just get the indicator
           ↪ parameter for particles that will be eroded.
6:       else
7:          $\chi_p^{n+1}, D_p^{n+1} \leftarrow \text{constitutiveModel}[\text{matl}].\text{GETDAMAGEPARAMETER}(\chi_p^n, D_p^n)$ 
           ↪ Update the damage parameter in the constitutive model.
8:       end if
9:     end for
10:  end for
11:  return  $\chi_p^{n+1}, D_p^{n+1}$ 
12: end procedure

```

Interpolating back to the particles and update

This is the final step at which the particle velocities and positions are updated and the grid is reset. Particle that are to be removed are dealt with in a subsequent relocation step.

Algorithm 14 Interpolating back to the particles and position update

Require: $\Delta t, \mathbf{a}_g, \mathbf{v}_g^*, \mathbf{x}_p^n, \mathbf{v}_p^n, \mathbf{u}_p^n, \mathbf{h}_p^n, \chi_p^{n+1}, \mathbf{F}_p^{n+1}, V_p^{n+1}$, materialList, particleList, gridNodeList, mpmFlags

```

1: procedure INTERPOLATE TOPARTICLES AND UPDATE
2:   interpolator  $\leftarrow \text{CREATEINTERPOLATOR}(\text{mpmFlags})$ 
3:   for matl in materialList do
4:      $\mathbf{h}_p^{n+1} \leftarrow \mathbf{h}_p^n$ 
5:     for part in particleList do
6:        $n_{gp}, S_{gp} \leftarrow \text{interpolator.FINDCELLSANDWEIGHTS}(\mathbf{x}_p^n, \mathbf{h}_p^{n+1}, \mathbf{F}_p^{n+1})$ 

```

```

7:      v ← o, a ← o,
8:      for node in gridNodeList do
9:          v ← v + vg*[node] * Sgp[node]
10:         a ← a + ag[node] * Sgp[node]
11:     end for
12:     xpn+1 ← xpn + v * Δt
13:     upn+1 ← upn + v * Δt
14:     vpn+1 ← vpn + a * Δt
15: end for
16: end for
17: DELETEROGUEPARTICLES()
18: return Vpn+1, upn+1, vpn+1, xpn+1, mp, hpn+1
19: end procedure

```

▷ Update particle velocity
 ▷ Update particle acceleration
 ▷ Update position
 ▷ Update displacement
 ▷ Update velocity
 ▷ Delete particles that are to be eroded.

2 — MPM Material Models

In this chapter we discuss some general features of the MPM material models. Individual models are complex and are discussed in separate chapters. Notation and definitions that are used frequently are also elaborated upon here.

2.1 Notation and definitions

A primary assumption made in many of the material models in Vaango is that stresses and (moderate) strains can be additively decomposed into volumetric and deviatoric parts.

2.1.1 Volumetric-deviatoric decomposition

The volumetric-deviatoric decomposition of stress (σ) is expressed as

$$\sigma = p\mathbf{I} + \mathbf{s} \quad (2.1)$$

where the mean stress (p) and the deviatoric stress (\mathbf{s}) are given by

$$p = \frac{1}{3}\text{tr}(\sigma) = \frac{1}{3}\sigma : \mathbf{I} = \frac{1}{3}(\sigma_{11} + \sigma_{22} + \sigma_{33}) \quad \text{and} \quad \mathbf{s} = \sigma - p\mathbf{I} = \begin{bmatrix} \sigma_{11} - p & \sigma_{12} & \sigma_{13} \\ \sigma_{12} & \sigma_{22} - p & \sigma_{23} \\ \sigma_{13} & \sigma_{23} & \sigma_{33} - p \end{bmatrix}. \quad (2.2)$$

Similarly, the volumetric-deviatoric split of the strain (ϵ) is expressed as

$$\epsilon = \frac{1}{3}\epsilon_v\mathbf{I} + \epsilon_s \quad (2.3)$$

where the volumetric strain (ϵ_v) and the deviatoric strain (ϵ_s) are defined as

$$\epsilon_v = \text{tr}(\epsilon) = \epsilon : \mathbf{I} = \epsilon_{11} + \epsilon_{22} + \epsilon_{33} \quad \text{and} \quad \epsilon_s = \epsilon - \frac{1}{3}\epsilon_v\mathbf{I} = \begin{bmatrix} \epsilon_{11} - \frac{1}{3}\epsilon_v & \epsilon_{12} & \epsilon_{13} \\ \epsilon_{12} & \epsilon_{22} - \frac{1}{3}\epsilon_v & \epsilon_{23} \\ \epsilon_{13} & \epsilon_{23} & \epsilon_{33} - \frac{1}{3}\epsilon_v \end{bmatrix}. \quad (2.4)$$

2.1.2 Stress invariants

The principal invariants and principal deviatoric invariants of the stress are used in several models. Frequently used invariants are:

$$\begin{aligned}
 I_1 &= \text{tr}(\boldsymbol{\sigma}) = \sigma_{11} + \sigma_{22} + \sigma_{33} \\
 I_2 &= \frac{1}{2} [\text{tr}(\boldsymbol{\sigma})^2 - \text{tr}(\boldsymbol{\sigma}^2)] = \sigma_{11}\sigma_{22} + \sigma_{22}\sigma_{33} + \sigma_{33}\sigma_{11} - (\sigma_{12}^2 + \sigma_{23}^2 + \sigma_{13}^2) \\
 I_3 &= \det(\boldsymbol{\sigma}) = \sigma_{11}\sigma_{22}\sigma_{33} + 2\sigma_{12}\sigma_{23}\sigma_{13} - \sigma_{12}^2\sigma_{33} - \sigma_{23}^2\sigma_{11} - \sigma_{13}^2\sigma_{22} \\
 J_2 &= \frac{1}{2} \mathbf{s} : \mathbf{s} = \frac{1}{6} [(\sigma_{11} - \sigma_{22})^2 + (\sigma_{22} - \sigma_{33})^2 + (\sigma_{33} - \sigma_{11})^2] + (\sigma_{12}^2 + \sigma_{23}^2 + \sigma_{31}^2) \\
 J_3 &= \det(\mathbf{s}) = \frac{2}{27} I_1^3 - \frac{1}{3} I_1 I_2 + I_3
 \end{aligned} \tag{2.5}$$

Alternatives to I_1 , J_2 and J_3 are p , q , and θ , defined as

$$p := \frac{1}{3} I_1, \quad q := \sqrt{3J_2}, \quad \cos 3\theta := \left(\frac{r}{q} \right)^3 = \frac{3\sqrt{3}}{2} \frac{J_3}{J_2^{3/2}}, \quad r^3 = \frac{27}{2} J_3. \tag{2.6}$$

A geometric accurate view of the stress state and yield surfaces is obtained if the isomorphic cylindrical coordinates z , ρ , and θ are used instead, where

$$z := \frac{I_1}{\sqrt{3}} = \sqrt{3}p, \quad \rho := \sqrt{2J_2} = \sqrt{\frac{2}{3}}q, \quad \cos 3\theta := \frac{3\sqrt{3}}{2} \frac{J_3}{J_2^{3/2}}. \tag{2.7}$$

2.1.3 Effective stress and strain

The effective stress and strain (sometimes also referred to as the shear stress and shear strain in the code) are defined such that the product is equal to the plastic work done. These measures are strictly applicable only to J_2 plasticity models but have also been used elsewhere.

The effective stress is defined as

$$\sigma_{\text{eff}} = q = \sqrt{3J_2} = \sqrt{\frac{3}{2} \mathbf{s} : \mathbf{s}} = \sqrt{\frac{1}{2} [(\sigma_{11} - \sigma_{22})^2 + (\sigma_{22} - \sigma_{33})^2 + (\sigma_{33} - \sigma_{11})^2] + 3(\sigma_{12}^2 + \sigma_{23}^2 + \sigma_{31}^2)}. \tag{2.8}$$

The effective strain is defined as

$$\epsilon_{\text{eff}} = \sqrt{\frac{2}{3} \boldsymbol{\epsilon}_s : \boldsymbol{\epsilon}_s} \tag{2.9}$$

so that

$$\sigma_{\text{eff}} \epsilon_{\text{eff}} = \sqrt{(\mathbf{s} : \mathbf{s})(\boldsymbol{\epsilon}_s : \boldsymbol{\epsilon}_s)}. \tag{2.10}$$

From the definition of $\boldsymbol{\epsilon}_s$ we see that

$$\begin{aligned}
 \boldsymbol{\epsilon}_s : \boldsymbol{\epsilon}_s &= \boldsymbol{\epsilon} : \boldsymbol{\epsilon} - \frac{2}{3} \text{tr}(\boldsymbol{\epsilon}) \mathbf{I} : \boldsymbol{\epsilon} + \frac{1}{9} [\text{tr}(\boldsymbol{\epsilon})]^2 \mathbf{I} : \mathbf{I} = \boldsymbol{\epsilon} : \boldsymbol{\epsilon} - \frac{2}{3} [\text{tr}(\boldsymbol{\epsilon})]^2 + \frac{1}{3} [\text{tr}(\boldsymbol{\epsilon})]^2 = \boldsymbol{\epsilon} : \boldsymbol{\epsilon} - \frac{1}{3} [\text{tr}(\boldsymbol{\epsilon})]^2 \\
 &= \epsilon_{11}^2 + \epsilon_{22}^2 + \epsilon_{33}^2 + 2\epsilon_{12}^2 + 2\epsilon_{23}^2 + 2\epsilon_{13}^2 - \frac{1}{3} [\epsilon_{11}^2 + \epsilon_{22}^2 + \epsilon_{33}^2 + 2\epsilon_{11}\epsilon_{22} + 2\epsilon_{22}\epsilon_{33} + 2\epsilon_{11}\epsilon_{33}] \\
 &= \frac{1}{3} [(\epsilon_{11} - \epsilon_{22})^2 + (\epsilon_{22} - \epsilon_{33})^2 + (\epsilon_{33} - \epsilon_{11})^2] + 2(\epsilon_{12}^2 + \epsilon_{23}^2 + \epsilon_{13}^2)
 \end{aligned} \tag{2.11}$$

Therefore,

$$\epsilon_{\text{eff}} = \sqrt{\frac{2}{3} \left[\frac{1}{3} [(\epsilon_{11} - \epsilon_{22})^2 + (\epsilon_{22} - \epsilon_{33})^2 + (\epsilon_{33} - \epsilon_{11})^2] + 2(\epsilon_{12}^2 + \epsilon_{23}^2 + \epsilon_{13}^2) \right]} \tag{2.12}$$

For volume preserving plastic deformations, $\text{tr}(\boldsymbol{\epsilon}) = 0$, and we have

$$\epsilon_{\text{eff}} = \sqrt{\frac{2}{3} (\epsilon_{11}^2 + \epsilon_{22}^2 + \epsilon_{33}^2) + \frac{4}{3} (\epsilon_{12}^2 + \epsilon_{23}^2 + \epsilon_{13}^2)} = \sqrt{\frac{2}{3} (\epsilon_{11}^2 + \epsilon_{22}^2 + \epsilon_{33}^2) + \frac{1}{3} (\gamma_{12}^2 + \gamma_{23}^2 + \gamma_{13}^2)}. \tag{2.13}$$

2.1.4 Equivalent strain rate and plastic strain

The equivalent strain rate is defined as

$$\dot{\varepsilon}^{\text{eq}} = \sqrt{\dot{\varepsilon} : \dot{\varepsilon}} \quad (2.14)$$

where $\dot{\varepsilon}(t)$ is the strain rate tensor. The distortional equivalent strain rate is

$$\dot{\gamma}^{\text{eq}} = \sqrt{\frac{2}{3} \dot{\varepsilon}_s : \dot{\varepsilon}_s} \quad (2.15)$$

where $\dot{\varepsilon}_s(t)$ is the deviatoric strain rate tensor.

For models where an equivalent plastic strain is computed, we define a scalar equivalent plastic strain rate as

$$\dot{\varepsilon}_p^{\text{eq}} = \sqrt{\dot{\varepsilon}^p : \dot{\varepsilon}^p} \quad (2.16)$$

where $\dot{\varepsilon}^p(t)$ is the plastic strain rate tensor. The definition of the scalar equivalent plastic strain is

$$\varepsilon_p^{\text{eq}}(t) = \int_0^t \dot{\varepsilon}_p^{\text{eq}}(\tau) d\tau. \quad (2.17)$$

The corresponding distortional equivalent plastic strain rate and strain are defined as

$$\dot{\gamma}_p^{\text{eq}} = \sqrt{\frac{2}{3} \dot{\varepsilon}_s^p : \dot{\varepsilon}_s^p} \quad (2.18)$$

and

$$\gamma_p^{\text{eq}}(t) = \int_0^t \dot{\gamma}_p^{\text{eq}}(\tau) d\tau. \quad (2.19)$$

2.1.5 Velocity gradient, rate-of-deformation, deformation gradient

The velocity gradient is represented by \mathbf{I} and the deformation gradient by \mathbf{F} . The rate-of-deformation is

$$\mathbf{d} = \frac{1}{2}(\mathbf{I} + \mathbf{I}^T) = \frac{1}{2}(\nabla \mathbf{v} + \nabla \mathbf{v}^T). \quad (2.20)$$

2.1.6 Eigenvectors and coordinate transformations

For most situations, tensor components in VAANGO are expressed in terms of the basis vectors $\mathbf{e}_1 = (1, 0, 0)$, $\mathbf{e}_2 = (0, 1, 0)$, and $\mathbf{e}_3 = (0, 0, 1)$. However, in some situations tensor components have to be expressed in the eigenbasis of a second-order tensor. Let these eigenvectors be \mathbf{v}_1 , \mathbf{v}_2 and \mathbf{v}_3 . Then a vector \mathbf{a} with components (a_1, a_2, a_3) in the original basis has components (a'_1, a'_2, a'_3) in the eigenbasis. The two sets of components are related by

$$\begin{bmatrix} a'_1 \\ a'_2 \\ a'_3 \end{bmatrix} = \begin{bmatrix} \mathbf{e}_1 \cdot \mathbf{v}_1 & \mathbf{e}_2 \cdot \mathbf{v}_1 & \mathbf{e}_3 \cdot \mathbf{v}_1 \\ \mathbf{e}_1 \cdot \mathbf{v}_2 & \mathbf{e}_2 \cdot \mathbf{v}_2 & \mathbf{e}_3 \cdot \mathbf{v}_2 \\ \mathbf{e}_1 \cdot \mathbf{v}_3 & \mathbf{e}_2 \cdot \mathbf{v}_3 & \mathbf{e}_3 \cdot \mathbf{v}_3 \end{bmatrix} \begin{bmatrix} a_1 \\ a_2 \\ a_3 \end{bmatrix} = \begin{bmatrix} v_{11} & v_{12} & v_{13} \\ v_{21} & v_{22} & v_{23} \\ v_{31} & v_{32} & v_{33} \end{bmatrix} \begin{bmatrix} a_1 \\ a_2 \\ a_3 \end{bmatrix} = \mathbf{Q} \cdot \mathbf{a}. \quad (2.21)$$

The matrix that is used for this coordinate transformation, \mathbf{Q} , is given by

$$\mathbf{Q}^T := [\mathbf{v}_1 \quad \mathbf{v}_2 \quad \mathbf{v}_3] \quad (2.22)$$

where \mathbf{v}_1 , \mathbf{v}_2 , and \mathbf{v}_3 are **column vectors** representing the components of the eigenvectors in the reference basis.

The above coordinate transformation for vectors can be written in index notation as

$$a'_i = Q_{ij} a_j. \quad (2.23)$$

For transformations of second-order tensors, we have

$$T'_{ij} = Q_{ip} Q_{jq} T_{pq} . \quad (2.24)$$

For fourth-order tensors, the transformation relation is

$$C'_{ijkl} = Q_{im} Q_{jn} Q_{kp} Q_{\ell q} C_{mnpq} . \quad (2.25)$$

If the second-order tensor T is symmetric, we can express it in Mandel notation as a six-dimensional vector $\hat{\mathbf{t}}$:

$$\hat{\mathbf{t}} = [T_{11} \quad T_{22} \quad T_{33} \quad \sqrt{2}T_{23} \quad \sqrt{2}T_{31} \quad \sqrt{2}T_{12}]^T \quad (2.26)$$

Then the transformation matrix is a 6×6 matrix, $\hat{\mathbf{Q}}$, such that

$$\hat{\mathbf{t}}'_i = \hat{Q}_{ij} \hat{\mathbf{t}}_j . \quad (2.27)$$

The matrix $\hat{\mathbf{Q}}$ has components [19],

$$\hat{\mathbf{Q}} = \begin{bmatrix} Q_{11}^2 & Q_{12}^2 & Q_{13}^2 & \sqrt{2}Q_{12}Q_{13} & \sqrt{2}Q_{11}Q_{13} & \sqrt{2}Q_{11}Q_{12} \\ Q_{21}^2 & Q_{22}^2 & Q_{23}^2 & \sqrt{2}Q_{22}Q_{23} & \sqrt{2}Q_{21}Q_{23} & \sqrt{2}Q_{21}Q_{22} \\ Q_{31}^2 & Q_{32}^2 & Q_{33}^2 & \sqrt{2}Q_{32}Q_{33} & \sqrt{2}Q_{31}Q_{33} & \sqrt{2}Q_{31}Q_{32} \\ \sqrt{2}Q_{21}Q_{31} & \sqrt{2}Q_{22}Q_{32} & \sqrt{2}Q_{23}Q_{33} & Q_{22}Q_{33} + Q_{23}Q_{32} & Q_{21}Q_{33} + Q_{31}Q_{23} & Q_{21}Q_{32} + Q_{31}Q_{22} \\ \sqrt{2}Q_{11}Q_{31} & \sqrt{2}Q_{12}Q_{32} & \sqrt{2}Q_{13}Q_{33} & Q_{12}Q_{33} + Q_{32}Q_{13} & Q_{11}Q_{33} + Q_{13}Q_{31} & Q_{11}Q_{32} + Q_{31}Q_{12} \\ \sqrt{2}Q_{11}Q_{31} & \sqrt{2}Q_{12}Q_{22} & \sqrt{2}Q_{13}Q_{23} & Q_{12}Q_{23} + Q_{22}Q_{13} & Q_{11}Q_{23} + Q_{21}Q_{13} & Q_{11}Q_{22} + Q_{21}Q_{12} \end{bmatrix} \quad (2.28)$$

Similarly, the transformation relation for fourth-order tensors simplifies to

$$\hat{C}'_{ij} = \hat{Q}_{ip} \hat{Q}_{jq} \hat{C}_{pq} \quad (2.29)$$

where

$$\hat{\mathbf{C}} = \begin{bmatrix} C_{1111} & C_{1122} & C_{1133} & \sqrt{2}C_{1123} & \sqrt{2}C_{1131} & \sqrt{2}C_{1112} \\ C_{2211} & C_{2222} & C_{2233} & \sqrt{2}C_{2223} & \sqrt{2}C_{2231} & \sqrt{2}C_{2212} \\ C_{3311} & C_{3322} & C_{3333} & \sqrt{2}C_{3323} & \sqrt{2}C_{3331} & \sqrt{2}C_{3312} \\ \sqrt{2}C_{2311} & \sqrt{2}C_{2322} & \sqrt{2}C_{2333} & 2C_{2323} & 2C_{2331} & 2C_{2312} \\ \sqrt{2}C_{3111} & \sqrt{2}C_{3122} & \sqrt{2}C_{3133} & 2C_{3123} & 2C_{3131} & 2C_{3112} \\ \sqrt{2}C_{1211} & \sqrt{2}C_{1222} & \sqrt{2}C_{1233} & 2C_{1223} & 2C_{1231} & 2C_{1212} \end{bmatrix} \quad (2.30)$$

2.2 Material models available in Vaango

The MPM material models implemented in VAANGO were originally chosen for the following purposes:

- To verify the **accuracy** of the material point method (MPM) and to validate the **coupling** between the computational fluid dynamics code (ICE) and MPM.
- To model the elastic-plastic deformation of **metals** and the consequent damage in the regimes of both high and low strain rates and high and low temperatures.
- To model **polymer bonded explosives** and **polymers** under various strain rates and temperatures.
- To model the deformation of **biological tissues**.
- To model the explosive deformation of **rocks and soils**.

As of VAANGO Version 23 .4 .6 , the material models that have been implemented are:

1. Rigid material

2. Ideal gas material
3. Water material
4. Membrane material
5. Programmed burn material
6. Tabular equation of state
7. Murnaghan equation of state
8. JWL++ equation of state
9. Hypoelastic material
10. Hypoelastic material with manufactured solutions
11. Hypoelastic material implementation in FORTRAN
12. Polar-orthotropic hypoelastic material
13. Compressible neo-Hookean hyperelastic material
14. Compressible neo-Hookean hyperelastic material with manufactured solutions
15. Compressible neo-Hookean hyperelastic material with damage
16. Unified explicit/implicit compressible Neo-Hookean hyperelastic material with damage
17. Compressible Neo-Hookean hyperelastic- J_2 plastic material with damage
18. Compressible Mooney-Rivlin hyperelastic material
19. Compressible neo-Hookean material for shells
20. Transversely isotropic hyperelastic material
21. The p - α model for porous materials
22. Viscoelastic material written in FORTRAN for damping
23. Simplified Maxwell viscoelastic material
24. Visco-SCRAM model for viscoelastic materials with cracks
25. Visco-SCRAM hotspot model
26. Tabular plasticity model
27. Tabular plasticity model with cap
28. Hypoelastic J_2 plasticity model with damage for high-rates
29. Viscoplastic J_2 plasticity model
30. Mohr-Coulomb material
31. Drucker-Prager material with deformation induced elastic anisotropy
32. CAM-Clay model for soils
33. Nonlocal Drucker-Prager material
34. Arenisca material for rocks and soils
35. Arenisca3 material for rocks and soils
36. Arena material for partially saturated soils
37. Arena-mixture material for mixes of partially saturated sand and clay
38. Brannon's soil model
39. Soil foam model

A small subset of these models also have implementations that can be used with Implicit **MPM** .

Some of these models can work with multiple sub-models such as elasticity model or yield condition. As of VAANGO Version 23 .4 .6 , the implemented sub-models are:

1. Equations of state:
 - (a) Pressure model for Air
 - (b) Pressure model for Borja's CAMClay
 - (c) Pressure model for Granite
 - (d) Pressure model for hyperelastic materials
 - (e) Pressure model for Hypoelastic materials
 - (f) Pressure model for Mie-Gruneisen equation of state
 - (g) Mie-Gruneisen energy-based equation of state for pressure
 - (h) Pressure model for Water

2. Shear modulus models:
 - (a) Constant shear modulus model
 - (b) Shear modulus model for Borja's CAMClay
 - (c) Shear modulus model by Nadal and LePoac
 - (d) Mechanical Threshold Stress shear modulus model
 - (e) Preston-Tonks-Wallace shear modulus model
 - (f) Steinberg-Guinan shear modulus model
3. Combined elastic modulus models:
 - (a) Constant elastic modulus model
 - (b) Tabular elastic modulus model
 - (c) Neural net elastic modulus model
 - (d) Arena elastic modulus model
 - (e) Arena mixture elastic modulus model
 - (f) Arenisca elastic modulus model
4. Yield condition models:
 - (a) Yield condition for Arena model
 - (b) Yield condition for Arena mixture model
 - (c) Yield condition for Arenisca3 model
 - (d) Yield condition for CamClay model
 - (e) Yield condition for Gurson model
 - (f) Yield condition for Tabular plasticity with Cap
 - (g) Yield condition for Tabular plasticity with
 - (h) Yield condition for vonMises J_2 plasticity
 - (i) Classic Mohr-Coulomb model
 - (j) Sheng's Mohr-Coulomb model
5. Plastic flow stress models
 - (a) Isotropic hardening plastic flow model
 - (b) Johnson-Cook plastic flow model
 - (c) Mechanical Threshold Stress plastic flow model
 - (d) Preston-Tonks-Wallace plastic flow model
 - (e) Steinberg-Guinan plastic flow model
 - (f) SuvicI viscoplastic flow model
 - (g) Zerilli-Armstrong metal plastic flow model
 - (h) Zerilli-Armstrong polymer plastic flow model
6. Plastic internal variable models:
 - (a) Arena internal variable model
 - (b) Borja internal variable model
 - (c) Brannan's soil model internal variable model
 - (d) Tabular plasticity with cap internal variable model
7. Kinematic hardening models:
 - (a) Prager kinematic hardening model
 - (b) Armstrong-Frederick kinematic hardening model
 - (c) Arena kinematic hardening model
8. Damage models
 - (a) Becker's damage model
 - (b) Drucker and Becker combined damage model
 - (c) Drucker loss of stability model
 - (d) Johnson-Cook damage model
 - (e) Hancock-MacKenzie damage model
9. Melting model
 - (a) Constant melting temperature model

- (b) Linear melting temperature model
 - (c) BPS melting model
 - (d) Steinberg-Guinan melting temperature model
10. Specific heat model
- (a) Constant specific heat
 - (b) Cubic specific heat model
 - (c) Copper specific heat model
 - (d) Steel specific heat model

3 — Special material models

VAANGO contains a few material models that are designed for special problems. These are discussed in this chapter.

3.1 Rigid material

Applicable to: explicit and implicit MPM

This material model assumes that

$$\sigma(F, t) = \mathbf{0} \quad \text{and} \quad F(t) = I. \quad (3.1)$$

The model is a rough approximation of a rigid body as long as there is no contact between objects. Upon contact, the model should ideally transition into the form

$$\sigma(F, t) = \infty \quad \text{and} \quad F(t) = I. \quad (3.2)$$

This situation is approximated using the **specified body contact** algorithm which is applicable only in certain directions. Rigid materials were designed to act as rigid surfaces against which deformable objects could be compressed. The specified body contact algorithm can simulate the interaction of a single “master” rigid body with deformable objects.

3.2 Ideal gas material

Applicable to: explicit MPM only

The ideal gas material assumes that the stress at a particle is

$$\sigma(F, t) = \begin{cases} \bar{p}(F) I & \text{for } p \geq 0 \\ \mathbf{0} & \text{for } p < 0 \end{cases} \quad (3.3)$$

where $\bar{p} = -p$, and the pressure p is computed with an isentropic ideal gas equation of state:

$$p = p_{\text{ref}} [\exp(\gamma \bar{\epsilon}_v) - 1] ; \quad \bar{\epsilon}_v = \begin{cases} -\ln(J) & \text{for } J < 1 \\ 0 & \text{for } J \geq 1 \end{cases} \quad (3.4)$$

where $J = \det(\mathbf{F})$.

A rate of change of temperature (T) can also be computed by the model:

$$\frac{dT}{dt} = \frac{1}{\Delta t} \left(1 - \frac{J_{n+1}}{J_n} \right) \left(\frac{p}{\rho C_v} \right) \quad (3.5)$$

where $J_{n+1} = J(t_{n+1})$, $J_n = J(t_n)$, ρ is the mass density, and C_v is the constant volume specific heat.

3.3 Water material

Applicable to: explicit MPM only

This material models water [20], and assumes that the stress is given by

$$\boldsymbol{\sigma}(\mathbf{F}, t) = \bar{p}(\mathbf{F})\mathbf{I} + 2\mu\boldsymbol{\eta}. \quad (3.6)$$

where μ is a shear viscosity, \mathbf{d} is the symmetric part of the velocity gradient,

$$\bar{p} = -p \quad \text{and} \quad \boldsymbol{\eta} = \mathbf{d} - \frac{1}{3}\text{tr}(\mathbf{d})\mathbf{I}. \quad (3.7)$$

The pressure is given by:

$$p = \kappa [J^{-\gamma} - 1], \quad J = \det(\mathbf{F}) \quad (3.8)$$

where κ the bulk modulus and γ is a model parameter. It has not been validated, but gives qualitatively reasonable behavior.

3.4 Murnaghan material

Applicable to: explicit MPM only

This material is based on the equation of state proposed in [21]. The stress is given by

$$\boldsymbol{\sigma}(\mathbf{F}, t) = \bar{p}(\mathbf{F})\mathbf{I} + 2\mu\boldsymbol{\eta}. \quad (3.9)$$

where μ is a shear viscosity, \mathbf{d} is the symmetric part of the velocity gradient,

$$\bar{p} = -p \quad \text{and} \quad \boldsymbol{\eta} = \mathbf{d} - \frac{1}{3}\text{tr}(\mathbf{d})\mathbf{I}. \quad (3.10)$$

The pressure is given by:

$$p = \frac{\kappa}{\kappa'} [J^{-\kappa'} - 1], \quad J = \det(\mathbf{F}) \quad (3.11)$$

where κ the initial bulk modulus and $\kappa' = d\kappa/dp$ is a constant.

3.5 JWL++ material

Applicable to: explicit MPM only

The JWL++ material is a combination of the Murnaghan and JWL models along with a burn algorithm to convert from one to the other [22]. A small viscous component is added to the JWL model to stabilize behavior.

The stress is given by

$$\boldsymbol{\sigma}(\mathbf{F}, t) = \bar{p}(\mathbf{F})\mathbf{I} + 2\mu\boldsymbol{\eta}. \quad (3.12)$$

where μ is a shear viscosity, \mathbf{d} is the symmetric part of the velocity gradient,

$$\bar{p} = -p \quad \text{and} \quad \boldsymbol{\eta} = \mathbf{d} - \frac{1}{3}\text{tr}(\mathbf{d})\mathbf{I}. \quad (3.13)$$

The burn rate is computed as

$$\dot{f} = (1 - f)G p^b \quad (3.14)$$

where f is the volume fraction of the reactant, G, b are fit parameters, and p is the pressure, computed using

$$p = (1 - f)p_m + f p_{\text{jwl}}. \quad (3.15)$$

The Murnaghan pressure (p_m) is given by:

$$p_m = \frac{1}{nK} [J^{-n} - 1], \quad J = \det(\mathbf{F}) \quad (3.16)$$

where $K = 1/\kappa$, κ is the initial bulk modulus, and $n = \kappa' = d\kappa/dp$ is a constant.

The JWL pressure (p_{jwl}) is given by

$$p_{\text{jwl}} = A \exp(-R_1 J) + B \exp(-R_2 J) + C J^{-(1+\omega)} \quad (3.17)$$

where A, B, C, ω are fit parameters, R_1, R_2 are fit rate parameters, and $J = \det \mathbf{F}$.

4 — Elastic material models

4.1 Hypoelastic material

Applicable to: explicit and implicit MPM

Hypoelastic materials have stress-deformation relationships of the form

$$\dot{\sigma}(\mathbf{F}) = \mathbb{C}(\mathbf{F}) : \mathbf{d}(\mathbf{F}) \quad (4.1)$$

where \mathbb{C} is an elastic stiffness tensor and \mathbf{d} is the symmetric part of the velocity gradient.

The base hypoelastic material implemented in Vaango is linear and isotropic:

$$\dot{\sigma} = \left(\kappa - \frac{2}{3}\mu \right) \text{tr}(\mathbf{d}) \mathbf{I} + 2\mu \mathbf{d} \quad (4.2)$$

where μ is the shear modulus and κ is the bulk modulus.

To ensure frame indifference, both σ and \mathbf{d} are unrotated using the beginning of the timestep deformation gradient polar decomposition before any constitutive relations are evaluated. The updated stress is rotated back using the deformation gradient decomposition at the end of the time step.

4.2 Hyperelastic Material Models

Several hyperelastic material models have been implemented in VAANGO. Other models can be easily implemented using the available infrastructure. The general model has the form

$$\sigma = \frac{1}{J} \frac{\partial W}{\partial \mathbf{F}} \cdot \mathbf{F}^T \quad (4.3)$$

where W is a strain energy function and $J = \det \mathbf{F}$. For isotropic hyperelastic functions that are expressed in terms of the invariants (I_1, I_2, J) of the right Cauchy-Green deformation ($\mathbf{C} = \mathbf{F}^T \cdot \mathbf{F}$), the Cauchy stress is given by

$$\sigma = \frac{2}{J} \left[\frac{1}{J^{2/3}} \left(\frac{\partial W}{\partial \bar{I}_1} + \bar{I}_1 \frac{\partial W}{\partial \bar{I}_2} \right) \mathbf{B} - \frac{1}{J^{4/3}} \frac{\partial W}{\partial \bar{I}_2} \mathbf{B} \cdot \mathbf{B} \right] + \left[\frac{\partial W}{\partial J} - \frac{2}{3J} \left(\bar{I}_1 \frac{\partial W}{\partial \bar{I}_1} + 2 \bar{I}_2 \frac{\partial W}{\partial \bar{I}_2} \right) \right] \mathbf{I} \quad (4.4)$$

where $\mathbf{B} = \mathbf{F} \cdot \mathbf{F}^T$, and

$$J = \det \mathbf{F}, \quad \bar{I}_1 = J^{-2/3} I_1, \quad \bar{I}_2 = J^{-4/3} I_2, \quad I_1 = \text{tr} \mathbf{C}, \quad I_2 = \frac{1}{2} [(\text{tr} \mathbf{C})^2 - \text{tr}(\mathbf{C} \cdot \mathbf{C})] \quad (4.5)$$

Note that I_1 and I_2 are identical for \mathbf{C} and \mathbf{B} . Alternatively,

$$\boldsymbol{\sigma} = \frac{2}{J} \left[\left(\frac{\partial W}{\partial I_1} + I_1 \frac{\partial W}{\partial I_2} \right) \mathbf{B} - \frac{\partial W}{\partial I_2} \mathbf{B} \cdot \mathbf{B} \right] + 2J \frac{\partial W}{\partial I_3} \mathbf{I} \quad (4.6)$$

where $I_3 = J^2$.

The P-wave speed (c) needed to estimate the timestep can be computed using

$$c_i^2 = \frac{1}{\rho J} \frac{\partial^2 W}{\partial \lambda_i^2} = \frac{1}{\rho J} \left[\frac{\partial W}{\partial I_1} \frac{\partial^2 I_1}{\partial \lambda_i^2} + \frac{\partial W}{\partial I_2} \frac{\partial^2 I_2}{\partial \lambda_i^2} + \frac{\partial W}{\partial I_3} \frac{\partial^2 I_3}{\partial \lambda_i^2} \right] \quad (4.7)$$

where λ_i are the principal stretches, i.e., $I_1 = \sum_i \lambda_i^2$, $I_2 = \lambda_1^2 \lambda_2^2 + \lambda_2^2 \lambda_3^2 + \lambda_1^2 \lambda_3^2$ and $I_3 = \lambda_1^2 \lambda_2^2 \lambda_3^2$.

4.2.1 Compressible neo-Hookean material

Applicable to: **explicit** and **implicit MPM**

The default strain energy function for the compressible neo-Hookean material model implemented in VAANGO is ([23], p.307):

$$W = \frac{\kappa}{2} \left[\frac{1}{2} (J^2 - 1) - \ln J \right] + \frac{\mu}{2} [\bar{I}_1 - 3] \quad (4.8)$$

The Cauchy stress corresponding to this function is

$$\boldsymbol{\sigma} = \frac{\kappa}{2} \left(J - \frac{1}{J} \right) \mathbf{I} + \frac{\mu}{J} (\bar{\mathbf{B}} - \frac{1}{3} \bar{I}_1 \mathbf{I}) \quad (4.9)$$

where $\bar{\mathbf{B}} = J^{-2/3} \mathbf{B} = J^{-2/3} \mathbf{F} \cdot \mathbf{F}^T$ and $J = \det \mathbf{F}$. Consistency with linear elasticity requires that $\kappa = K$ and $\mu = G$ where K and G are the linear elastic bulk and shear moduli, respectively.

Alternative expressions for the bulk modulus factor are allowed and defined in the equation-of-state sub-models.

4.2.2 Compressible Mooney-Rivlin material

Applicable to: **explicit MPM** only

The compressible Mooney-Rivlin material implemented in VAANGO has the form

$$W = C_1(I_1 - 3) + C_2(I_2 - 3) + C_3 \left(\frac{1}{I_3^2} - 1 \right) + C_4(I_3 - 1)^2 \quad (4.10)$$

where C_1 , C_2 and ν are parameters and

$$C_3 = \frac{1}{2}(C_1 + 2C_2), \quad C_4 = \frac{1}{2} \left[\frac{C_1(5\nu - 2) + C_2(11\nu - 5)}{1 - 2\nu} \right]. \quad (4.11)$$

The corresponding Cauchy stress is

$$\boldsymbol{\sigma} = \frac{2}{J} \left[(C_1 + C_2 I_1) \mathbf{B} - C_2 \mathbf{B} \cdot \mathbf{B} + J^2 \left[-\frac{2C_3}{I_3^3} + 2C_4(I_3 - 1) \right] \right]. \quad (4.12)$$

4.2.3 Transversely isotropic hyperelastic material

Applicable to: **explicit** and **implicit** MPM

The transversely isotropic material model implemented in VAANGO is based on [24]. The model assumes a stiffer, “fiber”, direction denoted $\hat{\mathbf{f}}$ and isotropy orthogonal to that direction.

The strain energy density function for the model has the form

$$W = W_v + W_d \quad (4.13)$$

where W_v is the volumetric part and W_d is the deviatoric (volume preserving) part. The volumetric part of the strain energy is given by

$$W_v = \frac{1}{2} \kappa (\ln J)^2 \quad (4.14)$$

where κ is the bulk modulus and $J = \det \mathbf{F}$. The deviatoric part, W_d , is given by

$$W_d = \begin{cases} C_1(\bar{I}_1 - 3) + C_2(\bar{I}_2 - 3) + C_3 [\exp(C_4(\bar{\lambda} - 1)) - 1] & \text{for } \bar{\lambda} < \lambda^* \\ C_1(\bar{I}_1 - 3) + C_2(\bar{I}_2 - 3) + C_5 \bar{\lambda} + C_6 \ln \bar{\lambda} & \text{for } \bar{\lambda} \geq \lambda^* \end{cases} \quad (4.15)$$

where $C_1, C_2, C_3, C_4, C_5, \lambda^*$ are model parameters, and

$$C_6 = C_3 [\exp(C_4(\lambda^* - 1)) - 1] - C_5 \lambda^* \quad (4.16)$$

$$\bar{\lambda} = \sqrt{\bar{I}_4}, \quad \bar{I}_4 = \hat{\mathbf{f}} \cdot (\bar{\mathbf{C}} \cdot \hat{\mathbf{f}}), \quad \bar{\mathbf{C}} = J^{-2/3} \mathbf{C}.$$

The fiber direction is updated using

$$\hat{\mathbf{f}}_{n+1} = \frac{J^{-1/3}}{\bar{\lambda}} \mathbf{F} \cdot \hat{\mathbf{f}}_n. \quad (4.17)$$

The Cauchy stress is given by

$$\boldsymbol{\sigma} = p \mathbf{I} + \boldsymbol{\sigma}_d + \boldsymbol{\sigma}_f \quad (4.18)$$

where

$$p = \kappa \frac{\ln(J)}{J}$$

$$\boldsymbol{\sigma}_d = \frac{2}{J} \left[(C_1 + C_2 \bar{I}_1) \bar{\mathbf{B}} - C_2 \bar{\mathbf{B}} \cdot \bar{\mathbf{B}} - \frac{1}{3} (C_1 \bar{I}_1 + 2C_2 \bar{I}_2) \mathbf{I} \right] \quad (4.19)$$

$$\boldsymbol{\sigma}_f = \frac{\bar{\lambda}}{J} \frac{\partial W_d}{\partial \bar{\lambda}} \left(\hat{\mathbf{f}}_{n+1} \otimes \hat{\mathbf{f}}_{n+1} - \frac{1}{3} \mathbf{I} \right)$$

The model also contains a failure feature that sets $\boldsymbol{\sigma}_d = \mathbf{0}$ when the maximum shear strain, defined as the difference between the maximum and minimum eigenvalues of \mathbf{C} , exceeds a critical shear strain value. Also, a fiber stretch failure criterion can be used that compares $\sqrt{\bar{I}_4}$ with a critical stretch value and sets $\boldsymbol{\sigma}_f = \mathbf{0}$ if this value is exceeded.

4.3 Elastic modulus models

Applicable to: **Hypoelastic** **Tabular** material models

For selected material models that use isotropic hypoelasticity models and require bulk and shear moduli, specialized elastic moduli models can be used. Some of these models are discussed in this section.

4.3.1 Support vector regression model

The support vector regression (SVR) approach [25, 26] can be used to fit bulk modulus models to data without the need for closed form expressions. The advantage of this approach is that the resulting model requires few function evaluations and can, in principle, be computed as fast as a closed-form model.

For the purpose of fitting a bulk modulus model we assume that the input (training) data are of the form $\{(\boldsymbol{\varepsilon}_1, p_1), (\boldsymbol{\varepsilon}_2, p_2), \dots, (\boldsymbol{\varepsilon}_m, p_m)\} \subset \mathbb{R}^2 \times \mathbb{R}$. Here $\boldsymbol{\varepsilon}_i = (\boldsymbol{\varepsilon}_i, \varepsilon_i^p)$ where $\boldsymbol{\varepsilon}$ is the total volumetric strain and ε^p is the plastic volumetric strain and p_i is the mean stress (assumed positive in compression). The aim of SVR is to find a function $p = f(\boldsymbol{\varepsilon})$ that fits the data such that the function is as flat as possible (in $d + 1$ -dimensional space), and deviates from p_i by at most ϵ (a small quantity).

In nonlinear support vector regression we fit functions of the form

$$p = f(\boldsymbol{\varepsilon}) = \mathbf{w} \cdot \boldsymbol{\phi}(\boldsymbol{\varepsilon}) + b \quad (4.20)$$

where \mathbf{w} is a vector of parameters, $\boldsymbol{\phi}(\boldsymbol{\varepsilon})$ are vector-valued basis functions, (\cdot) is an inner product, and b is a scalar offset. The fitting process can be posed as the following primal convex optimization problem [27]:

$$\begin{aligned} & \underset{\mathbf{w}, b, \xi, \xi^*}{\text{minimize}} && \frac{1}{2} \mathbf{w} \cdot \mathbf{w} + C \sum_{i=1}^m (\xi_i + \xi_i^*) \\ & \text{subject to} && \begin{cases} -(\xi_i + \epsilon) \leq p_i - \mathbf{w} \cdot \boldsymbol{\phi}(\boldsymbol{\varepsilon}_i) - b \leq \xi_i^* + \epsilon \\ \xi_i, \xi_i^* \geq 0, \quad i = 1 \dots m \end{cases} \end{aligned} \quad (4.21)$$

where C is a constraint multiplier, m is the number of data points, and ξ_i, ξ_i^* are constraints.

In practice, it is easier to solve the dual problem for which the expansion for $f(\boldsymbol{\varepsilon})$ becomes

$$p = f(\boldsymbol{\varepsilon}) = \sum_{i=1}^m (\lambda_i^* - \lambda_i) K(\boldsymbol{\varepsilon}_i, \boldsymbol{\varepsilon}) + b, \quad K(\boldsymbol{\varepsilon}_i, \boldsymbol{\varepsilon}) = \boldsymbol{\phi}(\boldsymbol{\varepsilon}_i) \cdot \boldsymbol{\phi}(\boldsymbol{\varepsilon}) \quad (4.22)$$

where $\boldsymbol{\varepsilon}_i$ are the sample vectors, λ_i and λ_i^* are dual coefficients, and $K(\boldsymbol{\varepsilon}_i, \boldsymbol{\varepsilon})$ is a kernel function. The dual convex optimization problem has the form

$$\begin{aligned} & \underset{\lambda, \lambda^*}{\text{minimize}} && \frac{1}{2} \sum_{i,j=1}^m (\lambda_i - \lambda_i^*) K(\boldsymbol{\varepsilon}_i, \boldsymbol{\varepsilon}_j) (\lambda_j - \lambda_j^*) + \epsilon \sum_{i=1}^m (\lambda_i + \lambda_i^*) + \sum_{i=1}^m p_i (\lambda_i - \lambda_i^*) \\ & \text{subject to} && \begin{cases} \sum_{i=1}^m (\lambda_i - \lambda_i^*) = 0 \\ \lambda_i, \lambda_i^* \in [0, C], \quad i = 1 \dots m. \end{cases} \end{aligned} \quad (4.23)$$

The free parameters for the fitting process are the quantities ϵ and C . SVR accuracy also depends strongly on the choice of kernel function. In this paper, we use the Gaussian radial basis function:

$$K(\boldsymbol{\varepsilon}_i, \boldsymbol{\varepsilon}_j) = \exp \left[-\frac{(\boldsymbol{\varepsilon}_i - \boldsymbol{\varepsilon}_j) \cdot (\boldsymbol{\varepsilon}_i - \boldsymbol{\varepsilon}_j)}{\sigma^2 d} \right] = \exp \left[-\gamma \|\boldsymbol{\varepsilon}_i - \boldsymbol{\varepsilon}_j\|^2 \right], \quad \gamma := \frac{1}{\sigma^2 d} \quad (4.24)$$

where d is the dimension of $\boldsymbol{\varepsilon}$ and σ^2 is the width of the support of the kernel (assumed to be equal to the norm of the covariance matrix of the training data in this paper).

The minimization problem solves for the difference in the dual coefficients $(\lambda - \lambda^*)$ and the intercept (b), and outputs a reduced set ($m_{SV} < m$) of values of $\boldsymbol{\varepsilon}_i$ called “support vectors”. Given these quantities, the function (4.22) can be evaluated quite efficiently, particularly if the number of support vectors is small. SVR fits to data can be computed using software such as the **LIBSVM** library [28]. A variation of the above approach, called ν -SVR [25] can also be used if sufficient computational resources are available.

The bulk modulus can be computed from (4.22) using

$$\kappa(\boldsymbol{\varepsilon}) = \frac{\partial p}{\partial \varepsilon^e} = \frac{\partial p}{\partial \varepsilon} = \sum_{i=1}^{m_{SV}} (\lambda_i^* - \lambda_i) \frac{\partial K_i}{\partial \varepsilon}, \quad K_i := K(\boldsymbol{\varepsilon}_i, \boldsymbol{\varepsilon}) \quad (4.25)$$

From (4.24),

$$\frac{\partial K_i}{\partial \varepsilon} = 2\gamma(\varepsilon_i - \varepsilon) \exp[-\gamma \|\boldsymbol{\varepsilon}_i - \boldsymbol{\varepsilon}\|^2] \quad (4.26)$$

Therefore, the bulk modulus is given by,

$$\kappa(\boldsymbol{\varepsilon}) = \sum_{i=1}^{m_{SV}} 2\gamma(\lambda_i^* - \lambda_i)(\varepsilon_i - \varepsilon) \exp[-\gamma \|\boldsymbol{\varepsilon}_i - \boldsymbol{\varepsilon}\|^2] \quad (4.27)$$

If we need to account for elastic-plastic coupling, we may also need the derivative

$$\frac{\partial \kappa}{\partial \varepsilon^p} = \sum_{i=1}^{m_{SV}} 4\gamma^2(\lambda_i^* - \lambda_i)(\varepsilon_i - \varepsilon)(\varepsilon_i^p - \varepsilon^p) \exp[-\gamma \|\boldsymbol{\varepsilon}_i - \boldsymbol{\varepsilon}\|^2] \quad (4.28)$$

The bulk modulus model is also associated with a shear modulus model that computes the value of μ using a Poisson's ratio (ν) based on the value of κ . The VAANGO implementation can be accessed in the tabular plasticity models, using the tag `<elastic_moduli_model type="support_vector">`.



5 — Plasticity

Most plasticity models in VAANGO are implemented as stand-alone models with their own elasticity law, yield condition, flow rule, and internal variable evolution rules. However, because of the large number of possible combinations of these, a few metal plasticity models are available that allow the user to swap out one set of rules for another.

The list below is not comprehensive. Please see the following chapters for details of the models actually available in VAANGO .

The plasticity implementations typically contain the following:

1. **An elasticity model :**
 - Isotropic linear elastic model.
 - Anisotropic linear elastic models.
 - Isotropic nonlinear elastic models.
 - Anisotropic nonlinear elastic models.
 - **Equation of state** to determine the pressure (or volumetric response), for example,
 - Mie-Gruneisen equation of state.
 - **Deviatoric stress model** to determine the shear response.
 - Nadal-LePoac shear modulus model
 - Steinberg-Guinan shear modulus model
2. **A yield condition :**
 - von Mises yield condition.
 - Drucker-Prager yield condition.
 - Mohr-Coulomb yield condition.
 - Gurson-Needleman-Tvergaard yield condition.
3. **A flow rule :**
 - Associated flow.
 - Non-Associated flow using either a flow potential or a material parameter.
4. **Isotropic hardening :**
 - Perfect plasticity (no hardening).
 - Johnson-Cook plasticity.
 - Mechanical Threshold Stress (MTS) plasticity.
5. **Kinematic hardening :**
 - Isotropic backstress.

- Deviatoric backstress.
- 6. **Isotropic hardening internal variable evolution rules :**
 - Mechanical threshold stress evolution.
 - Gurson's porosity evolution law.
- 7. **Kinematic hardening internal variable evolution rules :**
 - Ziegler-Prager evolution rule.
 - Armstrong-Frederick evolution rule
- 8. **Damage evolution rules :**
 - Johnson-Cook damage model.
 - Brittle damage model.
- 9. **Melting temperature models**
- 10. **Specific heat models**
- 11. **Material stability-based localization models :**
 - Acoustic tensor.
 - Drucker stability.

The models used by the main plasticity codes in the current implementation of VAANGO are described in the following chapters, followed by descriptions of the plasticity algorithms themselves.

6 — Equation of state models

In the isotropic metal plasticity models implemented in VAANGO, the volumetric part of the Cauchy stress can be calculated using an equation of state. The equations of state that are implemented in VAANGO are described below.

6.1 Hypoelastic equation of state

In this case we assume that the stress rate is given by

$$\dot{\boldsymbol{\sigma}} = \lambda \operatorname{tr}(\mathbf{d}^e) \mathbf{I} + 2 \mu \mathbf{d}^e \quad (6.1)$$

where $\boldsymbol{\sigma}$ is the Cauchy stress, \mathbf{d}^e is the elastic part of the rate of deformation, and λ, μ are constants.

If $\operatorname{dev}(\mathbf{d}^e)$ is the deviatoric part of \mathbf{d}^e then we can write

$$\dot{\boldsymbol{\sigma}} = \left(\lambda + \frac{2}{3} \mu \right) \operatorname{tr}(\mathbf{d}^e) \mathbf{I} + 2 \mu \operatorname{dev}(\mathbf{d}^e) = \kappa \operatorname{tr}(\mathbf{d}^e) \mathbf{I} + 2 \mu \operatorname{dev}(\mathbf{d}^e) . \quad (6.2)$$

If we split $\boldsymbol{\sigma}$ into a volumetric and a deviatoric part, i.e., $\boldsymbol{\sigma} = p \mathbf{I} + \mathbf{s}$, take the time derivative to get $\dot{\boldsymbol{\sigma}} = \dot{p} \mathbf{I} + \dot{\mathbf{s}}$, and compare the result with (6.2), we see that

$$\dot{p} = \kappa \operatorname{tr}(\mathbf{d}^e) . \quad (6.3)$$

In addition we assume that $\mathbf{d} = \mathbf{d}^e + \mathbf{d}^p$. If we also assume that the plastic volume change is negligible ($\operatorname{tr}(\mathbf{d}^p) \approx 0$), which is reasonable for a void-free metal matrix, we have

$$\dot{p} = \kappa \operatorname{tr}(\mathbf{d}) . \quad (6.4)$$

This is the equation that is used to calculate the pressure p in the default hypoelastic equation of state. For a forward Euler integration step,

$$p_{n+1} = p_n + \kappa \operatorname{tr}(\mathbf{d}_{n+1}) \Delta t . \quad (6.5)$$

To get the derivative of p with respect to J , where $J = \det(\mathbf{F})$, we note that

$$\dot{p} = \frac{\partial p}{\partial J} \dot{J} = \frac{\partial p}{\partial J} J \operatorname{tr}(\mathbf{d}) . \quad (6.6)$$

Therefore,

$$\frac{\partial p}{\partial J} = \frac{\kappa}{J}. \quad (6.7)$$

This model is invoked in VAANGO using

```
<equation_of_state type="default_hypo">
</equation_of_state>
```

6.2 Default hyperelastic equation of state

In this model the pressure is computed using the relation

$$p = \frac{1}{2} \kappa \left(J^e - \frac{1}{J^e} \right) \quad (6.8)$$

where κ is the bulk modulus and J^e is determinant of the elastic part of the deformation gradient.

We can also compute

$$\frac{dp}{dJ} = \frac{1}{2} \kappa \left(1 + \frac{1}{(J^e)^2} \right). \quad (6.9)$$

The metal plasticity implementations in VAANGO assume that the volume change of the matrix during plastic deformation can be neglected, i.e., $J^e = J$.

This model is invoked using

```
<equation_of_state type="default_hyper">
</equation_of_state>
```

6.3 Mie-Grüneisen equation of state

The pressure (p) is calculated using a Mie-Grüneisen equation of state of the form ([14, 29])

$$p = -\frac{\rho_0 C_0^2 (1 - J^e) [1 - \Gamma_0 (1 - J^e)/2]}{[1 - S_\alpha (1 - J^e)]^2} - \Gamma_0 E; \quad J^e := \det \mathbf{F}^e \quad (6.10)$$

where C_0 is the bulk speed of sound, ρ_0 is the initial mass density, Γ_0 is the Grüneisen's gamma at the reference state, $S_\alpha = dU_s/dU_p$ is a linear Hugoniot slope coefficient, U_s is the shock wave velocity, U_p is the particle velocity, and E is the internal energy density (per unit reference volume), \mathbf{F}^e is the elastic part of the deformation gradient. For isochoric plasticity,

$$J^e = J = \det(\mathbf{F}) = \frac{\rho_0}{\rho}.$$

The internal energy is computed using

$$E = \frac{1}{V_0} \int C_v dT \approx \frac{C_v (T - T_0)}{V_0} \quad (6.11)$$

where $V_0 = 1/\rho_0$ is the reference specific volume at temperature $T = T_0$, and C_v is the specific heat at constant volume.

Also,

$$\frac{\partial p}{\partial J^e} = \frac{\rho_o C_o^2 [1 + (S_\alpha - \Gamma_o) (1 - J^e)]}{[1 - S_\alpha (1 - J^e)]^3} - \Gamma_o \frac{\partial E}{\partial J^e}. \quad (6.12)$$

We neglect the $\frac{\partial E}{\partial J^e}$ term in our calculations.

This model is invoked in Vaango using

```
<equation_of_state type="mie_gruneisen">
  <C_0>5386</C_0>
  <Gamma_0>1.99</Gamma_0>
  <S_alpha>1.339</S_alpha>
  <rho_0> 7200 </rho_0>
</equation_of_state>
```

An alternative formulation is also available that can be used for models where a linear Hugoniot is not accurate enough. A cubic model can be used in that formulation.

$$p_{n+1} = -\frac{\rho_o C_o^2 (1 - J_{n+1}^e) [1 - \Gamma_o (1 - J_{n+1}^e)/2]}{[1 - S_\alpha (1 - J_{n+1}^e) - S_2 (1 - J_{n+1}^e)^2 - S_3 (1 - J_{n+1}^e)^3]^2} - \Gamma_o e_{n+1}; \quad J^e := \det \mathbf{F}^e \quad (6.13)$$

This model is invoked using the label **mie_gruneisen_energy**.

6.4 Equations of state used in the ARENA model

In many models, a tangent bulk modulus is computed using the equation of state and the pressure is updated using an integration step. While this approach less accurate than directly evaluating the equation of state, it is useful when a composite material is being simulated that does not have well-characterized equations of state at all states.

The equations of state used by the ARENA model for soils are described below. The bars above quantities indicate negation.

6.4.1 Solid matrix material

The pressure in the solid matrix is expressed as

$$\bar{p}_s = K_s \bar{\epsilon}_v^s; \quad \bar{\epsilon}_v^s := \ln \left(\frac{V_{so}}{V_s} \right) \quad (6.14)$$

where $\bar{p}_s = -p_s$ is the solid matrix pressure, K_s is the solid bulk modulus, $\bar{\epsilon}_v^s$ is the volumetric strain, V_{so} is the initial volume of the solid, and V_s is the current volume of the solid. The solid bulk modulus is assumed to modeled by the Murnaghan equation:

$$K_s(\bar{p}_s) = K_{so} + n_s (\bar{p}_s - \bar{p}_{so}) \quad (6.15)$$

where K_{so} and n_s are material properties, and \bar{p}_{so} is a reference pressure.

6.4.2 Pore water

The equation of state of the pore water is

$$\bar{p}_w = K_w \bar{\epsilon}_v^w + \bar{p}_o; \quad \bar{\epsilon}_v^w := \ln \left(\frac{V_{wo}}{V_w} \right) \quad (6.16)$$

where $\bar{p}_w = -p_w$ is the water pressure, K_w is the water bulk modulus, V_{w0} is the initial volume of water, V_w is the current volume of water, \bar{p}_0 is the initial water pressure, and $\bar{\varepsilon}_v^w$ is the volumetric strain in the water. We use the isothermal Murnaghan bulk modulus model for water:

$$K_w(\bar{p}_w) = K_{w0} + n_w (\bar{p}_w - \bar{p}_{w0}) \quad (6.17)$$

where K_{w0} and n_w are material properties, and \bar{p}_{w0} is a reference pressure.

6.4.3 Pore air

The isentropic ideal gas equation of state for the pore air is

$$\bar{p}_a = \bar{p}_r [\exp(\gamma \bar{\varepsilon}_v^a) - 1] ; \quad \bar{\varepsilon}_v^a := \ln \left(\frac{V_{a0}}{V_a} \right) \quad (6.18)$$

where the quantities with subscript a represent quantities for the air model analogous to those for the water model in (??), \bar{p}_r is a reference pressure (101325 Pa) and $\gamma = 1.4$. The bulk modulus of air (K_a) varies with the volumetric strain in the air:

$$K_a = \frac{d\bar{p}_a}{d\bar{\varepsilon}_v^a} = \gamma \bar{p}_r \exp(\gamma \bar{\varepsilon}_v^a) = \gamma (\bar{p}_a + \bar{p}_r) . \quad (6.19)$$



7 — Deviatoric stress models

Isotropic plasticity models in VAANGO typically assume hypoelasticity, for which the stress rate is given by

$$\dot{\boldsymbol{\sigma}} = \dot{p} \mathbf{I} + \dot{\mathbf{s}} = \kappa \operatorname{tr}(\mathbf{d}^e) \mathbf{I} + 2 \mu \operatorname{dev}(\mathbf{d}^e) \quad (7.1)$$

where $\boldsymbol{\sigma} = p \mathbf{I} + \mathbf{s}$ is the Cauchy stress, $p = \operatorname{tr}(\boldsymbol{\sigma})$, \mathbf{s} is the deviatoric stress, \mathbf{d}^e is the elastic part of the rate of deformation, and κ, μ are the bulk and shear moduli.

The pressure is computed using an equation of state as described in the chapter 6. The deviatoric stress is computed using the relation

$$\dot{\mathbf{s}} = 2 \mu \operatorname{dev}(\mathbf{d}^e). \quad (7.2)$$

If a forward Euler stress update is used, we have

$$\mathbf{s}_{n+1} = \mathbf{s}_n + 2 \mu \operatorname{dev}(\mathbf{d}_{n+1}^e) \Delta t. \quad (7.3)$$

For linear elastic materials, the shear modulus can vary with temperature and pressure. Several shear modulus models are available in VAANGO for computing the value for a given state.

For linear viscoelastic materials to be used with plasticity, a Maxwell model is available in VAANGO where the deviatoric stress is computed as a sum of Maxwell elements:

$$\mathbf{s}_{n+1} = \mathbf{s}_n + 2 \sum_j \mu_j \operatorname{dev}(\mathbf{d}_{n+1}^e) \Delta t. \quad (7.4)$$

7.1 Shear modulus models

Shear modulus models that are available in VAANGO are described below.

7.1.1 Constant shear modulus

The default model gives a constant shear modulus. The model is invoked using

```
<shear_modulus_model type="constant_shear">
  <shear_modulus> 1.0e8 </shear_modulus>
</shear_modulus_model>
```

7.1.2 Mechanical Threshold Stress shear modulus

The simplest model is of the form suggested by [30] ([31])

$$\mu(T) = \mu_o - \frac{D}{\exp(T_o/T) - 1} \quad (7.5)$$

where μ_o is the shear modulus at oK, and D , T_o are material constants.

The model is invoked using

```
<shear_modulus_model type="mts_shear">
  <mu_0>28.0e9</mu_0>
  <D>4.50e9</D>
  <T_0>294</T_0>
</shear_modulus_model>
```

7.1.3 SCG shear modulus

The Steinberg-Cochran-Guinan (SCG) shear modulus model ([29, 32]) is pressure dependent and has the form

$$\mu(p, T) = \mu_o + \frac{\partial \mu}{\partial p} \frac{p}{\eta^{1/3}} + \frac{\partial \mu}{\partial T} (T - 300); \quad \eta = \rho/\rho_o \quad (7.6)$$

where, μ_o is the shear modulus at the reference state ($T = 300$ K, $p = 0$, $\eta = 1$), p is the pressure, and T is the temperature. When the temperature is above T_m , the shear modulus is instantaneously set to zero in this model.

The model is invoked using

```
<shear_modulus_model type="scg_shear">
  <mu_0> 81.8e9 </mu_0>
  <A> 20.6e-12 </A>
  <B> 0.16e-3 </B>
</shear_modulus_model>
```

7.1.4 Nadal-LePoac (NP) shear modulus

A modified version of the SCG model has been developed by [33] that attempts to capture the sudden drop in the shear modulus close to the melting temperature in a smooth manner. The Nadal-LePoac (NP) shear modulus model has the form

$$\mu(p, T) = \frac{1}{\mathcal{J}(\hat{T})} \left[\left(\mu_o + \frac{\partial \mu}{\partial p} \frac{p}{\eta^{1/3}} \right) (1 - \hat{T}) + \frac{\rho}{Cm} k_b T \right]; \quad C := \frac{(6\pi^2)^{2/3}}{3} f^2 \quad (7.7)$$

where

$$\mathcal{J}(\hat{T}) := 1 + \exp \left[-\frac{1 + 1/\zeta}{1 + \zeta/(1 - \hat{T})} \right] \quad \text{for} \quad \hat{T} := \frac{T}{T_m} \in [0, 1 + \zeta], \quad (7.8)$$

μ_o is the shear modulus at o K and ambient pressure, ζ is a material parameter, k_b is the Boltzmann constant, m is the atomic mass, and f is the Lindemann constant.

The model is invoked using

```
<shear_modulus_model type="np_shear">
  <mu_0>26.5e9</mu_0>
  <zeta>0.04</zeta>
  <slope_mu_p_over_mu0>65.0e-12</slope_mu_p_over_mu0>
  <C> 0.047 </C>
  <m> 26.98 </m>
</shear_modulus_model>
```


7.1.5 Preston-Tonks-Wallace (PTW) shear modulus

The PTW shear model [34] is a simplified version of the SCG shear model. This model suggests computing the shear modulus using

$$\mu(p, T) = \mu_o \left(1 + \beta \frac{\bar{p}}{\eta^{1/3}} \right) \left(1 - \alpha_p \frac{T}{T_m} \right) \quad (7.9)$$

where μ_o is the shear modulus at room temperature and pressure, $\bar{p} = -p$, α_p is a material parameter, T_m is the melting temperature, and

$$\eta = \frac{\rho}{\rho_o}, \quad \beta = \frac{d\mu}{dp}. \quad (7.10)$$

7.1.6 Borja's shear modulus model

Borja's deviatoric stress model [35] assumes that the deviatoric part of the elastic strain energy density has the form

$$W_{\text{dev}}(\epsilon_v^e, \epsilon_s^e) = \frac{3}{2} \mu (\epsilon_s^e)^2 \quad (7.11)$$

where $\epsilon_v^e = \text{tr}(\epsilon_v^e)$ is the volumetric part of the elastic strain, $\epsilon_s^e = \sqrt{2/3 \text{dev}(\epsilon_v^e) : \text{dev}(\epsilon_v^e)}$ is the deviatoric part of the elastic strain, and μ is the shear modulus.

The shear modulus in the Borja model is computed as

$$\mu(p) = \mu_o - \alpha p_o \exp\left(-\frac{\epsilon_v^e - \epsilon_{v_o}^e}{\tilde{\kappa}}\right) \quad (7.12)$$

where μ_o is a reference shear modulus, $\epsilon_{v_o}^e$ is the volumetric strain corresponding to a mean normal compressive stress p_o , and $\tilde{\kappa}$ is the elastic compressibility index.

8 — Yield condition

The yield condition models in VAANGO are of two types: yield conditions that are tightly tied to material models such as CamClay, Arenisca3, Arena, Mohr-Coulomb etc. and those that can be switched in the input file. This chapter discusses those yield conditions that can be easily substituted while simulating isotropic metal plasticity. The other yield conditions are described in the chapters that deal with specific models.

8.1 von Mises yield

The von Mises yield function implemented in VAANGO has the form

$$f = \sigma_{\text{eff}}^{\xi} - \sigma_y(\varepsilon_p^{\text{eq}}, \dot{\varepsilon}_p^{\text{eq}}, \phi, T, \dot{\varepsilon}^{\text{eq}}, \dots) \quad (8.1)$$

where σ_y is the flow stress, $\varepsilon_p^{\text{eq}}$ is the equivalent plastic strain, $\dot{\varepsilon}_p^{\text{eq}}$ is the equivalent plastic strain rate, ϕ is the porosity, and T is the temperature. The equivalent stress is defined as

$$\sigma_{\text{eff}}^{\xi} = \sqrt{3J_2^{\xi}} = \sqrt{\frac{3}{2}\xi : \xi}, \quad \xi = \mathbf{s} - \text{dev}(\boldsymbol{\beta}), \quad \mathbf{s} = \boldsymbol{\sigma} - \frac{1}{3}\text{tr}(\boldsymbol{\sigma})\mathbf{I} \quad (8.2)$$

where $\boldsymbol{\sigma}$ is the Cauchy stress and $\boldsymbol{\beta}$ is the kinematic hardening backstress.

The normal to the yield surface is

$$\mathbf{N} = \frac{\partial f}{\partial \boldsymbol{\sigma}} = \frac{\partial f}{\partial \xi} : \frac{\partial \xi}{\partial \boldsymbol{\sigma}} = \frac{\partial f}{\partial \xi} : \frac{\partial \xi}{\partial \mathbf{s}} : \frac{\partial \mathbf{s}}{\partial \boldsymbol{\sigma}} \quad (8.3)$$

Noting that

$$\frac{\partial \mathbf{s}}{\partial \boldsymbol{\sigma}} = \text{symm}(\mathbb{I}) - \frac{1}{3}\mathbf{I} \otimes \mathbf{I} \quad \text{and} \quad \frac{\partial \xi}{\partial \mathbf{s}} = \text{symm}(\mathbb{I}) \quad (8.4)$$

where \mathbb{I} is the fourth-order identity tensor and \mathbf{I} is the second-order identity tensor, we have

$$\begin{aligned} \mathbf{N} &= \frac{\partial f}{\partial \xi} : \text{symm}(\mathbb{I}) : (\text{symm}(\mathbb{I}) - \frac{1}{3}\mathbf{I} \otimes \mathbf{I}) = \frac{\partial f}{\partial \xi} : (\text{symm}(\mathbb{I}) - \frac{1}{3}\mathbf{I} \otimes \mathbf{I}) \\ &= \frac{\partial f}{\partial \xi} - \frac{1}{3}\text{tr}\left(\frac{\partial f}{\partial \xi}\right)\mathbf{I}. \end{aligned} \quad (8.5)$$

Next we compute the derivative of f :

$$\frac{\partial f}{\partial \xi} = \frac{\partial f}{\partial \sigma_{\text{eff}}^{\xi}} \frac{\partial \sigma_{\text{eff}}^{\xi}}{\partial \xi} = \sqrt{\frac{3}{2}} \frac{\xi}{\sqrt{\xi : \xi}} \implies \text{tr} \left(\frac{\partial f}{\partial \xi} \right) = 0. \quad (8.6)$$

Therefore,

$$\mathbf{N} = \sqrt{\frac{3}{2}} \frac{\xi}{\|\xi\|} \quad (8.7)$$

The unit normal to the yield surface is

$$\hat{\mathbf{N}} = \frac{\xi}{\|\xi\|}. \quad (8.8)$$

The von Mises yield condition is the default for metal plasticity and can be invoked using the tag

```
<yield_condition type="von_mises"/>
```

8.2 The Gurson-Tvergaard-Needleman (GTN) yield condition

The Gurson-Tvergaard-Needleman (GTN) yield condition [36, 37] depends on porosity. The GTN yield function can be written as

$$f = \left(\frac{\sigma_{\text{eff}}^{\xi}}{\sigma_y} \right)^2 + 2q_1\phi_* \cosh \left(q_2 \frac{\text{tr}(\sigma^{\xi})}{2\sigma_y} \right) - (1 + q_3\phi_*^2) \quad (8.9)$$

where $\sigma^{\xi} = \sigma - \beta$, σ is the Cauchy stress, β is the backstress, $\sigma_{\text{eff}}^{\xi}$ is the equivalent stress defined in (8.2), σ_y is the flow stress of the void-free material, q_1, q_2, q_3 are material constants, and ϕ_* is the porosity function defined as

$$\phi_* = \begin{cases} \phi & \text{for } \phi \leq \phi_c, \\ \phi_c + k(\phi - \phi_c) & \text{for } \phi > \phi_c \end{cases} \quad (8.10)$$

where k is a constant and ϕ is the porosity (void volume fraction).

The normal to the yield surface is

$$\mathbf{N} = \frac{\partial f}{\partial \sigma} = \frac{\partial f}{\partial \xi} : \frac{\partial \xi}{\partial \sigma} + \frac{\partial f}{\partial I_1^{\xi}} \frac{\partial I_1^{\xi}}{\partial \sigma} = \frac{\partial f}{\partial \xi} : \frac{\partial \xi}{\partial s} : \frac{\partial s}{\partial \sigma} + \frac{\partial f}{\partial I_1^{\xi}} \frac{\partial I_1^{\xi}}{\partial I_1} \frac{\partial I_1}{\partial \sigma} \quad (8.11)$$

where $I_1 = \text{tr}(\sigma)$ and $I_1^{\xi} = \text{tr}(\sigma^{\xi}) = \text{tr}(\sigma - \beta)$. Using (8.5),

$$\mathbf{N} = \frac{\partial f}{\partial \xi} - \frac{1}{3} \text{tr} \left(\frac{\partial f}{\partial \xi} \right) \mathbf{I} + \frac{\partial f}{\partial I_1^{\xi}} \frac{\partial I_1^{\xi}}{\partial I_1} \frac{\partial I_1}{\partial \sigma}. \quad (8.12)$$

Noting that

$$\frac{\partial I_1^{\xi}}{\partial I_1} = 1 \quad \text{and} \quad \frac{\partial I_1}{\partial \sigma} = \mathbf{I} \quad (8.13)$$

we have

$$\mathbf{N} = \frac{\partial f}{\partial \xi} - \frac{1}{3} \text{tr} \left(\frac{\partial f}{\partial \xi} \right) \mathbf{I} + \frac{\partial f}{\partial I_1^{\xi}} \mathbf{I}. \quad (8.14)$$

Computation of the derivatives of f gives

$$\frac{\partial f}{\partial \xi} = \frac{\partial f}{\partial \sigma_{\text{eff}}^{\xi}} \frac{\partial \sigma_{\text{eff}}^{\xi}}{\partial \xi} = \sqrt{\frac{3}{2}} \left(\frac{2\sigma_{\text{eff}}^{\xi}}{\sigma_y^2} \right) \frac{\xi}{\|\xi\|} = \frac{3\xi}{\sigma_y^2} \implies \text{tr} \left(\frac{\partial f}{\partial \xi} \right) = 0. \quad (8.15)$$

and

$$\frac{\partial f}{\partial I_1^{\xi}} = \frac{q_1 q_2 \phi_*}{\sigma_y} \sinh \left(q_2 \frac{\text{tr}(\sigma^{\xi})}{2\sigma_y} \right). \quad (8.16)$$

Therefore,

$$\mathbf{N} = \frac{3\xi}{\sigma_y^2} + \frac{q_1 q_2 \phi_*}{\sigma_y} \sinh \left(q_2 \frac{\text{tr}(\sigma^{\xi})}{2\sigma_y} \right) \mathbf{I}. \quad (8.17)$$

The unit normal to the GTN yield surface is given by

$$\hat{\mathbf{N}} = \frac{\mathbf{N}}{\|\mathbf{N}\|}. \quad (8.18)$$

The GTN yield condition is invoked using

```
<yield_condition type="gurson">
  <q1> 1.5 </q1>
  <q2> 1.0 </q2>
  <q3> 2.25 </q3>
  <k> 4.0 </k>
  <f_c> 0.05 </f_c>
</yield_condition>
```

8.3 The Rousselier yield condition

The Rousselier yield condition [38] is another porosity-based yield condition that has been used for ductile tearing simulations.

The yield function is

$$f = \frac{\sigma_{\text{eff}}^{\xi}}{1 - \phi} + D\sigma_1\phi \exp \left(\frac{\text{tr}(\sigma^{\xi})}{3(1 - \phi)\sigma_1} \right) - \sigma_y \quad (8.19)$$

where D, σ_1 are material constants, and the remaining quantities have been defined in the previous section.

The normal to the yield surface is

$$\mathbf{N} = \frac{\partial f}{\partial \xi} - \frac{1}{3} \text{tr} \left(\frac{\partial f}{\partial \xi} \right) \mathbf{I} + \frac{\partial f}{\partial I_1^{\xi}} \mathbf{I} \quad (8.20)$$

where

$$\frac{\partial f}{\partial \xi} = \frac{\partial f}{\partial \sigma_{\text{eff}}^{\xi}} \frac{\partial \sigma_{\text{eff}}^{\xi}}{\partial \xi} = \sqrt{\frac{3}{2}} \frac{1}{1 - \phi} \frac{\xi}{\|\xi\|} \implies \text{tr} \left(\frac{\partial f}{\partial \xi} \right) = 0 \quad (8.21)$$

and

$$\frac{\partial f}{\partial I_1^{\xi}} = \frac{D\phi}{3(1 - \phi)} \exp \left(\frac{\text{tr}(\sigma^{\xi})}{3(1 - \phi)\sigma_1} \right). \quad (8.22)$$

Therefore,

$$\mathbf{N} = \frac{1}{1 - \phi} \left[\sqrt{\frac{3}{2}} \frac{\xi}{\|\xi\|} + \frac{D\phi}{3} \exp \left(\frac{\text{tr}(\sigma^{\xi})}{3(1 - \phi)\sigma_1} \right) \right]. \quad (8.23)$$

9 — Flow rule

Plastic flow rules in VAANGO have the form

$$\mathbf{d}^p = \dot{\boldsymbol{\epsilon}}^p = \dot{\lambda} \mathbf{M} \quad (9.1)$$

where $\mathbf{d}^p = \dot{\boldsymbol{\epsilon}}^p$ is the plastic strain rate tensor, λ is the consistency parameter, and \mathbf{M} is a unit tensor in the direction of the plastic strain rate.

9.1 Associated plasticity

For associated plasticity, VAANGO uses the classical approach in plasticity theory and assumes that $\mathbf{M} = \hat{\mathbf{N}}$ is the unit normal to the yield surface:

$$\dot{\boldsymbol{\epsilon}}^p = \dot{\lambda} \hat{\mathbf{N}}, \quad \hat{\mathbf{N}} = \frac{\frac{\partial f}{\partial \boldsymbol{\sigma}}}{\left\| \frac{\partial f}{\partial \boldsymbol{\sigma}} \right\|} \quad (9.2)$$

where f is the yield function.

9.2 Non-associated plasticity

VAANGO use two approaches for non-associated plasticity ($\mathbf{M} \neq \hat{\mathbf{N}}$). The first approach, implemented in the Mohr-Coulomb model, is to use a separate plastic potential (g) to compute \mathbf{M} :

$$\dot{\boldsymbol{\epsilon}}^p = \dot{\lambda} \hat{\mathbf{M}}, \quad \hat{\mathbf{M}} = \frac{\frac{\partial g}{\partial \boldsymbol{\sigma}}}{\left\| \frac{\partial g}{\partial \boldsymbol{\sigma}} \right\|} \quad (9.3)$$

The plastic potential is assumed to have the same form as the yield function, but different parameters to match experimental data on dilatation.

An alternative approach, used in Arenisca3 and Arena, is to compute the direction of the plastic strain rate tensor using

$$\dot{\boldsymbol{\epsilon}}^p = \dot{\lambda} \hat{\mathbf{M}}, \quad \hat{\mathbf{M}} = \frac{\text{dev}(\mathbf{N}) + \beta \text{tr}(\mathbf{N})}{\left\| \text{dev}(\mathbf{N}) + \beta \text{tr}(\mathbf{N}) \right\|} \quad (9.4)$$

where β is an adjustable parameter.



10 — Isotropic hardening models

Several flow stress models have been implemented in VAANGO . These are described in this chapter.

10.1 Linear hardening model

The linear hardening model in VAANGO has the form

$$\sigma_y(\epsilon_p^{\text{eq}}) = \sigma_0 + K\epsilon_p^{\text{eq}} \quad (10.1)$$

where σ_0 is the initial yield stress, K is a hardening modulus, and ϵ_p^{eq} is the equivalent plastic strain.

The linear hardening model can be invoked using

```
<flow_model type="linear">
  <sigma_0> 700.0e6 </sigma_0>
  <K>1.5e6</K>
</flow_model>
```

10.2 Johnson-Cook model

The Johnson-Cook (JC) model ([39]) has the following relation for the flow stress (σ_y)

$$\sigma_y(\epsilon_p^{\text{eq}}, \dot{\epsilon}^{\text{eq}}, T) = [A + B(\epsilon_p^{\text{eq}})^n] [1 + C \ln(\dot{\epsilon}^*)] [1 - (T^*)^m] \quad (10.2)$$

where ϵ_p^{eq} is the equivalent plastic strain, A , B , C , n , m are material constants, and

$$\dot{\epsilon}^* = \frac{\dot{\epsilon}^{\text{eq}}}{\dot{\epsilon}^0}; \quad T^* = \frac{(T - T_0)}{(T_m - T_0)}. \quad (10.3)$$

In the above equations, $\dot{\epsilon}^{\text{eq}}$ is the equivalent strain rate, $\dot{\epsilon}^0$ is a reference strain rate, T_0 is a reference temperature, and T_m is the melt temperature. For conditions where $T^* < 0$, we assume that $m = 1$.

The inputs for this model have the form

```
<flow_model type="johnson_cook">
  <A>792.0e6</A>
  <B>510.0e6</B>
  <C>0.014</C>
```

```

<n>0.26</n>
<m>1.03</m>
<T_r>298.0</T_r>
<T_m>1793.0</T_m>
<epdot_0>1.0</epdot_0>
</flow_model>

```

10.3 Steinberg-Guinan model

The Steinberg-Cochran-Guinan-Lund (SCG) model is a semi-empirical model that was developed by [32] for high strain rate situations and extended to low strain rates and bcc materials by [40]. The flow stress in this model is given by

$$\sigma_y(\varepsilon_p^{\text{eq}}, \dot{\varepsilon}_p^{\text{eq}}, T) = [\sigma_a f(\varepsilon_p^{\text{eq}}) + \sigma_t(\dot{\varepsilon}_p^{\text{eq}}, T)] \frac{\mu(p, T)}{\mu_o} \quad (10.4)$$

where σ_a is the athermal component of the flow stress, $f(\varepsilon_p^{\text{eq}})$ is a function that represents strain hardening, σ_t is the thermally activated component of the flow stress, $\mu(p, T)$ is the shear modulus, and μ_o is the shear modulus at standard temperature and pressure. The strain hardening function has the form

$$f(\varepsilon_p^{\text{eq}}) = [1 + \beta(\varepsilon_p^{\text{eq}} + \varepsilon_{pi})]^n; \quad \sigma_a f(\varepsilon_p^{\text{eq}}) \leq \sigma_{\text{max}} \quad (10.5)$$

where β, n are work hardening parameters, and ε_{pi} is the initial equivalent plastic strain. The thermal component σ_t is computed using a bisection algorithm from the following equation (based on the work of [41])

$$\dot{\varepsilon}_p^{\text{eq}} = \left[\frac{1}{C_1} \exp \left[\frac{2U_k}{k_b T} \left(1 - \frac{\sigma_t}{\sigma_p} \right)^2 \right] + \frac{C_2}{\sigma_t} \right]^{-1}; \quad \sigma_t \leq \sigma_p \quad (10.6)$$

where $2U_k$ is the energy to form a kink-pair in a dislocation segment of length L_d , k_b is the Boltzmann constant, σ_p is the Peierls stress. The constants C_1, C_2 are given by the relations

$$C_1 := \frac{\rho_d L_d a b^2 v}{2w^2}; \quad C_2 := \frac{D}{\rho_d b^2} \quad (10.7)$$

where ρ_d is the dislocation density, L_d is the length of a dislocation segment, a is the distance between Peierls valleys, b is the magnitude of the Burgers' vector, v is the Debye frequency, w is the width of a kink loop, and D is the drag coefficient.

The inputs for this model are of the form

```

<flow_model type="steinberg-cochran-guinan">
  <mu_0> 81.8e9 </mu_0>
  <sigma_0> 1.15e9 </sigma_0>
  <Y_max> 0.25e9 </Y_max>
  <beta> 2.0 </beta>
  <n> 0.50 </n>
  <A> 20.6e-12 </A>
  <B> 0.16e-3 </B>
  <T_m0> 2310.0 </T_m0>
  <Gamma_0> 3.0 </Gamma_0>
  <a> 1.67 </a>
  <epsilon_p0> 0.0 </epsilon_p0>
</flow_model>

```

10.4 Zerilli-Armstrong model

The Zerilli-Armstrong (ZA) model ([42–44]) is based on simplified dislocation mechanics. The general form of the equation for the flow stress is

$$\sigma_y(\epsilon_p^{\text{eq}}, \dot{\epsilon}_p^{\text{eq}}, T) = \sigma_a + B \exp(-\beta(\dot{\epsilon}_p^{\text{eq}})T) + B_o \sqrt{\epsilon_p^{\text{eq}}} \exp(-\alpha(\epsilon_p^{\text{eq}})T) \quad (10.8)$$

where σ_a is the athermal component of the flow stress given by

$$\sigma_a := \sigma_g + \frac{k_h}{\sqrt{l}} + K(\epsilon_p^{\text{eq}})^n, \quad (10.9)$$

σ_g is the contribution due to solutes and initial dislocation density, k_h is the microstructural stress intensity, l is the average grain diameter, K is zero for fcc materials, B, B_o are material constants. The functional forms of the exponents α and β are

$$\alpha = \alpha_o - \alpha_1 \ln(\dot{\epsilon}_p^{\text{eq}}); \quad \beta = \beta_o - \beta_1 \ln(\dot{\epsilon}_p^{\text{eq}}); \quad (10.10)$$

where $\alpha_o, \alpha_1, \beta_o, \beta_1$ are material parameters that depend on the type of material (fcc, bcc, hcp, alloys). The Zerilli-Armstrong model has been modified by [45] for better performance at high temperatures. However, we have not used the modified equations in our computations.

The input for this model is of the form

```
<flow_model type="zerilli_armstrong">
  <sigma_g>      46.5e6    </sigma_g>
  <k_H>          5.0e6    </k_H>
  <sqr_t_l_inv>   3.7      </sqr_t_l_inv>
  <B>            0.0      </B>
  <beta_0>       0.0      </beta_0>
  <beta_1>       0.0      </beta_1>
  <B_0>         890.0e6   </B_0>
  <alpha_0>      0.0028   </alpha_0>
  <alpha_1>      0.000115 </alpha_1>
  <K>           0.0      </K>
  <n>           0.0      </n>
</flow_model>
```

10.5 Polymer Zerilli-Armstrong model

The Zerilli-Armstrong model for polymers has the form:

$$\sigma_y(\epsilon_p^{\text{eq}}, \dot{\epsilon}_p^{\text{eq}}, T) = \sigma_g + B \exp(-\beta T^*) + B_o \sqrt{\omega \epsilon_p^{\text{eq}}} \exp(-\alpha T^*) \quad (10.11)$$

where σ_g is the athermal component of the flow stress and

$$\omega = \omega_a + \omega_b \ln(\dot{\epsilon}_p^{\text{eq}}) + \omega_p \sqrt{\bar{p}} \quad (10.12)$$

where $\omega_a, \omega_b, \omega_p$ are material parameters and $\bar{p} = -p$ is the pressure (positive in compression). The functional forms of the exponents α and β are

$$\alpha = \alpha_o - \alpha_1 \ln(\dot{\epsilon}_p^{\text{eq}}); \quad \beta = \beta_o - \beta_1 \ln(\dot{\epsilon}_p^{\text{eq}}); \quad (10.13)$$

where $\alpha_o, \alpha_1, \beta_o, \beta_1$ are material parameters. The factors B and B_o are defined as

$$B = B_{pa} \left(1 + B_{pb} \sqrt{\bar{p}} \right)^{B_{pn}}, \quad B_o = B_{opa} \left(1 + B_{opb} \sqrt{\bar{p}} \right)^{B_{opn}} \quad (10.14)$$

where B_{pa} , B_{opa} , B_{pb} , B_{opb} , B_{pn} , and B_{opn} are material parameters. Also,

$$T^* = \frac{T}{T_o} \quad (10.15)$$

where T_o is a reference temperature.

The input tags for the polymer ZA model are:

```
<flow_model type="zerilli_armstrong_polymer">
  <sigma_g> 46.5e6 </sigma_g>
  <B_pa> 0.0 </B_pa>
  <B_pb> 0.0 </B_pb>
  <B_pn> 1.0 </B_pn>
  <beta_0> 0.0 </beta_0>
  <beta_1> 0.0 </beta_1>
  <T_0> 300.0 </T_0>
  <B_0pa> 890.0e6 </B_0pa>
  <B_0pb> 0.0 </B_0pb>
  <B_0pn> 1.0 </B_0pn>
  <omega_a> 0.0 </omega_a>
  <omega_b> 0.0 </omega_b>
  <omega_p> 0.0 </omega_p>
</flow_model>
```

10.6 Mechanical threshold stress model

The Mechanical Threshold Stress (MTS) model ([46–48]) gives the following form for the flow stress

$$\sigma_y(\epsilon_p^{\text{eq}}, \dot{\epsilon}_p^{\text{eq}}, T) = \sigma_a + (S_i \sigma_i + S_e \sigma_e) \frac{\mu(p, T)}{\mu_o} \quad (10.16)$$

where σ_a is the athermal component of mechanical threshold stress, μ_o is the shear modulus at 0 K and ambient pressure, σ_i is the component of the flow stress due to intrinsic barriers to thermally activated dislocation motion and dislocation-dislocation interactions, σ_e is the component of the flow stress due to microstructural evolution with increasing deformation (strain hardening), (S_i, S_e) are temperature and strain rate dependent scaling factors. The scaling factors take the Arrhenius form

$$S_i = \left[1 - \left(\frac{k_b T}{g_{oi} b^3 \mu(p, T)} \ln \frac{\dot{\epsilon}_{poi}}{\dot{\epsilon}_p^{\text{eq}}} \right)^{1/q_i} \right]^{1/p_i} \quad (10.17)$$

$$S_e = \left[1 - \left(\frac{k_b T}{g_{oe} b^3 \mu(p, T)} \ln \frac{\dot{\epsilon}_{poe}}{\dot{\epsilon}_p^{\text{eq}}} \right)^{1/q_e} \right]^{1/p_e} \quad (10.18)$$

where k_b is the Boltzmann constant, b is the magnitude of the Burgers' vector, (g_{oi}, g_{oe}) are normalized activation energies, $(\dot{\epsilon}_{poi}, \dot{\epsilon}_{poe})$ are constant reference strain rates, and (q_i, p_i, q_e, p_e) are constants. The strain hardening component of the mechanical threshold stress (σ_e) is given by a modified Voce law

$$\frac{d\sigma_e}{d\epsilon_p^{\text{eq}}} = \theta(\sigma_e) \quad (10.19)$$

where

$$\theta(\sigma_e) = \theta_0[1 - F(\sigma_e)] + \theta_{IV}F(\sigma_e) \quad (10.20)$$

$$\theta_0 = a_0 + a_1 \ln \dot{\epsilon}_p^{\text{eq}} + a_2 \sqrt{\dot{\epsilon}_p^{\text{eq}}} - a_3 T \quad (10.21)$$

$$F(\sigma_e) = \frac{\tanh\left(\alpha \frac{\sigma_e}{\sigma_{es}}\right)}{\tanh(\alpha)} \quad (10.22)$$

$$\ln\left(\frac{\sigma_{es}}{\sigma_{oes}}\right) = \left(\frac{kT}{g_{oes} b^3 \mu(p, T)}\right) \ln\left(\frac{\dot{\epsilon}_p^{\text{eq}}}{\dot{\epsilon}_{poes}}\right) \quad (10.23)$$

and θ_0 is the hardening due to dislocation accumulation, θ_{IV} is the contribution due to stage-IV hardening, $(a_0, a_1, a_2, a_3, \alpha)$ are constants, σ_{es} is the stress at zero strain hardening rate, σ_{oes} is the saturation threshold stress for deformation at 0 K, g_{oes} is a constant, and $\dot{\epsilon}_{poes}$ is the maximum strain rate. Note that the maximum strain rate is usually limited to about $10^7/\text{s}$.

The inputs for this model are of the form

```
<flow_model type="mechanical_threshold_stress">
  <sigma_a>363.7e6</sigma_a>
  <mu_0>28.0e9</mu_0>
  <D>4.50e9</D>
  <T_0>294</T_0>
  <koverbcubed>0.823e6</koverbcubed>
  <g_0i>0.0</g_0i>
  <g_0e>0.71</g_0e>
  <edot_0i>0.0</edot_0i>
  <edot_0e>2.79e9</edot_0e>
  <p_i>0.0</p_i>
  <q_i>0.0</q_i>
  <p_e>1.0</p_e>
  <q_e>2.0</q_e>
  <sigma_i>0.0</sigma_i>
  <a_0>211.8e6</a_0>
  <a_1>0.0</a_1>
  <a_2>0.0</a_2>
  <a_3>0.0</a_3>
  <theta_IV>0.0</theta_IV>
  <alpha>2</alpha>
  <edot_es0>3.42e8</edot_es0>
  <g_0es>0.15</g_0es>
  <sigma_es0>1679.3e6</sigma_es0>
</flow_model>
```

10.7 Preston-Tonks-Wallace model

The Preston-Tonks-Wallace (PTW) model ([34]) attempts to provide a model for the flow stress for extreme strain rates (up to $10^{11}/\text{s}$) and temperatures up to melt. The flow stress is given by

$$\sigma_y(\epsilon_p^{\text{eq}}, \dot{\epsilon}_p^{\text{eq}}, T) = \begin{cases} 2 \left[\tau_s + \alpha \ln \left[1 - \varphi \exp \left(-\beta - \frac{\theta \epsilon_p^{\text{eq}}}{\alpha \varphi} \right) \right] \right] \mu(p, T) & \text{thermal regime} \\ 2\tau_s \mu(p, T) & \text{shock regime} \end{cases} \quad (10.24)$$

with

$$\alpha := \frac{s_0 - \tau_y}{d}; \quad \beta := \frac{\tau_s - \tau_y}{\alpha}; \quad \varphi := \exp(\beta) - 1 \quad (10.25)$$

where τ_s is a normalized work-hardening saturation stress, s_0 is the value of τ_s at 0K, τ_y is a normalized yield stress, θ is the hardening constant in the Voce hardening law, and d is a dimensionless material

parameter that modifies the Voce hardening law. The saturation stress and the yield stress are given by

$$\tau_s = \max \left\{ s_0 - (s_0 - s_\infty) \operatorname{erf} \left[\kappa \hat{T} \ln \left(\frac{\gamma \dot{\xi}}{\dot{\varepsilon}_p^{\text{eq}}} \right) \right], s_0 \left(\frac{\dot{\varepsilon}_p^{\text{eq}}}{\gamma \dot{\xi}} \right)^{s_1} \right\} \quad (10.26)$$

$$\tau_y = \max \left\{ \gamma_0 - (\gamma_0 - \gamma_\infty) \operatorname{erf} \left[\kappa \hat{T} \ln \left(\frac{\gamma \dot{\xi}}{\dot{\varepsilon}_p^{\text{eq}}} \right) \right], \min \left\{ \gamma_1 \left(\frac{\dot{\varepsilon}_p^{\text{eq}}}{\gamma \dot{\xi}} \right)^{\gamma_2}, s_0 \left(\frac{\dot{\varepsilon}_p^{\text{eq}}}{\gamma \dot{\xi}} \right)^{s_1} \right\} \right\} \quad (10.27)$$

where s_∞ is the value of τ_s close to the melt temperature, $(\gamma_0, \gamma_\infty)$ are the values of τ_y at 0K and close to melt, respectively, (κ, γ) are material constants, $\hat{T} = T/T_m$, $(s_1, \gamma_1, \gamma_2)$ are material parameters for the high strain rate regime, and

$$\dot{\xi} = \frac{1}{2} \left(\frac{4\pi\rho}{3M} \right)^{1/3} \left(\frac{\mu(p, T)}{\rho} \right)^{1/2} \quad (10.28)$$

where ρ is the density, and M is the atomic mass.

The inputs for this model are of the form

```
<flow_model type="preston_tonks_wallace">
  <theta> 0.025 </theta>
  <p> 2.0 </p>
  <s0> 0.0085 </s0>
  <sinf> 0.00055 </sinf>
  <kappa> 0.11 </kappa>
  <gamma> 0.00001 </gamma>
  <y0> 0.0001 </y0>
  <yinf> 0.0001 </yinf>
  <y1> 0.094 </y1>
  <y2> 0.575 </y2>
  <beta> 0.25 </beta>
  <M> 63.54 </M>
  <G0> 518e8 </G0>
  <alpha> 0.20 </alpha>
  <alphap> 0.20 </alphap>
</flow_model>
```

10.8 SUVIC-I model

SUVIC-I is a viscoplastic model for ice that has been used for modeling the interaction of tires with ice [49, 50]. The model is an extension of the SUVIC model (Strain-rate history dependent Unified Viscoplastic model with Internal Variables for Crystalline materials). The model is applicable for strain rates in the range of 10^{-8} to 10^{-2} s^{-1} . Further details on the range of applicability of the model can be found in [49].

This model is driven by a specialized viscoplastic constitutive model for which the yield criterion is given by

$$\left\langle \frac{X_{ae} - R}{K} \right\rangle, \quad \langle x \rangle = \begin{cases} x & \text{for } x > 0 \\ 0 & \text{for } x \leq 0 \end{cases} \quad (10.29)$$

where the effective reduced stress is defined as

$$X_{ae} := \sqrt{\frac{3}{2}(\mathbf{s} - \boldsymbol{\beta}) : (\mathbf{s} - \boldsymbol{\beta})} \quad (10.30)$$

and R is the yield stress, K is the drag stress, $\mathbf{s} = \operatorname{dev}(\boldsymbol{\sigma})$ is the deviatoric stress, $\boldsymbol{\beta}$ is the deviatoric backstress.

The inelastic strain rate is given by

$$\dot{\boldsymbol{\varepsilon}}^i = \left[A \left\langle \frac{X_{ae} - R}{K} \right\rangle^N \exp \left(-\frac{Q}{RT} \right) \right] \mathbf{n}, \quad \mathbf{n} = \frac{3}{2} \left(\frac{\mathbf{s} - \boldsymbol{\beta}}{X_{ae}} \right) \quad (10.31)$$

where A is a kinetic-law material constants, and Q, R, T are the activation energy, Universal gas constant and the absolute temperature, respectively.

The equivalent inelastic strain rate for the model is defined as

$$\dot{\epsilon}_i^{\text{eq}} = \sqrt{\frac{2}{3} \dot{\epsilon}^i : \dot{\epsilon}^i} = A \left(\frac{X_{ae} - R}{K} \right)^N \exp \left(-\frac{Q}{RT} \right). \quad (10.32)$$

The evolution of the deviatoric backstress is given by

$$\dot{\beta} = \frac{2}{3} A_1 \dot{\epsilon}^i - A_1 (\beta_{\text{sat}})^{-1} \dot{\epsilon}_i^{\text{eq}} \beta - A_2 (\beta_{\text{sat}}^{\text{eff}})^{q-1} C^{-q} \beta \quad (10.33)$$

where A_1 is a constant that is fitted to the kinematic hardening and dynamic recovery curves, β_{sat} is a saturation value of the backstress, and A_2, q, C are constants fitted to static recovery curves. The isotropic hardening yield stress evolves as

$$\dot{R} = \frac{A_3}{d_g} \dot{\epsilon}_i^{\text{eq}} \left(1 - \frac{R}{R_{\text{sat}}} \right) - \frac{A_4}{d_g} \frac{(R - R_{\text{sat}})^p}{C} \quad (10.34)$$

where A_3 is a constant, d_g is the grain size, R_{sat} is the saturation value of R , and A_4, p, C are constants associated with static recovery. The drag stress evolves as

$$\dot{K} = \frac{A_5}{d_g} \dot{\epsilon}_i^{\text{eq}} \left(1 - \frac{K}{K_{\text{sat}}} \right) - \frac{A_6}{d_g} \frac{(K - K_{\text{sat}})^q}{C} \quad (10.35)$$

and has the same form as the yield stress evolution rule. The static recovery terms are ignored in the VAANGO implementation. The saturation value for the effective stress is given by

$$\sigma_{\text{sat}}^{\text{eff}} = \sigma_o \left(\frac{\dot{\epsilon}_i^{\text{eq}}}{\dot{\epsilon}_o} \right)^{1/n} \quad (10.36)$$

where σ_o and $\dot{\epsilon}_o$ are reference values and n is a constant. Similar relations are assumed for the reference values of the other quantities:

$$\beta_{\text{sat}}^{\text{eff}} = \beta_o \left(\frac{\dot{\epsilon}_i^{\text{eq}}}{\dot{\epsilon}_o} \right)^{1/n} ; R_{\text{sat}} = R_o \left(\frac{\dot{\epsilon}_i^{\text{eq}}}{\dot{\epsilon}_o} \right)^{1/n} \quad (10.37)$$

The drag stress saturation value is given by

$$K_{\text{sat}} = \left[\frac{\dot{\epsilon}_i^{\text{eq}}}{A \exp \left(\frac{-Q}{RT} \right)} \right] (X_{\text{sat}} - R_{\text{sat}}) \quad (10.38)$$

where X_{sat} is the saturation value of X_{ae} .

A typical input deck for the **SUVIC-I** model is shown below.

```
<constitutive_model type="visco_plastic">
  <shear_modulus>3.52e9</shear_modulus>
  <bulk_modulus>8.9e9</bulk_modulus>
  <remove_particles> false </remove_particles>
  <zero_stress_upon_failure> false </zero_stress_upon_failure>
  <stability_check type="none"> </stability_check>
  <equation_of_state type="default_hypo">
    <bulk_modulus>8.9e9</bulk_modulus>
  </equation_of_state>
  <viscoplastic_flow_model type="suvic_i">
    <coeff_backstressevol>75e6</coeff_backstressevol>
    <exponent_backstressevol> 1</exponent_backstressevol>
    <normalizing_backstress> 1e6</normalizing_backstress>
    <coeff_saturation_backstress> 0.1e6</coeff_saturation_backstress>
    <exponent_backstress> 4</exponent_backstress>
```

```
<ref_strainrate>7.794e-08</ref_strainrate>
<normalizing_inelastic_strainrate>5.0e9 </normalizing_inelastic_strainrate>
<activation_energy> 67500.0</activation_energy>
<universal_gas_constant>8.3144 </universal_gas_constant>
<temperature>269.15</temperature>
<exponent_inelastic_strainrate>4.0 </exponent_inelastic_strainrate>
<coeff_yieldstress_saturation>0.8e6 </coeff_yieldstress_saturation>
<exponent_yieldstress>4.0 </exponent_yieldstress>
<coeff_yieldstress_evol> 1600.0e6</coeff_yieldstress_evol>
<exponent_dragstress> 4.0</exponent_dragstress>
<coeff_dragstress_evol>95e6 </coeff_dragstress_evol>
<coeff_stress_saturation>1.0e6</coeff_stress_saturation>
<intial_drag>0.05e6</intial_drag>
<initial_yield> 0.0</initial_yield>
<integration_parameter_theta> 0.5</integration_parameter_theta>
</viscoplastic_flow_model>
</constitutive_model>
```




11 — Kinematic hardening models

Kinematic hardening in VAANGO is modeled with a backstress (β) that is subtracted from the stress while evaluating the yield condition. In Arena, the pore water pressure ($\bar{p}_w = -p_w$) acts as a backstress, i.e.,

$$\beta = \bar{p}_w I. \quad (11.1)$$

For metals, the backstress can either be ignored or modeled using the approaches described in this chapter.

11.1 Ziegler-Prager model

If the evolution of the backstress is given by the Ziegler-Prager kinematic hardening rule, we have

$$\dot{\beta} = \frac{2}{3} \beta H \dot{\epsilon}^p \quad (11.2)$$

where β is the backstress, βH is a constant hardening modulus, and $\dot{\epsilon}^p$ is the plastic strain rate.

The Prager model is invoked using

```
<kinematic_hardening_model type="prager_hardening">
  <beta> 1.0 </beta>
  <hardening_modulus>1.5e6</hardening_modulus>
</kinematic_hardening_model>
```

11.2 Armstrong-Frederick model

The Armstrong-Frederick model evolves the backstress using

$$\dot{\beta} = \frac{2}{3} \beta H_1 \dot{\epsilon}^p - \beta H_2 \beta \|\dot{\epsilon}^p\| \quad (11.3)$$

where β , H_1 and H_2 are material parameters.

The Armstrong-Frederick model is invoked using

```
<kinematic_hardening_model type="armstrong_frederick_hardening">
  <beta> 1.0 </beta>
  <hardening_modulus_1>1.5e6</hardening_modulus_1>
  <hardening_modulus_2>1.5e4</hardening_modulus_2>
</kinematic_hardening_model>
```


12 — Internal variable evolution

Internal variables are used to model isotropic hardening/softening behavior in VAANGO . The evolution of these internal variables is assumed to be given by first-order differential equations of the form

$$\dot{\boldsymbol{\eta}} = \dot{\lambda} \mathbf{h}_{\boldsymbol{\eta}} \quad (12.1)$$

where $\boldsymbol{\eta}$ is the internal variable, λ is the consistency parameter, and $\mathbf{h}_{\boldsymbol{\eta}}$ is a hardening/softening modulus.

The kinematic hardening backstress is also an internal variable. Equations for the evolution of backstress are given in Chapter 11. Other internal variables that are specific to CamCay, Arena, Tabular plasticity, etc. are discussed in separate chapters associated with these models.

12.1 Equivalent plastic strain

Recall from the flow rule (9.1) that

$$\dot{\boldsymbol{\varepsilon}}^P = \dot{\lambda} \mathbf{M} \quad (12.2)$$

where \mathbf{M} is a unit tensor ($\mathbf{M} : \mathbf{M} = 1$). Therefore, using the definition of the equivalent plastic strain rate from (2.16),

$$\dot{\boldsymbol{\varepsilon}}^P : \dot{\boldsymbol{\varepsilon}}^P = (\dot{\lambda})^2 \implies \dot{\lambda} = \sqrt{\dot{\boldsymbol{\varepsilon}}^P : \dot{\boldsymbol{\varepsilon}}^P} = \dot{\varepsilon}_p^{\text{eq}}. \quad (12.3)$$

Therefore, from the definition of the equivalent plastic strain in (2.17), we see that the evolution rule for the equivalent plastic strain can be expressed in the the form (12.1) as

$$\dot{\varepsilon}_p^{\text{eq}} = \dot{\lambda} h_{\varepsilon_p}, \quad h_{\varepsilon_p} = 1. \quad (12.4)$$

12.2 Porosity

The evolution of porosity is assumed to be given by the sum of the rate of void growth and the rate of void nucleation [51]. In VAANGO these rates are computed as [52]:

$$\dot{\phi} = \dot{\phi}_{\text{nucl}} + \dot{\phi}_{\text{grow}} \quad (12.5)$$

$$\dot{\phi}_{\text{grow}} = (1 - \phi) \text{tr}(\dot{\boldsymbol{\varepsilon}}^P) \quad (12.6)$$

$$\dot{\phi}_{\text{nucl}} = \frac{f_n}{(s_n \sqrt{2\pi})} \exp \left[-\frac{1}{2} \frac{(\varepsilon_p^{\text{eq}} - \varepsilon_n)^2}{s_n^2} \right] \dot{\varepsilon}_p^{\text{eq}} \quad (12.7)$$

where $\dot{\epsilon}_p$ is the plastic strain rate, f_n is the volume fraction of void nucleating particles, ϵ_n is the mean of the distribution of nucleation strains, and s_n is the standard deviation of the distribution.

From the flow rule (9.1),

$$\text{tr}(\dot{\epsilon}^p) = \dot{\lambda} \text{tr}(\mathbf{M}) \quad (12.8)$$

Therefore, using (12.3),

$$\dot{\phi} = \dot{\lambda} h_\phi, \quad h_\phi = (1 - \phi) \text{tr}(\mathbf{M}) + \frac{f_n}{(s_n \sqrt{2\pi})} \exp\left(-\frac{1}{2} \frac{(\epsilon_p^{\text{eq}} - \epsilon_n)^2}{s_n^2}\right). \quad (12.9)$$

VAANGO allows for the possibly of porosity to be different in each MPM particle. The inputs tags for defining the porosity and its distribution are:

```
<evolve_porosity> true </evolve_porosity>
<initial_mean_porosity> 0.005 </initial_mean_porosity>
<initial_std_porosity> 0.001 </initial_std_porosity>
<critical_porosity> 0.3 </critical_porosity>
<frac_nucleation> 0.1 </frac_nucleation>
<meanstrain_nucleation> 0.3 </meanstrain_nucleation>
<stddevstrain_nucleation> 0.1 </stddevstrain_nucleation>
<initial_porosity_distrib> gauss </initial_porosity_distrib>
```

12.3 Backstress

The backstress evolution rule can also be expressed in terms of the consistency parameter in the form

$$\dot{\beta} = \dot{\lambda} \mathbf{h}_\beta \quad (12.10)$$

For the Ziegler-Prager model in (11.2),

$$\mathbf{h}_\beta = \frac{2}{3} \beta \mathbf{H} \mathbf{M} \quad (12.11)$$

where \mathbf{M} is the unit tensor in the direction of the plastic flow rate.

For the Armstrong-Frederick model in (11.3),

$$\mathbf{h}_\beta = \frac{2}{3} \beta H_1 \mathbf{M} - \beta H_2 \beta. \quad (12.12)$$

12.4 Damage

The evolution of damage models in VAANGO is detailed in Chapter 15. These models have the general form

$$\dot{D} = g(\boldsymbol{\sigma}, T) \dot{\epsilon}_p^{\text{eq}} = \dot{\lambda} h_D, \quad h_D = g(\boldsymbol{\sigma}, T) \quad (12.13)$$

where D is the damage parameter and $g(\boldsymbol{\sigma}, T)$ is a damage function.

12.5 Temperature

The rise in temperature due to plastic dissipation can also be treated as an internal variable that causes softening. This may be considered to be equivalent to treating the plastic work as an internal variable.

The evolution of temperature (T) due to plastic work is given by the equation

$$\dot{T} = \frac{\chi}{\rho C_p} \boldsymbol{\sigma} : \dot{\epsilon}^p \quad (12.14)$$

where χ is the Taylor-Quinney coefficient, ρ is the density, and C_p is the specific heat. Expressed in terms of the consistency parameter,

$$\dot{T} = \dot{\lambda} h_T, \quad h_T = \frac{\chi}{\rho C_p} \boldsymbol{\sigma} : \boldsymbol{M} \quad (12.15)$$

where \boldsymbol{M} is the plastic flow rate direction defined in the flow rule.



13 — Melting temperature models

The melting temperature is used by several models in VAANGO to compute the shear modulus. Failure and transitioning into fluid-like behavior is also controlled by the melting temperature. The melt temperature models implemented in VAANGO are described below.

13.1 Constant melting temperature

The default is to use a constant melting temperature. This model is invoked using

```
<melting_temp_model type="constant_Tm">
</melting_temp_model>
```

13.2 Steinberg-Cochran-Guinan melting temperature

A pressure dependent relation to determine the melting temperature (T_m) in the Steinberg-Cochran-Guinan (SCG) melt model ([32]).

This model is based on a modified Lindemann law and has the form

$$T_m(\rho) = T_{m0} \exp \left[2a \left(1 - \frac{1}{\eta} \right) \right] \eta^{2(\Gamma_0 - a - 1/3)}; \quad \eta = \frac{\rho}{\rho_0} \quad (13.1)$$

where T_{m0} is the melt temperature at $\eta = 1$, a is the coefficient of the first order volume correction to Grüneisen's gamma (Γ_0).

This model is invoked with

```
<melting_temp_model type="scg_Tm">
  <T_m0> 2310.0 </T_m0>
  <Gamma_0> 3.0 </Gamma_0>
  <a> 1.67 </a>
</melting_temp_model>
```

13.3 Burakovsky-Preston-Silbar melting temperature

The Burakovsky-Preston-Silbar (BPS) model is based on dislocation-mediated phase transitions [53]. The BPS model has the form

$$T_m(p) = T_m(o) \left[\frac{1}{\eta} + \frac{1}{\eta^{4/3}} \frac{\mu'_o}{\mu_o} p \right]; \quad \eta = \left(1 + \frac{K'_o}{K_o} p \right)^{1/K'_o} \quad (13.2)$$

$$T_m(o) = \frac{\kappa \lambda \mu_o \nu_{WS}}{8\pi \ln(z-1) k_b} \ln \left(\frac{\alpha^2}{4 b^2 \rho_c(T_m)} \right) \quad (13.3)$$

where p is the pressure, $\eta = \rho/\rho_o$ is the compression, μ_o is the shear modulus at room temperature and zero pressure, $\mu'_o = \partial\mu/\partial p$ is the derivative of the shear modulus at zero pressure, K_o is the bulk modulus at room temperature and zero pressure, $K'_o = \partial K/\partial p$ is the derivative of the bulk modulus at zero pressure, κ is a constant, $\lambda = b^3/\nu_{WS}$ where b is the magnitude of the Burgers' vector, ν_{WS} is the Wigner-Seitz volume, z is the coordination number, α is a constant, $\rho_c(T_m)$ is the critical density of dislocations, and k_b is the Boltzmann constant.

This model is invoked with

```
<melting_temp_model type="bps_Tm">
  <B0> 137e9 </B0>
  <dB_dp0> 5.48 <dB_dp0>
  <G0> 47.7e9 <G0>
  <dG_dp0> 1.4 <dG_dp0>
  <kappa> 1.25 <kappa>
  <z> 12 <z>
  <b2rhoTm> 0.64 <b2rhoTm>
  <alpha> 2.9 <alpha>
  <lambda> 1.41 <lambda>
  <a> 3.6147e-9 <a>
  <v_ws_a3_factor> 1/4 <v_ws_a3_factor>
  <Boltzmann_Constant> <Boltzmann_Constant>
</melting_temp_model>
```




14 — Adiabatic heating and specific heat

A part of the plastic work done is converted into heat and used to update the temperature of a particle. The increase in temperature (ΔT) due to an increment in plastic strain ($\Delta \epsilon_p^{\text{eq}}$) is given by the equation

$$\Delta T = \frac{\chi \sigma_y}{\rho C_p} \Delta \epsilon_p^{\text{eq}} \quad (14.1)$$

where χ is the Taylor-Quinney coefficient, and C_p is the specific heat. The value of the Taylor-Quinney coefficient is taken to be 0.9 in all our simulations (see [54] for more details on the variation of χ with strain and strain rate).

The Taylor-Quinney coefficient is taken as input using the tags

```
<taylor_quinney_coeff> 0.9 </taylor_quinney_coeff>
```

The heat generated at a material point is conducted away at the end of a time step using the transient heat equation. The effect of conduction on material point temperature is negligible (but non-zero) for the high strain-rate problems simulated using Vaango.

14.1 Constant specific heat model

The default model returns a constant specific heat and is invoked using

```
<specific_heat_model type="constant_Cp">
</specific_heat_model>
```

14.2 Specific heat model for copper

The specific heat model for copper is of the form

$$C_p = \begin{cases} A_0 T^3 - B_0 T^2 + C_0 T - D_0 & \text{if } T < T_0 \\ A_1 T + B_1 & \text{if } T \geq T_0 \end{cases} \quad (14.2)$$

The model is invoked using

```
<specific_heat_model type = "copper_Cp"> </specific_heat_model>
```

14.3 Specific heat model for steel

A relation for the dependence of C_p upon temperature is used for the steel ([55]).

$$C_p = \begin{cases} A_1 + B_1 t + C_1 |t|^{-\alpha} & \text{if } T < T_c \\ A_2 + B_2 t + C_2 t^{-\alpha'} & \text{if } T > T_c \end{cases} \quad (14.3)$$

$$t = \frac{T}{T_c} - 1 \quad (14.4)$$

where T_c is the critical temperature at which the phase transformation from the α to the γ phase takes place, and $A_1, A_2, B_1, B_2, \alpha, \alpha'$ are constants.

The model is invoked using

```
<specific_heat_model type = "steel_Cp"> </specific_heat_model>
```

15 — Damage models

The damage models implemented in VAANGO are described in this chapter. The most common model evolves a scalar damage parameter that can either be used to flag failure when a critical value is reached or to modify the stress as in continuum damage mechanics.

15.1 Hancock-MacKenzie model

The Hancock-MacKenzie model [56] evolves a scalar damage parameter (D) using the rule:

$$\dot{D} = \frac{1}{1.65} \dot{\epsilon}_p^{\text{eq}} \exp\left(\frac{\text{tr}(\boldsymbol{\sigma})}{2\sigma_{\text{eff}}}\right) \quad (15.1)$$

where $D = 0$ for virgin material, $\dot{\epsilon}_p$ is the equivalent plastic strain rate, $\boldsymbol{\sigma}$ is the Cauchy stress, and $\sigma_{\text{eq}} = \sqrt{3J_2}$ is the von Mises equivalent stress.

Expressed as an evolution equation in terms of the plastic consistency parameter, the above can be written as

$$\dot{D} = \dot{\lambda} h_D, \quad h_D = \frac{1}{1.65} \exp\left(\frac{\text{tr}(\boldsymbol{\sigma})}{2\sigma_{\text{eff}}}\right). \quad (15.2)$$

The input tags for the damage model are :

```
<damage_model type="hancock_mackenzie">
  <D0>0.05</D1>
  <Dc>3.44</D2>
</damage_model>
```

15.2 Johnson-Cook model

The Johnson-Cook damage model [57] depends on temperature, plastic strain, and strain rate. The damage evolution rule for the damage parameter (D) can be written as

$$\dot{D} = \frac{\dot{\epsilon}_p^{\text{eq}}}{\epsilon_p^f}, \quad \epsilon_p^f = [D_1 + D_2 \exp(D_3 \sigma^*)] [1 + D_4 \ln(\dot{\epsilon}_p^*)] [1 + D_5 T^*]. \quad (15.3)$$

The damage parameter D has a value of 0 for virgin material and a value of 1 at fracture, ϵ_p^f is the fracture strain, D_1, D_2, D_3, D_4, D_5 are constants. In the above equation,

$$\sigma^* = \frac{\text{tr}(\boldsymbol{\sigma})}{3\sigma_{\text{eff}}} \quad (15.4)$$

where $\boldsymbol{\sigma}$ is the Cauchy stress and σ_{eff} is the von Mises equivalent stress. The scaled plastic strain rate and temperature are defined as

$$\dot{\epsilon}_p^* = \frac{\dot{\epsilon}_p^{\text{eq}}}{\dot{\epsilon}_{p0}}, \quad T^* = \frac{T - T_0}{T_m - T_0} \quad (15.5)$$

where $\dot{\epsilon}_{p0}$ is a reference strain rate and T_0 is a reference temperature, T_m is the melting temperature, and $\dot{\epsilon}_p^{\text{eq}}$ is the equivalent plastic strain rate.

When expressed in terms of the consistency parameter, the Johnson-Cook damage model has the form,

$$\dot{D} = \dot{\lambda} h_D, \quad h_D = \left[[D_1 + D_2 \exp(D_3 \sigma^*)] [1 + D_4 \ln(\dot{\epsilon}_p^*)] [1 + D_5 T^*] \right]^{-1}. \quad (15.6)$$

The input tags for the damage model are :

```
<damage_model type="johnson_cook">
  <D1>0.05</D1>
  <D2>3.44</D2>
  <D3>-2.12</D3>
  <D4>0.002</D4>
  <D5>0.61</D5>
</damage_model>
```

An initial damage distribution can be created using the following tags

```
<evolve_damage> true </evolve_damage>
<initial_mean_scalar_damage> 0.005 </initial_mean_scalar_damage>
<initial_std_scalar_damage> 0.001 </initial_std_scalar_damage>
<critical_scalar_damage> 1.0 </critical_scalar_damage>
<initial_scalar_damage_distrib> gauss </initial_scalar_damage_distrib>
```



16 — Material failure

16.1 Introduction

The primary technique used in VAANGO to simulate failure is damage evolution. A particle is tagged as “failed” when its temperature is greater than the melting point of the material at the applied pressure. Failure is also flagged when the porosity of a particle is greater critical limit (typically 0.9) and the strain exceeds the fracture strain of the material.

An alternative approach that can be used in the metal plasticity models implemented in VAANGO is to test material stability conditions to determine and propagate failure. Upon failure detection, a particle is either removed from the computation by setting the stress to zero or is converted into a material with a different velocity field which interacts with the remaining particles via contact. Either approach leads to the simulation of a newly created surface. More details of the approach can be found in [58–60].

16.2 Erosion algorithm

In metal plasticity simulations, the heat generated at a material point is conducted away at the end of a time step using the heat equation. If special adiabatic conditions apply (such as in impact problems), the heat is accumulated at a material point and is not conducted to the surrounding particles. This localized heating can be used to determine whether a material point has melted.

The determination of whether a particle has failed can be made on the basis of either or all of the following conditions:

- The particle temperature exceeds the melting temperature.
- The TEPLA-F fracture condition [61] is satisfied. This condition can be written as

$$\left(\frac{\phi}{\phi_c}\right)^2 + \left(\frac{\varepsilon_p^{\text{eq}}}{\varepsilon_p^f}\right)^2 = 1 \quad (16.1)$$

where ϕ is the current porosity, ϕ_c is the maximum allowable porosity, $\varepsilon_p^{\text{eq}}$ is the current equivalent plastic strain, and ε_p^f is the equivalent plastic strain at fracture.

- An alternative to ad-hoc damage criteria is to use the concept of material stability bifurcation to determine whether a particle has failed or not.

Since the material unloads locally after fracture, the hypoelastic-plastic stress update may not work accurately under certain circumstances. An improvement would be to use a hyperelastic-plastic stress update

algorithm. Also, the plasticity models are temperature dependent. Hence there is the issue of severe mesh dependence due to change of the governing equations from hyperbolic to elliptic in the softening regime [62–64]. Viscoplastic stress update models or nonlocal/gradient plasticity models [65, 66] can be used to eliminate some of these effects. Such models that have been implemented in VAANGO are discussed later.

The tags used to control the erosion algorithm are in two places. In the <MPM> </MPM> section the following flags can be set

```
<erosion_algorithm = "ZeroStress"/>
<create_new_particles>         false      </create_new_particles>
<manual_new_material>         false      </manual_new_material>
```

If the erosion algorithm is "none" then no particle failure is done.

In the <constitutive_model type="elastic_plastic"> section, the following flags can be set

```
<evolve_porosity>             true      </evolve_porosity>
<evolve_damage>               true      </evolve_damage>
<do_melting>                   true      </do_melting>
<useModifiedEOS>               true      </useModifiedEOS>
<check_TEPLA_failure_criterion> true      </check_TEPLA_failure_criterion>
<check_max_stress_failure>     false    </check_max_stress_failure>
<critical_stress>              12.0e9   </critical_stress>
```

16.3 Material stability conditions

16.3.1 Drucker's condition

The simplest criterion that can be used is the Drucker stability postulate [67] which states that time rate of change of the rate of work done by a material cannot be negative. Therefore, the material is assumed to become unstable (and a particle fails) when

$$\dot{\sigma} : d^p \leq 0 \quad (16.2)$$

16.3.2 Acoustic tensor criterion

Another stability criterion that is less restrictive is the acoustic tensor criterion which states that the material loses stability if the determinant of the acoustic tensor changes sign [68–70].

We assume that the strain is localized in a thin band with normal \mathbf{n} . The band is assumed be homogeneous but has slightly different material properties than the surrounding material.

To develop the bifurcation relations [69], assume that \mathbf{v}^b is the velocity of a material point in the band (Ω_b) and \mathbf{v}^o is the velocity of the material outside the band (Ω_o). The deformation of the material outside the band is assumed to be uniform. The deformation within the band is also assumed to be homogeneous.

We assume that stresses and rates of deformation have been rotated to the undeformed configuration using the polar decomposition of the deformation gradient.

Consider the case where the local coordinates of points in the band are expressed in terms of an orthonormal basis $\mathbf{e}_1, \mathbf{e}_2, \mathbf{e}_3$ where $\mathbf{e}_2 = \mathbf{n}$. Then a point \mathbf{x} inside (or outside) the band can be expressed as $\mathbf{x} = x_i \mathbf{e}_i$.

Continuity and the homogeneity of deformation in the two regions requires that only the velocity in the \mathbf{n} direction can be different in the two regions. This implies

$$\mathbf{v}^b(\mathbf{x}) - \mathbf{v}^o(\mathbf{x}) = \mathbf{f}(\mathbf{n} \cdot \mathbf{x}) = \mathbf{f}(x_2) \quad (16.3)$$

where \mathbf{f} is an unknown function. The velocity gradient can be computed from the above relation as

$$\nabla \mathbf{v}^b = \nabla \mathbf{v}^o + \frac{d\mathbf{f}}{dx_2} \otimes \mathbf{n} = \nabla \mathbf{v}^o + \mathbf{q} \otimes \mathbf{n} \quad (16.4)$$

where

$$\mathbf{q} := \frac{d\mathbf{f}}{dx_2} = \begin{cases} \mathbf{o} & \text{for } \mathbf{x} \in \Omega_o \\ \mathbf{q} & \text{for } \mathbf{x} \in \Omega_b \end{cases} \quad (16.5)$$

The rate of deformation in the band is

$$\mathbf{d}^b = \frac{1}{2} [\nabla \mathbf{v}^b + (\nabla \mathbf{v}^b)^T] = \frac{1}{2} [\nabla \mathbf{v}^o + (\nabla \mathbf{v}^o)^T] + \frac{1}{2} (\mathbf{q} \otimes \mathbf{n} + \mathbf{n} \otimes \mathbf{q}) = \mathbf{d}^o + \frac{1}{2} (\mathbf{q} \otimes \mathbf{n} + \mathbf{n} \otimes \mathbf{q}). \quad (16.6)$$

The stress rate is related to the rate of deformation by

$$\dot{\boldsymbol{\sigma}}^o = \mathbb{C}^o : \mathbf{d}^o, \quad \dot{\boldsymbol{\sigma}}^b = \mathbb{C}^b : \mathbf{d}^b = \mathbb{C}^b : \mathbf{d}^o + \frac{1}{2} \mathbb{C}^b : (\mathbf{q} \otimes \mathbf{n} + \mathbf{n} \otimes \mathbf{q}). \quad (16.7)$$

The minor symmetry of \mathbb{C} implies that

$$\dot{\boldsymbol{\sigma}}^b = \mathbb{C}^b : \mathbf{d}^o + \mathbb{C}^b : (\mathbf{q} \otimes \mathbf{n}). \quad (16.8)$$

Homogeneity of the deformation also implies that

$$\mathbf{n} \cdot \boldsymbol{\sigma}^b = \mathbf{n} \cdot \boldsymbol{\sigma}^o. \quad (16.9)$$

Taking the material time derivative of the above gives

$$\dot{\mathbf{n}} \cdot \boldsymbol{\sigma}^b + \mathbf{n} \cdot \dot{\boldsymbol{\sigma}}^b = \dot{\mathbf{n}} \cdot \boldsymbol{\sigma}^o + \mathbf{n} \cdot \dot{\boldsymbol{\sigma}}^o. \quad (16.10)$$

We need an expression for $\dot{\mathbf{n}}$. To find that, note that if \mathbf{n}_o and \mathbf{n} are the unit normals to the band in the reference and current configurations, using Nanson's formula, we have

$$\mathbf{n} da = J(\mathbf{F}^{-T} \cdot \mathbf{n}_o) dA, \quad J = \det \mathbf{F}. \quad (16.11)$$

Taking the time derivative of (16.11),

$$\dot{\mathbf{n}} da + \mathbf{n} \dot{da} = \frac{dJ}{dt} (\mathbf{F}^{-T} \cdot \mathbf{n}_o) dA + J \left(\frac{d\mathbf{F}^{-1}}{dt} \right)^T \cdot \mathbf{n}_o dA \quad (16.12)$$

For the derivative of J , we have

$$\frac{dJ}{dt} = \frac{\partial J}{\partial \mathbf{F}} : \dot{\mathbf{F}} = J \mathbf{F}^{-T} : \dot{\mathbf{F}} = J \text{tr}(\dot{\mathbf{F}} \cdot \mathbf{F}^{-1}) = J \text{tr}(\nabla \mathbf{v}). \quad (16.13)$$

We can also show that

$$\frac{d\mathbf{F}^{-1}}{dt} = -\mathbf{F}^{-1} \cdot \dot{\mathbf{F}} \cdot \mathbf{F}^{-1} = -\mathbf{F}^{-1} \cdot \nabla \mathbf{v}. \quad (16.14)$$

Therefore, using (16.11),

$$\begin{aligned} \dot{\mathbf{n}} da + \mathbf{n} \dot{da} &= J \text{tr}(\nabla \mathbf{v}) (\mathbf{F}^{-T} \cdot \mathbf{n}_o) dA - J (\nabla \mathbf{v})^T \cdot \mathbf{F}^{-T} \cdot \mathbf{n}_o dA \\ &= \mathbf{n} \cdot [\text{tr}(\nabla \mathbf{v}) \mathbf{I} - \nabla \mathbf{v}] da. \end{aligned} \quad (16.15)$$

To find \dot{da} , we compute a dot product of both sides of (16.11) to get

$$da^2 = J^2 (\mathbf{F}^{-T} \cdot \mathbf{n}_o) \cdot (\mathbf{F}^{-T} \cdot \mathbf{n}_o) dA^2 = J^2 \mathbf{n}_o \cdot (\mathbf{F}^{-1} \cdot \mathbf{F}^{-T}) \cdot \mathbf{n}_o dA^2. \quad (16.16)$$

The material time derivative of the above expression is

$$2dada = 2J \frac{dJ}{dt} \mathbf{n}_o \cdot (\mathbf{F}^{-1} \cdot \mathbf{F}^{-T}) \cdot \mathbf{n}_o dA^2 + J^2 \mathbf{n}_o \cdot \frac{d}{dt} (\mathbf{F}^{-1} \cdot \mathbf{F}^{-T}) \cdot \mathbf{n}_o dA^2 \quad (16.17)$$

For the derivative of the \mathbf{F}^{-1} product, we have

$$\begin{aligned} \frac{d}{dt}(\mathbf{F}^{-1} \cdot \mathbf{F}^{-T}) &= \frac{d\mathbf{F}^{-1}}{dt} \cdot \mathbf{F}^{-T} + \mathbf{F}^{-1} \cdot \left(\frac{d\mathbf{F}^{-1}}{dt} \right)^T = -\mathbf{F}^{-1} \cdot \dot{\mathbf{F}} \cdot \mathbf{F}^{-1} \cdot \mathbf{F}^{-T} - \mathbf{F}^{-1} \cdot \mathbf{F}^{-T} \cdot \dot{\mathbf{F}}^T \cdot \mathbf{F}^{-T} \\ &= -\mathbf{F}^{-1} \cdot \nabla \mathbf{v} \cdot \mathbf{F}^{-T} - \mathbf{F}^{-1} \cdot (\nabla \mathbf{v})^T \cdot \mathbf{F}^{-T} = -2\mathbf{F}^{-1} \cdot \mathbf{d} \cdot \mathbf{F}^{-T}. \end{aligned} \quad (16.18)$$

Substitution into (16.17) gives

$$\begin{aligned} da da &= J^2 \text{tr}(\nabla \mathbf{v}) \mathbf{n}_o \cdot (\mathbf{F}^{-1} \cdot \mathbf{F}^{-T}) \cdot \mathbf{n}_o dA^2 - J^2 \mathbf{n}_o \cdot (\mathbf{F}^{-1} \cdot \mathbf{d} \cdot \mathbf{F}^{-T}) \cdot \mathbf{n}_o dA^2 \\ &= \text{tr}(\nabla \mathbf{v}) (J\mathbf{F}^{-T} \cdot \mathbf{n}_o dA) \cdot (J\mathbf{F}^{-T} \cdot \mathbf{n}_o dA) - (J\mathbf{F}^{-T} \cdot \mathbf{n}_o dA) \cdot \mathbf{d} \cdot (J\mathbf{F}^{-T} \cdot \mathbf{n}_o dA) \\ &= \text{tr}(\nabla \mathbf{v}) \mathbf{n} \cdot \mathbf{n} da^2 - \mathbf{n} \cdot \mathbf{d} \cdot \mathbf{n} da^2 = \text{tr}(\nabla \mathbf{v}) da^2 - \mathbf{n} \cdot \mathbf{d} \cdot \mathbf{n} da^2. \end{aligned} \quad (16.19)$$

Therefore,

$$\dot{da} = [\text{tr}(\nabla \mathbf{v}) - \mathbf{n} \cdot \mathbf{d} \cdot \mathbf{n}] da = [\text{tr}(\nabla \mathbf{v}) - \mathbf{n} \cdot \nabla \mathbf{v} \cdot \mathbf{n}] da. \quad (16.20)$$

Plugging (16.20) into (16.15), we have

$$\dot{\mathbf{n}} da + \mathbf{n} [\text{tr}(\nabla \mathbf{v}) - \mathbf{n} \cdot \mathbf{d} \cdot \mathbf{n}] da = \mathbf{n} \cdot [\text{tr}(\nabla \mathbf{v}) \mathbf{I} - \nabla \mathbf{v}] da. \quad (16.21)$$

That gives us the expression for $\dot{\mathbf{n}}$ that we seek,

$$\dot{\mathbf{n}} = \mathbf{n} \cdot [\mathbf{d} \cdot (\mathbf{n} \otimes \mathbf{n}) - \nabla \mathbf{v}] = \mathbf{n} \cdot \nabla \mathbf{v} \cdot (\mathbf{n} \otimes \mathbf{n} - \mathbf{I}). \quad (16.22)$$

Using (16.22) in (16.10), we have

$$\mathbf{n} \cdot [(\dot{\boldsymbol{\sigma}}^b - \dot{\boldsymbol{\sigma}}^o) + \nabla \mathbf{v}^b \cdot (\mathbf{n} \otimes \mathbf{n} - \mathbf{I}) \cdot (\boldsymbol{\sigma}^b - \boldsymbol{\sigma}^o)] = \mathbf{o}. \quad (16.23)$$

Substituting equations (16.7), (16.8), and (16.4),

$$\mathbf{n} \cdot [(\mathbb{C}^b : \mathbf{d}^o + \mathbb{C}^b : (\mathbf{q} \otimes \mathbf{n}) - \mathbb{C}^o : \mathbf{d}^o) + (\nabla \mathbf{v}^o + \mathbf{q} \otimes \mathbf{n}) \cdot (\mathbf{n} \otimes \mathbf{n} - \mathbf{I}) \cdot (\boldsymbol{\sigma}^b - \boldsymbol{\sigma}^o)] = \mathbf{o}. \quad (16.24)$$

Using the symmetry of stress and the projection $\mathbf{n} \otimes \mathbf{n} - \mathbf{I}$, we can reorganize the above expression into

$$\mathbf{n} \cdot [(\mathbb{C}^b + (\boldsymbol{\sigma}^b - \boldsymbol{\sigma}^o) \cdot (\mathbf{n} \otimes \mathbf{n} - \mathbf{I}) \cdot \mathbb{I}) : (\mathbf{q} \otimes \mathbf{n}) + (\mathbb{C}^b - \mathbb{C}^o) : \mathbf{d}^o + (\boldsymbol{\sigma}^b - \boldsymbol{\sigma}^o) \cdot (\mathbf{n} \otimes \mathbf{n} - \mathbf{I}) \cdot \nabla \mathbf{v}^o] = \mathbf{o}. \quad (16.25)$$

Further rearrangement leads to

$$[\mathbf{n} \cdot (\mathbb{C}^b + (\boldsymbol{\sigma}^b - \boldsymbol{\sigma}^o) \cdot (\mathbf{n} \otimes \mathbf{n} - \mathbf{I}) \cdot \mathbb{I}) \cdot \mathbf{n}] \cdot \mathbf{q} = -\mathbf{n} \cdot [(\mathbb{C}^b - \mathbb{C}^o) : \mathbf{d}^o + (\boldsymbol{\sigma}^b - \boldsymbol{\sigma}^o) \cdot (\mathbf{n} \otimes \mathbf{n} - \mathbf{I}) \cdot \nabla \mathbf{v}^o] \quad (16.26)$$

This equation has a solution (\mathbf{q}) only if

$$\det[\mathbf{n} \cdot (\mathbb{C}^b + (\boldsymbol{\sigma}^b - \boldsymbol{\sigma}^o) \cdot (\mathbf{n} \otimes \mathbf{n} - \mathbf{I}) \cdot \mathbb{I}) \cdot \mathbf{n}] \neq \mathbf{o}. \quad (16.27)$$

The canonical bifurcation condition is obtained if $\boldsymbol{\sigma}^b = \boldsymbol{\sigma}^o$:

$$\det(\mathbf{A}) := \det(\mathbf{n} \cdot \mathbb{C} \cdot \mathbf{n}) = \mathbf{o} \quad (16.28)$$

where \mathbf{A} is the **acoustic tensor**.

Evaluation of the acoustic tensor requires a search for a normal vector around the material point and is therefore computationally expensive.

16.3.3 Becker's simplification

A simplification of this criterion is a check which assumes that the direction of instability lies in the plane of the maximum and minimum principal stress [71].

Let the principal stresses be $\sigma_1 > \sigma_2 > \sigma_3$, and the corresponding principal directions (eigenvectors) are E_1, E_2, E_3 . We can express the unit normal to the band in this basis as $\mathbf{n} = n_i E_i$.

The components of the tangent modulus in this coordinate system are given by

$$C'_{ijk\ell} = Q_{im} Q_{jn} Q_{kp} Q_{\ell q} C_{mnpq}. \quad (16.29)$$

where the 3×3 matrix used for this coordinate transformation, \mathbf{Q} , is given by

$$\mathbf{Q}^T := [\mathbf{E}_1 \quad \mathbf{E}_2 \quad \mathbf{E}_3] \quad (16.30)$$

Then the acoustic tensor in (16.28) has the components

$$A_{jk} = C'_{ijk\ell} n_i n_\ell \quad (16.31)$$

If $\det(A_{jk}) = 0$, then $q_j = df_j/dx_2$ can be arbitrary and there is a possibility of strain localization. Also, this condition indicates when a material transitions from stable behavior where $\det(A_{jk}) > 0$. If this condition for loss of hyperbolicity is met, then a particle deforms in an unstable manner and failure can be assumed to have occurred at that particle.

Becker's simplification is to consider only selected components of the acoustic tensor by assuming that the stress state in the band can be approximated as a planar tension problem. Then the acoustic tensor takes the form

$$\mathbf{A} = \begin{bmatrix} C'_{1111}n_1^2 + C'_{3113}n_3^2 & 0 & (C'_{1133} + C'_{3131})n_1n_3 \\ 0 & C'_{1221}n_1^2 + C'_{3223}n_3^2 & 0 \\ (C'_{3311} + C'_{1313})n_1n_3 & 0 & C'_{1331}n_1^2 + C'_{3333}n_3^2 \end{bmatrix} \quad (16.32)$$

Without loss of generality, we can divide this matrix by n_1^2 to get

$$\tilde{\mathbf{A}} = \begin{bmatrix} C'_{1111} + C'_{3113} \frac{n_3^2}{n_1^2} & 0 & (C'_{1133} + C'_{3131}) \frac{n_3}{n_1} \\ 0 & C'_{1221} + C'_{3223} \frac{n_3^2}{n_1^2} & 0 \\ (C'_{3311} + C'_{1313}) \frac{n_3}{n_1} & 0 & C'_{1331} + C'_{3333} \frac{n_3^2}{n_1^2} \end{bmatrix} \quad (16.33)$$

Let $\alpha := n_3/n_1$. Then we can write

$$\tilde{\mathbf{A}} = \begin{bmatrix} C'_{1111} + C'_{3113}\alpha^2 & 0 & (C'_{1133} + C'_{3131})\alpha \\ 0 & C'_{1221} + C'_{3223}\alpha^2 & 0 \\ (C'_{3311} + C'_{1313})\alpha & 0 & C'_{1331} + C'_{3333}\alpha^2 \end{bmatrix} \quad (16.34)$$

and we have

$$\det(\tilde{\mathbf{A}}) = (C'_{1111} + C'_{3113}\alpha^2)\alpha^2(C'_{1331} + C'_{3333}\alpha^2) - (C'_{1133} + C'_{3131})\alpha(C'_{1221} + C'_{3223}\alpha^2)(C'_{3311} + C'_{1313})\alpha \quad (16.35)$$

Setting the determinant to zero allows us to get the following quadratic equation in $\beta := \alpha^2$:

$$(C'_{1111} + C'_{3113}\beta)(C'_{1331} + C'_{3333}\beta) - (C'_{1133} + C'_{3131})(C'_{1221} + C'_{3223}\beta)(C'_{3311} + C'_{1313}) = 0. \quad (16.36)$$

We can express the above in Voigt notation (convention 11, 22, 33, 23, 31, 12) as

$$(\hat{C}_{11} + \hat{C}_{55}\beta)(\hat{C}_{55} + \hat{C}_{33}\beta) - (\hat{C}_{13} + \hat{C}_{55})(\hat{C}_{66} + \hat{C}_{44}\beta)(\hat{C}_{31} + \hat{C}_{55}) = 0. \quad (16.37)$$

or

$$a_1\beta^2 + a_2\beta + a_3 = 0 \quad (16.38)$$

where,

$$\begin{aligned} a_1 &= \hat{C}_{33}\hat{C}_{55} \\ a_2 &= \hat{C}_{11}\hat{C}_{33} - \hat{C}_{13}\hat{C}_{31}\hat{C}_{44} - \hat{C}_{13}\hat{C}_{44}\hat{C}_{55} - \hat{C}_{31}\hat{C}_{44}\hat{C}_{55} - \hat{C}_{44}\hat{C}_{55}^2 + \hat{C}_{55}^2 \\ a_3 &= \hat{C}_{11}\hat{C}_{55} - \hat{C}_{13}\hat{C}_{31}\hat{C}_{66} - \hat{C}_{13}\hat{C}_{55}\hat{C}_{66} - \hat{C}_{31}\hat{C}_{55}\hat{C}_{66} . \end{aligned} \quad (16.39)$$

The four roots are

$$\frac{n_3}{n_1} = \pm \sqrt{\frac{-a_2 \pm \sqrt{a_2^2 - 4a_1a_3}}{2a_1}} . \quad (16.40)$$

If there are no real roots, a band cannot form and there is no bifurcation. If there are four real roots then bifurcation is possible. Two real roots indicate an intermediate condition that may not be realized in practice but is considered stable in VAANGO .

More explicitly, for unstable deformation,

$$a_2^2 - 4a_1a_3 \geq 0 \quad \text{and} \quad \frac{-a_2 \pm \sqrt{a_2^2 - 4a_1a_3}}{2a_1} \geq 0 . \quad (16.41)$$

If these conditions are satisfied, the **MPM** particle is assumed to have failed.



17 — Isotropic metal plasticity

The deformation gradient (\mathbf{F}) can be decomposed into a rotation tensor (\mathbf{R}) and a stretch tensor (\mathbf{U}) with the polar decomposition $\mathbf{F} = \mathbf{R} \cdot \mathbf{U}$. In the isotropic metal plasticity model implemented in VAANGO, \mathbf{R} is used to rotate the stress ($\boldsymbol{\sigma}$) and the rate of deformation (\mathbf{d}) into the unrotated configuration before the updated stress is computed:

$$\hat{\boldsymbol{\sigma}} = \mathbf{R}^T \cdot \boldsymbol{\sigma} \cdot \mathbf{R}; \quad \hat{\dot{\boldsymbol{\epsilon}}} = \mathbf{R}^T \cdot \mathbf{d} \cdot \mathbf{R} \quad (17.1)$$

where $\dot{\boldsymbol{\epsilon}}$ is a “natural” strain rate. After the stress has been updated, it is rotated back using

$$\boldsymbol{\sigma} = \mathbf{R} \cdot \hat{\boldsymbol{\sigma}} \cdot \mathbf{R}^T. \quad (17.2)$$

In the following discussion, all equations should be treated as referring to the hatted quantities even though we drop the hats for convenience.

17.1 The model

The metal plasticity model assumes that we know the total strain rate ($\dot{\boldsymbol{\epsilon}}^t$) and that this strain rate can be decomposed into a mechanical component ($\dot{\boldsymbol{\epsilon}}$) and a thermal expansion component ($\dot{\boldsymbol{\epsilon}}^\alpha$):

$$\dot{\boldsymbol{\epsilon}}^t = \dot{\boldsymbol{\epsilon}} + \dot{\boldsymbol{\epsilon}}^\alpha. \quad (17.3)$$

The thermal expansion component is assumed to be of the rate form

$$\dot{\boldsymbol{\epsilon}}^\alpha = \frac{\partial \boldsymbol{\epsilon}^\alpha}{\partial T} \dot{T} = \alpha \dot{T} \quad (17.4)$$

where T is the temperature and α is a coefficient of thermal expansion. Then the mechanical strain rate can be expressed as

$$\dot{\boldsymbol{\epsilon}} = \dot{\boldsymbol{\epsilon}}^t - \alpha \dot{T}. \quad (17.5)$$

The primary function of the metal plasticity model is to compute the stress when a mechanical strain rate $\dot{\boldsymbol{\epsilon}}$ is given, which we assume can be additively decomposed into elastic ($\dot{\boldsymbol{\epsilon}}^e$) and plastic ($\dot{\boldsymbol{\epsilon}}^p$) parts:

$$\dot{\boldsymbol{\epsilon}} = \dot{\boldsymbol{\epsilon}}^e + \dot{\boldsymbol{\epsilon}}^p. \quad (17.6)$$

The Cauchy stress ($\boldsymbol{\sigma}$) is decomposed into volumetric and deviatoric parts:

$$\boldsymbol{\sigma} = p \mathbf{I} + \mathbf{s} \quad \text{where} \quad p = \frac{1}{3} \text{tr}(\boldsymbol{\sigma}) \quad \text{and} \quad \mathbf{s} = \text{dev}(\boldsymbol{\sigma}) = \boldsymbol{\sigma} - \frac{1}{3} \text{tr}(\boldsymbol{\sigma}) \mathbf{I}. \quad (17.7)$$

In the above $p = \sigma_m$ is the mean stress and \mathbf{s} is the deviatoric stress. An alternative decomposition that can be used for the isotropic metal plasticity models implemented in VAANGO is

$$\boldsymbol{\sigma} = \sigma_p \hat{\mathbf{I}} + \sigma_s \hat{\mathbf{s}}, \quad \hat{\mathbf{I}} = \frac{1}{\sqrt{3}} \mathbf{I}, \quad \hat{\mathbf{s}} = \frac{\mathbf{s}}{\|\mathbf{s}\|}, \quad \sigma_p = \sqrt{3} p, \quad \sigma_s = \|\mathbf{s}\|. \quad (17.8)$$

This decomposition is useful because $\hat{\mathbf{I}}$ and $\hat{\mathbf{s}}$ form a basis that can be used to express several other quantities in the metal plasticity models implemented in VAANGO. The time derivative of stress can then be expressed as

$$\dot{\boldsymbol{\sigma}} = \dot{p} \mathbf{I} + \dot{\mathbf{s}} = \dot{\sigma}_p \hat{\mathbf{I}} + \dot{\sigma}_s \hat{\mathbf{s}}. \quad (17.9)$$

The isotropy of the material allows us to compute the mean stress using an equation of state if desired. The deviatoric stress is computed using a rate-form stress-strain relation. For convenience, we assume that rate-form relations are used for both the mean stress and the deviatoric stress.

17.1.1 Purely elastic loading/unloading

The elastic constitutive relation is assumed to be of the form

$$\dot{\boldsymbol{\epsilon}}^e = \frac{\partial \boldsymbol{\sigma}}{\partial \boldsymbol{\epsilon}^e} : \dot{\boldsymbol{\epsilon}}^e = \mathbb{C}^e : \dot{\boldsymbol{\epsilon}}^e, \quad \mathbb{C}^e = \left(\kappa - \frac{2}{3} \mu \right) \mathbf{I} \otimes \mathbf{I} + 2\mu \text{symm}(\mathbb{I}) \quad (17.10)$$

or,

$$\dot{\boldsymbol{\sigma}}^e = \left(\kappa - \frac{2}{3} \mu \right) \text{tr}(\dot{\boldsymbol{\epsilon}}^e) \mathbf{I} + 2\mu \dot{\boldsymbol{\epsilon}}^e. \quad (17.11)$$

In the above, $\mu(\rho, p, T, \phi, D)$ is the shear modulus, $\kappa(\rho, p, T, \phi, D)$ is the tangent bulk modulus, \mathbf{I} is the second-order identity tensor and \mathbb{I} is the fourth-order identity tensor. Also, ρ is the mass density, p is the pressure, T is the current temperature, ϕ is the current porosity and D is a scalar damage parameter.

The inverse relationship is

$$\dot{\boldsymbol{\epsilon}}^e = \mathbb{S}^e : \dot{\boldsymbol{\sigma}}^e, \quad \mathbb{S}^e = \frac{1}{3} \left(\frac{1}{3\kappa} - \frac{1}{2\mu} \right) \mathbf{I} \otimes \mathbf{I} + \frac{1}{2\mu} \text{symm}(\mathbb{I}) \quad (17.12)$$

Using the decomposition (17.8), we can write

$$\dot{\boldsymbol{\epsilon}}^e = \mathbb{S}^e : (\dot{\sigma}_p \hat{\mathbf{I}} + \dot{\sigma}_s \hat{\mathbf{s}}) = \frac{\dot{\sigma}_p}{3\kappa} \hat{\mathbf{I}} + \frac{\dot{\sigma}_s}{2\mu} \hat{\mathbf{s}}. \quad (17.13)$$

17.1.2 Yield condition

The isotropic metal plasticity yield conditions implemented in VAANGO have the form

$$f(\boldsymbol{\sigma}_\beta, \epsilon_p^{\text{eq}}, \dot{\epsilon}_p^{\text{eq}}, \phi, D, T, \dot{\epsilon}^{\text{eq}}, \dots) = 0, \quad \boldsymbol{\sigma}_\beta := \boldsymbol{\sigma} - \beta. \quad (17.14)$$

The quantity $\boldsymbol{\sigma}_\beta$ is further decomposed into isotropic and deviatoric parts:

$$\boldsymbol{\sigma}_\beta = p_\beta \mathbf{I} + \boldsymbol{\xi} \quad (17.15)$$

where $\boldsymbol{\xi} = \text{dev}(\boldsymbol{\sigma}_\beta)$ and $p_\beta = \text{tr}(\boldsymbol{\sigma}_\beta)/3$. Most of the metal yield conditions in VAANGO use this notation. Derivatives of f with respect to the stress ($\boldsymbol{\sigma}$) can therefore be expressed as

$$\frac{\partial f}{\partial \boldsymbol{\sigma}} = \frac{\partial f}{\partial \boldsymbol{\sigma}_\beta} : \frac{\partial \boldsymbol{\sigma}_\beta}{\partial \boldsymbol{\sigma}} = \frac{\partial f}{\partial \boldsymbol{\sigma}_\beta} = \frac{\partial f}{\partial p_\beta} \frac{\partial p_\beta}{\partial \boldsymbol{\sigma}_\beta} + \frac{\partial f}{\partial \boldsymbol{\xi}} : \frac{\partial \boldsymbol{\xi}}{\partial \boldsymbol{\sigma}_\beta} = \frac{1}{3} \frac{\partial f}{\partial p_\beta} \mathbf{I} + \frac{\partial f}{\partial \boldsymbol{\xi}} - \frac{1}{3} \text{tr} \left(\frac{\partial f}{\partial \boldsymbol{\xi}} \right) \mathbf{I}. \quad (17.16)$$

The isotropic metal yield conditions in VAANGO are expressed in terms of $\sigma_{\text{eff}}^\xi = \sqrt{3J_2^\xi} = \sqrt{\frac{3}{2}\xi:\xi}$. Therefore,

$$\frac{\partial f}{\partial \sigma} = \frac{1}{3} \frac{\partial f}{\partial p_\beta} \mathbf{I} + \frac{\partial f}{\partial \sigma_{\text{eff}}^\xi} \frac{\partial \sigma_{\text{eff}}^\xi}{\partial \xi} = \frac{1}{3} \frac{\partial f}{\partial p_\beta} \mathbf{I} + \sqrt{\frac{3}{2}} \frac{\partial f}{\partial \sigma_{\text{eff}}^\xi} \frac{\xi}{\|\xi\|}. \quad (17.17)$$

If we express both \mathbf{I} and ξ in terms of the basis $\hat{\mathbf{I}}$ and $\hat{\mathbf{s}}$, we have

$$\mathbf{I} = \sqrt{3}\hat{\mathbf{I}}, \quad \xi = \xi_s \hat{\mathbf{s}}, \quad \xi_s = \xi : \hat{\mathbf{s}} \quad \text{and} \quad \|\xi\| = \xi_s \quad \implies \quad \frac{\xi}{\|\xi\|} = \hat{\mathbf{s}}. \quad (17.18)$$

Therefore,

$$\mathbf{N} = \frac{\partial f}{\partial \sigma} = \frac{1}{\sqrt{3}} \frac{\partial f}{\partial p_\beta} \hat{\mathbf{I}} + \sqrt{\frac{3}{2}} \frac{\partial f}{\partial \sigma_{\text{eff}}^\xi} \hat{\mathbf{s}}, \quad \|\mathbf{N}\| = \sqrt{\frac{1}{3} \left(\frac{\partial f}{\partial p_\beta} \right)^2 + \frac{3}{2} \left(\frac{\partial f}{\partial \sigma_{\text{eff}}^\xi} \right)^2}, \quad \hat{\mathbf{N}} = \frac{\mathbf{N}}{\|\mathbf{N}\|}. \quad (17.19)$$

The Kuhn-Tucker loading-unloading conditions are

$$\dot{\lambda} \geq 0; \quad f \leq 0; \quad \dot{\lambda} f = 0 \quad (17.20)$$

and the consistency condition is $\dot{\lambda} \dot{f} = 0$.

17.1.3 Flow rule

We assume that the plastic rate of deformation is given by the flow rule

$$\dot{\epsilon}^p = \dot{\lambda} \hat{\mathbf{M}}. \quad (17.21)$$

For the isotropic metal plasticity models in VAANGO, we assume associated plasticity:

$$\dot{\epsilon}^p = \dot{\lambda} \hat{\mathbf{N}} = \frac{\dot{\lambda}}{\|\mathbf{N}\|} \left[\frac{1}{\sqrt{3}} \frac{\partial f}{\partial p_\beta} \hat{\mathbf{I}} + \sqrt{\frac{3}{2}} \frac{\partial f}{\partial \sigma_{\text{eff}}^\xi} \hat{\mathbf{s}} \right]. \quad (17.22)$$

17.1.4 Isotropic and kinematic hardening/softening rules

The equivalent plastic strain (ϵ_p^{eq}) evolves according to the relation

$$\dot{\epsilon}_p^{\text{eq}} = \dot{\lambda} h^{\epsilon_p}. \quad (17.23)$$

The back stress (β) evolves according to the relation

$$\dot{\beta} = \dot{\lambda} h^\beta. \quad (17.24)$$

The porosity (ϕ) is assumed to evolve according to the relation

$$\dot{\phi} = \dot{\lambda} h^\phi. \quad (17.25)$$

The damage parameter (D) evolves as

$$\dot{D} = \dot{\lambda} h^D. \quad (17.26)$$

The temperature (T_p) due to plastic dissipation evolves as

$$\dot{T}_p = \dot{\lambda} h^T. \quad (17.27)$$

17.1.5 Elastic-plastic loading/unloading

During purely elastic loading and unloading

$$\dot{\lambda} = 0, \quad \dot{\boldsymbol{\varepsilon}}^p = \mathbf{0}, \quad \dot{\boldsymbol{\varepsilon}} = \dot{\boldsymbol{\varepsilon}}^e. \quad (17.28)$$

In that situation, the stress is updated using (17.10).

However, during elastic-plastic deformation, $\dot{\lambda} > 0$, and we have

$$\begin{aligned} \dot{\boldsymbol{\sigma}} &= \frac{\partial \boldsymbol{\sigma}}{\partial \boldsymbol{\varepsilon}^e} : \dot{\boldsymbol{\varepsilon}}^e + \frac{\partial \boldsymbol{\sigma}}{\partial \boldsymbol{\beta}} : \dot{\boldsymbol{\beta}} + \frac{\partial \boldsymbol{\sigma}}{\partial \varepsilon_p^{\text{eq}}} \dot{\varepsilon}_p^{\text{eq}} + \frac{\partial \boldsymbol{\sigma}}{\partial \phi} \dot{\phi} + \frac{\partial \boldsymbol{\sigma}}{\partial D} \dot{D} + \frac{\partial \boldsymbol{\sigma}}{\partial T_p} \dot{T}_p \\ &= \mathbb{C}^e : \dot{\boldsymbol{\varepsilon}}^e + \dot{\lambda} \left[\frac{\partial \boldsymbol{\sigma}}{\partial \boldsymbol{\beta}} : \mathbf{h}^\beta + \frac{\partial \boldsymbol{\sigma}}{\partial \varepsilon_p^{\text{eq}}} h^{\varepsilon_p} + \frac{\partial \boldsymbol{\sigma}}{\partial \phi} h^\phi + \frac{\partial \boldsymbol{\sigma}}{\partial D} h^D + \frac{\partial \boldsymbol{\sigma}}{\partial T_p} h^T \right] \\ &= \mathbb{C}^e : \dot{\boldsymbol{\varepsilon}} - \dot{\lambda} \left[\mathbb{C}^e : \hat{\mathbf{M}} - \frac{\partial \boldsymbol{\sigma}}{\partial \boldsymbol{\beta}} : \mathbf{h}^\beta - \frac{\partial \boldsymbol{\sigma}}{\partial \varepsilon_p^{\text{eq}}} h^{\varepsilon_p} - \frac{\partial \boldsymbol{\sigma}}{\partial \phi} h^\phi - \frac{\partial \boldsymbol{\sigma}}{\partial D} h^D - \frac{\partial \boldsymbol{\sigma}}{\partial T_p} h^T \right] \end{aligned} \quad (17.29)$$

Define

$$\mathbf{P} := \mathbb{C}^e : \hat{\mathbf{M}} - \frac{\partial \boldsymbol{\sigma}}{\partial \boldsymbol{\beta}} : \mathbf{h}^\beta - \frac{\partial \boldsymbol{\sigma}}{\partial \varepsilon_p^{\text{eq}}} h^{\varepsilon_p} - \frac{\partial \boldsymbol{\sigma}}{\partial \phi} h^\phi - \frac{\partial \boldsymbol{\sigma}}{\partial D} h^D - \frac{\partial \boldsymbol{\sigma}}{\partial T_p} h^T. \quad (17.30)$$

Then,

$$\dot{\boldsymbol{\sigma}} = \mathbb{C}^e : \dot{\boldsymbol{\varepsilon}} - \dot{\lambda} \mathbf{P} = \dot{\boldsymbol{\sigma}}^{\text{trial}} - \dot{\lambda} \mathbf{P} \quad \text{where} \quad \dot{\boldsymbol{\sigma}}^{\text{trial}} := \mathbb{C}^e : \dot{\boldsymbol{\varepsilon}}. \quad (17.31)$$

In VAANGO, we assume that the coupling terms $\partial \boldsymbol{\sigma} / \partial \boldsymbol{\beta}$ are zero and $T = T_p$ for elastic-plastic coupling. From (17.10) we have

$$\dot{\boldsymbol{\sigma}}^e = \left(\kappa - \frac{2}{3} \mu \right) \text{tr}(\dot{\boldsymbol{\varepsilon}}^e) \mathbf{I} + 2\mu \dot{\boldsymbol{\varepsilon}}^e \quad (17.32)$$

We can use this relation to estimate the coupling terms for the internal variables $\eta \in \{\varepsilon_p^{\text{eq}}, \phi, D, T\}$:

$$\frac{\partial \boldsymbol{\sigma}}{\partial \eta} = \left(\frac{\partial \kappa}{\partial \eta} - \frac{2}{3} \frac{\partial \mu}{\partial \eta} \right) \text{tr}(\boldsymbol{\varepsilon}^e) \mathbf{I} + 2 \frac{\partial \mu}{\partial \eta} \boldsymbol{\varepsilon}^e \quad (17.33)$$

Similarly, from (17.13), choosing the basis to be $\hat{\mathbf{I}}$ and $\hat{\mathbf{s}}^{\text{trial}} = \text{dev}(\boldsymbol{\sigma}^{\text{trial}}) / \|\text{dev}(\boldsymbol{\sigma}^{\text{trial}})\|$,

$$\boldsymbol{\varepsilon}^e = \frac{\sigma_p^e}{3\kappa} \hat{\mathbf{I}} + \frac{\sigma_s^e \sigma_{ss}}{2\mu} \hat{\mathbf{s}}^{\text{trial}} \quad \text{and} \quad \text{tr}(\boldsymbol{\varepsilon}^e) = \frac{\sigma_p^e}{\sqrt{3}\kappa} \quad (17.34)$$

where $\sigma_{ss} = \hat{\mathbf{s}}^e : \hat{\mathbf{s}}^{\text{trial}}$. Substitution into (17.33) leads to

$$\frac{\partial \boldsymbol{\sigma}}{\partial \eta} = \frac{1}{\kappa} \frac{\partial \kappa}{\partial \eta} \sigma_p^e \hat{\mathbf{I}} + \frac{1}{\mu} \frac{\partial \mu}{\partial \eta} \sigma_s^e \sigma_{ss} \hat{\mathbf{s}}^{\text{trial}}. \quad (17.35)$$

Also, for associated plasticity and using (17.19),

$$\mathbb{C}^e : \hat{\mathbf{M}} = \frac{1}{\|\mathbf{N}\|} \left[\sqrt{3}\kappa \frac{\partial f}{\partial p_\beta} \hat{\mathbf{I}} + 2\sqrt{\frac{3}{2}}\mu \frac{\partial f}{\partial \sigma_{\text{eff}}^\xi} \hat{\mathbf{s}} \right] = \frac{1}{\|\mathbf{N}\|} \left[\sqrt{3}\kappa \frac{\partial f}{\partial p_\beta} \hat{\mathbf{I}} + \sqrt{6}\mu \frac{\partial f}{\partial \sigma_{\text{eff}}^\xi} \sigma_{ss} \hat{\mathbf{s}}^{\text{trial}} \right] \quad (17.36)$$

Therefore,

$$\mathbf{P} = \left[\frac{\sqrt{3}\kappa}{\|\mathbf{N}\|} \frac{\partial f}{\partial p_\beta} - \frac{1}{\kappa} \sum_\eta \frac{\partial \kappa}{\partial \eta} \sigma_p^e \right] \hat{\mathbf{I}} + \left[\frac{\sqrt{6}\mu}{\|\mathbf{N}\|} \frac{\partial f}{\partial \sigma_{\text{eff}}^\xi} - \frac{1}{\mu} \sum_\eta \frac{\partial \mu}{\partial \eta} \sigma_s^e \right] \sigma_{ss} \hat{\mathbf{s}}^{\text{trial}} \quad (17.37)$$

For an elastic-plastic load step, we can compute the plastic strain rate using (17.13):

$$\dot{\boldsymbol{\varepsilon}}^p = \dot{\boldsymbol{\varepsilon}} - \frac{\dot{\sigma}_p^e}{3\kappa} \hat{\mathbf{I}} - \frac{\dot{\sigma}_s^e}{2\mu} \hat{\mathbf{s}}^{\text{trial}}. \quad (17.38)$$

17.1.6 Consistency condition

The consistency condition requires that, when $\dot{\lambda} > 0$,

$$\dot{f}(\boldsymbol{\sigma}, \boldsymbol{\beta}, \varepsilon_p^{\text{eq}}, \dot{\varepsilon}_p^{\text{eq}}, \phi, D, T, \dot{\varepsilon}^{\text{eq}}, \dots) = 0. \quad (17.39)$$

For rate-independent plasticity, from the chain rule,

$$\dot{f} = \frac{\partial f}{\partial \boldsymbol{\sigma}} : \dot{\boldsymbol{\sigma}} + \frac{\partial f}{\partial \boldsymbol{\beta}} : \dot{\boldsymbol{\beta}} + \frac{\partial f}{\partial \varepsilon_p^{\text{eq}}} \dot{\varepsilon}_p^{\text{eq}} + \frac{\partial f}{\partial \phi} \dot{\phi} + \frac{\partial f}{\partial D} \dot{D} + \frac{\partial f}{\partial T_p} \dot{T}_p = 0. \quad (17.40)$$

Using the hardening/softening rules,

$$\frac{\partial f}{\partial \boldsymbol{\sigma}} : \dot{\boldsymbol{\sigma}} + \dot{\lambda} \left[\frac{\partial f}{\partial \boldsymbol{\beta}} : \mathbf{h}^\beta + \frac{\partial f}{\partial \varepsilon_p^{\text{eq}}} h^{\varepsilon_p} + \frac{\partial f}{\partial \phi} h^\phi + \frac{\partial f}{\partial D} h^D + \frac{\partial f}{\partial T_p} h^T \right] = 0 \quad (17.41)$$

or

$$\frac{\partial f}{\partial \boldsymbol{\sigma}} : \dot{\boldsymbol{\sigma}} + \dot{\lambda} H = 0. \quad (17.42)$$

Define,

$$\mathbf{N} := \frac{\partial f}{\partial \boldsymbol{\sigma}}, \quad \hat{\mathbf{N}} := \frac{\mathbf{N}}{\|\mathbf{N}\|}, \quad \hat{H} := \frac{H}{\|\mathbf{N}\|}. \quad (17.43)$$

Then,

$$\hat{\mathbf{N}} : \dot{\boldsymbol{\sigma}} + \dot{\lambda} \hat{H} = 0. \quad (17.44)$$

Combining the stress-rate equation (17.31) with the consistency equation (17.44), we have

$$\hat{\mathbf{N}} : \dot{\boldsymbol{\sigma}}^{\text{trial}} = \hat{\mathbf{N}} : \mathbb{C}^e : \dot{\boldsymbol{\varepsilon}} = \dot{\lambda} (\hat{\mathbf{N}} : \mathbf{P} - \hat{H}). \quad (17.45)$$

Therefore,

$$\dot{\lambda} = \frac{\hat{\mathbf{N}} : \dot{\boldsymbol{\sigma}}^{\text{trial}}}{\hat{\mathbf{N}} : \mathbf{P} - \hat{H}} = \frac{\hat{\mathbf{N}} : \mathbb{C}^e : \dot{\boldsymbol{\varepsilon}}}{\hat{\mathbf{N}} : \mathbf{P} - \hat{H}} \quad (17.46)$$

Substituting this expression to (17.31), we have

$$\dot{\boldsymbol{\sigma}} = \dot{\boldsymbol{\sigma}}^{\text{trial}} - \frac{\hat{\mathbf{N}} : \dot{\boldsymbol{\sigma}}^{\text{trial}}}{\hat{\mathbf{N}} : \mathbf{P} - \hat{H}} \mathbf{P} = \dot{\boldsymbol{\sigma}}^{\text{trial}} - \frac{\mathbf{P} \otimes \hat{\mathbf{N}}}{\hat{\mathbf{N}} : \mathbf{P} - \hat{H}} : \dot{\boldsymbol{\sigma}}^{\text{trial}} \quad (17.47)$$

or,

$$\dot{\boldsymbol{\sigma}} = \mathbb{C}^e : \dot{\boldsymbol{\varepsilon}} - \frac{(\mathbf{P} \otimes \hat{\mathbf{N}}) : \mathbb{C}^e}{\hat{\mathbf{N}} : \mathbf{P} - \hat{H}} : \dot{\boldsymbol{\varepsilon}} = \mathbb{C}^{ep} : \dot{\boldsymbol{\varepsilon}}. \quad (17.48)$$

The quantity \mathbb{C}^{ep} is the continuum elastic-plastic tangent modulus.

17.2 Stress update

The first step in the stress update procedure is to compute a trial stress state from

$$\dot{\boldsymbol{\sigma}}^{\text{trial}} = \mathbb{C}^e : \dot{\boldsymbol{\varepsilon}}. \quad (17.49)$$

We assume that

$$\boldsymbol{\sigma}^{\text{trial}} = \boldsymbol{\sigma}_n + \Delta t (\mathbb{C}_n^e : \dot{\boldsymbol{\varepsilon}}_{n+1}) \quad (17.50)$$

where σ_n is the stress at the end of time t_n , \mathbb{C}_n^e is the elastic modulus at that time, $\dot{\epsilon}_{n+1}$ is the strain rate computed from the symmetric part of the unrotated velocity gradient, and $\Delta t = t_{n+1} - t_n$ is the timestep size.

The trial state contains the vector

$$\eta^{\text{trial}} = [\sigma^{\text{trial}}, \beta_n, (\epsilon_p^{\text{eq}})_n, (\dot{\epsilon}_p^{\text{eq}})_n, \phi_n, D_n, T_n, \dot{\epsilon}_n^{\text{eq}}, \kappa_n, \mu_n, \dots] \quad (17.51)$$

where the subscript (n) indicates the state at the end of time t_n .

The trial state is used to compute the yield function

$$f_y = f[\sigma^{\text{trial}}, \beta_n, (\epsilon_p^{\text{eq}})_n, (\dot{\epsilon}_p^{\text{eq}})_n, \phi_n, D_n, T_n, \dot{\epsilon}_n^{\text{eq}}, \kappa_n, \mu_n, \dots] \quad (17.52)$$

If $f_y \leq 0$, the trial state is in the elastic regime and we update the stress using

$$\begin{aligned} \sigma_{n+1} &= \sigma^{\text{trial}}, \quad \beta_{n+1} = \beta_n, \quad (\epsilon_p^{\text{eq}})_{n+1} = (\epsilon_p^{\text{eq}})_n, \quad (\dot{\epsilon}_p^{\text{eq}})_{n+1} = (\dot{\epsilon}_p^{\text{eq}})_n \\ \phi_{n+1} &= \phi_n, \quad D_{n+1} = D_n, \quad T_{n+1} = T_n \\ \kappa_{n+1} &= \kappa(p_{n+1}, T_n), \quad \mu_{n+1} = \mu(p_{n+1}, T_n). \end{aligned} \quad (17.53)$$

If $f_y > 0$, the trial state is outside the yield surface in the elastic-plastic regime. We can use a backward Euler algorithm to compute the updated stress state:

$$\frac{\sigma_{n+1} - \sigma_n}{\Delta t} = \frac{\sigma^{\text{trial}} - \sigma_n}{\Delta t} - \frac{\lambda_{n+1} - \lambda_n}{\Delta t} \mathbf{P}_{n+1} \quad \text{or} \quad \sigma_{n+1} = \sigma^{\text{trial}} - \Delta \lambda_{n+1} \mathbf{P}_{n+1}. \quad (17.54)$$

The plastic strain and the internal variables can similarly be updated using

$$\begin{aligned} \epsilon_{n+1}^p &= \epsilon_n^p + \Delta \lambda_{n+1} \hat{\mathbf{M}}_{n+1} \\ (\epsilon_p^{\text{eq}})_{n+1} &= (\epsilon_p^{\text{eq}})_n + \Delta \lambda_{n+1} h_{n+1}^{\epsilon_p} \\ \beta_{n+1} &= \beta_n + \Delta \lambda_{n+1} h_{n+1}^\beta \\ \phi_{n+1} &= \phi_n + \Delta \lambda_{n+1} h_{n+1}^\phi \\ D_{n+1} &= D_n + \Delta \lambda_{n+1} h_{n+1}^D \\ (T_p)_{n+1} &= (T_p)_n + \Delta \lambda_{n+1} h_{n+1}^T. \end{aligned} \quad (17.55)$$

In addition, the stress state has to lie on the yield surface:

$$f(\sigma^{\text{trial}} - \Delta \lambda_{n+1} \mathbf{P}_{n+1}) = 0. \quad (17.56)$$

Finally, the consistency condition needs to be satisfied:

$$\hat{\mathbf{N}}_{n+1} : (\sigma_{n+1} - \sigma_n) + \Delta \lambda_{n+1} \hat{H}_{n+1} = 0 \quad (17.57)$$

or,

$$\hat{\mathbf{N}}_{n+1} : (\sigma^{\text{trial}} - \sigma_n) = \Delta \lambda_{n+1} (\hat{\mathbf{N}}_{n+1} : \mathbf{P}_{n+1} - \hat{H}_{n+1}). \quad (17.58)$$

17.2.1 Iterative solution

VAANGO assumes associated plasticity for isotropic metals, i.e., $\hat{\mathbf{M}} = \hat{\mathbf{N}}$. Therefore, the following coupled equations, not all of which are independent, have to be solved for $\Gamma := \Delta \lambda_{n+1}$ and the updated state

$[\boldsymbol{\sigma}_{n+1}, \boldsymbol{\kappa}_{n+1}, \boldsymbol{\mu}_{n+1}, \boldsymbol{\varepsilon}_{n+1}^p, (\boldsymbol{\varepsilon}_p^{\text{eq}})_{n+1}, \boldsymbol{\beta}_{n+1}, \phi_{n+1}, D_{n+1}, (T_p)_{n+1}]$:

$$\begin{aligned}
\boldsymbol{\sigma}_{n+1} &= \boldsymbol{\sigma}^{\text{trial}} - \Gamma \mathbf{P}_{n+1} \\
\boldsymbol{\varepsilon}_{n+1}^p &= \boldsymbol{\varepsilon}_n^p + \Gamma \hat{\mathbf{N}}_{n+1} \\
\boldsymbol{\beta}_{n+1} &= \boldsymbol{\beta}_n + \Gamma \mathbf{h}_{n+1}^\beta \\
(\boldsymbol{\varepsilon}_p^{\text{eq}})_{n+1} &= (\boldsymbol{\varepsilon}_p^{\text{eq}})_n + \Gamma \mathbf{h}_{n+1}^{\varepsilon_p} \\
\phi_{n+1} &= \phi_n + \Gamma \mathbf{h}_{n+1}^\phi \\
D_{n+1} &= D_n + \Gamma \mathbf{h}_{n+1}^D \\
(T_p)_{n+1} &= (T_p)_n + \Gamma \mathbf{h}_{n+1}^T \\
\hat{\mathbf{N}}_{n+1} : (\boldsymbol{\sigma}^{\text{trial}} - \boldsymbol{\sigma}_n) - \Gamma(\hat{\mathbf{N}}_{n+1} : \mathbf{P}_{n+1} - \hat{H}_{n+1}) &= 0 \\
f_{n+1} &= f(\boldsymbol{\sigma}^{\text{trial}} - \Gamma \mathbf{P}_{n+1}) = 0
\end{aligned} \tag{17.59}$$

where

$$\begin{aligned}
\mathbf{P}_{n+1} &= \mathbb{C}_{n+1}^e : \hat{\mathbf{N}}_{n+1} - \frac{\partial \boldsymbol{\sigma}}{\partial \boldsymbol{\beta}} \bigg|_{n+1} : \mathbf{h}_{n+1}^\beta - \frac{\partial \boldsymbol{\sigma}}{\partial \boldsymbol{\varepsilon}_p^{\text{eq}}} \bigg|_{n+1} \mathbf{h}_{n+1}^{\varepsilon_p} - \frac{\partial \boldsymbol{\sigma}}{\partial \phi} \bigg|_{n+1} \mathbf{h}_{n+1}^\phi - \frac{\partial \boldsymbol{\sigma}}{\partial D} \bigg|_{n+1} \mathbf{h}_{n+1}^D - \frac{\partial \boldsymbol{\sigma}}{\partial T_p} \bigg|_{n+1} \mathbf{h}_{n+1}^T \\
\hat{\mathbf{N}}_{n+1} &= \frac{\mathbf{N}_{n+1}}{\|\mathbf{N}_{n+1}\|}, \quad \mathbf{N}_{n+1} = \frac{\partial f}{\partial \boldsymbol{\sigma}} \bigg|_{n+1} \\
\hat{H}_{n+1} &= \frac{H_{n+1}}{\|\mathbf{N}_{n+1}\|}, \quad H_{n+1} = \frac{\partial f}{\partial \boldsymbol{\beta}} \bigg|_{n+1} : \mathbf{h}_{n+1}^\beta + \frac{\partial f}{\partial \boldsymbol{\varepsilon}_p^{\text{eq}}} \bigg|_{n+1} \mathbf{h}_{n+1}^{\varepsilon_p} + \frac{\partial f}{\partial \phi} \bigg|_{n+1} \mathbf{h}_{n+1}^\phi + \frac{\partial f}{\partial D} \bigg|_{n+1} \mathbf{h}_{n+1}^D + \frac{\partial f}{\partial T_p} \bigg|_{n+1} \mathbf{h}_{n+1}^T.
\end{aligned} \tag{17.60}$$

Let us express the stresses and strains as vectors:

$$\mathbf{S} := [\sigma_{11}, \sigma_{22}, \sigma_{33}, \sqrt{2}\sigma_{23}, \sqrt{2}\sigma_{31}, \sqrt{2}\sigma_{12}] \quad \mathbf{E}^p := [\varepsilon_{11}^p, \varepsilon_{22}^p, \varepsilon_{33}^p, \sqrt{2}\varepsilon_{23}^p, \sqrt{2}\varepsilon_{31}^p, \sqrt{2}\varepsilon_{12}^p]. \tag{17.61}$$

We can also write

$$\mathbf{N} := \left[\frac{\partial f}{\partial \sigma_{11}}, \frac{\partial f}{\partial \sigma_{22}}, \frac{\partial f}{\partial \sigma_{33}}, \sqrt{2} \frac{\partial f}{\partial \sigma_{23}}, \sqrt{2} \frac{\partial f}{\partial \sigma_{31}}, \sqrt{2} \frac{\partial f}{\partial \sigma_{12}} \right], \quad \hat{\mathbf{N}} = \frac{\mathbf{N}}{\|\mathbf{N}\|}. \tag{17.62}$$

Because of the isotropy of the elasticity tensor, we have

$$\begin{aligned}
\mathbb{C}^e : \hat{\mathbf{N}} = \mathbf{C} = & \left[2\mu N_1 + (\kappa - \frac{2}{3}\mu)(N_1 + N_2 + N_3), 2\mu N_2 + (\kappa - \frac{2}{3}\mu)(N_1 + N_2 + N_3), \right. \\
& \left. 2\mu N_3 + (\kappa - \frac{2}{3}\mu)(N_1 + N_2 + N_3), 2\sqrt{2}\mu N_4, 2\sqrt{2}\mu N_5, 2\sqrt{2}\mu N_6 \right]
\end{aligned} \tag{17.63}$$

where N_i are the components of the vector $\hat{\mathbf{N}}$. If we ignore the elastic-plastic coupling term $\partial \boldsymbol{\sigma} / \partial \boldsymbol{\beta}$, and define

$$\begin{aligned}
\mathbf{Z}^{\varepsilon_p} &:= \left[\frac{\partial \sigma_{11}}{\partial \varepsilon_p^{\text{eq}}} h^{\varepsilon_p}, \frac{\partial \sigma_{22}}{\partial \varepsilon_p^{\text{eq}}} h^{\varepsilon_p}, \frac{\partial \sigma_{33}}{\partial \varepsilon_p^{\text{eq}}} h^{\varepsilon_p}, \sqrt{2} \frac{\partial \sigma_{23}}{\partial \varepsilon_p^{\text{eq}}} h^{\varepsilon_p}, \sqrt{2} \frac{\partial \sigma_{31}}{\partial \varepsilon_p^{\text{eq}}} h^{\varepsilon_p}, \sqrt{2} \frac{\partial \sigma_{12}}{\partial \varepsilon_p^{\text{eq}}} h^{\varepsilon_p} \right] \\
\mathbf{Z}^\phi &:= \left[\frac{\partial \sigma_{11}}{\partial \phi} h^\phi, \frac{\partial \sigma_{22}}{\partial \phi} h^\phi, \frac{\partial \sigma_{33}}{\partial \phi} h^\phi, \sqrt{2} \frac{\partial \sigma_{23}}{\partial \phi} h^\phi, \sqrt{2} \frac{\partial \sigma_{31}}{\partial \phi} h^\phi, \sqrt{2} \frac{\partial \sigma_{12}}{\partial \phi} h^\phi \right] \\
\mathbf{Z}^D &:= \left[\frac{\partial \sigma_{11}}{\partial D} h^D, \frac{\partial \sigma_{22}}{\partial D} h^D, \frac{\partial \sigma_{33}}{\partial D} h^D, \sqrt{2} \frac{\partial \sigma_{23}}{\partial D} h^D, \sqrt{2} \frac{\partial \sigma_{31}}{\partial D} h^D, \sqrt{2} \frac{\partial \sigma_{12}}{\partial D} h^D \right] \\
\mathbf{Z}^{T_p} &:= \left[\frac{\partial \sigma_{11}}{\partial T_p} h^T, \frac{\partial \sigma_{22}}{\partial T_p} h^T, \frac{\partial \sigma_{33}}{\partial T_p} h^T, \sqrt{2} \frac{\partial \sigma_{23}}{\partial T_p} h^T, \sqrt{2} \frac{\partial \sigma_{31}}{\partial T_p} h^T, \sqrt{2} \frac{\partial \sigma_{12}}{\partial T_p} h^T \right]
\end{aligned} \tag{17.64}$$

we have

$$\mathbf{P} = \mathbf{C} - \mathbf{Z}^{\varepsilon_p} - \mathbf{Z}^\phi - \mathbf{Z}^D - \mathbf{Z}^{T_p}. \quad (17.65)$$

Noting that $\boldsymbol{\beta}$ is required to be symmetric for the conservation of angular momentum, we can express the internal variables as a vector such that

$$\begin{aligned} \mathbf{Q} &:= [\beta_{11}, \beta_{22}, \beta_{33}, \sqrt{2}\beta_{23}, \sqrt{2}\beta_{31}, \sqrt{2}\beta_{12}, \varepsilon_p^{\text{eq}}, \phi, D, T_p] \\ \mathbf{H} &:= [h_{11}^\beta, h_{22}^\beta, h_{33}^\beta, \sqrt{2}h_{23}^\beta, \sqrt{2}h_{31}^\beta, \sqrt{2}h_{12}^\beta, h^{\varepsilon_p}, h^\phi, h^D, h^T] \\ \frac{\partial f}{\partial \mathbf{Q}} &:= \left[\frac{\partial f}{\partial \beta_{11}}, \frac{\partial f}{\partial \beta_{22}}, \frac{\partial f}{\partial \beta_{33}}, \sqrt{2} \frac{\partial f}{\partial \beta_{23}}, \sqrt{2} \frac{\partial f}{\partial \beta_{31}}, \sqrt{2} \frac{\partial f}{\partial \beta_{12}}, \frac{\partial f}{\partial \varepsilon_p^{\text{eq}}}, \frac{\partial f}{\partial \phi}, \frac{\partial f}{\partial D}, \frac{\partial f}{\partial T_p} \right] \end{aligned} \quad (17.66)$$

Therefore,

$$H = \frac{\partial f}{\partial \mathbf{Q}} \cdot \mathbf{H}, \quad \hat{H} = \frac{H}{\|\mathbf{N}\|}. \quad (17.67)$$

Then (17.59), can be written in vector form as

$$\begin{aligned} \mathbf{S}_{n+1} &= \mathbf{S}^{\text{trial}} - \Gamma \mathbf{P}_{n+1} \\ \mathbf{E}_{n+1}^p &= \mathbf{E}_n^p + \Gamma \hat{\mathbf{N}}_{n+1} \\ \mathbf{Q}_{n+1} &= \mathbf{Q}_n + \Gamma \mathbf{H}_{n+1} \\ \hat{\mathbf{N}}_{n+1} \cdot (\mathbf{S}^{\text{trial}} - \mathbf{S}_n) - \Gamma (\hat{\mathbf{N}}_{n+1} \cdot \mathbf{P}_{n+1} - \hat{H}_{n+1}) &= 0 \implies \Gamma = \frac{\hat{\mathbf{N}}_{n+1} \cdot (\mathbf{S}^{\text{trial}} - \mathbf{S}_n)}{(\hat{\mathbf{N}}_{n+1} \cdot \mathbf{P}_{n+1} - \hat{H}_{n+1})} \\ f_{n+1} &= f(\mathbf{S}^{\text{trial}} - \Gamma \mathbf{P}_{n+1}) = 0 \end{aligned} \quad (17.68)$$

Since $\mathbf{P} = \mathbf{P}(\mathbf{S}, \mathbf{E}^p, \mathbf{Q})$, $\mathbf{N} = \mathbf{N}(\mathbf{S}, \mathbf{E}^p, \mathbf{Q})$, $\mathbf{H} = \mathbf{H}(\mathbf{S}, \mathbf{E}^p, \mathbf{Q})$, and $H = H(\mathbf{S}, \mathbf{E}^p, \mathbf{Q})$, we can write the equations above as residuals:

$$\begin{aligned} \mathbf{r}_S(\Gamma, \mathbf{S}, \mathbf{E}^p, \mathbf{Q}) &:= -\mathbf{S}_{n+1} + \mathbf{S}^{\text{trial}} - \Gamma \mathbf{P}_{n+1}(\mathbf{S}, \mathbf{E}^p, \mathbf{Q}) = 0 \\ \mathbf{r}_E(\Gamma, \mathbf{S}, \mathbf{E}^p, \mathbf{Q}) &:= -\mathbf{E}_{n+1}^p + \mathbf{E}_n^p + \Gamma \hat{\mathbf{N}}_{n+1}(\mathbf{S}, \mathbf{E}^p, \mathbf{Q}) = 0 \\ \mathbf{r}_Q(\Gamma, \mathbf{S}, \mathbf{E}^p, \mathbf{Q}) &:= -\mathbf{Q}_{n+1} + \mathbf{Q}_n + \Gamma \mathbf{H}_{n+1}(\mathbf{S}, \mathbf{E}^p, \mathbf{Q}) = 0 \\ r_f(\Gamma, \mathbf{S}, \mathbf{E}^p, \mathbf{Q}) &:= f(\mathbf{S}_{n+1}, \mathbf{E}_{n+1}^p, \mathbf{Q}_{n+1}) = 0 \end{aligned} \quad (17.69)$$

First-order Taylor series expansions of these functions at $(\Gamma, \mathbf{S}_n, \mathbf{E}_n^p, \mathbf{Q}_n)$, give

$$\begin{aligned} \mathbf{r}_S(\Gamma, \mathbf{S}, \mathbf{E}^p, \mathbf{Q}) &\approx \mathbf{r}_S(\Gamma, \mathbf{S}_n, \mathbf{E}_n^p, \mathbf{Q}_n) + \\ &\quad \left. \frac{\partial \mathbf{r}_S}{\partial \Gamma} \right|_n (\Gamma - \Gamma_n) + \left. \frac{\partial \mathbf{r}_S}{\partial \mathbf{S}} \right|_n \cdot (\mathbf{S} - \mathbf{S}_n) + \left. \frac{\partial \mathbf{r}_S}{\partial \mathbf{E}^p} \right|_n \cdot (\mathbf{E}^p - \mathbf{E}_n^p) + \left. \frac{\partial \mathbf{r}_S}{\partial \mathbf{Q}} \right|_n \cdot (\mathbf{Q} - \mathbf{Q}_n) \\ \mathbf{r}_E(\Gamma, \mathbf{S}, \mathbf{E}^p, \mathbf{Q}) &\approx \mathbf{r}_E(\Gamma, \mathbf{S}_n, \mathbf{E}_n^p, \mathbf{Q}_n) + \\ &\quad \left. \frac{\partial \mathbf{r}_E}{\partial \Gamma} \right|_n (\Gamma - \Gamma_n) + \left. \frac{\partial \mathbf{r}_E}{\partial \mathbf{S}} \right|_n \cdot (\mathbf{S} - \mathbf{S}_n) + \left. \frac{\partial \mathbf{r}_E}{\partial \mathbf{E}^p} \right|_n \cdot (\mathbf{E}^p - \mathbf{E}_n^p) + \left. \frac{\partial \mathbf{r}_E}{\partial \mathbf{Q}} \right|_n \cdot (\mathbf{Q} - \mathbf{Q}_n) \\ \mathbf{r}_Q(\Gamma, \mathbf{S}, \mathbf{E}^p, \mathbf{Q}) &\approx \mathbf{r}_Q(\Gamma, \mathbf{S}_n, \mathbf{E}_n^p, \mathbf{Q}_n) + \\ &\quad \left. \frac{\partial \mathbf{r}_Q}{\partial \Gamma} \right|_n (\Gamma - \Gamma_n) + \left. \frac{\partial \mathbf{r}_Q}{\partial \mathbf{S}} \right|_n \cdot (\mathbf{S} - \mathbf{S}_n) + \left. \frac{\partial \mathbf{r}_Q}{\partial \mathbf{E}^p} \right|_n \cdot (\mathbf{E}^p - \mathbf{E}_n^p) + \left. \frac{\partial \mathbf{r}_Q}{\partial \mathbf{Q}} \right|_n \cdot (\mathbf{Q} - \mathbf{Q}_n) \\ r_f(\Gamma, \mathbf{S}, \mathbf{E}^p, \mathbf{Q}) &\approx r_f(\Gamma, \mathbf{S}_n, \mathbf{E}_n^p, \mathbf{Q}_n) + \\ &\quad \left. \frac{\partial r_f}{\partial \Gamma} \right|_n (\Gamma - \Gamma_n) + \left. \frac{\partial r_f}{\partial \mathbf{S}} \right|_n \cdot (\mathbf{S} - \mathbf{S}_n) + \left. \frac{\partial r_f}{\partial \mathbf{E}^p} \right|_n \cdot (\mathbf{E}^p - \mathbf{E}_n^p) + \left. \frac{\partial r_f}{\partial \mathbf{Q}} \right|_n \cdot (\mathbf{Q} - \mathbf{Q}_n) \end{aligned} \quad (17.70)$$

Since the residuals are required to be zero at the end of the timestep, we get the following rule for the k -th iteration,

$$\begin{aligned}
\left. \frac{\partial \mathbf{r}_S}{\partial \Gamma} \right|_k \Delta \Gamma + \left. \frac{\partial \mathbf{r}_S}{\partial \mathbf{S}} \right|_k \cdot \Delta \mathbf{S} + \left. \frac{\partial \mathbf{r}_S}{\partial \mathbf{E}^p} \right|_k \cdot \Delta \mathbf{E}^p + \left. \frac{\partial \mathbf{r}_S}{\partial \mathbf{Q}} \right|_k \cdot \Delta \mathbf{Q} &= -\mathbf{r}_S(\Gamma_k, \mathbf{S}_k, \mathbf{E}_k^p, \mathbf{Q}_k) \\
\left. \frac{\partial \mathbf{r}_E}{\partial \Gamma} \right|_k \Delta \Gamma + \left. \frac{\partial \mathbf{r}_E}{\partial \mathbf{S}} \right|_k \cdot \Delta \mathbf{S} + \left. \frac{\partial \mathbf{r}_E}{\partial \mathbf{E}^p} \right|_k \cdot \Delta \mathbf{E}^p + \left. \frac{\partial \mathbf{r}_E}{\partial \mathbf{Q}} \right|_k \cdot \Delta \mathbf{Q} &= -\mathbf{r}_E(\Gamma_k, \mathbf{S}_k, \mathbf{E}_k^p, \mathbf{Q}_k) \\
\left. \frac{\partial \mathbf{r}_Q}{\partial \Gamma} \right|_k \Delta \Gamma + \left. \frac{\partial \mathbf{r}_Q}{\partial \mathbf{S}} \right|_k \cdot \Delta \mathbf{S} + \left. \frac{\partial \mathbf{r}_Q}{\partial \mathbf{E}^p} \right|_k \cdot \Delta \mathbf{E}^p + \left. \frac{\partial \mathbf{r}_Q}{\partial \mathbf{Q}} \right|_k \cdot \Delta \mathbf{Q} &= -\mathbf{r}_Q(\Gamma_k, \mathbf{S}_k, \mathbf{E}_k^p, \mathbf{Q}_k) \\
\left. \frac{\partial r_f}{\partial \Gamma} \right|_k \Delta \Gamma + \left. \frac{\partial r_f}{\partial \mathbf{S}} \right|_k \cdot \Delta \mathbf{S} + \left. \frac{\partial r_f}{\partial \mathbf{E}^p} \right|_k \cdot \Delta \mathbf{E}^p + \left. \frac{\partial r_f}{\partial \mathbf{Q}} \right|_k \cdot \Delta \mathbf{Q} &= -r_f(\Gamma_k, \mathbf{S}_k, \mathbf{E}_k^p, \mathbf{Q}_k)
\end{aligned} \tag{17.71}$$

where

$$\Delta \Gamma = \Gamma_{k+1} - \Gamma_k, \quad \Delta \mathbf{S} = \mathbf{S}_{k+1} - \mathbf{S}_k, \quad \Delta \mathbf{E}^p = \mathbf{E}_{k+1}^p - \mathbf{E}_k^p, \quad \Delta \mathbf{Q} = \mathbf{Q}_{k+1} - \mathbf{Q}_k. \tag{17.72}$$

The derivatives of the residuals are (dropping subscripts $n + 1$ for convenience),

$$\begin{aligned}
\frac{\partial \mathbf{r}_S}{\partial \Gamma} &= -\mathbf{P}, \quad \frac{\partial \mathbf{r}_E}{\partial \Gamma} = \hat{\mathbf{N}}, \quad \frac{\partial \mathbf{r}_Q}{\partial \Gamma} = \mathbf{H}, \quad \frac{\partial r_f}{\partial \Gamma} = 0 \\
\frac{\partial \mathbf{r}_S}{\partial \mathbf{S}} &= -[\mathbf{I}] - \Gamma \frac{\partial \mathbf{P}}{\partial \mathbf{S}}, \quad \frac{\partial \mathbf{r}_E}{\partial \mathbf{S}} = \Gamma \frac{\partial \hat{\mathbf{N}}}{\partial \mathbf{S}}, \quad \frac{\partial \mathbf{r}_Q}{\partial \mathbf{S}} = \Gamma \frac{\partial \mathbf{H}}{\partial \mathbf{S}}, \quad \frac{\partial r_f}{\partial \mathbf{S}} = \frac{\partial f}{\partial \mathbf{S}} \\
\frac{\partial \mathbf{r}_S}{\partial \mathbf{E}^p} &= -\Gamma \frac{\partial \mathbf{P}}{\partial \mathbf{E}^p}, \quad \frac{\partial \mathbf{r}_E}{\partial \mathbf{E}^p} = -[\mathbf{I}] + \Gamma \frac{\partial \hat{\mathbf{N}}}{\partial \mathbf{E}^p}, \quad \frac{\partial \mathbf{r}_Q}{\partial \mathbf{E}^p} = \Gamma \frac{\partial \mathbf{H}}{\partial \mathbf{E}^p}, \quad \frac{\partial r_f}{\partial \mathbf{E}^p} = \frac{\partial f}{\partial \mathbf{E}^p} \\
\frac{\partial \mathbf{r}_S}{\partial \mathbf{Q}} &= -\Gamma \frac{\partial \mathbf{P}}{\partial \mathbf{Q}}, \quad \frac{\partial \mathbf{r}_E}{\partial \mathbf{Q}} = \Gamma \frac{\partial \hat{\mathbf{N}}}{\partial \mathbf{Q}}, \quad \frac{\partial \mathbf{r}_Q}{\partial \mathbf{Q}} = -[\mathbf{I}] + \Gamma \frac{\partial \mathbf{H}}{\partial \mathbf{Q}}, \quad \frac{\partial r_f}{\partial \mathbf{Q}} = \frac{\partial f}{\partial \mathbf{Q}}
\end{aligned} \tag{17.73}$$

Therefore, using $\mathbf{N} = \partial f / \partial \mathbf{S}$,

$$\begin{aligned}
-\mathbf{P}_k \Delta \Gamma - \left([\mathbf{I}] + \Gamma_k \frac{\partial \mathbf{P}}{\partial \mathbf{S}} \right) \cdot \Delta \mathbf{S} - \Gamma_k \frac{\partial \mathbf{P}}{\partial \mathbf{E}^p} \cdot \Delta \mathbf{E}^p - \Gamma_k \frac{\partial \mathbf{P}}{\partial \mathbf{Q}} \cdot \Delta \mathbf{Q} &= -\mathbf{r}_S(\Gamma_k, \mathbf{S}_k, \mathbf{E}_k^p, \mathbf{Q}_k) \\
\hat{\mathbf{N}}_k \Delta \Gamma + \Gamma_k \frac{\partial \hat{\mathbf{N}}}{\partial \mathbf{S}} \cdot \Delta \mathbf{S} - \left([\mathbf{I}] - \Gamma_k \frac{\partial \hat{\mathbf{N}}}{\partial \mathbf{E}^p} \right) \cdot \Delta \mathbf{E}^p + \Gamma_k \frac{\partial \hat{\mathbf{N}}}{\partial \mathbf{Q}} \cdot \Delta \mathbf{Q} &= -\mathbf{r}_E(\Gamma_k, \mathbf{S}_k, \mathbf{E}_k^p, \mathbf{Q}_k) \\
\mathbf{H}_k \Delta \Gamma + \Gamma_k \frac{\partial \mathbf{H}}{\partial \mathbf{S}} \cdot \Delta \mathbf{S} + \Gamma_k \frac{\partial \mathbf{H}}{\partial \mathbf{E}^p} \cdot \Delta \mathbf{E}^p - \left([\mathbf{I}] - \Gamma_k \frac{\partial \mathbf{H}}{\partial \mathbf{Q}} \right) \cdot \Delta \mathbf{Q} &= -\mathbf{r}_Q(\Gamma_k, \mathbf{S}_k, \mathbf{E}_k^p, \mathbf{Q}_k) \\
\mathbf{N}_k \cdot \Delta \mathbf{S} + \left. \frac{\partial f}{\partial \mathbf{E}^p} \right|_k \cdot \Delta \mathbf{E}^p + \left. \frac{\partial f}{\partial \mathbf{Q}} \right|_k \cdot \Delta \mathbf{Q} &= -r_f(\Gamma_k, \mathbf{S}_k, \mathbf{E}_k^p, \mathbf{Q}_k)
\end{aligned} \tag{17.74}$$

Because the derivatives of $\hat{\mathbf{N}}$, \mathbf{P} , \mathbf{H} with respect to \mathbf{S} , \mathbf{E}^p , \mathbf{Q} may be difficult to calculate, it is more convenient to use a semi-implicit scheme where the quantities $\hat{\mathbf{N}}$, \mathbf{P} , \mathbf{H} are evaluated at t_n . In that case we have

$$\begin{aligned}
-\mathbf{P}_k \Delta \Gamma - \Delta \mathbf{S} &= -\mathbf{r}_S(\Gamma_k, \mathbf{S}_k, \mathbf{E}_k^p, \mathbf{Q}_k) \\
\hat{\mathbf{N}}_k \Delta \Gamma - \Delta \mathbf{E}^p &= -\mathbf{r}_E(\Gamma_k, \mathbf{S}_k, \mathbf{E}_k^p, \mathbf{Q}_k) \\
\mathbf{H}_k \Delta \Gamma - \Delta \mathbf{Q} &= -\mathbf{r}_Q(\Gamma_k, \mathbf{S}_k, \mathbf{E}_k^p, \mathbf{Q}_k) \\
\mathbf{N}_k \cdot \Delta \mathbf{S} + \left. \frac{\partial f}{\partial \mathbf{E}^p} \right|_k \cdot \Delta \mathbf{E}^p + \left. \frac{\partial f}{\partial \mathbf{Q}} \right|_k \cdot \Delta \mathbf{Q} &= -r_f(\Gamma_k, \mathbf{S}_k, \mathbf{E}_k^p, \mathbf{Q}_k)
\end{aligned} \tag{17.75}$$

We now force \mathbf{r}_S , \mathbf{r}_E , and \mathbf{r}_Q to be zero at all times, leading to the expressions

$$\begin{aligned}
\Delta \mathbf{S} &= -\mathbf{P}_k \Delta \Gamma \\
\Delta \mathbf{E}^p &= \hat{\mathbf{N}}_k \Delta \Gamma \\
\Delta \mathbf{Q} &= \mathbf{H}_k \Delta \Gamma \\
r_f(\Gamma_k, \mathbf{S}_k, \mathbf{E}_k^p, \mathbf{Q}_k) + \mathbf{N}_k \cdot \Delta \mathbf{S} + \left. \frac{\partial f}{\partial \mathbf{E}^p} \right|_k \cdot \Delta \mathbf{E}^p + \left. \frac{\partial f}{\partial \mathbf{Q}} \right|_k \cdot \Delta \mathbf{Q} &= 0
\end{aligned} \tag{17.76}$$

Plugging the expressions for $\Delta \mathbf{S}$, $\Delta \mathbf{E}^p$, $\Delta \mathbf{Q}$ from the first three equations into the fourth gives us

$$r_f(\Gamma_k, \mathbf{S}_k, \mathbf{E}_k^p, \mathbf{Q}_k) - \mathbf{N}_k \cdot \mathbf{P}_k \Delta \Gamma + \left. \frac{\partial f}{\partial \mathbf{E}^p} \right|_k \cdot \hat{\mathbf{N}}_k \Delta \Gamma + \left. \frac{\partial f}{\partial \mathbf{Q}} \right|_k \cdot \mathbf{H}_k \Delta \Gamma = 0 \quad (17.77)$$

or

$$\Delta \Gamma = \frac{f(\mathbf{S}_k, \mathbf{E}_k^p, \mathbf{Q}_k)}{\mathbf{N}_k \cdot \mathbf{P}_k - \left. \frac{\partial f}{\partial \mathbf{E}^p} \right|_k \cdot \hat{\mathbf{N}}_k - \left. \frac{\partial f}{\partial \mathbf{Q}} \right|_k \cdot \mathbf{H}_k} \quad (17.78)$$

In the metal plasticity models implemented in VAANGO, there is no direct dependence of f on \mathbf{E}^p . Therefore, using (17.67),

$$\Gamma_{k+1} = \Gamma_k + \frac{f(\mathbf{S}_k, \mathbf{Q}_k)}{\mathbf{N}_k \cdot \mathbf{P}_k - H_k}. \quad (17.79)$$

All quantities on the right hand side of the above equation are known, and we can compute Γ_{k+1} . The other variables can now be updated using

$$\mathbf{S}_{k+1} = \mathbf{S}_k - \mathbf{P}_k \Delta \Gamma, \quad \mathbf{E}_{k+1}^p = \mathbf{E}_k^p + \hat{\mathbf{N}}_k \Delta \Gamma, \quad \mathbf{Q}_{k+1} = \mathbf{Q}_k + \mathbf{H}_k \Delta \Gamma \quad (17.80)$$

The iterative process can be stopped when r_f is close to 0 and Γ_{k+1} is close to the value required to satisfy consistency given in (17.68).

17.2.2 Stress update in reduced stress space

The isotropic metal yield functions in VAANGO depend only on two invariants of stress. Therefore, the return mapping can be carried out in the reduced stress space spanned by $\hat{\mathbf{I}}$ and $\hat{\mathbf{s}}^{\text{trial}}$ where

$$\hat{\mathbf{I}} = \frac{\mathbf{I}}{\|\mathbf{I}\|} = \frac{\mathbf{I}}{\sqrt{3}} \quad \text{and} \quad \hat{\mathbf{s}}^{\text{trial}} = \frac{\mathbf{s}^{\text{trial}}}{\|\mathbf{s}^{\text{trial}}\|} = \frac{\text{dev}(\boldsymbol{\sigma}^{\text{trial}})}{\|\text{dev}(\boldsymbol{\sigma}^{\text{trial}})\|}. \quad (17.81)$$

The stress can be expressed in terms of this basis as,

$$\boldsymbol{\sigma}_{n+1} = (\sigma_p)_{n+1} \hat{\mathbf{I}} + (\sigma_s)_{n+1} \hat{\mathbf{s}}^{\text{trial}} \quad \text{where} \quad (\sigma_p)_{n+1} = \boldsymbol{\sigma}_{n+1} : \hat{\mathbf{I}} = \frac{\text{tr}(\boldsymbol{\sigma}_{n+1})}{\sqrt{3}}, \quad (\sigma_s)_{n+1} = \boldsymbol{\sigma}_{n+1} : \hat{\mathbf{s}}^{\text{trial}}. \quad (17.82)$$

As before,

$$\boldsymbol{\sigma}^{\text{trial}} = \boldsymbol{\sigma}_n + \Delta t (\mathbb{C}_n^e : \dot{\boldsymbol{\epsilon}}_{n+1}) = \boldsymbol{\sigma}_n + \Delta t \left[\left(\kappa_n - \frac{2}{3} \mu_n \right) \text{tr}(\dot{\boldsymbol{\epsilon}}_{n+1}) \mathbf{I} + 2 \mu_n \dot{\boldsymbol{\epsilon}}_{n+1} \right] \quad (17.83)$$

The trial stress is then decomposed into

$$\boldsymbol{\sigma}^{\text{trial}} = \sigma_p^{\text{trial}} \hat{\mathbf{I}} + \sigma_s^{\text{trial}} \hat{\mathbf{s}}^{\text{trial}} \quad \text{where} \quad \sigma_p^{\text{trial}} = \frac{\text{tr}(\boldsymbol{\sigma}^{\text{trial}})}{\sqrt{3}}, \quad \sigma_s^{\text{trial}} = \boldsymbol{\sigma}^{\text{trial}} : \hat{\mathbf{s}}^{\text{trial}} = \|\mathbf{s}^{\text{trial}}\|. \quad (17.84)$$

The yield function is computed using

$$f_y = f[\boldsymbol{\sigma}_\beta^{\text{trial}}, (\epsilon_p^{\text{eq}})_n, (\dot{\epsilon}_p^{\text{eq}})_n, \phi_n, D_n, T_n, \dot{\epsilon}_n^{\text{eq}}, \kappa_n, \mu_n, \dots], \quad \boldsymbol{\sigma}_\beta^{\text{trial}} = \boldsymbol{\sigma}^{\text{trial}} - \boldsymbol{\beta}_n. \quad (17.85)$$

If $f_y \leq 0$, the state is updated using

$$\begin{aligned} \boldsymbol{\sigma}_{n+1} &= \boldsymbol{\sigma}^{\text{trial}}, \quad \boldsymbol{\beta}_{n+1} = \boldsymbol{\beta}_n, \quad (\epsilon_p^{\text{eq}})_{n+1} = (\epsilon_p^{\text{eq}})_n, \quad (\dot{\epsilon}_p^{\text{eq}})_{n+1} = (\dot{\epsilon}_p^{\text{eq}})_n \\ \phi_{n+1} &= \phi_n, \quad D_{n+1} = D_n, \quad T_{n+1} = T_n \\ \kappa_{n+1} &= \kappa(p_{n+1}, T_n), \quad \mu_{n+1} = \mu(p_{n+1}, T_n). \end{aligned} \quad (17.86)$$

If $f_y > 0$, integration of the stress rate by backward Euler leads to

$$\boldsymbol{\sigma}_{n+1} = \boldsymbol{\sigma}^{\text{trial}} - \Delta\lambda_{n+1} \mathbf{P}_{n+1}. \quad (17.87)$$

Expressed in terms of the trial basis using (17.37), and noting that $\boldsymbol{\sigma}_{n+1} = \boldsymbol{\sigma}_{n+1}^e$ and $(\sigma_{ss})_{n+1} = \hat{\mathbf{s}}_{n+1} : \hat{\mathbf{s}}^{\text{trial}}$,

$$\begin{aligned} \mathbf{P}_{n+1} = & \left[\frac{\sqrt{3}\kappa_{n+1}}{\|\mathbf{N}_{n+1}\|} \frac{\partial f_{n+1}}{\partial p_\beta} - \frac{1}{\kappa_{n+1}} \sum_\eta \frac{\partial \kappa_{n+1}}{\partial \eta} (\sigma_p)_{n+1} \right] \hat{\mathbf{I}} \\ & + \left[\frac{\sqrt{6}\mu_{n+1}}{\|\mathbf{N}_{n+1}\|} \frac{\partial f_{n+1}}{\partial \sigma_{\text{eff}}^\xi} - \frac{1}{\mu_{n+1}} \sum_\eta \frac{\partial \mu_{n+1}}{\partial \eta} (\sigma_s)_{n+1} \right] (\sigma_{ss})_{n+1} \hat{\mathbf{s}}^{\text{trial}} \end{aligned} \quad (17.88)$$

Therefore,

$$\begin{aligned} (\sigma_p)_{n+1} &= \sigma_p^{\text{trial}} - \Delta\lambda_{n+1} \left[\frac{\sqrt{3}\kappa_{n+1}}{\|\mathbf{N}_{n+1}\|} \frac{\partial f_{n+1}}{\partial p_\beta} - \frac{1}{\kappa_{n+1}} \sum_\eta \frac{\partial \kappa_{n+1}}{\partial \eta} (\sigma_p)_{n+1} \right] \\ (\sigma_s)_{n+1} &= \sigma_s^{\text{trial}} - \Delta\lambda_{n+1} \left[\frac{\sqrt{6}\mu_{n+1}}{\|\mathbf{N}_{n+1}\|} \frac{\partial f_{n+1}}{\partial \sigma_{\text{eff}}^\xi} - \frac{1}{\mu_{n+1}} \sum_\eta \frac{\partial \mu_{n+1}}{\partial \eta} (\sigma_s)_{n+1} \right] (\sigma_{ss})_{n+1} \end{aligned} \quad (17.89)$$

The plastic strain can be updated using (17.38):

$$\boldsymbol{\varepsilon}_{n+1}^p = \boldsymbol{\varepsilon}_n^p + \Delta t \dot{\boldsymbol{\varepsilon}}_{n+1} - \left(\frac{(\sigma_p)_{n+1} - (\sigma_p)_n}{3\kappa_{n+1}} \right) \hat{\mathbf{I}} - \left(\frac{(\sigma_s)_{n+1} - (\sigma_s)_n}{2\mu_{n+1}} \right) \hat{\mathbf{s}}^{\text{trial}}. \quad (17.90)$$

The internal variables can be updated using

$$\boldsymbol{\eta}_{n+1} = \boldsymbol{\eta}_n + \Delta\lambda_{n+1} \mathbf{h}_{n+1}^\eta \quad (17.91)$$

Also, as before, the stress state has to lie on the yield surface:

$$f(\boldsymbol{\sigma}^{\text{trial}} - \Delta\lambda_{n+1} \mathbf{P}_{n+1}) = 0 \quad (17.92)$$

and the consistency condition needs to be satisfied:

$$\hat{\mathbf{N}}_{n+1} : (\boldsymbol{\sigma}^{\text{trial}} - \boldsymbol{\sigma}_n) = \Delta\lambda_{n+1} (\hat{\mathbf{N}}_{n+1} : \mathbf{P}_{n+1} - \hat{H}_{n+1}) \quad (17.93)$$

where

$$\hat{\mathbf{N}}_{n+1} = \frac{\mathbf{N}_{n+1}}{\|\mathbf{N}_{n+1}\|}, \quad \mathbf{N}_{n+1} = \frac{1}{\sqrt{3}} \frac{\partial f_{n+1}}{\partial p_\beta} \hat{\mathbf{I}} + \sqrt{\frac{3}{2}} \frac{\partial f_{n+1}}{\partial \sigma_{\text{eff}}^\xi} \hat{\mathbf{s}}^{\text{trial}}. \quad (17.94)$$

We can now attempt to express the iterative semi-implicit stress update algorithm given in (17.79) and (17.80) in terms of the trial basis. Recall that

$$\Gamma_{k+1} = \Gamma_k + \frac{f(\mathbf{S}_k, \mathbf{Q}_k)}{\mathbf{N}_k \cdot \mathbf{P}_k - H_k}, \quad \mathbf{E}_{k+1}^p = \mathbf{E}_k^p + \hat{\mathbf{N}}_k \Delta\Gamma, \quad \mathbf{S}_{k+1} = \mathbf{S}_k - \mathbf{P}_k \Delta\Gamma, \quad \mathbf{Q}_{k+1} = \mathbf{Q}_k + \mathbf{H}_k \Delta\Gamma \quad (17.95)$$

Reverting back to tensor notation,

$$\Gamma_{k+1} = \Gamma_k + \frac{f(\boldsymbol{\sigma}_k, \boldsymbol{\eta}_k)}{\|\mathbf{N}_k\| (\hat{\mathbf{N}}_k : \mathbf{P}_k - \hat{H}_k)}, \quad \boldsymbol{\varepsilon}_{k+1}^p = \boldsymbol{\varepsilon}_k^p + \hat{\mathbf{N}}_k \Delta\Gamma, \quad \boldsymbol{\sigma}_{k+1} = \boldsymbol{\sigma}_k - \mathbf{P}_k \Delta\Gamma, \quad \boldsymbol{\eta}_{k+1} = \boldsymbol{\eta}_k + \mathbf{H}_k \Delta\Gamma \quad (17.96)$$

Using (17.94) and (17.88), we have

$$\begin{aligned} \|\mathbf{N}_k\| (\hat{\mathbf{N}}_k : \mathbf{P}_k) = & \frac{1}{\sqrt{3}} \frac{\partial f_k}{\partial p_\beta} \left[\sqrt{3}\kappa_k \frac{\partial f_k}{\partial p_\beta} - \frac{\|\mathbf{N}_k\|}{\kappa_k} \sum_\eta \frac{\partial \kappa_k}{\partial \eta} (\sigma_p)_k \right] + \\ & \sqrt{\frac{3}{2}} \frac{\partial f_k}{\partial \sigma_{\text{eff}}^\xi} \left[\sqrt{6}\mu_k \frac{\partial f_k}{\partial \sigma_{\text{eff}}^\xi} - \frac{\|\mathbf{N}_k\|}{\mu_k} \sum_\eta \frac{\partial \mu_k}{\partial \eta} (\sigma_s)_k \right] (\sigma_{ss})_k \end{aligned} \quad (17.97)$$

Also,

$$\|N_k\| \hat{H}_k = \frac{\partial f_k}{\partial \beta} : (h^\beta)_k + \frac{\partial f_k}{\partial \varepsilon_p^{\text{eq}}} (h^{\varepsilon_p})_k + \frac{\partial f_k}{\partial \phi} (h^\phi)_k + \frac{\partial f_k}{\partial D} (h^D)_k + \frac{\partial f_k}{\partial T_p} (h^T)_k. \quad (17.98)$$

At the end of the iterative process, the plastic strain tensor may also be updated using (17.90) and a non-hardening return used to force the computed stress state on the final yield surface.

17.2.3 Algorithm 1

Two implementations of the model described in this chapter have been implemented in VAANGO. The algorithm described in this section is used when the `elastic_plastic_hp` algorithm is invoked in an input file. This plastic return algorithm is more robust but does not include kinematic hardening or softening due to damage and temperature changes. Softening and damage are treated in an uncoupled manner after the stress has been updated. Also, elastic-plastic coupling is ignored. For this algorithm, the timestep is divided into substeps and the following algorithm is applied at each substep. At the end of the last substep, the stress state is projected back to the updated yield surface without any changes to the internal variables.

1. Inputs:

$$\begin{aligned} \text{Timestep size: } & \Delta t \\ \text{New strain rate: } & \dot{\varepsilon}_{n+1}, \dot{\varepsilon}_{n+1}^{\text{eq}} \\ \text{Old stress: } & \sigma_n \\ \text{Old moduli: } & \kappa_n, \mu_n \\ \text{Old plastic strain: } & \varepsilon_n^p \\ \text{Old equivalent plastic rate: } & (\dot{\varepsilon}_p^{\text{eq}})_n \\ \text{Old internal variables: } & (\varepsilon_p^{\text{eq}})_n, \phi_n, T_n \\ \text{Trial stress: } & \sigma^{\text{trial}} = \sigma_n + \Delta t \left[\left(\kappa_n - \frac{2}{3} \mu_n \right) \text{tr}(\dot{\varepsilon}_{n+1}) \mathbf{I} + 2 \mu_n \dot{\varepsilon}_{n+1} \right] \end{aligned} \quad (17.99)$$

2. Decompose trial stress

$$\begin{aligned} p^{\text{trial}} &= \frac{1}{3} \text{tr}(\sigma^{\text{trial}}), \quad \mathbf{s}^{\text{trial}} = \sigma^{\text{trial}} - \frac{1}{3} \text{tr}(\sigma^{\text{trial}}) \mathbf{I}, \quad \hat{\mathbf{s}}^{\text{trial}} = \frac{\mathbf{s}^{\text{trial}}}{\|\mathbf{s}^{\text{trial}}\|} \\ \sigma^{\text{trial}} &= \sigma_p^{\text{trial}} \hat{\mathbf{I}} + \sigma_s^{\text{trial}} \hat{\mathbf{s}}^{\text{trial}}, \quad \sigma_p^{\text{trial}} = \sqrt{3} p^{\text{trial}}, \quad \sigma_s^{\text{trial}} = \|\mathbf{s}^{\text{trial}}\| \end{aligned} \quad (17.100)$$

3. Decompose start-of-timestep stress

$$\begin{aligned} \sigma_n &= p_n \mathbf{I} + \mathbf{s}_n = (\sigma_p)_n \hat{\mathbf{I}} + (\sigma_s)_n \hat{\mathbf{s}}^{\text{trial}}, \quad (\sigma_{\text{eff}})_n = \sqrt{\frac{3}{2} \mathbf{s}_n : \mathbf{s}_n} \\ (\sigma_p)_n &= \sigma_n : \hat{\mathbf{I}}, \quad (\sigma_s)_n = \sigma_n : \hat{\mathbf{s}}^{\text{trial}} = \mathbf{s}_n : \hat{\mathbf{s}}^{\text{trial}} \end{aligned} \quad (17.101)$$

4. Compute f_n and derivatives

$$f_n = f(\mathbf{s}_n, p_n, (\varepsilon_p^{\text{eq}})_n, (\dot{\varepsilon}_p^{\text{eq}})_n, \phi_n, T_n, \kappa_n, \mu_n, \dot{\varepsilon}_{n+1}^{\text{eq}}, \dots), \quad \frac{\partial f_n}{\partial p}, \quad \frac{\partial f_n}{\partial \sigma_{\text{eff}}} \quad (17.102)$$

5. Compute components of N_n and $\|N_n\|$

$$\begin{aligned} N_n &= (N_p)_n \hat{\mathbf{I}} + (N_s)_n \hat{\mathbf{s}}^{\text{trial}}, \quad \|N_n\| = \sqrt{(N_p)_n^2 + (N_s)_n^2} \\ (N_p)_n &= \frac{1}{\sqrt{3}} \frac{\partial f_n}{\partial p}, \quad (N_s)_n = \sqrt{\frac{3}{2}} \frac{\partial f_n}{\partial \sigma_{\text{eff}}} \end{aligned} \quad (17.103)$$

6. Compute components of \mathbf{P}_n

$$\begin{aligned} \mathbf{P}_n &= (P_p)_n \hat{\mathbf{I}} + (P_s)_n \hat{\mathbf{s}}^{\text{trial}} \\ (P_p)_n &= \frac{\sqrt{3}\kappa_n}{\|\mathbf{N}_n\|} \frac{\partial f_n}{\partial p}, \quad (P_s)_n = \frac{\sqrt{6}\mu_n}{\|\mathbf{N}_n\|} \frac{\partial f_n}{\partial \sigma_{\text{eff}}} \end{aligned} \quad (17.104)$$

7. Initialize:

$$\begin{aligned} k &= 0, \quad \Gamma = 0 \\ \boldsymbol{\sigma}_k &= \boldsymbol{\sigma}^{\text{trial}} \end{aligned} \quad (17.105)$$

8. Decompose current stress

$$\begin{aligned} \boldsymbol{\sigma}_k &= p_k \mathbf{I} + \mathbf{s}_k = (\sigma_p)_k \hat{\mathbf{I}} + (\sigma_s)_k \hat{\mathbf{s}}^{\text{trial}}, \quad (\sigma_{\text{eff}})_k = \sqrt{\frac{3}{2} \mathbf{s}_k : \mathbf{s}_k} \\ (\sigma_p)_k &= \boldsymbol{\sigma}_k : \hat{\mathbf{I}}, \quad (\sigma_s)_k = \boldsymbol{\sigma}_k : \hat{\mathbf{s}}^{\text{trial}} = \mathbf{s}_k : \hat{\mathbf{s}}^{\text{trial}}, \quad (\sigma_{ss})_k = \frac{\mathbf{s}_k}{\|\mathbf{s}_k\|} : \hat{\mathbf{s}}^{\text{trial}} = 1 \end{aligned} \quad (17.106)$$

9. Compute f_k and derivatives

$$f_k = f(\mathbf{s}_k, p_k, (\varepsilon_p^{\text{eq}})_k, (\dot{\varepsilon}_p^{\text{eq}})_k, \phi_k, T_n, \kappa_n, \mu_n, \dot{\varepsilon}_{n+1}^{\text{eq}}, \dots), \quad \frac{\partial f_k}{\partial p}, \quad \frac{\partial f_k}{\partial \sigma_{\text{eff}}} \quad (17.107)$$

10. Compute components of \mathbf{N}_k and $\|\mathbf{N}_k\|$

$$\begin{aligned} \mathbf{N}_k &= (N_p)_k \hat{\mathbf{I}} + (N_s)_k \hat{\mathbf{s}}^{\text{trial}}, \quad \|\mathbf{N}_k\| = \sqrt{(N_p)_k^2 + (N_s)_k^2} \\ (N_p)_k &= \frac{1}{\sqrt{3}} \frac{\partial f_k}{\partial p}, \quad (N_s)_k = \sqrt{\frac{3}{2}} \frac{\partial f_k}{\partial \sigma_{\text{eff}}}. \end{aligned} \quad (17.108)$$

11. Compute $\mathbf{N}_k : \mathbf{P}_n$

$$\mathbf{N}_k : \mathbf{P}_n = (N_p)_k (P_p)_n + (N_s)_k (P_s)_n \quad (17.109)$$

12. Compute updated $\Delta\Gamma$

$$\Gamma_{k+1} = \Gamma_k + \frac{f_k}{\mathbf{N}_k : \mathbf{P}_n}, \quad \Delta\Gamma = \Gamma_{k+1} - \Gamma_k \quad (17.110)$$

13. Compute updated stress components:

$$(\sigma_p)_{k+1} = (\sigma_p)_k - (P_p)_n \Delta\Gamma, \quad (\sigma_s)_{k+1} = (\sigma_s)_k - (P_s)_n \Delta\Gamma \quad (17.111)$$

14. Compute f_{k+1}

$$f_{k+1} = f(\mathbf{s}_{k+1}, p_{k+1}, (\varepsilon_p^{\text{eq}})_k, (\dot{\varepsilon}_p^{\text{eq}})_{k+1}, \phi_{k+1}, D_{k+1}, T_{k+1}, \kappa_{k+1}, \mu_{k+1}, \dot{\varepsilon}_{n+1}^{\text{eq}}, \dots) \quad (17.112)$$

15. If $|f_{k+1}| < f_{\text{tolerance}}$ and $|\Gamma_{k+1} - \Gamma_k| < \Gamma_{\text{tolerance}}$ go to step 18.

16. Set $k \leftarrow k + 1$ and go to step 8.

17. Update the stress:

$$\boldsymbol{\sigma}_{n+1} = (\sigma_p)_{k+1} \hat{\mathbf{I}} + (\sigma_s)_{k+1} \hat{\mathbf{s}}^{\text{trial}} \quad (17.113)$$

18. Compute internal variable hardening/softening moduli

$$(h^{\varepsilon_p})_{k+1}, \quad (h^{\phi})_{k+1} \quad (17.114)$$

19. Compute updated internal variables

$$(\varepsilon_p^{\text{eq}})_{n+1} = (\varepsilon_p^{\text{eq}})_n + (h^{\varepsilon_p})_{k+1} \Delta \Gamma, \quad \phi_{n+1} = \phi_n + (h^\phi)_{k+1} \Delta \Gamma, \quad (17.115)$$

20. Compute updated elastic strain

$$\varepsilon_{n+1}^e = \varepsilon_n^e + \left(\frac{(\sigma_p)_{k+1} - (\sigma_p)_n}{3\kappa_n} \right) \hat{\mathbf{I}} - \left(\frac{(\sigma_s)_{k+1} - (\sigma_s)_n}{2\mu_n} \right) \hat{\mathbf{s}}^{\text{trial}}. \quad (17.116)$$

21. Compute the updated plastic strain

$$\varepsilon_{n+1}^p = \varepsilon_n^e + \varepsilon_n^p + \Delta t \dot{\varepsilon}_{n+1} - \varepsilon_{n+1}^e, \quad (\dot{\varepsilon}_p^{\text{eq}})_{n+1} = \|\varepsilon_{n+1}^p\| \quad (17.117)$$

22. Compute updated elastic moduli

$$\kappa_{n+1} = \kappa((\sigma_p)_{k+1}, \varepsilon_{n+1}^e, (T_p)_n), \quad \mu_{n+1} = \mu((\sigma_p)_{k+1}, \varepsilon_{n+1}^e, (T_p)_n) \quad (17.118)$$

17.2.4 Algorithm 2

The following stress update algorithm is used for each (plastic) time step for models that require kinematic hardening.

1. Inputs:

$$\begin{aligned} \text{Timestep size: } & \Delta t \\ \text{New strain rate: } & \dot{\varepsilon}_{n+1}, \dot{\varepsilon}_{n+1}^{\text{eq}} \\ \text{Old stress: } & \sigma_n \\ \text{Old moduli: } & \kappa_n, \mu_n \\ \text{Old plastic strain: } & \varepsilon_n^p \\ \text{Old equivalent plastic rate: } & (\dot{\varepsilon}_p^{\text{eq}})_n \\ \text{Old internal variables: } & \beta_n, (\varepsilon_p^{\text{eq}})_n, \phi_n, D_n, (T_p)_n \\ \text{Trial stress: } & \sigma^{\text{trial}} = \sigma_n + \Delta t \left[\left(\kappa_n - \frac{2}{3} \mu_n \right) \text{tr}(\dot{\varepsilon}_{n+1}) \mathbf{I} + 2\mu_n \dot{\varepsilon}_{n+1} \right] \end{aligned} \quad (17.119)$$

2. Decompose trial stress:

$$\begin{aligned} p^{\text{trial}} &= \frac{1}{3} \text{tr}(\sigma^{\text{trial}}), \quad \mathbf{s}^{\text{trial}} = \sigma^{\text{trial}} - \frac{1}{3} \text{tr}(\sigma^{\text{trial}}) \mathbf{I}, \quad \hat{\mathbf{s}}^{\text{trial}} = \frac{\mathbf{s}^{\text{trial}}}{\|\mathbf{s}^{\text{trial}}\|} \\ \sigma^{\text{trial}} &= \sigma_p^{\text{trial}} \hat{\mathbf{I}} + \sigma_s^{\text{trial}} \hat{\mathbf{s}}^{\text{trial}}, \quad \sigma_p^{\text{trial}} = \sqrt{3} p^{\text{trial}}, \quad \sigma_s^{\text{trial}} = \|\mathbf{s}^{\text{trial}}\| \end{aligned} \quad (17.120)$$

3. Initialize:

$$\begin{aligned} k &= 0, \quad \Gamma = 0 \\ \sigma_k &= \sigma^{\text{trial}}, \quad \kappa_k = \kappa_n, \quad \mu_k = \mu_n, \quad \varepsilon_k^p = \varepsilon_n^p \\ (\varepsilon_p^{\text{eq}})_k &= (\varepsilon_p^{\text{eq}})_n, \quad \beta_k = \beta_n, \quad \phi_k = \phi_n, \quad D_k = D_n, \quad (T_p)_k = (T_p)_n \\ (\dot{\varepsilon}_p^{\text{eq}})_k &= (\dot{\varepsilon}_p^{\text{eq}})_n, \quad \dot{\varepsilon}^{\text{eq}} = \dot{\varepsilon}_{n+1}^{\text{eq}} \end{aligned} \quad (17.121)$$

4. Compute shifted stress using backstress:

$$(\sigma_\beta)_k = \sigma_k - \beta_k, \quad (p_\beta)_k = \frac{1}{3} \text{tr}(\sigma_\beta)_k, \quad \xi_k = (\sigma_\beta)_k - (p_\beta)_k \mathbf{I}, \quad (\sigma_{\text{eff}}^\xi)_k = \sqrt{\frac{3}{2} \xi_k : \xi_k} \quad (17.122)$$

5. Compute f_k and derivatives

$$f_k = f(\xi_k, (p_\beta)_k, (\varepsilon_p^{\text{eq}})_k, (\dot{\varepsilon}_p^{\text{eq}})_k, \phi_k, D_k, T_k, \kappa_k, \mu_k, \dot{\varepsilon}_{n+1}^{\text{eq}}, \dots), \quad \frac{\partial f_k}{\partial p_\beta}, \quad \frac{\partial f_k}{\partial \sigma_{\text{eff}}^\xi} \quad (17.123)$$

6. Compute components of \mathbf{N}_k and $\|\mathbf{N}_k\|$

$$\begin{aligned}\mathbf{N}_k &= (N_p)_k \hat{\mathbf{I}} + (N_s)_k \hat{\mathbf{s}}^{\text{trial}}, \quad \|\mathbf{N}_k\| = \sqrt{(N_p)_k^2 + (N_s)_k^2} \\ (N_p)_k &= \frac{1}{\sqrt{3}} \frac{\partial f_k}{\partial p_\beta}, \quad (N_s)_k = \sqrt{\frac{3}{2}} \frac{\partial f_k}{\partial \sigma_{\text{eff}}^\xi}.\end{aligned}\quad (17.124)$$

7. Compute derivatives of bulk and shear modulus with respect to internal variables

$$\frac{\partial \kappa_k}{\partial \varepsilon_p^{\text{eq}}}, \frac{\partial \kappa_k}{\partial \phi}, \frac{\partial \kappa_k}{\partial D_k}, \frac{\partial \kappa_k}{\partial T_k}, \quad \frac{\partial \mu_k}{\partial \varepsilon_p^{\text{eq}}}, \frac{\partial \mu_k}{\partial \phi}, \frac{\partial \mu_k}{\partial D_k}, \frac{\partial \mu_k}{\partial T_k} \quad (17.125)$$

8. Decompose current stress

$$\begin{aligned}\boldsymbol{\sigma}_k &= p_k \mathbf{I} + \mathbf{s}_k = (\sigma_p)_k \hat{\mathbf{I}} + (\sigma_s)_k \hat{\mathbf{s}}^{\text{trial}} \\ (\sigma_p)_k &= \boldsymbol{\sigma}_k : \hat{\mathbf{I}}, \quad (\sigma_s)_k = \boldsymbol{\sigma}_k : \hat{\mathbf{s}}^{\text{trial}} = \mathbf{s}_k : \hat{\mathbf{s}}^{\text{trial}}, \quad (\sigma_{ss})_k = \frac{\mathbf{s}_k}{\|\mathbf{s}_k\|} : \hat{\mathbf{s}}^{\text{trial}} = 1\end{aligned}\quad (17.126)$$

9. Compute components of \mathbf{P}_k

$$\begin{aligned}\mathbf{P}_k &= (P_p)_k \hat{\mathbf{I}} + (P_s)_k \hat{\mathbf{s}}^{\text{trial}} \\ (P_p)_k &= \left[\frac{\sqrt{3} \kappa_k}{\|\mathbf{N}_k\|} \frac{\partial f_k}{\partial p_\beta} - \frac{1}{\kappa_k} \sum_\eta \frac{\partial \kappa_k}{\partial \eta} (\sigma_p)_k \right] \\ (P_s)_k &= \left[\frac{\sqrt{6} \mu_k}{\|\mathbf{N}_k\|} \frac{\partial f_k}{\partial \sigma_{\text{eff}}^\xi} - \frac{1}{\mu_k} \sum_\eta \frac{\partial \mu_k}{\partial \eta} (\sigma_s)_k \right] (\sigma_{ss})_k\end{aligned}\quad (17.127)$$

10. Compute $\|\mathbf{N}_k\| (\hat{\mathbf{N}}_k : \mathbf{P}_k)$

$$\|\mathbf{N}_k\| (\hat{\mathbf{N}}_k : \mathbf{P}_k) = (N_p)_k (P_p)_k + (N_s)_k (P_s)_k \quad (17.128)$$

11. Compute derivatives of f_k with respect to internal variables

$$\frac{\partial f_k}{\partial \boldsymbol{\beta}}, \quad \frac{\partial f_k}{\partial \varepsilon_p^{\text{eq}}}, \quad \frac{\partial f_k}{\partial \phi}, \quad \frac{\partial f_k}{\partial D}, \quad \frac{\partial f_k}{\partial T_p} \quad (17.129)$$

12. Compute internal variable hardening/softening moduli

$$(\mathbf{h}^\beta)_k, \quad (h^{\varepsilon_p})_k, \quad (h^\phi)_k, \quad (h^D)_k, \quad (h^T)_k \quad (17.130)$$

13. Compute $\|\mathbf{N}_k\| \hat{H}_k$

$$\|\mathbf{N}_k\| \hat{H}_k = \frac{\partial f_k}{\partial \boldsymbol{\beta}} : (\mathbf{h}^\beta)_k + \frac{\partial f_k}{\partial \varepsilon_p^{\text{eq}}} (h^{\varepsilon_p})_k + \frac{\partial f_k}{\partial \phi} (h^\phi)_k + \frac{\partial f_k}{\partial D} (h^D)_k + \frac{\partial f_k}{\partial T_p} (h^T)_k. \quad (17.131)$$

14. Compute updated $\Delta\Gamma$

$$\Gamma_{k+1} = \Gamma_k + \frac{f_k}{\|\mathbf{N}_k\| (\hat{\mathbf{N}}_k : \mathbf{P}_k - \hat{H}_k)}, \quad \Delta\Gamma = \Gamma_{k+1} - \Gamma_k \quad (17.132)$$

15. Compute updated stress components:

$$(\sigma_p)_{k+1} = (\sigma_p)_k - (P_p)_k \Delta\Gamma, \quad (\sigma_s)_{k+1} = (\sigma_s)_k - (P_s)_k \Delta\Gamma \quad (17.133)$$

16. Compute updated internal variables:

$$\begin{aligned}\boldsymbol{\beta}_{k+1} &= \boldsymbol{\beta}_k + \mathbf{h}^\beta \Delta\Gamma, \quad (\varepsilon_p^{\text{eq}})_{k+1} = (\varepsilon_p^{\text{eq}})_k + h^{\varepsilon_p} \Delta\Gamma \\ \phi_{k+1} &= \phi_k + h^\phi \Delta\Gamma, \quad D_{k+1} = D_k + h^D \Delta\Gamma, \quad (T_p)_{k+1} = (T_p)_k + h^T \Delta\Gamma\end{aligned}\quad (17.134)$$

17. Compute updated elastic strain:

$$\boldsymbol{\varepsilon}_{k+1}^e = \boldsymbol{\varepsilon}_n^e + \left(\frac{(\sigma_p)_{k+1} - (\sigma_p)_n}{3\kappa_k} \right) \hat{\mathbf{I}} - \left(\frac{(\sigma_s)_{k+1} - (\sigma_s)_n}{2\mu_k} \right) \hat{\mathbf{s}}^{\text{trial}}. \quad (17.135)$$

18. Compute the updated plastic strain:

$$\boldsymbol{\varepsilon}_{k+1}^p = \boldsymbol{\varepsilon}_n^e + \boldsymbol{\varepsilon}_n^p + \Delta t \dot{\boldsymbol{\varepsilon}}_{n+1} - \boldsymbol{\varepsilon}_{k+1}^e, \quad (\dot{\boldsymbol{\varepsilon}}_p^{\text{eq}})_{k+1} = \|\boldsymbol{\varepsilon}_{k+1}^p\| \quad (17.136)$$

19. Compute updated elastic moduli

$$\kappa_{k+1} = \kappa((\sigma_p)_{k+1}, \boldsymbol{\varepsilon}_{k+1}^e, (T_p)_{k+1}), \quad \mu_{k+1} = \mu((\sigma_p)_{k+1}, \boldsymbol{\varepsilon}_{k+1}^e, (T_p)_{k+1}) \quad (17.137)$$

20. Compute f_{k+1}

$$f_{k+1} = f(\boldsymbol{\xi}_{k+1}, (p_\beta)_{k+1}, (\boldsymbol{\varepsilon}_p^{\text{eq}})_{k+1}, (\dot{\boldsymbol{\varepsilon}}_p^{\text{eq}})_{k+1}, \phi_{k+1}, D_{k+1}, T_{k+1}, \kappa_{k+1}, \mu_{k+1}, \dot{\boldsymbol{\varepsilon}}_{n+1}^{\text{eq}}, \dots) \quad (17.138)$$

21. If $|f_{k+1}| < f_{\text{tolerance}}$ and $|\Gamma_{k+1} - \Gamma_k| < \Gamma_{\text{tolerance}}$ go to step 23.

22. Set $k \leftarrow k + 1$ and go to step 4.

23. Update the state:

$$\begin{aligned} \boldsymbol{\sigma}_{n+1} &= (\sigma_p)_{k+1} \hat{\mathbf{I}} + (\sigma_s)_{k+1} \hat{\mathbf{s}}^{\text{trial}}, \quad \boldsymbol{\beta}_{n+1} = \boldsymbol{\beta}_{k+1}, \quad (\boldsymbol{\varepsilon}_p^{\text{eq}})_{n+1} = (\boldsymbol{\varepsilon}_p^{\text{eq}})_{k+1} \\ \phi_{n+1} &= \phi_{k+1}, \quad D_{n+1} = D_{k+1}, \quad (T_p)_{n+1} = (T_p)_{k+1}, \quad (\dot{\boldsymbol{\varepsilon}}_p^{\text{eq}})_{n+1} = (\dot{\boldsymbol{\varepsilon}}_p^{\text{eq}})_{k+1} \\ \kappa_{n+1} &= \kappa_k, \quad \mu_{n+1} = \mu_k \\ \boldsymbol{\varepsilon}_{n+1}^e &= \boldsymbol{\varepsilon}_n^p + \left(\frac{(\sigma_p)_{k+1} - (\sigma_p)_n}{3\kappa_{n+1}} \right) \hat{\mathbf{I}} - \left(\frac{(\sigma_s)_{k+1} - (\sigma_s)_n}{2\mu_{n+1}} \right) \hat{\mathbf{s}}^{\text{trial}} \\ \boldsymbol{\varepsilon}_{n+1}^p &= \boldsymbol{\varepsilon}_n^e + \boldsymbol{\varepsilon}_n^p + \Delta t \dot{\boldsymbol{\varepsilon}}_{n+1} - \boldsymbol{\varepsilon}_{n+1}^e \end{aligned} \quad (17.139)$$

17.3 Example 1: von Mises plasticity

Consider the case of J_2 plasticity with the yield condition

$$f := \sqrt{\frac{3}{2}} \|\mathbf{s} - \text{dev}(\boldsymbol{\beta})\| - \sigma_y(\boldsymbol{\varepsilon}_p^{\text{eq}}, \dot{\boldsymbol{\varepsilon}}_p^{\text{eq}}, \phi, T, \dots) = \sqrt{\frac{3}{2}} \|\boldsymbol{\xi}\| - \sigma_y(\boldsymbol{\varepsilon}_p^{\text{eq}}, \dot{\boldsymbol{\varepsilon}}_p^{\text{eq}}, \phi, T, \dots) \leq 0 \quad (17.140)$$

where $\|\boldsymbol{\xi}\| = \sqrt{\frac{3}{2}} \|\mathbf{s} - \text{dev}(\boldsymbol{\beta})\|$. The derivatives of the yield function with respect to the internal variables are

$$\frac{\partial f}{\partial \boldsymbol{\beta}} = -\sqrt{\frac{3}{2}} \frac{\boldsymbol{\xi}}{\|\boldsymbol{\xi}\|}, \quad \frac{\partial f}{\partial \boldsymbol{\varepsilon}_p^{\text{eq}}} = -\frac{\partial \sigma_y}{\partial \boldsymbol{\varepsilon}_p^{\text{eq}}}, \quad \frac{\partial f}{\partial \phi} = -\frac{\partial \sigma_y}{\partial \phi}, \quad \frac{\partial f}{\partial D} = -\frac{\partial \sigma_y}{\partial D}, \quad \frac{\partial f}{\partial T_p} = -\frac{\partial \sigma_y}{\partial T_p} \quad (17.141)$$

Assume the associated flow rule

$$\mathbf{d}^p = \dot{\lambda} \hat{\mathbf{N}} = \dot{\lambda} \frac{\mathbf{N}}{\|\mathbf{N}\|} \quad \text{where} \quad \mathbf{N} = \frac{\partial f}{\partial \boldsymbol{\sigma}} = \frac{\partial f}{\partial \boldsymbol{\xi}} = \sqrt{\frac{3}{2}} \frac{\boldsymbol{\xi}}{\|\boldsymbol{\xi}\|}, \quad \|\mathbf{N}\| = \sqrt{\frac{3}{2}} \quad (17.142)$$

Then

$$\mathbf{d}^p = \dot{\lambda} \frac{\boldsymbol{\xi}}{\|\boldsymbol{\xi}\|}; \quad \text{dev}(\mathbf{d}^p) = \mathbf{d}^p, \quad \text{tr}(\mathbf{d}^p) = 0, \quad \|\mathbf{d}^p\| = \dot{\boldsymbol{\varepsilon}}_p^{\text{eq}} = \dot{\lambda}. \quad (17.143)$$

The evolution of the equivalent plastic strain is given by

$$\dot{\boldsymbol{\varepsilon}}_p^{\text{eq}} = \dot{\lambda} h^{\boldsymbol{\varepsilon}_p} \implies h^{\boldsymbol{\varepsilon}_p} = 1. \quad (17.144)$$

The evolution of porosity is given by (there is no evolution of porosity)

$$\dot{\phi} = \dot{\lambda} h^\phi = 0 \implies h^\phi = 0. \quad (17.145)$$

The evolution of the back stress is given by the Prager kinematic hardening rule

$$\dot{\boldsymbol{\beta}} = \dot{\lambda} \mathbf{h}^\beta = H' d^p \implies \mathbf{h}^\beta = H' \frac{\boldsymbol{\xi}}{\|\boldsymbol{\xi}\|} \quad (17.146)$$

where H' is a hardening modulus. For the Armstrong-Frederick kinematic hardening model,

$$\dot{\boldsymbol{\beta}} = \dot{\lambda} \mathbf{h}^\beta = H_1 d^p - H_2 \boldsymbol{\beta} \|\mathbf{d}^p\| = \dot{\lambda} \left[H_1 \frac{\boldsymbol{\xi}}{\|\boldsymbol{\xi}\|} - H_2 \boldsymbol{\beta} \right] \implies \mathbf{h}^\beta = H_1 \frac{\boldsymbol{\xi}}{\|\boldsymbol{\xi}\|} - H_2 \boldsymbol{\beta} \quad (17.147)$$

17.4 Example 2: Gurson-type model

Consider a Gurson-type yield condition with kinematic hardening. In this case the yield condition can be written as

$$f := \frac{3}{2} \frac{(\sigma_{\text{eff}}^\xi)^2}{\sigma_y^2} + 2 q_1 \phi^* \cosh\left(\frac{3}{2} \frac{q_2 p_\beta}{\sigma_y}\right) - [1 + q_3 (\phi^*)^2] \quad (17.148)$$

where σ_y is the yield stress of the matrix material (zero-porosity),

$$\begin{aligned} \sigma_{\text{eff}}^\xi &= \boldsymbol{\xi} : \boldsymbol{\xi}, \quad \boldsymbol{\xi} = \text{dev}(\boldsymbol{\sigma} - \boldsymbol{\beta}), \quad p_\beta = \frac{1}{3} \text{tr}(\boldsymbol{\sigma} - \boldsymbol{\beta}) \\ \phi^* &= \begin{cases} \phi & \text{for } \phi \leq \phi_c \\ \phi_c - \frac{\phi_u^* - \phi_c}{\phi_f - \phi_c} (\phi - \phi_c) & \text{for } \phi > \phi_c \end{cases} \end{aligned} \quad (17.149)$$

and ϕ is the porosity. Final fracture occurs for $\phi = \phi_f$ or when $\phi_u^* = 1/q_1$. In this case, the derivatives of f are

$$\frac{\partial f}{\partial \sigma_{\text{eff}}^\xi} = \frac{3\sigma_{\text{eff}}^\xi}{\sigma_y^2}, \quad \frac{\partial f}{\partial p_\beta} = \frac{3q_1 q_2 \phi^*}{\sigma_y} \sinh\left(\frac{3}{2} \frac{q_2 p_\beta}{\sigma_y}\right), \quad \frac{\partial f}{\partial \sigma_y} = - \left[\frac{3(\sigma_{\text{eff}}^\xi)^2}{\sigma_y^3} + \frac{3q_1 q_2 p_\beta \phi^*}{\sigma_y^2} \sinh\left(\frac{3}{2} \frac{q_2 p_\beta}{\sigma_y}\right) \right] \quad (17.150)$$

and

$$\frac{\partial f}{\partial \boldsymbol{\beta}} = - \left[2 \frac{\partial f}{\partial \sigma_{\text{eff}}^\xi} \boldsymbol{\xi} + \frac{\partial f}{\partial p_\beta} \mathbf{I} \right], \quad \frac{\partial f}{\partial \varepsilon_p^{\text{eq}}} = \frac{\partial f}{\partial \sigma_y} \frac{\partial \sigma_y}{\partial \varepsilon_p^{\text{eq}}}, \quad \frac{\partial f}{\partial D} = \frac{\partial f}{\partial \sigma_y} \frac{\partial \sigma_y}{\partial D}, \quad \frac{\partial f}{\partial T_p} = \frac{\partial f}{\partial \sigma_y} \frac{\partial \sigma_y}{\partial T_p} \quad (17.151)$$

For the derivative with respect to ϕ ,

$$\frac{\partial f}{\partial \phi} = \frac{\partial f}{\partial \phi^*} \frac{\partial \phi^*}{\partial \phi} + \frac{\partial f}{\partial \sigma_y} \frac{\partial \sigma_y}{\partial \phi} = \frac{\partial f}{\partial \phi^*} \frac{\partial \phi^*}{\partial \phi} \quad (17.152)$$

where

$$\frac{\partial f}{\partial \phi^*} = 2q_1 \cosh\left(\frac{3}{2} \frac{q_2 p_\beta}{\sigma_y}\right) - 2q_3 \phi^* \quad \text{and} \quad \frac{\partial \phi^*}{\partial \phi} = \begin{cases} 1 & \text{for } \phi \leq \phi_c \\ -\frac{\phi_u^* - \phi_c}{\phi_f - \phi_c} & \text{for } \phi > \phi_c \end{cases} \quad (17.153)$$

Using an associated flow rule, we have

$$\mathbf{d}^p = \dot{\lambda} \hat{\mathbf{N}} = \dot{\lambda} \frac{\mathbf{N}}{\|\mathbf{N}\|}, \quad \mathbf{N} = \frac{\partial f}{\partial \boldsymbol{\sigma}} = 2 \frac{\partial f}{\partial \sigma_{\text{eff}}^\xi} \boldsymbol{\xi} + \frac{\partial f}{\partial p_\beta} \mathbf{I}, \quad \|\mathbf{N}\| = \sqrt{4 \left(\frac{\partial f}{\partial \sigma_{\text{eff}}^\xi} \|\boldsymbol{\xi}\| \right)^2 + 3 \left(\frac{\partial f}{\partial p_\beta} \right)^2} \quad (17.154)$$

For the evolution equation for the plastic strain we use

$$(\boldsymbol{\sigma} - \boldsymbol{\beta}) : \mathbf{d}^p = (1 - \phi) \sigma_y \dot{\varepsilon}_p^{\text{eq}} \quad (17.155)$$

where $\dot{\varepsilon}_p^{\text{eq}}$ is the equivalent plastic strain rate in the matrix material. Hence,

$$\dot{\varepsilon}_p^{\text{eq}} = \dot{\lambda} h^{\varepsilon_p} = \dot{\lambda} \frac{(p_\beta \mathbf{I} + \boldsymbol{\xi}) : \hat{\mathbf{N}}}{(1 - \phi) \sigma_y} \implies h^{\varepsilon_p} = \frac{3p_\beta \frac{\partial f}{\partial p_\beta} + 2 \frac{\partial f}{\partial \sigma_{\text{eff}}^\xi} \boldsymbol{\xi} : \boldsymbol{\xi}}{(1 - \phi) \sigma_y \|\mathbf{N}\|} \quad (17.156)$$

The evolution equation for the porosity is assumed to be given by

$$\dot{\phi} = (1 - \phi) \text{tr}(\mathbf{d}^p) + A \dot{\varepsilon}_p^{\text{eq}} \quad (17.157)$$

where

$$A = \frac{f_n}{\varepsilon_s \sqrt{2\pi}} \exp \left[-\frac{1}{2} \frac{(\varepsilon_p^{\text{eq}} - \varepsilon_m)^2}{\varepsilon_s^2} \right] \quad (17.158)$$

and f_n is the volume fraction of void nucleating particles, ε_m is the mean of the normal distribution of nucleation strains, and ε_s is the standard deviation of the distribution. Therefore,

$$\dot{\phi} = \dot{\lambda} h^\phi = \dot{\lambda} \left[(1 - \phi) \text{tr}(\hat{\mathbf{N}}) + A \frac{(p_\beta \mathbf{I} + \boldsymbol{\xi}) : \hat{\mathbf{N}}}{(1 - \phi) \sigma_y} \right] \implies h^\phi = \frac{1}{\|\mathbf{N}\|} \left[3(1 - \phi) \frac{\partial f}{\partial p_\beta} + A \frac{3p_\beta \frac{\partial f}{\partial p_\beta} + 2 \frac{\partial f}{\partial \sigma_{\text{eff}}^\xi} \boldsymbol{\xi} : \boldsymbol{\xi}}{(1 - \phi) \sigma_y} \right] \quad (17.159)$$

If the evolution of the backstress is given by the Prager kinematic hardening rule

$$\dot{\boldsymbol{\beta}} = \dot{\lambda} \mathbf{h}^\beta = H' \mathbf{d}^p \implies \mathbf{h}^\beta = \frac{H'}{\|\mathbf{N}\|} \left[2 \frac{\partial f}{\partial \sigma_{\text{eff}}^\xi} \boldsymbol{\xi} + \frac{\partial f}{\partial p_\beta} \mathbf{I} \right] \quad (17.160)$$

For the Armstrong-Frederick model,

$$\dot{\boldsymbol{\beta}} = \dot{\lambda} \mathbf{h}^\beta = H_1 \mathbf{d}^p - H_2 \boldsymbol{\beta} \|\mathbf{d}^p\| \implies \mathbf{h}^\beta = \frac{H_1}{\|\mathbf{N}\|} \left(2 \frac{\partial f}{\partial \sigma_{\text{eff}}^\xi} \boldsymbol{\xi} + \frac{\partial f}{\partial p_\beta} \mathbf{I} \right) - H_2 \boldsymbol{\beta}. \quad (17.161)$$

17.5 Example 3: Nonlinear elasticity and isotropic hardening

Let the flow stress be given by the Johnson-Cook model:

$$\sigma_y(\varepsilon_p^{\text{eq}}, \dot{\varepsilon}_p^{\text{eq}}, T) = [A + B(\varepsilon_p^{\text{eq}})^n] [1 + C \ln(\dot{\varepsilon}^*)] [1 - (T^*)^m] \quad (17.162)$$

The volumetric part of the stress in the intact metal is given by a Mie-Grüneisen equation of state:

$$p(J^e, T) = - \left[\frac{\rho_0 C_0^2 (1 - J^e) [1 - \Gamma_0 (1 - J^e)/2]}{[1 - S_\alpha (1 - J^e)]^2} + \Gamma_0 E \right], \quad J^e = \det \mathbf{F}^e, \quad E \approx \frac{\rho C_v (T - T_0)}{V} \quad (17.163)$$

The tangent bulk modulus of the intact metal is defined as

$$\kappa_m(p, J^e, T) = V^e \frac{\partial p}{\partial V^e} = V^e \frac{\partial p}{\partial J^e} \frac{\partial J^e}{\partial V^e} = \frac{V^e}{V_0} \frac{\partial p}{\partial J^e} = J^e \frac{\partial p}{\partial J^e} \approx \frac{\rho_0 J^e C_0^2 [1 + (S_\alpha - \Gamma_0)(1 - J^e)]}{[1 - S_\alpha (1 - J^e)]^3}. \quad (17.164)$$

Since the rate of deformation is unrotated in the VAANGO metal plasticity implementation, we can identify $\text{tr}(\boldsymbol{\epsilon}^e)$ with $\ln(J^e)$ [72] and use that quantity in the calculation. The deviatoric part of the stress in the intact metal is given by the Steinberg-Cochran-Guinan (SCG) shear modulus model:

$$\mu_m(p, J^e, T) = \mu_o + p \frac{\partial \mu_m}{\partial p} (J^e)^{1/3} + \frac{\partial \mu_m}{\partial T} (T - T_o) \quad (17.165)$$

When we include porosity-dependence for the bulk and shear moduli, we have

$$\begin{aligned} \kappa(p, J^e, \phi, T) &= \frac{(1 - \phi)\kappa_m}{1 - (1 - K)\phi}, \quad K = \frac{3\kappa_m + 4\mu_m}{4\mu_m} \\ \mu(p, J^e, \phi, T) &= \frac{(1 - \phi)\mu_m}{1 - (1 - G)\phi}, \quad G = \frac{5(3\kappa_m + 4\mu_m)}{9\kappa_m + 8\mu_m} \end{aligned} \quad (17.166)$$

The derivatives of σ_y , κ , and μ required for the algorithm can be calculated from these expressions.

18 — Metal plasticity : traditional approach

18.1 Preamble

Let \mathbf{F} be the deformation gradient, $\boldsymbol{\sigma}$ be the Cauchy stress, and \mathbf{d} be the rate of deformation tensor. We first decompose the deformation gradient into a stretch and a rotations using $\mathbf{F} = \mathbf{R} \cdot \mathbf{U}$. The rotation \mathbf{R} is then used to rotate the stress and the rate of deformation into the material configuration to give us

$$\hat{\boldsymbol{\sigma}} = \mathbf{R}^T \cdot \boldsymbol{\sigma} \cdot \mathbf{R} ; \quad \hat{\mathbf{d}} = \mathbf{R}^T \cdot \mathbf{d} \cdot \mathbf{R} \quad (18.1)$$

This is equivalent to using a Green-Naghdi objective stress rate. In the following all equations are with respect to the hatted quantities and we drop the hats for convenience.

Let us split the Cauchy stress into a mean (isotropic) and a deviatoric part

$$\boldsymbol{\sigma} = \boldsymbol{\sigma}_{\text{iso}} + \boldsymbol{\sigma}_{\text{dev}} = \sigma_m \mathbf{1} + \boldsymbol{\sigma}_{\text{dev}} ; \quad \sigma_m = \frac{1}{3} \text{tr}(\boldsymbol{\sigma}) . \quad (18.2)$$

Taking the time derivative gives us the rate-form of the stress

$$\dot{\boldsymbol{\sigma}} = \dot{\sigma}_m \mathbf{1} + \dot{\boldsymbol{\sigma}}_{\text{dev}} . \quad (18.3)$$

Similarly, we can split the rate of deformation (symmetric part of the spatial velocity gradient) into volumetric (d_v) and isochoric distortional (\mathbf{d}_{dis}) parts:

$$\mathbf{d} = \mathbf{d}_{\text{vol}} + \mathbf{d}_{\text{dis}} = \frac{1}{3} d_v \mathbf{1} + \mathbf{d}_{\text{dis}} . \quad (18.4)$$

The rate of deformation is additively decomposed into an elastic (\mathbf{d}^e) and a plastic part (\mathbf{d}^p):

$$\mathbf{d} = \mathbf{d}^e + \mathbf{d}^p .$$

We may also split \mathbf{d}^e into volumetric (d_v^e) and isochoric ($\mathbf{d}_{\text{dis}}^e$) parts as

$$\mathbf{d}^e = \frac{1}{3} d_v^e \mathbf{1} + \mathbf{d}_{\text{dis}}^e ; \quad d_v^e = \text{tr}(\mathbf{d}^e) . \quad (18.5)$$

Similarly, we can split \mathbf{d}^p into a volumetric part (d_v^p) and a trace-free part ($\mathbf{d}_{\text{dis}}^p$), i.e.,

$$\mathbf{d}^p = \frac{1}{3} d_v^p \mathbf{1} + \mathbf{d}_{\text{dis}}^p ; \quad d_v^p = \text{tr}(\mathbf{d}^p) . \quad (18.6)$$

Therefore,

$$d_v = d_v^e + d_v^p , \quad \mathbf{d}_{\text{dis}} = \mathbf{d}_{\text{dis}}^e + \mathbf{d}_{\text{dis}}^p . \quad (18.7)$$

18.2 Elastic relation

We assume that the elastic response of the material is isotropic. The constitutive relation for a hypoelastic material of grade 0 can be expressed as

$$\dot{\boldsymbol{\sigma}}^e = \left[\lambda \operatorname{tr}(\mathbf{d}^e) - 3 \kappa \alpha \frac{d}{dt}(T - T_0) \right] \mathbf{1} + 2 \mu \mathbf{d}^e = \left[\lambda \operatorname{tr}(\mathbf{d}^e) - 3 \kappa \alpha \dot{T} \right] \mathbf{1} + 2 \mu \mathbf{d}^e \quad (18.8)$$

where \mathbf{d}^e is the elastic part of the rate of deformation tensor, λ, μ are the Lamé tangent moduli, κ is the bulk modulus, α is the coefficient of thermal expansion, T_0 is the reference temperature, and T is the current temperature. In terms of the volumetric and deviatoric parts of the rate of deformation, we can write

$$\dot{\boldsymbol{\sigma}}^e = \left[\left(\lambda + \frac{2}{3} \mu \right) d_v^e - 3 \kappa \alpha \dot{T} \right] \mathbf{1} + 2 \mu \mathbf{d}_{\text{dis}}^e = \kappa \left[d_v^e - 3 \alpha \dot{T} \right] \mathbf{1} + 2 \mu \mathbf{d}_{\text{dis}}^e \quad (18.9)$$

Therefore, we have

$$\dot{\boldsymbol{\sigma}}_{\text{dev}}^e = 2 \mu \mathbf{d}_{\text{dis}}^e . \quad (18.10)$$

and

$$\dot{\sigma}_m^e = \kappa \left[d_v^e - 3 \alpha \dot{T} \right] . \quad (18.11)$$

We will use a standard elastic-plastic stress update algorithm to integrate the rate equation for the deviatoric stress. However, we will assume that the volumetric part of the Cauchy stress of the intact metal (excluding voids) can be computed using an equation of state. Then the final Cauchy stress will be given by

$$\boldsymbol{\sigma}^e = \left[\sigma_m^e(J^e) - 3 \kappa \alpha (T - T_0) \right] \mathbf{1} + \boldsymbol{\sigma}_{\text{dev}}^e ; \quad J^e = \det(\mathbf{F}^e) ; \kappa := J^e \frac{d\sigma_m^e(J^e)}{dJ^e} . \quad (18.12)$$

We assume that the plastic part of the deformation of the intact metal is volume preserving. For Gurson-type models, a separate algorithm is needed, and the use of the algorithm discussed in this chapter will lead to a small error in the computed value of $\boldsymbol{\sigma}$.

The moduli κ and μ may depend on the deformation gradient, temperature, and strain rate. Since the temperature and porosity depend on the amount of plastic deformation, this implies that the elastic and plastic responses are coupled. However, in this algorithm we ignore that coupling with the assumption that the errors will be small. The consequence of this assumption is that the moduli are computed only at the beginning of each time step on the basis of the mean stress and temperature at that point in the simulation.

18.3 Flow rule

We assume that the flow rule is given by

$$\mathbf{d}^p = \dot{\gamma} \hat{\mathbf{M}} \quad (18.13)$$

where $\hat{\mathbf{M}}$ is a **unit** tensor ($\hat{\mathbf{M}} : \hat{\mathbf{M}} = 1$) in the direction of the plastic flow rate, and $\dot{\gamma}$ is the plastic multiplier. Then, using the flow rule, we have the volumetric part:

$$d_v^p = \operatorname{tr}(\mathbf{d}^p) = \dot{\gamma} \operatorname{tr}(\hat{\mathbf{M}}) =: \dot{\gamma} M_v$$

or,

$$\mathbf{d}_{\text{vol}}^p = \frac{1}{3} \dot{\gamma} M_v \mathbf{1} =: \dot{\gamma} \mathbf{M}_{\text{iso}} . \quad (18.14)$$

In the same way, we can write the deviatoric part of the flow rule as

$$\mathbf{d}_{\text{dis}}^p = \dot{\gamma} \left(\hat{\mathbf{M}} - \frac{1}{3} \text{tr}(\hat{\mathbf{M}}) \mathbf{1} \right) =: \dot{\gamma} \mathbf{M}_{\text{dev}} . \quad (18.15)$$

Note that \mathbf{M}_{dev} is *not* a unit tensor and an appropriate normalizing factor is needed to make it a unit tensor.

18.4 Hardening, porosity evolution, and plastic dissipation

We could assume that the strain rate, temperature, and porosity can be fixed at the beginning of a time step and consider only the evolution of plastic strain and the back stress while calculating the current stress. However, that causes problems of convergence and it is probably more appropriate to simultaneously consider all the ordinary differential equations that contain rates of change.

We assume that the equivalent plastic strain evolves according to the relation

$$\dot{\varepsilon}^p = \dot{\gamma} h^\alpha \quad (18.16)$$

We also assume that the back stress evolves according to the relation

$$\dot{\boldsymbol{\beta}} = \dot{\gamma} \mathbf{h}^\beta \quad (18.17)$$

where $\boldsymbol{\beta}$ is the back stress. If $\boldsymbol{\beta}_{\text{iso}}$ and $\boldsymbol{\beta}_{\text{dev}}$ are the volumetric and deviatoric parts of $\boldsymbol{\beta}$, respectively, we can write

$$\dot{\boldsymbol{\beta}}_{\text{iso}} = \dot{\gamma} h_{\text{iso}}^\beta \quad \dot{\boldsymbol{\beta}}_{\text{dev}} = \dot{\gamma} h_{\text{dev}}^\beta . \quad (18.18)$$

The porosity ϕ is assumed to evolve according to the relation

$$\dot{\phi} = \dot{\gamma} h^\phi . \quad (18.19)$$

The temperature change due to plastic dissipation is assumed to be given by the rate equation

$$\dot{T} = \frac{\chi}{\rho C_p} \sigma_y \dot{\varepsilon}^p = \dot{\gamma} h^T . \quad (18.20)$$

18.5 Yield condition

The yield condition is assumed to be of the form

$$f(\boldsymbol{\sigma}_{\text{iso}}, \boldsymbol{\sigma}_{\text{dev}}, \boldsymbol{\beta}_{\text{iso}}, \boldsymbol{\beta}_{\text{dev}}, \varepsilon^p, \phi, T, \dot{\varepsilon}, \dots) = f(\boldsymbol{\xi}_{\text{iso}}, \boldsymbol{\xi}_{\text{dev}}, \varepsilon^p, \phi, T, \dot{\varepsilon}, \dots) = 0 \quad (18.21)$$

where $\boldsymbol{\xi}_{\text{iso}} := \boldsymbol{\sigma}_{\text{iso}} - \boldsymbol{\beta}_{\text{iso}}$ and $\boldsymbol{\xi}_{\text{dev}} := \boldsymbol{\sigma}_{\text{dev}} - \boldsymbol{\beta}_{\text{dev}}$. The Kuhn-Tucker loading-unloading conditions are

$$\dot{\gamma} \geq 0 ; \quad f \leq 0 ; \quad \dot{\gamma} f = 0 \quad (18.22)$$

and the consistency condition is $\dot{f} = 0$.

18.6 Continuum elastic-plastic tangent modulus

To determine whether the material has undergone a loss of stability we need to compute the acoustic tensor which needs the computation of the continuum elastic-plastic tangent modulus.

Recall that

$$\boldsymbol{\sigma} = \boldsymbol{\sigma}_{\text{iso}} + \boldsymbol{\sigma}_{\text{dev}} = \sigma_m \mathbf{1} + \boldsymbol{\sigma}_{\text{dev}} \implies \dot{\boldsymbol{\sigma}} = \dot{\boldsymbol{\sigma}}_{\text{iso}} + \dot{\boldsymbol{\sigma}}_{\text{dev}} = \dot{\sigma}_m \mathbf{1} + \dot{\boldsymbol{\sigma}}_{\text{dev}}. \quad (18.23)$$

We assume that

$$\dot{\sigma}_m^e = J^e \frac{\partial \sigma_m^e}{\partial J^e} \text{tr}(\mathbf{d}^e) = \kappa \text{tr}(\mathbf{d}^e) \quad \text{and} \quad \dot{\boldsymbol{\sigma}}_{\text{dev}}^e = 2 \mu \mathbf{d}_{\text{dis}}^e. \quad (18.24)$$

The Kuhn-Tucker and consistency conditions require that the stress state is on the boundary of the elastic domain and therefore is directly related to the elastic part of the rate of deformation tensor. However, we don't know the fraction of the total deformation tensor that is elastic, and that is what we have to determine. Therefore, the consistency condition can be expressed as

$$\dot{f}(\boldsymbol{\sigma}_{\text{iso}}^e, \boldsymbol{\sigma}_{\text{dev}}^e, \boldsymbol{\beta}_{\text{iso}}, \boldsymbol{\beta}_{\text{dev}}, \varepsilon^p, \phi, T, \dot{\varepsilon}, \dots) = 0. \quad (18.25)$$

Keeping $\dot{\varepsilon}$ fixed over the time interval, we can use the chain rule to get

$$\dot{f} = \frac{\partial f}{\partial \boldsymbol{\sigma}_{\text{iso}}^e} : \dot{\boldsymbol{\sigma}}_{\text{iso}}^e + \frac{\partial f}{\partial \boldsymbol{\sigma}_{\text{dev}}^e} : \dot{\boldsymbol{\sigma}}_{\text{dev}}^e + \frac{\partial f}{\partial \boldsymbol{\beta}_{\text{iso}}} : \dot{\boldsymbol{\beta}}_{\text{iso}} + \frac{\partial f}{\partial \boldsymbol{\beta}_{\text{dev}}} : \dot{\boldsymbol{\beta}}_{\text{dev}} + \frac{\partial f}{\partial \varepsilon^p} \dot{\varepsilon}^p + \frac{\partial f}{\partial \phi} \dot{\phi} + \frac{\partial f}{\partial T} \dot{T} = 0. \quad (18.26)$$

The associated rate equations are

$$\begin{aligned} \dot{\boldsymbol{\sigma}}_{\text{iso}}^e &= \kappa \mathbf{d}_{\text{vol}}^e = \kappa (\mathbf{d}_{\text{vol}} - \mathbf{d}_{\text{vol}}^p) = \kappa [\mathbf{d}_{\text{vol}} - \dot{\gamma} \mathbf{M}_{\text{iso}}] \\ \dot{\boldsymbol{\sigma}}_{\text{dev}}^e &= 2 \mu \mathbf{d}_{\text{dis}}^e = 2 \mu (\mathbf{d}_{\text{dis}} - \mathbf{d}_{\text{dis}}^p) = 2 \mu [\mathbf{d}_{\text{dis}} - \dot{\gamma} \mathbf{M}_{\text{dev}}] \\ \dot{\boldsymbol{\beta}}_{\text{iso}} &= \dot{\gamma} \mathbf{h}_{\text{iso}}^\beta \\ \dot{\boldsymbol{\beta}}_{\text{dev}} &= \dot{\gamma} \mathbf{h}_{\text{dev}}^\beta \\ \dot{\varepsilon}^p &= \dot{\gamma} h^\alpha \\ \dot{\phi} &= \dot{\gamma} h^\phi \\ \dot{T} &= \dot{\gamma} h^T \end{aligned} \quad (18.27)$$

Plugging these into the expression for \dot{f} gives

$$\kappa \frac{\partial f}{\partial \boldsymbol{\sigma}_{\text{iso}}^e} : [\mathbf{d}_{\text{vol}} - \dot{\gamma} \mathbf{M}_{\text{iso}}] + 2 \mu \frac{\partial f}{\partial \boldsymbol{\sigma}_{\text{dev}}^e} : [\mathbf{d}_{\text{dis}} - \dot{\gamma} \mathbf{M}_{\text{dev}}] + \dot{\gamma} \frac{\partial f}{\partial \boldsymbol{\beta}_{\text{iso}}} : \mathbf{h}_{\text{iso}}^\beta + \dot{\gamma} \frac{\partial f}{\partial \boldsymbol{\beta}_{\text{dev}}} : \mathbf{h}_{\text{dev}}^\beta + \dot{\gamma} \frac{\partial f}{\partial \varepsilon^p} h^\alpha + \dot{\gamma} \frac{\partial f}{\partial \phi} h^\phi + \dot{\gamma} \frac{\partial f}{\partial T} h^T = 0 \quad (18.28)$$

or,

$$\dot{\gamma} = \frac{\kappa \mathbf{F}_{\sigma_v} : \mathbf{d}_{\text{vol}} + 2 \mu \mathbf{F}_{\sigma_d} : \mathbf{d}_{\text{dis}}}{H} \quad (18.29)$$

where

$$\mathbf{F}_{\sigma_v} := \frac{\partial f}{\partial \boldsymbol{\sigma}_{\text{iso}}^e}; \quad \mathbf{F}_{\sigma_d} := \frac{\partial f}{\partial \boldsymbol{\sigma}_{\text{dev}}^e}; \quad H := \kappa \frac{\partial f}{\partial \boldsymbol{\sigma}_{\text{iso}}^e} : \mathbf{M}_{\text{iso}} + 2 \mu \frac{\partial f}{\partial \boldsymbol{\sigma}_{\text{dev}}^e} : \mathbf{M}_{\text{dev}} - \frac{\partial f}{\partial \boldsymbol{\beta}_{\text{iso}}} : \mathbf{h}_{\text{iso}}^\beta - \frac{\partial f}{\partial \boldsymbol{\beta}_{\text{dev}}} : \mathbf{h}_{\text{dev}}^\beta - \frac{\partial f}{\partial \varepsilon^p} h^\alpha - \frac{\partial f}{\partial \phi} h^\phi - \frac{\partial f}{\partial T} h^T.$$

Plugging this expression for $\dot{\gamma}$ into the equations for $\dot{\boldsymbol{\sigma}}_{\text{iso}}^e$ and $\dot{\boldsymbol{\sigma}}_{\text{dev}}^e$, we get

$$\dot{\boldsymbol{\sigma}}_{\text{iso}}^e = \kappa \left[\mathbf{d}_{\text{vol}} - \left(\frac{\kappa \mathbf{F}_{\sigma_v} : \mathbf{d}_{\text{vol}} + 2 \mu \mathbf{F}_{\sigma_d} : \mathbf{d}_{\text{dis}}}{H} \right) \mathbf{M}_{\text{iso}} \right] \quad \dot{\boldsymbol{\sigma}}_{\text{dev}}^e = 2 \mu \left[\mathbf{d}_{\text{dis}} - \left(\frac{\kappa \mathbf{F}_{\sigma_v} : \mathbf{d}_{\text{vol}} + 2 \mu \mathbf{F}_{\sigma_d} : \mathbf{d}_{\text{dis}}}{H} \right) \mathbf{M}_{\text{dev}} \right].$$

(18.30)

These equations clearly indicate that the volumetric and deviatoric responses cannot be uncoupled unless the yield function depends only on the deviatoric stress. Since that assumption limits us to J2-plasticity and does not allow us to include Gurson-type models, we will not separate out the deviatoric and volumetric components of stress (or volumetric/isochoric deformation rates) in this model even though plastic deformation in the metal matrix is volume-preserving.

18.6.1 J2 plasticity

At this stage, note that a symmetric σ implies a symmetric σ_{dev} and hence a symmetric \mathbf{d}_{dis} . Also, \mathbf{M}_{dev} is symmetric, since we assume that the flow rule is associated, i.e.,

$$\hat{\mathbf{M}} = \frac{\mathbf{N}}{\|\mathbf{N}\|}, \quad \mathbf{N} := \frac{\partial f}{\partial \sigma}. \quad (18.31)$$

Then we can write,

$$\mathbf{d}_{\text{dis}} = \mathbb{I}^{4s} : \mathbf{d}_{\text{dis}} \quad \text{and} \quad \mathbf{M}_{\text{dev}} = \mathbb{I}^{4s} : \mathbf{M}_{\text{dev}} \quad (18.32)$$

where \mathbb{I}^{4s} is the fourth-order symmetric identity tensor. Also note that if \mathbf{A} , \mathbf{C} , \mathbf{D} are second order tensors and \mathbb{B} is a fourth order tensor, then

$$(\mathbf{A} : \mathbb{B} : \mathbf{C}) (\mathbb{B} : \mathbf{D}) \equiv A_{ij} B_{ijkl} C_{kl} B_{mnpq} D_{pq} = (B_{mnpq} D_{pq}) (A_{ij} B_{ijkl}) C_{kl} \equiv [(\mathbb{B} : \mathbf{D}) \otimes (\mathbf{A} : \mathbb{B})] : \mathbf{C}. \quad (18.33)$$

Therefore, we have,

$$\dot{\sigma}_{\text{dev}}^e = 2 \mu \left[\mathbb{I}^{4s} : \mathbf{d}_{\text{dis}} - \left(\frac{2 \mu [\mathbb{I}^{4s} : \mathbf{M}_{\text{dev}}] \otimes [\mathbf{F}_{\sigma} : \mathbb{I}^{4s}]}{H} \right) : \mathbf{d}_{\text{dis}} \right]. \quad (18.34)$$

Also,

$$\mathbb{I}^{4s} : \mathbf{M}_{\text{dev}} = \mathbf{M}_{\text{dev}} \quad \text{and} \quad \mathbf{F}_{\sigma} : \mathbb{I}^{4s} = \mathbf{F}_{\sigma}. \quad (18.35)$$

Hence we can write

$$\dot{\sigma}_{\text{dev}}^e = 2 \mu \left[\mathbb{I}^{4s} - \left(\frac{2 \mu \mathbf{M}_{\text{dev}} \otimes \mathbf{F}_{\sigma}}{H} \right) \right] : \mathbf{d}_{\text{dis}} \quad (18.36)$$

or,

$$\begin{aligned} \dot{\sigma}_{\text{dev}}^e &= \mathbb{B}^{ep} : \mathbf{d}_{\text{dis}} = \mathbb{B}^{ep} : \left[\mathbf{d} - \frac{1}{3} \text{tr}(\mathbf{d}) \mathbf{1} \right] = \mathbb{B}^{ep} : \mathbf{d} - \frac{1}{3} [\mathbb{B}^{ep} : (\mathbf{1} \otimes \mathbf{1})] : \mathbf{d} \\ &=: \mathbb{B}_{\text{dev}}^{ep} : \mathbf{d} \end{aligned} \quad (18.37)$$

where

$$\mathbb{B}^{ep} := 2 \mu \left[\mathbb{I}^{4s} - \left(\frac{2 \mu \mathbf{M}_{\text{dev}} \otimes \mathbf{F}_{\sigma}}{H} \right) \right], \quad \mathbb{B}_{\text{dev}}^{ep} := \mathbb{B}^{ep} - \frac{1}{3} [\mathbb{B}^{ep} : (\mathbf{1} \otimes \mathbf{1})] \quad (18.38)$$

For the mean stress component, we have

$$\begin{aligned} \dot{\sigma}_{\text{iso}}^e &= \dot{\sigma}_m^e \mathbf{1} = J^e \frac{\partial \sigma_m^e}{\partial J^e} [\text{tr}(\mathbf{d}) - \dot{\gamma} \text{tr}(\hat{\mathbf{M}})] \mathbf{1} \\ &= \kappa \left[\text{tr}(\mathbf{d}) - \frac{2 \mu \mathbf{F}_{\sigma} : \mathbf{d}_{\text{dis}}}{H} \text{tr}(\hat{\mathbf{M}}) \right] \mathbf{1} \\ &= \kappa \left[\text{tr}(\mathbf{d}) - \frac{2 \mu \text{tr}(\hat{\mathbf{M}})}{H} \mathbf{F}_{\sigma} : \left(\mathbf{d} - \frac{1}{3} \text{tr}(\mathbf{d}) \mathbf{1} \right) \right] \mathbf{1} \\ &= \kappa (\mathbf{1} \otimes \mathbf{1}) : \mathbf{d} - \frac{2 \mu \kappa \text{tr}(\hat{\mathbf{M}})}{H} \left[(\mathbf{1} \otimes \mathbf{F}_{\sigma}) : \mathbf{d} - \frac{1}{3} \text{tr}(\mathbf{F}_{\sigma}) (\mathbf{1} \otimes \mathbf{1}) : \mathbf{d} \right] \\ &=: \mathbb{B}_{\text{iso}}^{ep} : \mathbf{d} \end{aligned}$$

where,

$$\mathbb{B}_{\text{iso}}^{ep} = \kappa(\mathbf{1} \otimes \mathbf{1}) - \frac{2\mu\kappa \text{tr}(\hat{\mathbf{M}})}{H} \left[(\mathbf{1} \otimes \mathbf{F}_\sigma) - \frac{1}{3} \text{tr}(\mathbf{F}_\sigma)(\mathbf{1} \otimes \mathbf{1}) \right].$$

Adding the volumetric and deviatoric components gives

$$\begin{aligned} \dot{\boldsymbol{\sigma}}^e &= \dot{\boldsymbol{\sigma}}_{\text{iso}}^e + \dot{\boldsymbol{\sigma}}_{\text{dev}}^e \\ &= \mathbb{B}_{\text{iso}}^{ep} : \mathbf{d} + \mathbb{B}_{\text{dev}}^{ep} : \mathbf{d} =: \mathbb{C}^{ep} : \mathbf{d}. \end{aligned} \quad (18.39)$$

The quantity \mathbb{C}^{ep} is the continuum elastic-plastic tangent modulus. We also use the continuum elastic-plastic tangent modulus in the implicit version of the code. However, for improved accuracy and faster convergence, an algorithmically consistent tangent modulus should be used instead. That tangent modulus can be calculated in the usual manner and is left for development and implementation as an additional feature in the future.

18.6.2 J2-I1 plasticity

For J2-I1 plasticity, there is little advantage to be gained if we split the stress into volumetric and deviatoric components. Therefore, we use the total stress and the total rate of deformation:

$$\dot{\boldsymbol{\sigma}}^e = \left(\kappa - \frac{2}{3}\mu \right) \text{tr}(\mathbf{d}^e) \mathbf{1} + 2\mu \mathbf{d}^e$$

and

$$\mathbf{d}^e = \mathbf{d} - \mathbf{d}^p = \mathbf{d} - \dot{\gamma} \hat{\mathbf{M}}.$$

Then,

$$\dot{f} = \frac{\partial f}{\partial \boldsymbol{\sigma}^e} : \dot{\boldsymbol{\sigma}}^e + \frac{\partial f}{\partial \boldsymbol{\beta}} : \dot{\boldsymbol{\beta}} + \frac{\partial f}{\partial \varepsilon^p} \dot{\varepsilon}^p + \frac{\partial f}{\partial \phi} \dot{\phi} + \frac{\partial f}{\partial T} \dot{T} = 0$$

and we have

$$\dot{\gamma} = \frac{[(\kappa - \frac{2}{3}\mu) \text{tr}(\mathbf{F}_\sigma) \mathbf{1} + 2\mu \mathbf{F}_\sigma] : \mathbf{d}}{H}$$

where

$$H = (\kappa - \frac{2}{3}\mu) \text{tr}(\mathbf{F}_\sigma) \text{tr}(\hat{\mathbf{M}}) + 2\mu \mathbf{F}_\sigma : \hat{\mathbf{M}} - \frac{\partial f}{\partial \boldsymbol{\beta}} : \mathbf{h}^\beta - \frac{\partial f}{\partial \varepsilon^p} h^\alpha - \frac{\partial f}{\partial \phi} h^\phi - \frac{\partial f}{\partial T} h^T.$$

Therefore,

$$\mathbf{d}^e = \left[\mathbb{I}^{4s} - \frac{(\kappa - \frac{2}{3}\mu) \text{tr}(\mathbf{F}_\sigma) \hat{\mathbf{M}} \otimes \mathbf{1} + 2\mu \hat{\mathbf{M}} \otimes \mathbf{F}_\sigma}{H} \right] : \mathbf{d} =: \mathbb{D}^e : \mathbf{d}$$

and

$$\dot{\boldsymbol{\sigma}}^e = \left[\left(\kappa - \frac{2}{3}\mu \right) [(\mathbf{1} \otimes \mathbf{1}) : \mathbb{D}^e + 2\mu \mathbb{I}^{4s}] : \mathbf{d} =: \mathbb{C}^{ep} : \mathbf{d} \right].$$

18.7 Stress update

A standard return algorithm is used to compute the updated Cauchy stress.

18.7.1 Integrating the rate equations

J2 plasticity

Recall that the rate equation for the deviatoric stress is given by

$$\dot{\sigma}_{\text{dev}}^e = 2 \mu \mathbf{d}_{\text{dis}}^e. \quad (18.40)$$

Integration of the rate equation using a Backward Euler scheme gives

$$(\sigma_{\text{dev}}^e)_{n+1} - (\sigma_{\text{dev}}^e)_n = 2 \mu_{n+1} \Delta t (\mathbf{d}_{\text{dis}}^e)_{n+1} = 2 \mu_{n+1} \Delta t [(\mathbf{d}_{\text{dis}})_{n+1} - (\mathbf{d}_{\text{dis}}^p)_{n+1}] \quad (18.41)$$

Now, from the flow rule, we have

$$\mathbf{d}_{\text{dis}}^p = \dot{\gamma} \left(\hat{\mathbf{M}} - \frac{1}{3} \text{tr}(\hat{\mathbf{M}}) \mathbf{1} \right) = \dot{\gamma} \mathbf{M}_{\text{dev}}. \quad (18.42)$$

Identifying $\dot{\epsilon}_{\text{dis}}^p = \mathbf{d}_{\text{dis}}^p$, we can write the integrated strain as

$$(\epsilon_{\text{dis}}^p)_{n+1} = (\epsilon_{\text{dis}}^p)_n + \Delta \gamma_{n+1} (\mathbf{M}_{\text{dev}})_{n+1}. \quad (18.43)$$

Therefore,

$$(\sigma_{\text{dev}}^e)_{n+1} - (\sigma_{\text{dev}}^e)_n = 2 \mu_{n+1} \Delta t (\mathbf{d}_{\text{dis}})_{n+1} - 2 \mu_{n+1} \Delta \gamma_{n+1} (\mathbf{M}_{\text{dev}})_{n+1}. \quad (18.44)$$

where $\Delta \gamma := \dot{\gamma} \Delta t$. At this stage we ignore elastic-plastic coupling and assume that $\mu_{n+1} = \mu_n$. Define the trial stress

$$\sigma_{\text{dev}}^{\text{trial}} := (\sigma_{\text{dev}}^e)_n + 2 \mu_n \Delta t (\mathbf{d}_{\text{dis}})_{n+1}. \quad (18.45)$$

Then

$$(\sigma_{\text{dev}}^e)_{n+1} = \sigma_{\text{dev}}^{\text{trial}} - 2 \mu_n \Delta \gamma_{n+1} (\mathbf{M}_{\text{dev}})_{n+1}. \quad (18.46)$$

Also recall that the back stress is given by

$$\dot{\beta}_{\text{dev}} = \dot{\gamma} \mathbf{h}_{\text{dev}}^\beta \quad (18.47)$$

The evolution equation for the back stress can be integrated to get

$$(\beta_{\text{dev}})_{n+1} - (\beta_{\text{dev}})_n = \Delta \gamma_{n+1} (\mathbf{h}_{\text{dev}}^\beta)_{n+1}. \quad (18.48)$$

Define

$$\xi_{n+1} := (\sigma_{\text{dev}}^e)_{n+1} - (\beta_{\text{dev}})_{n+1}. \quad (18.49)$$

Plugging in the expressions for $(\sigma_{\text{dev}}^e)_{n+1}$ and $(\beta_{\text{dev}})_{n+1}$, we get

$$\xi_{n+1} = \sigma_{\text{dev}}^{\text{trial}} - 2 \mu_n \Delta \gamma_{n+1} (\mathbf{M}_{\text{dev}})_{n+1} - (\beta_{\text{dev}})_n - \Delta \gamma_{n+1} (\mathbf{h}_{\text{dev}}^\beta)_{n+1}. \quad (18.50)$$

Define

$$\xi^{\text{trial}} := \sigma_{\text{dev}}^{\text{trial}} - (\beta_{\text{dev}})_n. \quad (18.51)$$

Then

$$\xi_{n+1} = \xi^{\text{trial}} - \Delta \gamma_{n+1} \left[2 \mu_n (\mathbf{M}_{\text{dev}})_{n+1} + (\mathbf{h}_{\text{dev}}^\beta)_{n+1} \right]. \quad (18.52)$$

Similarly, the evolution of the plastic strain is given by

$$\epsilon_{n+1}^p = \epsilon_n^p + \Delta \gamma_{n+1} \mathbf{h}_{n+1}^\alpha. \quad (18.53)$$

The porosity evolves as

$$\phi_{n+1} = \phi_n + \Delta \gamma_{n+1} \mathbf{h}_{n+1}^\phi. \quad (18.54)$$

The temperature evolves as

$$T_{n+1} = T_n + \Delta \gamma_{n+1} \mathbf{h}_{n+1}^T. \quad (18.55)$$

The yield condition is discretized as

$$f((\sigma_{\text{dev}})_{n+1}, (\beta_{\text{dev}})_{n+1}, \epsilon_{n+1}^p, \phi_{n+1}, T_{n+1}, \dot{\epsilon}_{n+1}, \dots) = f(\xi_{n+1}, \epsilon_{n+1}^p, \phi_{n+1}, T_{n+1}, \dot{\epsilon}_{n+1}, \dots) = 0. \quad (18.56)$$

J2-I1 plasticity

In this case, we use the rate equation for the total stress is given by

$$\dot{\sigma}^e = \left(k - \frac{2}{3}\mu \right) \mathbf{d}^e : \mathbf{1} + 2\mu \mathbf{d}^e. \quad (18.57)$$

Backward Euler gives

$$\begin{aligned} \sigma_{n+1}^e - \sigma_n^e &= \Delta t \left(\kappa_{n+1} - \frac{2}{3}\mu_{n+1} \right) \mathbf{d}_{n+1}^e : \mathbf{1} + 2\Delta t \mu_{n+1} \mathbf{d}_{n+1}^e \\ &= \left(\kappa_{n+1} - \frac{2}{3}\mu_{n+1} \right) (\Delta t \mathbf{d}_{n+1} - \Delta t \mathbf{d}_{n+1}^p) : \mathbf{1} + 2\mu_{n+1} (\Delta t \mathbf{d}_{n+1} - \Delta t \mathbf{d}_{n+1}^p) \end{aligned} \quad (18.58)$$

Flow rule:

$$\mathbf{d}^p = \dot{\gamma} \hat{\mathbf{M}} \quad (18.59)$$

Set $\dot{\epsilon}^p := \mathbf{d}^p$, to write the integrated strain:

$$\epsilon_{n+1}^p = \epsilon_n^p + \Delta\gamma_{n+1} \hat{\mathbf{M}}_{n+1} \quad \leftrightarrow \quad \Delta t \mathbf{d}_{n+1}^p = \Delta\gamma_{n+1} \hat{\mathbf{M}}_{n+1}. \quad (18.60)$$

Then,

$$\sigma_{n+1}^e = \sigma_n^e + \left(\kappa_{n+1} - \frac{2}{3}\mu_{n+1} \right) (\Delta t \mathbf{d}_{n+1} - \Delta\gamma_{n+1} \hat{\mathbf{M}}_{n+1}) : \mathbf{1} + 2\mu_{n+1} (\Delta t \mathbf{d}_{n+1} - \Delta\gamma_{n+1} \hat{\mathbf{M}}_{n+1}) \quad (18.61)$$

where $\Delta\gamma := \dot{\gamma} \Delta t$. Ignore elastic-plastic coupling and assume $\kappa_{n+1} = \kappa_n$ and $\mu_{n+1} = \mu_n$. The trial stress is

$$\sigma^{\text{trial}} := \sigma_n^e + \left(\kappa_n - \frac{2}{3}\mu_n \right) \Delta t \mathbf{d}_{n+1} : \mathbf{1} + 2\mu_n \Delta t \mathbf{d}_{n+1}. \quad (18.62)$$

Then

$$\sigma_{n+1}^e = \sigma^{\text{trial}} - \left(\kappa_{n+1} - \frac{2}{3}\mu_{n+1} \right) \Delta\gamma_{n+1} \hat{\mathbf{M}}_{n+1} : \mathbf{1} - 2\mu_{n+1} \Delta\gamma_{n+1} \hat{\mathbf{M}}_{n+1}. \quad (18.63)$$

For the back stress,

$$\beta_{n+1} - \beta_n = \Delta\gamma_{n+1} \mathbf{h}_{n+1}^\beta. \quad (18.64)$$

Define

$$\xi_{n+1} := \sigma_{n+1}^e - \beta_{n+1} \quad (18.65)$$

to arrive at the combined stress equation

$$\xi_{n+1} = \sigma^{\text{trial}} - \left(\kappa_{n+1} - \frac{2}{3}\mu_{n+1} \right) \Delta\gamma_{n+1} \hat{\mathbf{M}}_{n+1} : \mathbf{1} - 2\mu_{n+1} \Delta\gamma_{n+1} \hat{\mathbf{M}}_{n+1} - \beta_n - \Delta\gamma_{n+1} \mathbf{h}_{n+1}^\beta. \quad (18.66)$$

Define

$$\xi^{\text{trial}} := \sigma^{\text{trial}} - \beta_n \quad (18.67)$$

to get

$$\xi_{n+1} = \xi^{\text{trial}} - \Delta\gamma_{n+1} \left[\left(\kappa_{n+1} - \frac{2}{3}\mu_{n+1} \right) \hat{\mathbf{M}}_{n+1} : \mathbf{1} - 2\mu_{n+1} \hat{\mathbf{M}}_{n+1} - \mathbf{h}_{n+1}^\beta \right]. \quad (18.68)$$

The other rate equations are integrated as before:

$$\begin{aligned} \epsilon_{n+1}^p &= \epsilon_n^p + \Delta\gamma_{n+1} \mathbf{h}_{n+1}^\alpha \\ \phi_{n+1} &= \phi_n + \Delta\gamma_{n+1} \mathbf{h}_{n+1}^\phi \\ T_{n+1} &= T_n + \Delta\gamma_{n+1} \mathbf{h}_{n+1}^T. \end{aligned} \quad (18.69)$$

The yield condition is discretized as

$$f(\sigma_{n+1}^e, \beta_{n+1}, \epsilon_{n+1}^p, \phi_{n+1}, T_{n+1}, \dot{\epsilon}_{n+1}, \dots) = f(\xi_{n+1}, \epsilon_{n+1}^p, \phi_{n+1}, T_{n+1}, \dot{\epsilon}_{n+1}, \dots) = 0. \quad (18.70)$$

18.7.2 Newton iterations

J2 plasticity

The following coupled equations have to be solved for the unknowns at t_{n+1} :

$$\begin{aligned}
 (\boldsymbol{\sigma}_{\text{dev}}^e)_{n+1} &= \boldsymbol{\sigma}_{\text{dev}}^{\text{trial}} - 2\mu_n \Delta\gamma_{n+1} (\mathbf{M}_{\text{dev}})_{n+1} \\
 (\boldsymbol{\varepsilon}_{\text{dis}}^p)_{n+1} &= (\boldsymbol{\varepsilon}_{\text{dis}}^p)_n + \Delta\gamma_{n+1} (\mathbf{M}_{\text{dev}})_{n+1} \\
 (\boldsymbol{\beta}_{\text{dev}})_{n+1} &= (\boldsymbol{\beta}_{\text{dev}})_n + \Delta\gamma_{n+1} (\mathbf{h}_{\text{dev}}^\beta)_{n+1} \\
 \boldsymbol{\varepsilon}_{n+1}^p &= \boldsymbol{\varepsilon}_n^p + \Delta\gamma_{n+1} \mathbf{h}_{n+1}^\alpha \\
 \phi_{n+1} &= \phi_n + \Delta\gamma_{n+1} \mathbf{h}_{n+1}^\phi \\
 T_{n+1} &= T_n + \Delta\gamma_{n+1} \mathbf{h}_{n+1}^T \\
 f_{n+1}(\boldsymbol{\xi}_{n+1}, \boldsymbol{\varepsilon}_{n+1}^p, \phi_{n+1}, T_{n+1}, \dot{\boldsymbol{\varepsilon}}_{n+1}, \dots) &= 0.
 \end{aligned} \tag{18.71}$$

Note that, for associated plasticity, the first two equations depend on f_{n+1} . Recognizing that the second equation is already incorporated into the first, and combining the stress and backstress equations, we can express the above equations in terms of residuals as,

$$\begin{aligned}
 \mathbf{r}_\xi &= \boldsymbol{\xi}_{n+1} - \boldsymbol{\xi}^{\text{trial}} + \Delta\gamma_{n+1} [2\mu_n (\mathbf{M}_{\text{dev}})_{n+1} + (\mathbf{h}_{\text{dev}}^\beta)_{n+1}] = \mathbf{0} \\
 \mathbf{r}_{\varepsilon^p} &= \boldsymbol{\varepsilon}_{n+1}^p - \boldsymbol{\varepsilon}_n^p - \Delta\gamma_{n+1} \mathbf{h}_{n+1}^\alpha = \mathbf{0} \\
 \mathbf{r}_\phi &= \phi_{n+1} - \phi_n - \Delta\gamma_{n+1} \mathbf{h}_{n+1}^\phi = 0 \\
 \mathbf{r}_T &= T_{n+1} - T_n - \Delta\gamma_{n+1} \mathbf{h}_{n+1}^T = 0 \\
 \mathbf{r}_f &= f_{n+1}(\boldsymbol{\xi}_{n+1}, \boldsymbol{\varepsilon}_{n+1}^p, \phi_{n+1}, T_{n+1}, \dot{\boldsymbol{\varepsilon}}_{n+1}, \dots) = 0.
 \end{aligned} \tag{18.72}$$

or, if $\mathbf{x} = (\boldsymbol{\xi}_{n+1}, \boldsymbol{\varepsilon}_{n+1}^p, \phi_{n+1}, T_{n+1}, \Delta\gamma_{n+1})$ is the vector of *independent* unknowns in the above equations,

$$\mathbf{r}(\mathbf{x}) = \mathbf{0}. \tag{18.73}$$

An iterative Newton method can be used to find the solution:

$$\mathbf{x}^{(k+1)} = \mathbf{x}^{(k)} - \left[\frac{\partial \mathbf{r}}{\partial \mathbf{x}} \right]_{(k)}^{-1} \mathbf{r}^{(k)} \quad \text{or} \quad -\mathbf{J}^{(k)} \delta \mathbf{x}^{(k)} = \mathbf{r}^{(k)}. \tag{18.74}$$

To simplify the notation, we drop the subscripts $(n+1)$ and “dev”, and set $\mathbf{x} \equiv (\mathbf{s}, \mathbf{b}, \varepsilon^p, \phi, T, \Delta\gamma)$. Also, for metal plasticity, we assume that $\hat{\mathbf{M}} = \mathbf{f}_\sigma / \|\mathbf{f}_\sigma\|$ where $\mathbf{f}_\sigma := \frac{\partial f}{\partial \boldsymbol{\sigma}}$. Now, with the isotropic-deviatoric split, and since f does not depend on the isotropic component of stress,

$$\mathbf{f}_\sigma = \mathbf{f}_s : \frac{\partial \mathbf{s}}{\partial \boldsymbol{\sigma}} + f_p \frac{\partial p}{\partial \boldsymbol{\sigma}} = \mathbf{f}_s : \frac{\partial \mathbf{s}}{\partial \boldsymbol{\sigma}} = \mathbf{f}_s - \frac{1}{3} \text{tr}(\mathbf{f}_s) \mathbf{1} = \mathbf{f}_s$$

(with $p := \sigma_{\text{iso}} : \mathbf{1} = \text{tr}(\boldsymbol{\sigma})$ and $\mathbf{s} := \boldsymbol{\sigma}_{\text{dev}} = \boldsymbol{\sigma} - \frac{1}{3} \text{tr}(\boldsymbol{\sigma}) \mathbf{1}$). Therefore,

$$\mathbf{M} := \mathbf{M}_{\text{dev}} = \hat{\mathbf{M}}.$$

Let us now compute the derivatives.

$$\begin{aligned}
 \frac{\partial \mathbf{r}_\xi}{\partial \boldsymbol{\xi}} &= \mathbb{I}^{4s} + \Delta\gamma \left[2\mu_n \frac{\partial \mathbf{M}}{\partial \boldsymbol{\xi}} + \frac{\partial \mathbf{h}^\beta}{\partial \boldsymbol{\xi}} \right], \quad \frac{\partial \mathbf{r}_\xi}{\partial \varepsilon^p} = \Delta\gamma \left[2\mu_n \frac{\partial \mathbf{M}}{\partial \varepsilon^p} + \frac{\partial \mathbf{h}^\beta}{\partial \varepsilon^p} \right], \quad \frac{\partial \mathbf{r}_\xi}{\partial \phi} = \Delta\gamma \left[2\mu_n \frac{\partial \mathbf{M}}{\partial \phi} + \frac{\partial \mathbf{h}^\beta}{\partial \phi} \right] \\
 \frac{\partial \mathbf{r}_\xi}{\partial T} &= \Delta\gamma \left[2\mu_n \frac{\partial \mathbf{M}}{\partial T} + \frac{\partial \mathbf{h}^\beta}{\partial T} \right], \quad \frac{\partial \mathbf{r}_\xi}{\partial \Delta\gamma} = 2\mu_n \mathbf{M} + \mathbf{h}^\beta
 \end{aligned}$$

$$\begin{aligned}
\frac{\partial r_{\varepsilon^p}}{\partial \xi} &= -\Delta\gamma \frac{\partial h^\alpha}{\partial \xi}, \frac{\partial r_{\varepsilon^p}}{\partial \varepsilon^p} = 1 - \Delta\gamma \frac{\partial h^\alpha}{\partial \varepsilon^p}, \frac{\partial r_{\varepsilon^p}}{\partial \phi} = -\Delta\gamma \frac{\partial h^\alpha}{\partial \phi}, \frac{\partial r_{\varepsilon^p}}{\partial T} = -\Delta\gamma \frac{\partial h^\alpha}{\partial T}, \frac{\partial r_{\varepsilon^p}}{\partial \Delta\gamma} = -h^\alpha \\
\frac{\partial r_\phi}{\partial \xi} &= -\Delta\gamma \frac{\partial h^\phi}{\partial \xi}, \frac{\partial r_\phi}{\partial \varepsilon^p} = -\Delta\gamma \frac{\partial h^\phi}{\partial \varepsilon^p}, \frac{\partial r_\phi}{\partial \phi} = 1 - \Delta\gamma \frac{\partial h^\phi}{\partial \phi}, \frac{\partial r_\phi}{\partial T} = -\Delta\gamma \frac{\partial h^\phi}{\partial T}, \frac{\partial r_\phi}{\partial \Delta\gamma} = -h^\phi \\
\frac{\partial r_T}{\partial \xi} &= -\Delta\gamma \frac{\partial h^T}{\partial \xi}, \frac{\partial r_T}{\partial \varepsilon^p} = -\Delta\gamma \frac{\partial h^T}{\partial \varepsilon^p}, \frac{\partial r_T}{\partial \phi} = -\Delta\gamma \frac{\partial h^T}{\partial \phi}, \frac{\partial r_T}{\partial T} = 1 - \Delta\gamma \frac{\partial h^T}{\partial T}, \frac{\partial r_T}{\partial \Delta\gamma} = -h^T \\
\frac{\partial r_f}{\partial \xi} &= \frac{\partial f}{\partial \xi} =: f_\xi, \frac{\partial r_f}{\partial \varepsilon^p} = \frac{\partial f}{\partial \varepsilon^p} =: f_\varepsilon, \frac{\partial r_f}{\partial \phi} = \frac{\partial f}{\partial \phi} =: f_\phi, \frac{\partial r_f}{\partial T} = \frac{\partial f}{\partial T} =: f_T, \frac{\partial r_f}{\partial \Delta\gamma} = 0
\end{aligned}$$

The system of equations can be expressed as

$$-\begin{bmatrix} \frac{\partial r_\xi}{\partial \xi} & \frac{\partial r_\xi}{\partial \varepsilon^p} & \frac{\partial r_\xi}{\partial \phi} & \frac{\partial r_\xi}{\partial T} & \frac{\partial r_\xi}{\partial \Delta\gamma} \\ \frac{\partial r_{\varepsilon^p}}{\partial \xi} & \frac{\partial r_{\varepsilon^p}}{\partial \varepsilon^p} & \frac{\partial r_{\varepsilon^p}}{\partial \phi} & \frac{\partial r_{\varepsilon^p}}{\partial T} & \frac{\partial r_{\varepsilon^p}}{\partial \Delta\gamma} \\ \frac{\partial r_\phi}{\partial \xi} & \frac{\partial r_\phi}{\partial \varepsilon^p} & \frac{\partial r_\phi}{\partial \phi} & \frac{\partial r_\phi}{\partial T} & \frac{\partial r_\phi}{\partial \Delta\gamma} \\ \frac{\partial r_T}{\partial \xi} & \frac{\partial r_T}{\partial \varepsilon^p} & \frac{\partial r_T}{\partial \phi} & \frac{\partial r_T}{\partial T} & \frac{\partial r_T}{\partial \Delta\gamma} \\ f_\xi & f_\varepsilon & f_\phi & f_T & 0 \end{bmatrix}^{(k)} \begin{bmatrix} \delta \xi \\ \delta \varepsilon^p \\ \delta \phi \\ \delta T \\ \delta \Delta\gamma \end{bmatrix}^{(k)} = \begin{bmatrix} r_\xi \\ r_{\varepsilon^p} \\ r_\phi \\ r_T \\ r_f \end{bmatrix}^{(k)}$$

We can statically condense the system by defining

$$[A] = \begin{bmatrix} \frac{\partial r_\xi}{\partial \xi} & \frac{\partial r_\xi}{\partial \varepsilon^p} & \frac{\partial r_\xi}{\partial \phi} & \frac{\partial r_\xi}{\partial T} \\ \frac{\partial r_{\varepsilon^p}}{\partial \xi} & \frac{\partial r_{\varepsilon^p}}{\partial \varepsilon^p} & \frac{\partial r_{\varepsilon^p}}{\partial \phi} & \frac{\partial r_{\varepsilon^p}}{\partial T} \\ \frac{\partial r_\phi}{\partial \xi} & \frac{\partial r_\phi}{\partial \varepsilon^p} & \frac{\partial r_\phi}{\partial \phi} & \frac{\partial r_\phi}{\partial T} \\ \frac{\partial r_T}{\partial \xi} & \frac{\partial r_T}{\partial \varepsilon^p} & \frac{\partial r_T}{\partial \phi} & \frac{\partial r_T}{\partial T} \end{bmatrix}, [B] = \begin{bmatrix} \frac{\partial r_\xi}{\partial \Delta\gamma} \\ \frac{\partial r_{\varepsilon^p}}{\partial \Delta\gamma} \\ \frac{\partial r_\phi}{\partial \Delta\gamma} \\ \frac{\partial r_T}{\partial \Delta\gamma} \end{bmatrix}, [C] = [f_\xi \ f_\varepsilon \ f_\phi \ f_T]$$

and

$$[X] = \begin{bmatrix} \delta \xi \\ \delta \varepsilon^p \\ \delta \phi \\ \delta T \end{bmatrix}, [R] = \begin{bmatrix} r_\xi \\ r_{\varepsilon^p} \\ r_\phi \\ r_T \end{bmatrix}$$

to get

$$\begin{bmatrix} [A] & [B] \\ [C] & 0 \end{bmatrix}^{(k)} \begin{bmatrix} [X] \\ \delta \Delta\gamma \end{bmatrix}^{(k)} = \begin{bmatrix} [R] \\ r_f \end{bmatrix}^{(k)}$$

We can eliminate $\delta \Delta\gamma$, to get the new system of equations

$$[A]^{(k)} [X]^{(k)} = [R]^{(k)} - \left[\frac{[C]^{(k)} [A]_{(k)}^{-1} [R]^{(k)} - r_f^{(k)}}{[C]^{(k)} [A]_{(k)}^{-1} [B]^{(k)}} \right] [B]^{(k)}, \delta \Delta\gamma^{(k)} = \frac{[C]^{(k)} [A]_{(k)}^{-1} [R]^{(k)} - r_f^{(k)}}{[C]^{(k)} [A]_{(k)}^{-1} [B]^{(k)}}.$$

The matrix $[A]$ may be difficult to invert because of its conditioning.

18.7.3 Algorithm

The following stress update algorithm is used for each (plastic) time step:

1. Initialize:

$$k = 0; (\varepsilon^p)^{(k)} = \varepsilon_n^p; \phi^{(k)} = \phi_n; \beta^{(k)} = \beta_n; \Delta\gamma^{(k)} = 0; \xi^{(k)} = \xi^{\text{trial}}. \quad (18.75)$$

2. Check yield condition:

$$f^{(k)} := f(\xi^{(k)}, (\varepsilon^p)^{(k)}, \phi^{(k)}, \dot{\varepsilon}_n, T_n, \dots) \quad (18.76)$$

If $f^{(k)} < \text{tolerance}$ then go to step 5 else go to step 3.

3. Compute updated $\delta\gamma^{(k)}$ using

$$\delta\gamma^{(k)} = \frac{f^{(k)}}{\frac{\partial f^{(k)}}{\partial \xi} : [2\mu (\mathbf{M}_{\text{dev}})_n + (\mathbf{h}_{\text{dev}}^\beta)_n] - h_n^\alpha \frac{\partial f^{(k)}}{\partial \varepsilon^p} - h_n^\phi \frac{\partial f^{(k)}}{\partial \phi}}. \quad (18.77)$$

Compute

$$\begin{aligned} \Delta\xi^{(k)} &= -[2\mu (\mathbf{M}_{\text{dev}})_n + (\mathbf{h}_{\text{dev}}^\beta)_n] \delta\gamma^{(k)} \\ (\Delta\varepsilon^p)^{(k)} &= h_n^\alpha \delta\gamma^{(k)} \\ \Delta\phi^{(k)} &= h_n^\phi \delta\gamma^{(k)} \end{aligned} \quad (18.78)$$

4. Update variables:

$$\begin{aligned} (\varepsilon^p)^{(k+1)} &= (\varepsilon^p)^{(k)} + (\Delta\varepsilon^p)^{(k)} \\ \phi^{(k+1)} &= \phi^{(k)} + \Delta\phi^{(k)} \\ \xi^{(k+1)} &= \xi^{(k)} + \Delta\xi^{(k)} \\ \Delta\gamma^{(k+1)} &= \Delta\gamma^{(k)} + \delta\gamma^{(k)} \end{aligned} \quad (18.79)$$

Set $k \leftarrow k + 1$ and go to step 2.

5. Update and calculate back stress and the deviatoric part of Cauchy stress:

$$\varepsilon_{n+1}^p = (\varepsilon^p)^{(k)}; \phi_{n+1} = \phi^{(k)}; \xi_{n+1} = \xi^{(k)}; \Delta\gamma_{n+1} = \Delta\gamma^{(k)} \quad (18.80)$$

and

$$\begin{aligned} \hat{\beta}_{n+1} &= \hat{\beta}_n + \Delta\gamma_{n+1} \mathbf{h}^\beta(\xi_{n+1}, \varepsilon_{n+1}^p, \phi_{n+1}) \\ \beta_{n+1} &= \hat{\beta}_{n+1} - \frac{1}{3} \text{tr}(\hat{\beta}_{n+1}) \mathbf{1} \\ (\sigma_{\text{dev}})_{n+1} &= \xi_{n+1} + \beta_{n+1} \end{aligned} \quad (18.81)$$

6. Update the temperature and the Cauchy stress

$$\begin{aligned} T_{n+1} &= T_n + \frac{\chi_{n+1} \Delta t}{\rho_{n+1} C_p} \sigma_y^{n+1} \varepsilon_{n+1}^p = T_n + \frac{\chi_{n+1} \Delta\gamma_{n+1}}{\rho_{n+1} C_p} \sigma_y^{n+1} h_{n+1}^\alpha \\ p_{n+1} &= p(J_{n+1}) \\ \kappa_{n+1} &= J_{n+1} \left[\frac{dp(J)}{dJ} \right]_{n+1} \\ \sigma_{n+1} &= [p_{n+1} - 3\kappa_{n+1} \alpha(T_{n+1} - T_0)] \mathbf{1} + (\sigma_{\text{dev}})_{n+1} \end{aligned} \quad (18.82)$$

18.8 Examples

Let us now look at a few examples.

18.8.1 Example 1

Consider the case of J_2 plasticity with the yield condition

$$f := \sqrt{\frac{3}{2}} \|\sigma_{\text{dev}} - \beta\| - \sigma_y(\varepsilon^p, \dot{\varepsilon}, T, \dots) = \sqrt{\frac{3}{2}} \|\xi\| - \sigma_y(\varepsilon^p, \dot{\varepsilon}, T, \dots) \leq 0 \quad (18.83)$$

where $\|\xi\| = \sqrt{\xi : \xi}$. Assume the associated flow rule

$$d^p = \dot{\gamma} r = \dot{\gamma} \frac{\partial f}{\partial \sigma} = \dot{\gamma} \frac{\partial f}{\partial \xi}. \quad (18.84)$$

Then

$$r = \frac{\partial f}{\partial \xi} = \sqrt{\frac{3}{2}} \frac{\xi}{\|\xi\|} \quad (18.85)$$

and

$$d^p = \sqrt{\frac{3}{2}} \dot{\gamma} \frac{\xi}{\|\xi\|}; \quad \|d^p\| = \sqrt{\frac{3}{2}} \dot{\gamma}. \quad (18.86)$$

The evolution of the equivalent plastic strain is given by

$$\dot{\varepsilon}^p = \dot{\gamma} h^\alpha = \sqrt{\frac{2}{3}} \|d^p\| = \dot{\gamma}. \quad (18.87)$$

This definition is consistent with the definition of equivalent plastic strain

$$\varepsilon^p = \int_0^t \dot{\varepsilon}^p d\tau = \int_0^t \sqrt{\frac{2}{3}} \|d^p\| d\tau. \quad (18.88)$$

The evolution of porosity is given by (there is no evolution of porosity)

$$\dot{\phi} = \dot{\gamma} h^\phi = 0 \quad (18.89)$$

The evolution of the back stress is given by the Prager kinematic hardening rule

$$\dot{\beta} = \dot{\gamma} h^\beta = \frac{2}{3} H' d^p \quad (18.90)$$

where $\hat{\beta}$ is the back stress and H' is a constant hardening modulus. Also, the trace of d^p is

$$\text{tr}(d^p) = \sqrt{\frac{3}{2}} \dot{\gamma} \frac{\text{tr}(\xi)}{\|\xi\|}. \quad (18.91)$$

Since ξ is deviatoric, $\text{tr}(\xi) = 0$ and hence $d^p = d_{\text{dis}}^p$. Hence, $\hat{\beta} = \beta$ (where β is the deviatoric part of $\hat{\beta}$), and

$$\dot{\beta} = \sqrt{\frac{2}{3}} H' \dot{\gamma} \frac{\xi}{\|\xi\|}. \quad (18.92)$$

These relation imply that

$$\begin{aligned} \mathbf{r} &= \sqrt{\frac{3}{2}} \frac{\boldsymbol{\xi}}{\|\boldsymbol{\xi}\|} \\ h^\alpha &= 1 \\ h^\phi &= 0 \\ \mathbf{h}^\beta &= \sqrt{\frac{2}{3}} H' \frac{\boldsymbol{\xi}}{\|\boldsymbol{\xi}\|}. \end{aligned} \quad (18.93)$$

We also need some derivatives of the yield function. These are

$$\begin{aligned} \frac{\partial f}{\partial \boldsymbol{\xi}} &= \mathbf{r} \\ \frac{\partial f}{\partial \varepsilon^p} &= -\frac{\partial \sigma_y}{\partial \varepsilon^p} \\ \frac{\partial f}{\partial \phi} &= 0. \end{aligned} \quad (18.94)$$

Let us change the kinematic hardening model and use the Armstrong-Frederick model instead, i.e.,

$$\dot{\boldsymbol{\beta}} = \dot{\gamma} \mathbf{h}^\beta = \frac{2}{3} H_1 \mathbf{d}^p - H_2 \boldsymbol{\beta} \|\mathbf{d}^p\|. \quad (18.95)$$

Since

$$\mathbf{d}^p = \sqrt{\frac{3}{2}} \dot{\gamma} \frac{\boldsymbol{\xi}}{\|\boldsymbol{\xi}\|} \quad (18.96)$$

we have

$$\|\mathbf{d}^p\| = \sqrt{\frac{3}{2}} \dot{\gamma} \frac{\|\boldsymbol{\xi}\|}{\|\boldsymbol{\xi}\|} = \sqrt{\frac{3}{2}} \dot{\gamma}. \quad (18.97)$$

Therefore,

$$\dot{\boldsymbol{\beta}} = \sqrt{\frac{2}{3}} H_1 \dot{\gamma} \frac{\boldsymbol{\xi}}{\|\boldsymbol{\xi}\|} - \sqrt{\frac{3}{2}} H_2 \dot{\gamma} \boldsymbol{\beta}. \quad (18.98)$$

Hence we have

$$\mathbf{h}^\beta = \sqrt{\frac{2}{3}} H_1 \frac{\boldsymbol{\xi}}{\|\boldsymbol{\xi}\|} - \sqrt{\frac{3}{2}} H_2 \boldsymbol{\beta}. \quad (18.99)$$

18.8.2 Example 2

Let us now consider a Gurson type yield condition with kinematic hardening. In this case the yield condition can be written as

$$f := \frac{3}{2} \frac{\boldsymbol{\xi} : \boldsymbol{\xi}}{\sigma_y^2} + 2 q_1 \phi^* \cosh\left(\frac{q_2 \operatorname{tr}(\boldsymbol{\sigma})}{2 \sigma_y}\right) - [1 + q_3 (\phi^*)^2] \quad (18.100)$$

where ϕ is the porosity and

$$\phi^* = \begin{cases} \phi & \text{for } \phi \leq \phi_c \\ \phi_c - \frac{\phi_u^* - \phi_c}{\phi_f - \phi_c} (\phi - \phi_c) & \text{for } \phi > \phi_c \end{cases} \quad (18.101)$$

Final fracture occurs for $\phi = \phi_f$ or when $\phi_u^* = 1/q_1$.

Let us use an associated flow rule

$$\mathbf{d}^p = \dot{\gamma} \mathbf{r} = \dot{\gamma} \frac{\partial f}{\partial \boldsymbol{\sigma}}. \quad (18.102)$$

Then

$$\mathbf{r} = \frac{\partial f}{\partial \boldsymbol{\sigma}} = \frac{3}{\sigma_y^2} \xi + \frac{q_1 q_2 \phi^*}{\sigma_y} \sinh\left(\frac{q_2 \text{tr}(\boldsymbol{\sigma})}{2 \sigma_y}\right) \mathbf{1}. \quad (18.103)$$

In this case

$$\text{tr}(\mathbf{r}) = \frac{3 q_1 q_2 \phi^*}{\sigma_y} \sinh\left(\frac{q_2 \text{tr}(\boldsymbol{\sigma})}{2 \sigma_y}\right) \neq 0 \quad (18.104)$$

Therefore,

$$\mathbf{d}^p \neq \mathbf{d}_{\text{dis}}^p. \quad (18.105)$$

For the evolution equation for the plastic strain we use

$$(\boldsymbol{\sigma} - \hat{\boldsymbol{\beta}}) : \mathbf{d}^p = (1 - \phi) \sigma_y \dot{\varepsilon}^p \quad (18.106)$$

where $\dot{\varepsilon}^p$ is the effective plastic strain rate in the matrix material. Hence,

$$\dot{\varepsilon}^p = \dot{\gamma} h^\alpha = \dot{\gamma} \frac{(\boldsymbol{\sigma} - \hat{\boldsymbol{\beta}}) : \mathbf{r}}{(1 - \phi) \sigma_y}. \quad (18.107)$$

The evolution equation for the porosity is given by

$$\dot{\phi} = (1 - \phi) \text{tr}(\mathbf{d}^p) + A \dot{\varepsilon}^p \quad (18.108)$$

where

$$A = \frac{f_n}{s_n \sqrt{2\pi}} \exp[-1/2(\varepsilon^p - \varepsilon_n)^2 / s_n^2] \quad (18.109)$$

and f_n is the volume fraction of void nucleating particles, ε_n is the mean of the normal distribution of nucleation strains, and s_n is the standard deviation of the distribution.

Therefore,

$$\dot{\phi} = \dot{\gamma} h^\phi = \dot{\gamma} \left[(1 - \phi) \text{tr}(\mathbf{r}) + A \frac{(\boldsymbol{\sigma} - \hat{\boldsymbol{\beta}}) : \mathbf{r}}{(1 - \phi) \sigma_y} \right]. \quad (18.110)$$

If the evolution of the back stress is given by the Prager kinematic hardening rule

$$\dot{\hat{\boldsymbol{\beta}}} = \dot{\gamma} h^\beta = \frac{2}{3} H' \mathbf{d}^p \quad (18.111)$$

where $\hat{\boldsymbol{\beta}}$ is the back stress, then

$$\dot{\hat{\boldsymbol{\beta}}} = \frac{2}{3} H' \dot{\gamma} \mathbf{r}. \quad (18.112)$$

Alternatively, if we use the Armstrong-Frederick model, then

$$\dot{\hat{\boldsymbol{\beta}}} = \dot{\gamma} \mathbf{h}^\beta = \frac{2}{3} H_1 \mathbf{d}^p - H_2 \hat{\boldsymbol{\beta}} \|\mathbf{d}^p\|. \quad (18.113)$$

Plugging in the expression for \mathbf{d}^p , we have

$$\dot{\hat{\boldsymbol{\beta}}} = \dot{\gamma} \left[\frac{2}{3} H_1 \mathbf{r} - H_2 \hat{\boldsymbol{\beta}} \|\mathbf{r}\| \right]. \quad (18.114)$$

Therefore, for this model,

$$\boxed{\begin{aligned} \mathbf{r} &= \frac{3}{\sigma_y^2} \boldsymbol{\xi} + \frac{q_1 q_2 \phi^*}{\sigma_y} \sinh\left(\frac{q_2 \text{tr}(\boldsymbol{\sigma})}{2 \sigma_y}\right) \mathbf{1} \\ h^\alpha &= \frac{(\boldsymbol{\sigma} - \hat{\boldsymbol{\beta}}) : \mathbf{r}}{(1 - \phi) \sigma_y} \\ h^\phi &= (1 - \phi) \text{tr}(\mathbf{r}) + A \frac{(\boldsymbol{\sigma} - \hat{\boldsymbol{\beta}}) : \mathbf{r}}{(1 - \phi) \sigma_y} \\ \mathbf{h}^\beta &= \frac{2}{3} H_1 \mathbf{r} - H_2 \hat{\boldsymbol{\beta}} \|\mathbf{r}\| \end{aligned}} \quad (18.115)$$

The other derivatives of the yield function that we need are

$$\begin{aligned} \frac{\partial f}{\partial \boldsymbol{\xi}} &= \frac{3}{\sigma_y^2} \boldsymbol{\xi} \\ \frac{\partial f}{\partial \varepsilon^p} &= \frac{\partial f}{\partial \sigma_y} \frac{\partial \sigma_y}{\partial \varepsilon^p} = - \left[\frac{3}{\sigma_y^3} \boldsymbol{\xi} : \boldsymbol{\xi} + \frac{q_1 q_2 \phi^* \text{tr}(\boldsymbol{\sigma})}{\sigma_y^2} \sinh\left(\frac{q_2 \text{tr}(\boldsymbol{\sigma})}{2 \sigma_y}\right) \right] \frac{\partial \sigma_y}{\partial \varepsilon^p} \\ \frac{\partial f}{\partial \phi} &= 2 q_1 \frac{d\phi^*}{d\phi} \cosh\left(\frac{q_2 \text{tr}(\boldsymbol{\sigma})}{2 \sigma_y}\right) - 2 q_3 \phi^* \frac{d\phi^*}{d\phi}. \end{aligned} \quad (18.116)$$